

Coal Characterisation and Combustion

Thesis submitted for the Degree of
Doctor of Philosophy

The University of Newcastle upon Tyne

NEWCASTLE UNIVERSITY LIBRARY

089 54096 1

Thesis L 3551

©*Stephen Leonard Bend*
November 1989

*I would like to dedicate this thesis
to my wife
and also to the memories of
Elzèar and James Ernest.*

Acknowledgements

I would like to thank my supervisor, Prof. H. Marsh, for the support extended to me over the past three years.

I also thank Dr. M.K. Thomas for critically reviewing my thesis.

In addition, I would like to thank: Dr. A. Cameron, Dr. R.C. Neavel, Dr. W. Livingston. Mr. J. Pearson for the kind donation of the coals.

I would also like to thank Dr I.A.S. Edwards and my fellow colleagues for making my stay in N.C.R.L. a memorable one.

To Dr. J.M. Jones for the loan of the Hamamatsu PMT, the uranyl glass and assorted specular standards.

Dr. D. Johnston (Leeds) for the TEM microtome service.

Dr. J. Senfile, ARCO, for the NMR analyses, Mr. C. Spracklin for conducting the surface area analyses and Mr D. Dunbar for the CHN and FT-IR analyses.

Mr. D. Stott (Leitz Instruments) for the loan of various photographic bits and pieces.

Mr. R. Graham and the 'workshop boys' for constructing my 'gadgets'.

Mrs. E. Watson for proof reading services.

Last, but not least, Phyllis, my wife: provider of moral support.

Contents

	<i>Page</i>
<i>Abstract</i>	<i>i</i>
Chapter One '<i>The Origin, Formation and Composition of Coal</i>'	
1.1 Introduction	1
1.2 'Coal Provincialism'	1
1.3 Coal Forming Periods and Influencing Factors	2
1.3.1 Palaeogeography and Climate	2
1.3.2 Evolutionary Trends within Coal Forming Flora	4
1.4 The Formation of Peat	8
1.4.1 Peat Forming Environments	8
1.4.2 The Influence of Temperature Upon the Formation of Peat	10
1.4.3 The Hydrology of the Peat-Forming Environments	10
1.5 The Formation of Coal	12
1.5.1 Precursor Material	12
1.5.2 Peatification	14
1.5.3 Gelification	16
1.6 Coalification	16
1.6.1 Time, Temperature and Pressure	16
1.6.2 Factors Responsible for Variations in Coalification	18
1.6.3 The Chemical and Physical Response to Coalification	18
1.7 The Petrographic Composition of Coal	20
1.7.1 The Lithotypes	20
1.7.2 The Macerals	20
1.7.2.1 The Vitrinites	21
1.7.2.2 The Liptinites	22
1.7.2.3 The Inertinites	23
1.7.3 The Macerals: Physical and Chemical Characteristics	23
1.8 In Retrospect	26
References	27
Chapter Two '<i>Coal Characterisation And Classification</i>'	
2.1 Introduction	31
<u>Coal Characterisation Part I: Petrographic Analysis</u>	
2.2 Sample Preparation	31

	<i>Page</i>
2.3 Maceral Analysis	32
2.4 Microlithotype Analysis	33
2.5 Reflectance	34
2.5.1 The Theoretical Basis	34
2.5.2 Vitrinite Reflectance	37
2.5.4 Automated Reflectance Techniques	38
2.6 Fluorescence Microscopy	39
<u>Coal Characterisation Part II: Standard Laboratory Tests</u>	
2.7 Introduction	40
2.7.1 Analysis 'Report Bases'	41
2.8 Proximate Analysis	41
2.8.1 The Determination of Moisture	42
2.8.2 The Determination of Volatile Matter	42
2.8.3 The Determination of Ash	43
2.8.4 Fixed Carbon	44
2.9 Ultimate Analysis	44
2.9.1 Carbon and Hydrogen Analysis	45
2.9.2 Nitrogen Analysis	45
2.9.3 Sulphur Analysis	45
2.9.4 Variation in Elemental Composition	46
2.10 The Determination of Calorific Value	46
2.11 The Determination of Grindability	47
2.12 Ash Fusibility	48
2.13 Behaviour upon Heating	48
2.13.1 General Considerations	48
2.13.2 Free Swelling Index	49
2.13.3 Gray-King Assay	49
2.13.4 Giesler Plastometer	49
2.13.5 Audibert-Arnu Dilatometer	49
2.13.6 Roga Test	49
<u>Coal Characterisation Part III: Coal Classification</u>	
2.14 General Considerations	50
2.15 Domestic Commercial Classification Systems	50
2.16 International Classification Systems	53
2.16.1 The International Hard Coal Classification by Type	53
2.16.2 The International Classification System for Medium and High Rank Coals	54
2.17 Scientific Classification Systems	56
2.17.1 Seyler's Classification System	56
2.17.2 Mott's Classification System	58
2.17.3 Recent Scientific Classification Systems	58
2.18 In Retrospect	59
References	60

Chapter Three *'Pulverised Coal Combustion'*

3.1	Introduction	62
3.2	Pulverised Coal Utility Boilers	62
3.2.1	Utility Boiler and Burner Configuration	62
3.2.2	The Modern Utility Boiler	64
3.2.3	Coal Feed Systems	66
3.2.4	Fly Ash Collection	66
3.3	Coal Combustion: An Overview	66
3.3.1	Background	66
3.3.2	The Classical View of Coal Combustion	67
3.3.3	Laboratory Based Studies, The Techniques and Rationale	68
3.4	Coal Combustion: Devolatilisation and Char Formation	70
3.5	Coal Combustion: The Combustion of Volatiles	74
3.6	Coal Combustion: Char Oxidation	76
3.7	Coal Combustion: The Effect of Coal Type and Rank	79
	References	82

Chapter Four *Objectives*

4.1	Overall Objectives	85
4.2	Specific Objectives	85
4.2.1	The Influence of Coal Rank upon Char Morphology and Combustion	85
4.2.2	Coal and Char Characterisation and Correlations	86
4.2.3	The Effects of Coal Oxidation and Weathering upon Coal Properties, Char Morphology and Combustion	86

Chapter Five *Experimental*

5.1	Coal Samples Used	87
5.1.1	Origin of Samples	87
5.1.2	Sample Preparation	88
5.2	Petrographic Characterisation Techniques	88
5.2.1	Sample Preparation	88
5.2.2	Maceral Analysis	89
5.2.2.1	Description of Apparatus	89
5.2.2.2	Procedure	89
5.2.2.3	Reproducibility of Data	89
5.2.3	Microlithotype Analysis	89
5.2.3.1	Description of Apparatus	89
5.2.3.2	Procedure	90
5.2.3.3	Reproducibility of Data	90
5.2.4	Vitrinite Reflectance	90

	<i>Page</i>
5.2.4.1 Description of Apparatus	90
5.2.4.2 Procedure and Calculations	90
5.2.4.3 Calibration of The Microscope Photometer	91
5.2.4.4 Reproducibility of Data	91
5.2.5 <i>Reflectance Scanning</i>	92
5.2.5.1 Description of Apparatus	92
5.2.5.2 Procedure	92
5.2.6 <i>Fluorescence Microphotometry</i>	93
5.2.6.1 Description of Apparatus	93
5.2.6.2 Procedure	94
5.3 Proximate Analysis	95
5.3.1 Introduction	95
5.3.2 Description of Apparatus	95
5.3.3 Procedure	95
5.3.4 Reproducibility of Data	96
5.4 Elemental Analysis	96
5.4.1 Description of Apparatus	96
5.4.2 Procedure	97
5.4.3 Reproducibility of Data	97
5.5 Calorific Value	98
5.5.1 Description of Apparatus	98
5.5.2 Procedure	98
5.5.3 Reproducibility of Data	99
5.6 Fourier Transform Infrared Spectroscopy	99
5.6.1 Description of Apparatus	99
5.6.2 Procedure	99
5.7 Nuclear Magnetic Resonance Spectroscopy	99
5.7.1 Description of Apparatus	99
5.8 Entrained Flow Reactor	99
5.8.1 Description of Apparatus	99
5.8.2 Procedure	102
5.8.2.1 Coal Pyrolysis Using N ₂	102
5.8.2.2 Char Combustion Using Air	103
5.9 Optical Char Characterisation (Morphology)	103
5.9.1 Sample Preparation	103
5.9.2 Description of Apparatus	103
5.9.3 Procedure	103
5.9.4 Char Classification Criteria	104
5.9.5 Reproducibility of Data	105
5.10 Macro Porosity Determinations	105
5.10.1 Description of Apparatus	105
5.10.2 Procedure	105
5.10.3 Reproducibility of Data	106

	<i>Page</i>
5.11 Scanning Electron Microscopy of Chars	106
5.11.1 Description of Apparatus	106
5.12 Transmitted Electron Microscopy of Chars	106
5.12.1 Description of Apparatus	106
5.13 TGA Reactivity Measurements of Coal	106
5.13.1 Description of Apparatus	106
5.13.2 Procedure	106
5.13.3 Reproducibility of Data	107
5.14 Surface Area Measurements of the Chars	107
5.14.1 Description of Apparatus	107
5.14.2 Procedure	107
5.14.3 Calculations	108
5.14.4 Reproducibility of Data	108
References	109

Chapter Six *Results*

6.1 The Influence of Coal Rank upon Char Morphology and Combustion	110
6.2 Coal and Char Characterisation and Correlations	110
6.3 The Effects of Coal Oxidation and Weathering upon Coal Properties, Char Morphology and Combustion	111

Chapter Seven *Discussion*

7.1 The Influence of Coal Rank upon Char Morphology and Combustion	
7.1.1 Introduction	121
7.1.2 Relationships Between Coal Rank and Char Morphology	122
7.1.3 Relationships Between Char Morphology and Coal Structure	126
7.1.4 Mechanism of Char Formation during Pyrolysis related to the Influence of Coal Rank	131
7.1.5 Char Reactivity and Burn-out	133
7.1.6 Review	135
7.2 Coal and Char Characterisation and Correlations	
7.2.1 Introduction	136
7.2.2 Coal Characterisation using Whole-Coal Reflectograms	136
7.2.3 Coal and Char Univariate and Multivariate Relationships	139
7.2.3.1 Univariate Relationships	139
7.2.3.2 Multivariate Relationships and 'Provincialism'	141
7.2.4 Review	143
7.3 The Effects of Coal Oxidation and Weathering upon Coal Characteristics, Char Morphology and Combustion	144
7.3.1 Introduction	144
7.3.2 Coal Characterisation: Oxidation and Weathering Effects	145

	<i>Page</i>
7.3.3 Char Morphology and Combustion: Oxidation and Weathering Effects	156
7.3.4 The Relationship Between Char Formation and Coal Elemental Oxygen Content	160
7.3.5 Review	161
References	163

Chapter Eight *Conclusions*

8.1 Overall Conclusions	165
8.2 Specific Conclusions	165
8.2.1 The Influence of Coal Rank upon Char Morphology and Combustion	165
8.2.2 Coal and Char Characterisation and Correlations	167
8.2.3 The Effects of Coal Oxidation and Weathering upon Coal Properties, Char Morphology and Combustion	168
References	170

Appendices:

A	Glossary of Terms Used
B	Line Drawings

Abstract

There are three related studies within this thesis that examine the relationships between the properties of coals and the characteristics of the chars produced during rapid pyrolysis in a laboratory based Entrained Flow Reactor (EFR) which simulates the rapid rates of heating (10^4 to 10^5 °C s⁻¹) typical of pulverised fuel boilers.

The first study, using a suite of nine coals, investigates the influence of coal rank upon the generation of specific types of char, their respective physical and structural characteristics and their relative combustibilities.

The second study, using a suite of twenty-two coals, examines various coal characterisation techniques and the correlations between those techniques and the associated char, and specifically investigates petrographic techniques as a means of characterising coal feedstock.

The third study, using freshly mined coals, investigates the effects of oxidation (100°C, air) and weathering (ambient) upon standard analytical techniques and relates such changes to the physical, structural and combustion characteristics of the associated char.

There is a common relationship between the *elemental oxygen content* of the parent coal and the generation of specific types of char for both vitrinite rich coals of differing coal rank and for the oxidised or weathered coals. There is also an inverse relationship ($R^2 = 0.97$) between the elemental oxygen content of a vitrinite rich coal and the proportion of cenospheres generated by pyrolysis at 1000°C using the EFR. Furthermore, the enhancement of char combustion at 1000°C (in an EFR) is related to the physical and structural characteristics of the char, i.e. the presence or absence of porosity (visible using SEM and TEM), the CO₂ surface area and optical texture.

A relationship exists ($R^2 = 0.83$) between the morphology of a char (1000°C / N₂) and the petrographic composition of the parent coal. The new term *microlithotype_v* is an amalgamation of various vitrinite rich microlithotype classes that simplifies the nomenclature. A combination of calorific value, *microlithotype_v* and coal rank (vitrinite reflectance) illustrates the influence of petrographic composition upon calorific value and also suggests a 'Province' dependency amongst the Cretaceous/Tertiary and Carboniferous coals studied. The coal properties calorific value, *microlithotype_v* and coal rank can be related ($R^2 = 0.91$) to the proportion of *porous chars* for the Cretaceous/Tertiary suite of coals, illustrating the use of multivariate analyses when characterising coal feedstock.

The effects of oxidation and weathering upon vitrinite fluorescence is also reported. The oxidation of coal at 100°C produces rims of quenched fluorescence which are not apparent within the weathered coals. Furthermore, the intensity of fluorescence at 650 nm (I₆₅₀) decreases due to progressive oxidation or weathering, but decreases at a rate that is dependent upon the severity (temperature) of the conditions employed. The proposed *oxidation quotient* ($O/Q = I_{650}/\%R_{0max}$) is a sensitive indicator of the oxidative conditions up to 100°C.

*Coal Characterisation
and
Combustion*

CHAPTER ONE

The Origin, Formation and Composition of Coal'

1.1 Introduction

There are two essential questions that are central to the theme of this chapter. Firstly, are there recognisable differences in the geochemical, petrological and utilisation characteristics between coals of different origin? Secondly, if differences do exist, to what extent are they attributable to the precursor materials from which coals are formed and to what extent are they a consequence of the processes of peatification and coalification?

1.2 'Coal Provincialism'

Without doubt, coal rank^{Ψ1} is the major factor that determines the suitability or the utilisation characteristics of a given coal. For example, measurable properties such as the swelling behaviour, fluidity, elemental composition and heating value vary with rank and form the basis of many classification schemes.^{1,2,3,4} However, coalification does not appear to occur with universal uniformity.⁵ Jones *et al*⁵ discuss the relationship of volatile-matter yield to vitrinite reflectance and carbon content and show that those properties are dependent upon the nature and coalification history of the vitrinite. The thesis of Jones *et al*⁵ is that those properties will show relative variations from coal bearing province to province as a function of coalification history.

The utilisation characteristics and intrinsic properties of coals do not appear to be governed solely by coal rank. Investigations of the interrelationships between the utilisation characteristics of coal and physical and chemical properties have indicated that coal rank is not the only factor that determines utilisation suitability. Given *et al*⁶ investigated the relationship between coal composition, coal rank and liquefaction behaviour for North American coals, and they determined that in addition to coal rank, the geological history and the petrographic composition of the coal determined the yield and nature of the liquefaction products. In a later study, Youtcheff and Given⁷ observed that a coal of Cretaceous age (Table 1.1, page 3) was associated with a lower yield of liquefaction products than equivalent Carboniferous coals. Differences were also shown to exist between Cretaceous and Carboniferous Canadian coals with respect to coking propensity,^{8,9} solvent extract yield, Giesler fluidity and oxidation behaviour.¹⁰ In each case, the coals were of comparable rank and the observed differences were attributed to petrographic composition, geological age and differences in coalification history. Petrographic composition has been

^{Ψ1} A glossary of terms used is given in Appendix A

largely regarded as the most significant discriminatory factor between the Carboniferous coals of Europe and North America, and the Permian coals of South Africa, India and Australia; the inappropriateness of chemical composition as a means of selecting such coals is well documented in the literature. Both Savage¹² and Sanyal¹³ report significant differences in gasification and carbonisation behaviour for South African coals when used under the same conditions as Carboniferous coals. There are also reports citing the anomalous coking behaviour of South African coals compared to Carboniferous coals of similar chemical analysis but varying in their petrographic composition.¹³ The relatively poor combustion characteristics of South African Permian coals are attributed by Sanyal¹² to the higher proportion of 'inertinite' in those coals compared to Carboniferous coals. The same maceral groups were also considered responsible for the poor combustion characteristics of Western Canadian Cretaceous coal by Nandi *et al.*¹⁴ These findings have subsequently been supported by systematic laboratory studies examining the combustion behaviour of such coals.^{15,16} The phenomena is now considered to show a possible 'province dependent' relationship.¹⁷ Multivariate analysis techniques have also been used by Metcalf *et al.*¹⁸ in which they successfully relate the compositional characteristics of lignites to variations in depositional environment using pyrolysis mass-spectroscopy, indicating that the concept of 'provincialism' is not only a phenomenon restricted to older coals.

There are several other studies that relate coal characteristics, excluding rank, to the conditions of deposition, the palaeogeography, palaeoclimate of the peat forming environment and the original peat forming flora. Early studies by Snyman¹⁹ and Hoffmann and Hoehne²⁰ on the Permian coals of South Africa and by Brown and Taylor²¹ on the Permian coals of Australia demonstrated that those coals were formed under conditions, and from flora, very different from those considered to have prevailed during earlier Carboniferous times. More recent studies^{22,23,24} have extensively developed the theories on Permian coal formation. Similar studies have been conducted on coals of all ages in China,^{25,26} on the Carboniferous and Jurassic coals of the USSR,^{27,28} the Carboniferous and Cretaceous coals of Canada^{29,30} and on the Cretaceous coals of New Zealand.³¹ However, there are many more publications, specific to Carboniferous coals, that discuss the petrological, geochemical and utilisation characteristics in relation to the origin, palaeogeography, climate and conditions of peatification and coalification (e.g.^{4,29,32,33,34,35}), underlying the importance such deposits have in the 'Western' world.^{3,4,5,10,36,37}

1.3 Coal Forming Periods and Influencing Factors

1.3.1 Palaeogeography and Climate

The development of a peat-forming environment requires a unique set of conditions.^{33,34} However, such conditions have only occurred sporadically in any given continent

throughout geological time³⁸ creating chronologically discontinuous deposits of coal and suggesting that the conditions necessary for the accumulation of economic deposits of coal are somewhat unique. A listing of the Geological periods is given in Table 1.1.

Table 1.1 Geological Periods and associated main coal forming taxa.

Era	Period	Age (Ma ⁻¹)	Duration (Ma ⁻¹)	Flora [†]	Coal Deposition
Cenozoic	Quaternary	2.0	2.0	A,g,p	minor
	Tertiary	65.0	63.0	A,g,p	
Mesozoic	Cretaceous	144.0	79.0	A,g,p	major
	Jurassic	213.0	69.0	a,G,p	minor
	Triassic	248.0	35.0	G,p	minimal
Palaeozoic	Permian	286.0	38.0	G,p	major [‡]
	U-Carboniferous	320.0	34.0	g,P	major
	L-Carboniferous	360.0	40.0	g,p	minor
	Devonian	408.0	48.0	p,z,r	minor
	Silurian	438.0	30.0	z,r	non-known
	Ordovician	505.0	67.0		
	Cambrian	590.0	85.0		

[†] The taxa indicated are: A,a angiosperms; G,g. gymnosperms; P,p. pteridophytes; in addition: z. zosterophyllum; r. rhynia. Increasing dominance indicated by: g→g→G→G

[‡] The Permian period was a period of major coal formation in the southern hemisphere.

One of the most underestimated major factors determining the type and the temporal and spatial distribution of coal is global palaeogeography. Butler *et al*³⁹ regarded climate, over and above palaeogeography, as the major coal forming determinant. However, global and local climate is dependent upon the juxtaposition and the spatial distribution of land mass in relation to the poles and the equator. Land mass has a profound effect upon the global zonal pattern of atmospheric circulation.^{40,41} The zonal pattern of atmospheric circulation (Figure 1.1) consists of a low pressure regime at the equator and high mid-latitudes, and a regime of high pressure at the poles and low mid-latitudes.

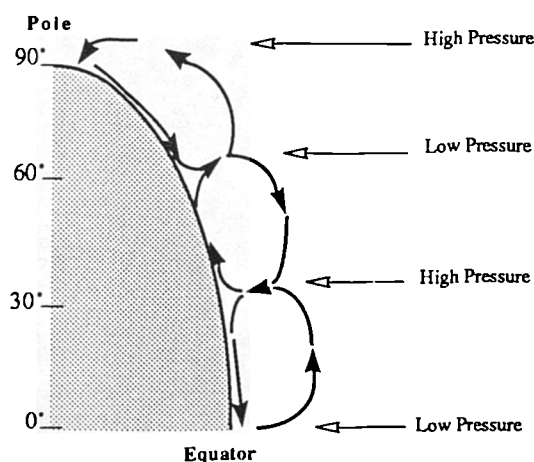


Figure 1.1 The circulation of the atmosphere due to the exchange of heat between the equator and the polar regions influenced by the coriolis force (→ indicates air movement).

The pressure regimes at the equator and poles are functions of temperature while the mid-latitude pressure regimes are due to the superimposition of the Coriolis force upon the direct exchange of heat between equator and the poles. The presence of a large continent extending from equator to pole would result in a fixation of the circulation cells,⁴² creating a narrow, intense, equatorial low-pressure belt (Inter-tropical Convergence Zone: ITCZ) with concomitant high levels of precipitation.⁴³ Such conditions prevailed upon the ancient continent of *Euramerica* (Figure 1.2) during the main coal forming period of the Carboniferous,^{40,43,44} whereas land positioned symmetrically about the equator would lessen the intensity of the equatorial low pressure belt and produce a much wider, less intense, equatorial low pressure belt, resulting in the drying-out of the equatorial zone and a wider dispersal of precipitation (monsoonal type) at mid-latitudes. This is now considered to be the main reason why lush equatorial-tropical forest swamps were replaced by arid conditions towards the close of the Carboniferous period in *Euramerica*.⁴⁴

1.3.2 Evolutionary Trends within the Coal Forming Flora

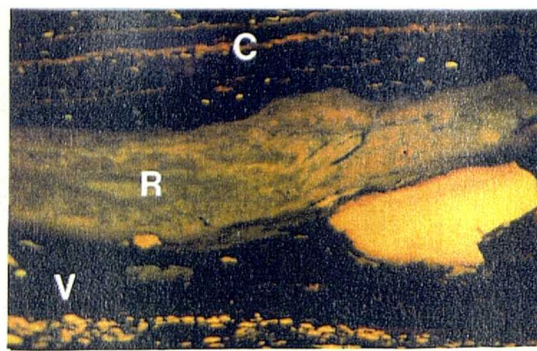
There have been three significant developments in vascular plant evolution throughout geological time and each development has led to a more successful taxa.⁴⁵ The earliest vascular plants belonged to the spore bearing, seedless plants known as Pteridophytes; the second development involved the evolution of seed-bearing plants known as Gymnosperms ('naked seeds') followed by the most successful group of all, the highly adaptable Angiosperms ('covered seeds').⁴⁶

The earliest known true coal deposit occurs in Kazakhstan in the USSR dating from the late Devonian period (c.a. 390 M.a.). This 'sapropelic-like' coal is formed from the primitive herbaceous forerunner of the Carboniferous Lycophyte: *Zosterophyllum*⁴⁷ (Plate 1a). Diversification, followed by rapid evolution during the later part of the Devonian (c.a. 390-360 M.a.), led to the emergence of the free-sporing, herbaceous variety of Pteridophytes (i.e. *Lycophytes*, *Sphenophytes* and Ferns).⁴⁶ Within the equatorial-tropical zones of *Euramerica* (Figure 1.2) during the early Carboniferous, an evolutionary explosion of plant varieties created competition within the peat forming environment, promoting the development of arborescence and habitat specialisation.^{46,48} The creation of lignified vascular tissue, through the secondary thickening of the apical stem, was a prerequisite to the development of arborescence⁴⁶ and is one of the most significant reasons why Carboniferous coals (Plates 1b) contain substantial amounts of vitrinite compared to those coals formed from more primitive plants (Plate 1a). Furthermore, the abundance of both mega and micro-spores (Plate 1b & 1c) in Carboniferous coals is explained by the primitive reproductive system of the Pteridophytes,^{45,46} which required the production of vast numbers of spores to compensate for a relatively crude reproductive system that relied upon the presence of ground water for sperm dispersal and fertilisation.^{46,48,49} The formation of small fresh-brackish water basins, such as the Central Pennine Basin⁵⁰ or shallow epic seas,⁴² provided suitable environments for the survival and growth of such plants during the Carboniferous period.



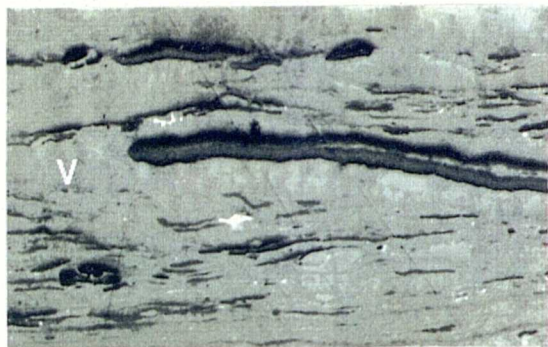
1a

50µm



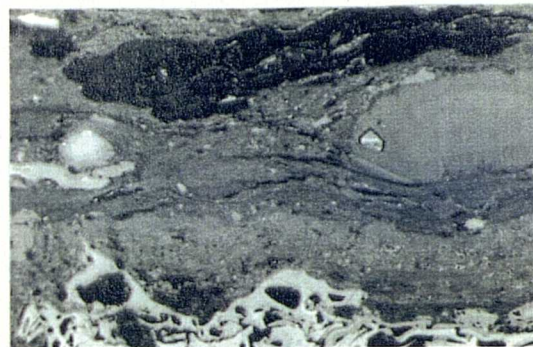
1e

50µm



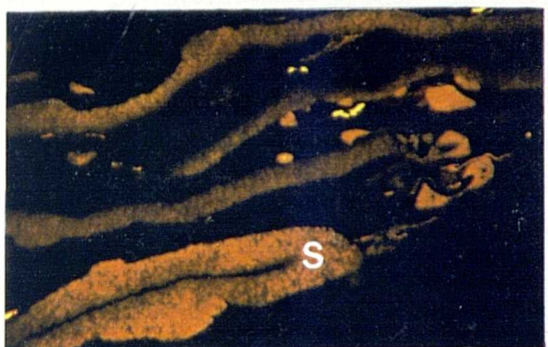
1b

50µm



1f

50µm



1c

50µm



1g

25µm



1d

50µm



1h

25µm

Plate 1 Coals of Various Geological ages

1a) Upper Devonian coal from Kazakhstania (USSR), composed predominantly of the maceral *sapromixtite* (Sp): fluorescent light. 1b) A *vitrinite* rich (V) Upper Carboniferous coal from Northumberland (UK): plane polarised light. 1c) Upper Carboniferous coal (UK) containing *sporinite* (S), fluorescent light. 1d) A Gondwanaland, Lower Permian, coal from India :plane polarised light. 1e) A Jurassic coal from Egypt (Sinai) containing much *resinite* (R), *cutinite* (C) and *vitrinite* (V): fluorescent light. 1f) Cretaceous coal from Western Canada containing macerals from the three main groups. 1g) A Tertiary coal (Miocene) from West Germany formed from reed-forest moorland showing severe decomposition. 1h) A Tertiary coal (Miocene) from Poland formed from an area dominated by the conifer *Taxodium* showing good cell structure.
(Leitz MPV3/Leica R4)

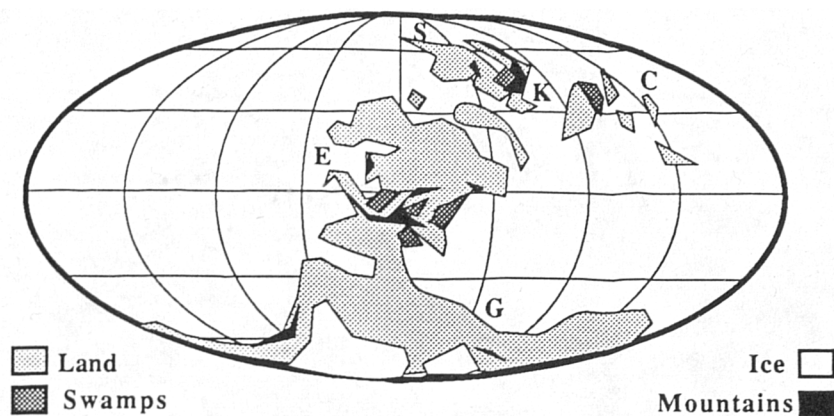


Figure 1.2 A palaeogeographical reconstruction of the Late Carboniferous.
E. Euramerica; G. Gondwanaland; K. Kazakhstan; C. China; S. Siberia.
(after Ziegler *et al*⁴³)

The morphological adaptations of the early plants are considered to have taken place from species to species, rather than a variability within species,⁴⁸ so that increased plant specialisation led to habitat specialisation, producing recognisable phytogeographic provinces.⁴⁰ Therefore, whole plant communities (i.e. *Lycopside*s, *Sigillaria*, *Sphenopsids* and *Cordiates*) perished when habitats changed at the close of the Carboniferous period. The formation of the super continent *Pangea* (Figure 1.3) was accompanied by the closure of epic seas and the melting of the southern ice-caps resulting in a rise in sea level,⁵¹ a general global warming trend,⁴⁴ the drying-out of the equatorial zones and the cessation of peat-forming conditions within the tropical-equatorial belt of *Pangea*.^{43,44}

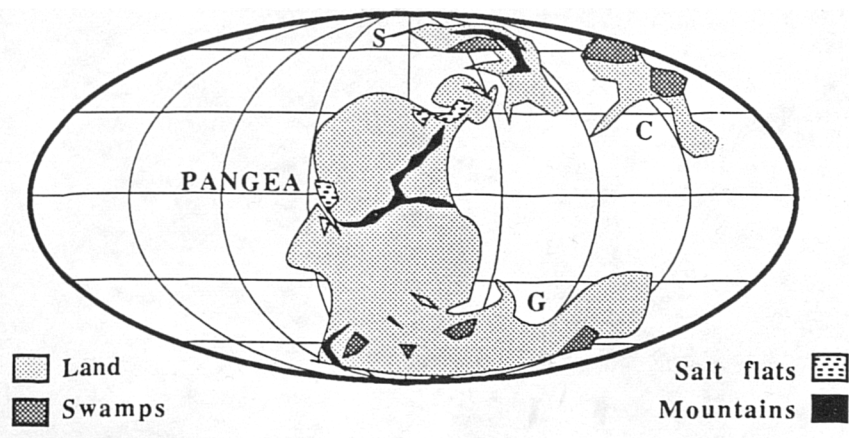


Figure 1.3 A Palaeogeographical reconstruction of the middle Permian.
S. Siberia; G. Gondwanaland; C. China. (after Dott and Batten⁴²)

However, the accumulation of thick coal deposits was not confined to the equatorial-tropical zones. Towards the end of the Carboniferous and during the following Permian period (c.a.

280-240 M.a.), peat-forming environments flourished under temperate-sub-arctic 280-240 M.a.), in the Southern continent of Gondwanaland (Figure 1.3)^{46,57} and in the sub-continents of Kazakhstania and Siberia.⁴⁰ The flora associated with those areas were very different to the predominant Pteridophyte flora of the equatorial-tropical zones of the Upper Carboniferous. Gondwanaland was dominated by the Gymnosperms, *Glossopteris* and *Gangompteris*,⁴⁶ whereas the temperate regions of Kazakhstania and Siberia were dominated by species of the Pteridospermea (i.e. *Medullosa*, *Neuropteris* and *Caulopteris*).⁴⁰ *Glossopteris* and *Medullosa* are both considered to have been arborescent because stumps of *Glossopteris*, up to 150 cm in diameter and showing pronounced regular growth rings, have been found.⁵³ Furthermore, *Glossopteris*, *Gangompteris* and *Neuropteris* are all considered to have been deciduous.⁴⁶

The peat-forming environments of Gondwanaland were in stark contrast to those that existed in the equatorial low latitude zone of the Euramerican Carboniferous peat-forming environments. The high inertinite content of Upper Carboniferous and Permian (Plate 1d) Gondwanaland coals (i.e. South Africa, Australia, India and Antarctica) has been attributed to the combined effects of weathering and ablation upon the plant debris during the peat forming stage⁵⁴ and seasonal rainfall in a cool-temperate climate.²² Support for theories regarding the seasonal nature of the Gondwanaland climate is given by the existence of rings of differential growth in *Glossopteris* stumps and the reported occurrence of frequent leaf abscission.^{33,46} There is no evidence to suggest the existence of seasonal growth within the equatorial low latitudes of Euramerica during the Carboniferous.⁴⁶

The global warming trend that began at the close of the Carboniferous period, due to the melting of polar ice and a weakening of the ITZC,⁴⁴ continued throughout the Permian and into the Mesozoic era, generating milder conditions than previously experienced.³⁵ Possibly, as a result, there was very little coal formation during the Triassic; the only known economic deposits are to be found in Vietnam³⁹ and the USSR.^{28,37} The Triassic period is regarded by Dobruskina⁵⁶ as a transitional period between the diverse flora of the Carboniferous and Permian and the more uniform flora of the middle to later Mesozoic (c.a. 190-65 M.a.). It was during this time that the decline of the Pteridophytes occurred, leaving the Gymnosperms as the dominant flora.⁴⁶

During the Jurassic period (c.a. 213 to 164 M.a.), the super continent of Pangea began to break-up^{42,57} accompanied by the opening of the North Atlantic, although, these events in themselves did not lead to sudden changes in climate. However, the absence of polar land mass and an increase in atmospheric CO₂, possibly due to volcanic activity, are regarded⁴³ as major factors responsible for the global warming trend that continued throughout the Mesozoic and into the Cretaceous period. Coal deposits formed during the Jurassic (Plate 1e) show very little maceral diversity from province to province despite their geographical spread (e.g. Australia, Walloon Coal Measures; USSR, Tuva coals; China Neimeng coals; Sinai, Maghara coal).^{26,28,57}

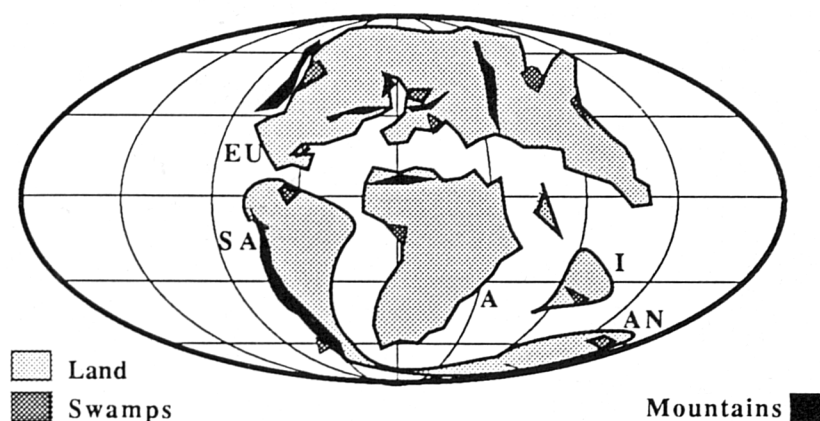


Figure 1.4 A Palaeogeographical reconstruction of the Cretaceous period.
EU. Euramerica; SA. South America; A. Africa; I. India; AN. Australia/New Zealand.
(after Dott and Batten⁴²)

The Cretaceous period (Figure 1.4) is regarded as the second great coal forming period.¹⁰ The breakup of Pangea coincident with the continued opening of the North and South Atlantic created a series of small epic seas. The global climate is estimated to have been 10° to 15° warmer than at present, with a tropical zone that extended from 30°N to 30°S palaeolatitude, generating a broad sub-tropical zone associated with low-seasonality.⁵⁵ By studying occurrences of late Mesozoic fossil wood, Creber and Chaloner⁵⁵ have indicated the existence of very high latitude forests (80°N and 70°S) associated with high rates of growth. They have further demonstrated that uniform growth, identified through the absence of growth rings, extended from c.a. 36°N through the equator to c.a. 31°S with concomitant high rates of plant productivity. The most significant development during the Cretaceous period, however, was the explosive, evolutionary development of the Angiosperms, although the Cretaceous flora is no longer considered to have been globally uniform as previously believed.^{10,32} Instead, four floral provinces are recognised.⁴⁶ Angiosperm colonisation and expansion is also considered to have been poleward, initial developments in the tropics followed by rapid migration of species towards the North and South poles. Coals formed from Cretaceous peats show great diversity in petrographic composition; from the vitrinite rich coals of Columbia, Poland and New Zealand, to coals that exhibit great petrographic diversity (i.e. Western Canada: Plate 1f).

The Cretaceous period was followed by a general global cooling trend⁴³ due to the poleward drift of Antarctica, the development of a polar ice cap and the intensification of the ITCZ.⁴³ Coals of the Tertiary are fairly diverse representing reed-forest (Plate 1g) peat forming environments³² or those areas dominated by the conifer (i.e. *Taxodium*) (Plate 1h).

1.4 The Formation of Peat

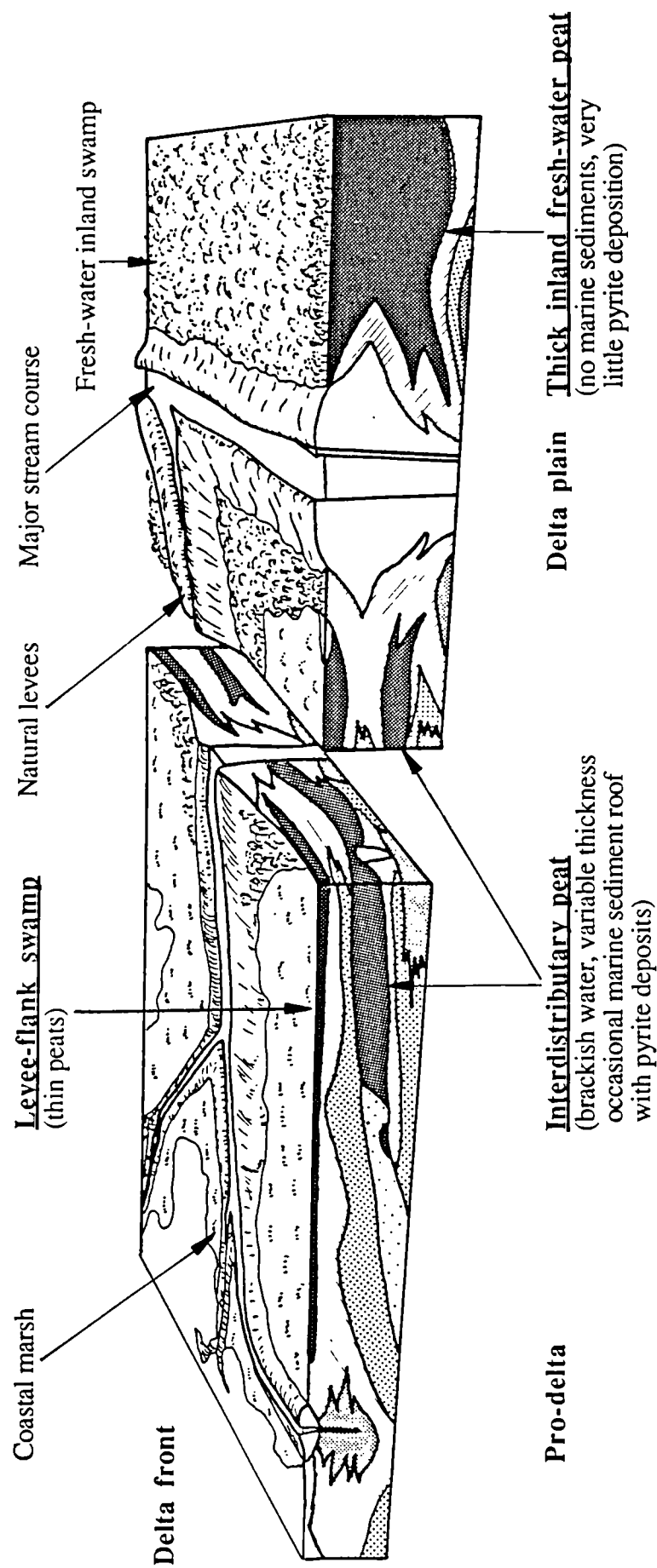
1.4.1 Peat Forming Environments

The accumulation of peat in a gently subsiding environment is considered a necessary prerequisite to the formation of coal.³² Peat represents the successful accumulation of organic detritus, formed predominantly from plant material, with minor amounts of inorganic (mineral) material.⁵⁸ Peat-forming environments, generically referred to as 'swamps',³² 'mires'⁵⁸ or 'marshes',³⁸ include all those water-logged environments (fresh to saline) that form a habitat for arborescent and/or herbaceous plant species in which there is a net accumulation of organic (plant) detritus.⁵⁸

This extremely broad definition of peat-forming environments indicates the nature of the problem: that there are, at present, a wide range of such environments, ranging from coastal to continental, from tropical to boreal and from fresh water to saline. Therefore, the suitability of modern peat-forming environments as analogues to past conditions is still keenly debated.^{32,34,38} However, the 'cyclothem' concept is no longer considered as an adequate descriptive model⁵⁹ and, currently, coal bearing sedimentary sequences are described as 'former environments of sediment accumulation' and given modern analogues, e.g. deltas.^{30,60} The delta (Figure 1.5) is a modern, generic, depositional model that is applied to both modern (i.e. Mississippi, Niger) and ancient peat-forming environments (i.e. Allegheny, Pocahontas and Cologne basin),^{32,60,61} in which coal deposits have been related to various peat forming environments within the delta (i.e. upper or lower delta plain, barrier coastal plain, interchannel peats).⁶⁰ Sediment characteristics or 'facies', the petrology of the coal and the presence of certain minerals (e.g. pyrite), are considered indicative of specific conditions within the peat-forming environment.^{29,32,50,60,61,62,63}

The application of modern tropical and sub-tropical deltaic analogues (i.e. Mississippi, Niger, Everglades) to the geological past does not meet with universal acceptance,^{23,30,64,65,66} the main objections being the extremely high inorganic content of modern deltas⁶⁶ and the occurrence of seasonal water fluctuations (e.g. Amazon, Niger) that would prevent extensive deposits of peat or promote peat oxidation.⁶⁵ Arguments against cool-temperate environments as major peat-forming (proto-coal) environments^{32,33} are also weak in the light of recent evidence.^{43,55,64,67} Furthermore, extensive work on the terrestrial ('telmatic' of Teichmüller³²) ombrogenous raised bogs within the tropical regions of Malaysia and Borneo⁶⁷ and the boreal bogs of the northern hemisphere^{64,66} invoke peat-surface 'doming' as a means of accumulating thick deposits of peat with very low inorganic content. Studies of the coal basins of South Africa^{23,24} India⁶⁸ and Australia²² have provided a better understanding of the peat forming environments that existed within Gondwanaland during the Carboniferous-Permian period. Modern deltaic analogues (i.e. Mississippi, Everglades) are not applicable to the peat-forming environments of the Permian coals of Gondwanaland which were either formed within continental fluvial or lacustrine

Figure 1.5 The Delta, a modern, generic type of peat forming environment. The figure shows the relationship between the depositional environment and peat type and thickness. Such a model is often used to describe the ancient peat forming environments of the past. (after Ferm⁶⁰)



environments ('limnic' of Teichmüller), in ice-scoured basins and lakes^{23,24,60} or continental-marginal foreland basins.⁶⁹ The high proportion of inertinite within Permian and Cretaceous coals (Plate 1d and 1f) is ascribed to the occurrence of in-situ (autochthonous) degradation and oxidation (weathering) of the peat surface^{23,54,69} rather than peat erosion and transportation (allochthonous) or forest fires.^{32,34}

1.4.2 The Influence of Temperature upon the Formation of Peat

Climate is purported to be the most important single peat-forming determinant³⁹ for the development, growth and sustainment of lush, vast, accumulations of plant material,³² although a closer examination of the facts and a comparison of the characteristics of the world's coals would appear to contradict these views. Gondwanaland coals, formed under cool-temperate conditions,^{52,54} are predominantly thicker (up to 133 m, Singrauli, India), but generally not as laterally extensive as northern hemisphere Carboniferous coals.⁶⁹ The importance attached to growth rates³² for the development of thick accumulations of peat is potentially misleading.⁶⁴ Growth rates for modern temperate-boreal bogs are much lower ($1\text{--}2\text{ kg m}^{-2}\text{ a}^{-1}$, dry) than for those in the tropics ($< 6\text{ kg m}^{-2}\text{ a}^{-1}$, dry) but comparisons of plant debris accumulation rates for temperate-boreal bogs ($< 0.5\text{ mm a}^{-1}$) compared to those within the tropics ($0.5\text{--}2.0\text{ mm a}^{-1}$) indicate that much material is lost in tropical and sub-tropical peat-forming environments.

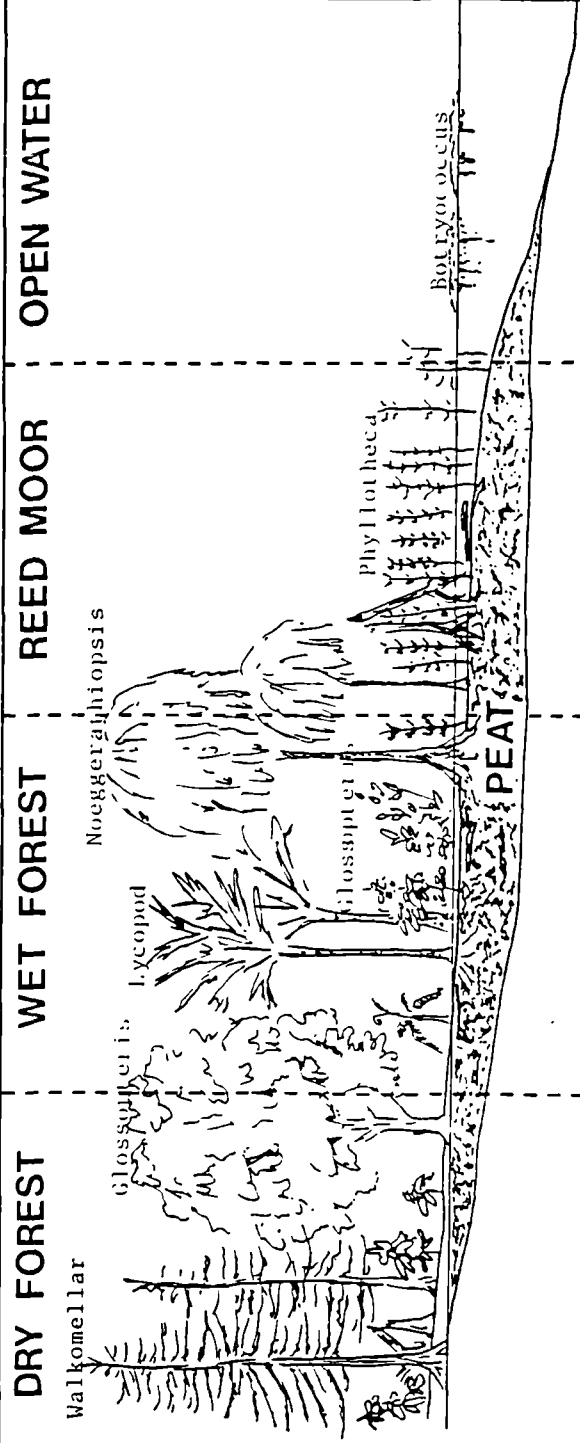
However, one aspect of climate that is vital to the development of the flora and the survival of the peat is adequate precipitation.^{32,43,44,58,67} For example, a lack of precipitation continuity, either within the catchment area on the peat-forming environment leads to water level fluctuations⁶⁵ promoting the oxidation of the exposed biomass.⁴³

1.4.3 The Hydrology of Peat-Forming Environments

The hydrological regime within the peat-forming environment has been shown to directly influence plant species success and the mode of peat preservation (Figure 1.6).^{46,71} There are two main hydrological models of peat formation, depending upon whether the peat-forming environment is predominantly rain-water fed (ombrotrophic) or ground-water fed (rheotrophic).^{32,64,67} Ombrotrophic peats, which are associated with raised or domed surfaces, are typically low in nutrients and minerals and produce low ash coals, whereas rheotrophic peats are nutrient and mineral rich and produce high ash coals.^{32,64,66} Clymo,⁶⁷ Moore⁶⁴ and Cohen *et al*⁶⁶ note that most Carboniferous, Permian, and Tertiary coals are low in ash. They therefore consider the ombrotrophic hydrological regime a more appropriate model for those peat-forming environments, a view not shared by Given.³³

Studies of miospore and megaspore successions^{71,72} in relation to paleoenvironment, palaeoflora and coal petrology recognize 'peat successions' within coal, marking the transition from 'palaeosoil' to emergent aerobic conditions through varying water-logged

Figure 1.6 A schematic cross-section of an ancient peat-forming environment relating various coal characteristics, such as type, lithotype and microlithotype to the conditions of decomposition, pH (acidity), organic activity, the type of flora and fauna and the availability of oxygen. According to the model, these are all related to extent of water cover.

	DRY FOREST	WET FOREST	REED MOOR	OPEN WATER
				
Water cover	None	Oscillating	Almost complete	Complete
Acidity	High	Medium	Low	Low
Atmospheric O ₂	Present	Partly present	Largely absent	Absent
Chemical reactions	Oxidation	Oxidation & reduction	Mainly reduction	Reduction
Organic activity	Fungi, insects & bacteria	Actinomycetes & bacteria	Anaerobic bacteria	Anaerobic bacteria
Decomposition	Rotting	Peatification	Peatification	Putrefication
Peat types	Humic	Woody & humic	Fibrous to earthy	Organic mud
Microlithotypes	Fusite to Durite	Vitrite to Trimacerite	Durite, Inertodetrite	Liptite, Trimacerite
Lithotype	Fusain & Durain	Vitrain & Clarain	Claro-durain & Durain	Cannel & Boghead coal
Coal type	SAPROPPELLIC			

(after Diessel, 1965)¹¹

stages within the peat-forming environment. In petrographic terms, this succession would be manifest as a transition from a *seat earth* through the microlithotypes *vitrinite*, through *trimacerite* and finally *durite*. The sequence could recommence by subsequent re-flooding and an influx of fresh sediment.⁷² A model such as this provides a mechanism whereby local and lateral (within seam) variations in coal type may occur, all within the same peat-forming environment (Figure 1.6). Long term variations in the hydrology of the whole peat-forming environment, such as the mid-Carboniferous eustatic event⁵¹ or alternating periods consisting of wet/dry/wet/dry conditions (i.e. late Carboniferous)^{43,44} are taken to be major factors in controlling both the colonisation ability and the survival of certain species within a given peat-forming environment.^{43,44,48}

Therefore, the hydrological regime of the peat-forming environment is a major factor that influences ultimate coal type. However, the characteristics of the peat-forming environment are also a response to the topography of the area, geographical location, climate (global and regional), the rainfall catchment area, the nature of the sediment (mineralogy, particle size), and the rate of subsidence, all of which ultimately influence the coal type either by controlling local variations in vegetation type or the conditions of preservation and decomposition.

1.5 The Formation of Coal

1.5.1 Precursor Material

The major assumption by those using modern analogues, such as deltas, for those processes considered responsible for the transformation of plant debris into peat, is that the biochemical processes that exist now were also in existence in the geological past and were responsible for the peatification of pteridophyte and gymnosperm plant debris. Research by those investigating the formation of specific coal maceral precursors⁷³ in modern peat-forming environments lead us to think that this is the case. The implicit assumption is that the basic plant polymers and molecules that constitute particular plant organs such as tannins, lignins, carbohydrates, glycosides, alkaloids, fats, waxes, and resins⁷⁴ (Figure 1.7), have remained basically unchanged throughout time, whereas, the spatial and temporal abundance of those plant polymers and substances, as peat-forming precursors, have varied as a function of plant type and peat-forming environment.

The chemical composition of certain macerals (e.g. resinite) is amenable to direct analysis and can be linked to specific chemical constituents (e.g. resin acids). In contrast, the link between vitrinite and specific plant polymers is not so clear cut although lignin represents the major single constituent in (modern) vascular plants,⁷⁵ usually accounting for 25 wt% of woody tissue.⁷⁶ The theory that lignin-derivatives represent the major

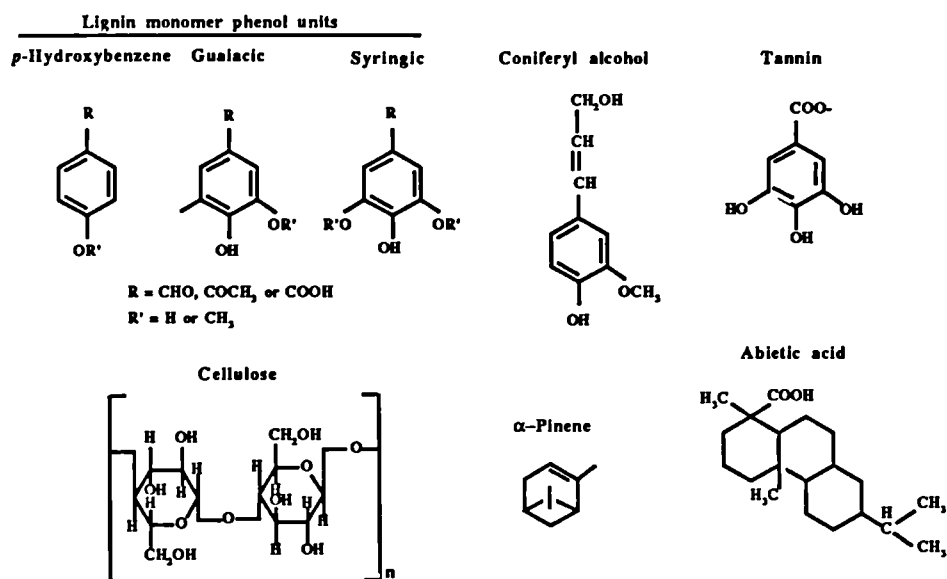


Figure 1.7 Examples of maceral precursor and maceral chemical constituents.

progenitors of humic coals, dates from the early work of Fischer and Schrader.⁷⁷ Lignins are considered to be polymers of phenyl-propyl compounds (Figure 1.7) such as coniferyl alcohol,^{75,78,79} although Hatcher goes further by defining lignin as a macromolecular biopolymer that is composed of cross-linked monomeric phenyl-propane units.⁷⁶ Recent studies using alkaline degradation techniques,⁷⁵ oxidative degradation,⁷⁹ infra-red analysis⁷⁴ and nuclear magnetic resonance (NMR) experiments⁷⁶ have not only confirmed the existence of lignin monomers, but have also demonstrated that lignin-like structural units exist in peats⁷⁴ and may survive un-altered in low rank coals.^{75,76}

It is reasonably well established that the composition of lignin varies with plant species.^{36,76,79,80} Using NMR spectroscopic techniques on natural lignins from degraded gymnosperm (Douglas fir) and angiosperm (Oak) woods, Hatcher⁷⁶ confirmed that hard wood lignins contain mostly syringyl phenyl-propane units whereas soft-woods contain *p*-hydroxyphenyl and guaiacyl phenyl-propane units. Similarly, Hurst and Burgess⁷⁹ report that the lignins from woody-dicotyledons (broad-leaf angiosperms) differ from those of the monocotyledons (narrow-leaf angiosperms, i.e. sedges). Indicating therefore, that the type and range of plant debris surviving peatification not only influences the range of biopolymers within peat, but will also depend upon the prevalent species of vascular plant within a given peat-forming environment from which the debris originated.

The process of peat-formation, which is the first stage in the transformation of organic detritus into coal, is largely due to microbial and chemical processes³³ and is, therefore, distinct from subsequent 'geochemical' processes that operate during 'coalification'.^{3,32,76} It is consequently convenient and customary to treat peatification as a separate process.

1.5.2 Peatification

Peatification begins with the accumulation of plant debris on the peat surface.^{32,33} The extensive alteration and degradation of plant debris³³ by bacteria, fungi, actinomyces and enzymes^{32,77,67} occur within the upper layers of the peat, although both the abundance and the population of micro-organisms show a regular variation with depth (Table 1.2).^{32,77,67}

TABLE 1.2 Abundance of micro-organisms in the surface layers of blanket peat in the Moor House National Nature Reserve (54° 65'N, 2° 45'W).

Depth (cm)	Zone	Fungi : stained Mycelium (m g ⁻¹)	Bacteria (10 ⁵ g ⁻¹ range)	
			Aerobic	Anaerobic
0-5	Litter	2450	9-260	9-250
5-12	Dark brown	1030	6-150	32-200
12-20	Green brown	750	11-76	16-500
20-32	Red brown	200	0.7-42	28-260

(from Clymo⁶⁷)

The availability of oxygen ('redox potential' of Teichmüller³²) is the determining factor governing the depth related distribution of micro-organisms.⁵⁸ This concept was the basis of a decomposition scheme devised by White⁸¹ (Figure 1.8) to explain the survival of some plant/lipid material during peatification. Where the consumption of oxygen is greater than that supplied by percolating ground water, anoxic or anaerobic conditions prevail.^{32,33,67} According to the model, a lower proportion of plant/lipid material will survive in an aerobic environment than an anaerobic one. Therefore, the input of plant or lipid material to successive peat and coal forming stages also reflects their mode of preservation.

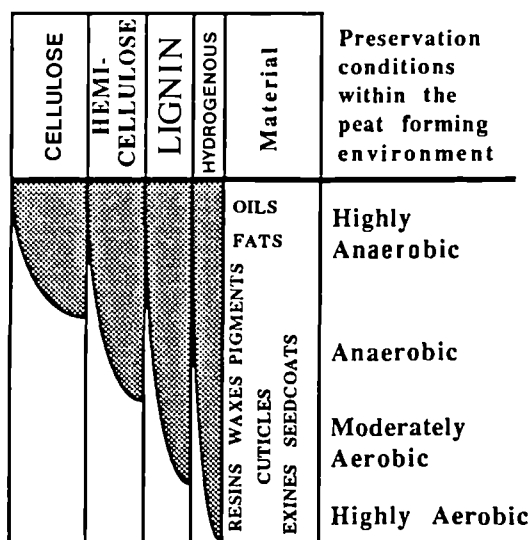


Figure 1.8 The decay of plant and lipid material due to the availability of oxygen, the shaded area indicates the relative proportion of each constituent. (after White⁸¹)

The diffusion of oxygen through stagnant water is 10⁻⁴ that of air⁶⁷ so that the transition

from aerobic to anaerobic conditions depends upon the presence or absence of percolating oxygenated water and the addition of fresh plant debris.^{32,58} Teichmüller³² considers this transition to occur approximately 0.5 m below the peat surface. Although factors such as the hydrological regime of the peat (salinity, water depth, flow rate and nutrient supply), the rate of plant debris accumulation, the nature of plant debris, pH of the peat and temperature are all important determinants that govern the transition.^{32,33,58,67,78} Flowing water through the peat-forming environment supplies dissolved oxygen, with the result that the decomposition of plant debris by aerobic microbes is the highest under such relatively oxygen rich conditions.^{3,32}

The scheme outlined by White⁸¹ is augmented by recent work conducted by Clymo⁸² who demonstrated that the loss of plant material within the upper aerobic zone of the peat ('acrotelm') from the process of peatification, is greatest when waterlogging is intermittent. Such a high loss is considered by Teichmüller³² to be due to physical disintegration (abiotic oxidation) or, in the presence of fungi, due to mouldering (fungal hydrolysis). White-rot attack⁸⁰ on the lignin molecule involves little depolymerisation with the formation of oxygen-bearing functional groups (i.e. carbonyl and carboxylic acids), the products of this process being ultimately incorporated into a coal as oxidised/partially oxidised material.^{61,70}

In peats, where the supply of oxygen is restricted, the plant polymers are transformed by highly selective and specific micro-organisms^{33,74} into humic substances, or 'geopolymers'.³² Bacteria preferentially attack the carbohydrate and proteinaceous portion of the plant material followed by more complex plant polymers, such as cellulose and lastly lignin.⁸⁰ However, the concept that lignin undergoes little or no change during peatification³² is not readily supported by present work.

Given³³ discusses several studies that indicate that certain parts (aqueous-dioxan soluble) of lignin undergo degradation, depolymerisation and re-condensation to generate molecules with higher molecular weight than are present in unaltered lignin. Furthermore, the degree of lignin alteration is also dependent upon the size of the woody precursor material; fine grained material being more prone to peripheral alteration and loss of polysaccharides than coarse material.³³ Furthermore, not all cellulose is destroyed during peatification^{33,74} as was previously thought^{3,32} which has also been recently shown to be a principle source of molecular oxygen in brown coals.⁷⁴

Peats also contain a variety of substances of low to moderate molecular weight inherited from the parent plants that do not undergo molecular transformation due to microbial processes.^{33,78} Tannins, for example, combine with proteins, condense and polymerise to form phlobaphenes which occasionally occur as cell in-fillings in brown coal.³³

1.5.3 Gelification

Little is known about the actual process of gelification.³³ However, the term refers to a series of processes that cause swelling, the degradation and the infilling of cell lumina and usually the destruction of recognisable plant cellular structure. Teichmüller³² considers this process to proceed via an 'in-situ' peptidization of the humic matter followed by a process of 'desiccation' that forms a 'gel'. More recently, the process of gelification has been related to the activity of micro-organisms⁸³ in which the principle changes observed were the loss of recognisable ligno-cellulose derived structures and the formation of a more random geopolymer, containing a higher proportion of aromatic carbon and less methoxyl substituents.^{85,86} Therefore, the presence of recognisable plant structure within the Huminite macerals of brown coal and the vitrinite macerals of sub-bituminous coals is due to the presence of polymers and molecular constituents that exhibit the cross-linked characteristics of lignin and cellulose, 'gelification' being a chemical homogenisation process.^{33,86}

1.6 Coalification

1.6.1 Time, Temperature and Pressure

Coalification represents the natural chemical and physical alteration of coal; firstly, by biochemical processes (Section 1.5.2) and subsequently by increases in temperature, pressure and time upon burial by sediments in a subsiding basin.^{32,87-89} It is a contemporary coal science axiom that a genetic relationship exists between peat-lignite-subbituminous-bituminous and anthracite coals. The relative position of a coal within the coalification series, based upon its chemical and physical properties, denotes the *rank* of a coal.^{3,32,36,87,88}

The relationship between burial depth and coal rank was first enunciated by Hilt in 1873 in which he noted that 'in a given shaft or a given borehole, the volatile matter decreases with increasing depth', (Hilt's law).³⁶ Subsequent efforts to determine the relationship and causality between burial depth and coal rank focused upon three factors: *time*, *static pressure* and *temperature*.⁸⁷

Early theories considered that coalification required very high temperatures in recognition that chemical reaction rates are sensitive to temperature changes.^{88,90} However, the artificial, laboratory based, coalification experiments by Bergius⁹¹ and later Briggs⁹² demonstrated that temperature alone was insufficient to generate coals of high rank. Static pressure was therefore considered⁹³ as a necessary prerequisite for coalification to proceed beyond the rank of lignite. The promotion of static pressure, as an agent during coalification, sought to reconcile the depth/rank relationship implicit in Hilt's law. However, static pressure was subsequently shown to retard chemical coalification⁹⁴⁻⁹⁶ and was

therefore discounted as a factor involved in coalification.³² It was not until the 1950's that the proposal by Bergius,⁹¹ in which he suggested that there was an exponential relationship between time and temperature, was serious consideration given by other workers to the relationship between the geothermal gradient and burial depth. An average geothermal gradient of 3°C/100 m, generating temperatures approximately 60° to 80°C at moderate depths, is considered sufficient for coalification to take place.^{32,96,97} The rank of the coal, therefore, is considered to be a function of the depth of burial related to specific minimum temperatures and the duration of burial. Such a relationship formed the basis of Karweil's⁹⁷ classic nomograph (Figure 1.9) in which it was theoretically possible to predict coal rank given the geothermal gradient and the burial history of a coal. Although, it was later acknowledged that such a model was too simplistic since the relative importance of time and

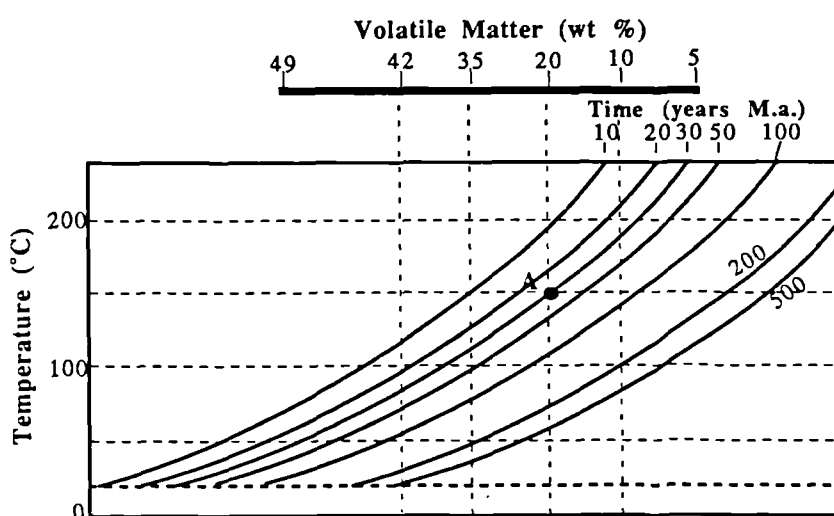


Figure 1.9 Karweil's nomograph relating coal rank (determined by volatile matter) to the length of time spent at a certain palaeotemperature. (after Karweil⁹⁷)
The x co-ordinate of any point along any time line represents the rank of a coal seam whose maximum palaeotemperature is given by the y co-ordinate of the same point. For example, at point 'A' a hypothetical coal has spent 30 million years at 150°C and consequently contains 20 wt% volatile matter corresponding to a rank of medium volatile bituminous.

temperature during coalification change as the temperature rises³² or the burial history of the coal changes.^{33,98} That minimum geotemperatures are necessary for coalification to proceed is demonstrated by the existence of the Moscow basin Carboniferous brown coals; coals that have never attained a rank higher than that of lignite despite their age (c.a. 330 Ma), due to their shallow depth of burial and low geotemperature (<50°C).³⁶

Overburden pressure, resulting from the burial of successive younger sediments on top of the coal, has an important influence upon certain physical properties of coals such as the pore volume and moisture content of low rank coals.^{32,36} Furthermore, the optical anisotropy of vitrinite would appear to be strongly influenced by overburden pressure through the orientation of the aromatic lamellae during coalification.^{32,62}

1.6.2 Factors Responsible for Variations in Coalification

The coal rank/depth of burial relationship discussed in Section 1.5.1 is not straightforward. The depth of burial and the temperature of a coal during coalification is far from constant,^{32,33,99} as is implied in Karweil's⁹⁷ nomogram (Figure 1.9). Coalification is not an isothermal process; the temperature and burial histories of coals A and B in Figure 1.20, for example, represent a complex situation. The highest temperatures (Figure 1.20) were attained for a short initial period of time following rapid burial, subsequent uplift exposed the coals to different, lower, geotemperatures with the result that coals A and B are of a different rank despite having been deposited in the same basin during the same coal-forming period (carboniferous).³³

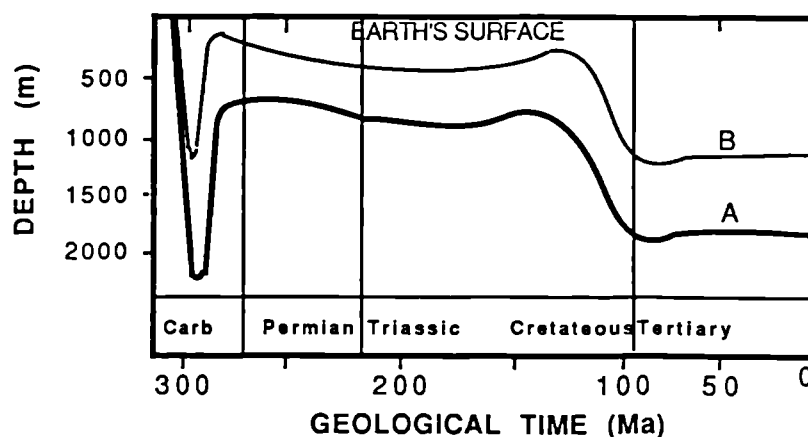


Figure 1.20 A time temperature history of two Carboniferous coal seams in the Ruhr, Germany, that are presently at two different stages of coalification due to relative differences in burial depth over time. (after Radke *et al.*, cited in Given³³)

Therefore, any theoretical coalification model must account for such non-isothermal conditions throughout the tectonic history of the coal.⁹⁹ Furthermore, coalification models are, at present, unable to determine whether equilibrium between temperature and the reacting organic matter was or has been attained.^{32,100} The suggestion that a 'hysteresis effect' exists with respect to changes in vitrinite reflectance during periods of rapid burial (160 m Ma^{-1}) was the result of studies that compared vitrinite reflectance values against mineral transformations.¹⁰¹ Although geothermal gradients can vary both in space and time, the concept that the average geothermal gradient was higher in the past than at present does not enjoy universal support.¹⁰² Local variations in geothermal gradient are more usually attributable to any one, or combinations of the following factors: differences in sediment conductivity,¹⁰³ hydrodynamic regimes,¹⁰⁴ crustal thinning,¹⁰⁵ local and regional igneous activity^{106,107} and radiogenic heat productivity.¹⁰⁸

1.6.3 The Chemical and Physical Response to Coalification

Changes in chemical and physical properties occur within coal during coalification. Among the physical changes that occur are the reduction in bed moisture content, a concomitant

decrease (increase in anthracites) in the porosity, changes in surface area and a non-linear increase in the refractive and absorptive indices.^{3,32,33,36} The chemical changes that occur are essentially those that involve condensation, polymerisation³⁶ or depolymerisation,^{38,109} aromatisation reactions and the loss of functional groups, the overall result being a gradual non-linear enrichment in carbon with increasing rank.^{32,36,38}

The aromaticity of coal increases with rank, as determined by X-ray diffraction,¹¹⁰ nuclear magnetic resonance spectroscopy (NMR),¹¹¹ and chemical degradation studies.³⁶ The increase in aromaticity has been shown to correspond to a near linear decrease of CH- and CH₂ carbons and the loss of CH₃- groups in the aliphatic region of NMR spectra, accompanied by an increase in the proportion of aromatic carbon. Changes in elemental carbon, hydrogen, oxygen and nitrogen, when plotted as atomic ratios (H/C, O/C) on a van Krevelen type diagram,³⁶ indicate that the initial changes that occur during the transformation from lignite to bituminous coal are due to the predominant loss of oxygen relative to carbon followed by the rapid loss of hydrogen and enrichment of carbon at higher levels of coalification. The identification of functional groups and studies of the carbon skeleton,³⁶ especially by infra-red spectroscopy¹¹² suggest that aromatic centers are generally linked by hydroaromatic and methylene bridges and fringed with methyl, hydroxyl, carboxyl, carbonyl, amino and other functional groups. The non-aromatic fraction of the coal structure is progressively eliminated during progressive coalification,^{32,36} resulting in the loss of oxygen-bearing functional groups with increasing rank (Figure 1.21) which, in conjunction with the loss of physi- and chemi-sorbed water, account for the progressive loss of elemental oxygen and moisture content.

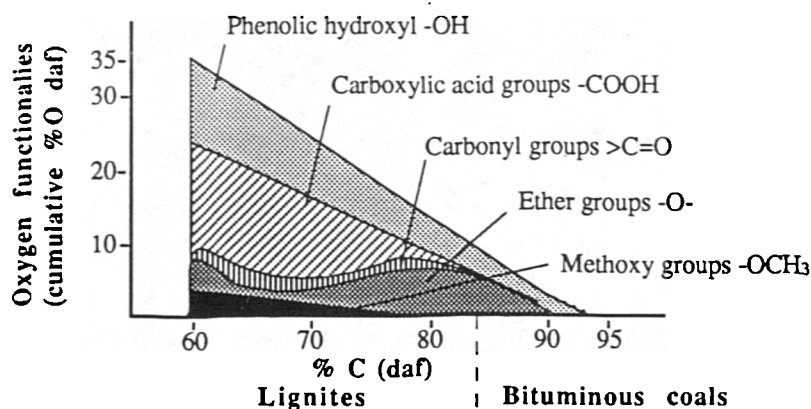


Figure 1.21 Mean content of different oxygen functionalities in coal. (after Wittehurst *et al*)¹¹³

Bulk properties such as moisture and volatile matter do not exhibit linear changes throughout the coalification series. Such properties either pass through a minima or maxima, or undergo sudden shifts or 'coalification jumps',³² during the course of coalification. Such trends have been attributed, in general, to the initial loss of bed moisture and the loss of oxygen-bearing functional groups throughout the lower rank stages, followed by the generation of aliphatic and hydro-aromatic material through the high volatile and medium

volatile bituminous rank stages accompanied by aromatic ring condensation, increasing molecular order and carbon enrichment.^{32,36,76}

1.7 The Petrographic Composition of Coal

1.7.1 The Lithotypes

The majority of humic bituminous coals have a banded appearance in a hand-specimen, due to the irregular alternation of lustrous layers that appear either glassy, silky, dull or fibrous.^{3,11,61,114} The banded variety of humic bituminous coals are derived predominantly from the organic detritus of vascular plants (Section 1.5), whereas non-banded coals of similar rank are often cannel or boghead coals and are considered sapropelic in type.^{35,115} The bands in humic coals represent different lithotypes which according to Stopes^{116,117} are recognisable as four distinct components in a hand specimen, the names of which all terminate in the suffix *-ain*:

- i. vitrain (lat. *vitrum*, glass) brilliant to vitreous lustre, conchoidal fracture
- ii. clarain (lat. *clarus*, bright) pearly to sub-vitreous lustre, striated
- iii. durain (lat. *durus*, hard) dull to greasy lustre, granular fracture
- iv. fusain (lat. *fusus*, a spindle) silky lustre, fibrous, friable^{61,114}

However, not all humic coals are banded.^{4,31,35,61,115} Such coals are either high rank coals (i.e. anthracite) where the banding becomes indistinct due to coalification,¹¹⁵ or low rank coals (lignite, sub-bituminous) where the absence of banding has been ascribed to conditions of preservation during deposition or peatification and the precursor material.^{3,32,78} Jacob¹¹⁸ considers the Eocene brown coals, which were deposited under a tropical climate, to be more strongly decomposed than the younger Miocene coals of the lower Rhine, which were deposited under sub-tropical conditions. Teichmüller,^{32,119} discussing the Miocene brown coals, notes that coals formed from lignin-poor reed-like vegetation are heavily decomposed, whereas those coals formed from forest vegetation (i.e. *Taxodium*) show good cell preservation (Plate 1h).

1.7.2 The Macerals

Even those coals exhibiting poor banding are composed of microscopically distinct entities termed macerals (lat. *macerare*, to soften, dissolve) which were considered by Stopes as analogous to rock minerals.¹¹⁷ A micropetrological serial terminology was devised¹¹⁷ that later became known as the Stopes-Heerling System¹¹⁴ in which each maceral was rendered distinct from the lithotype terminology by the incorporation of the suffix *-inite*. There are three maceral groups: *vitritinite*, *inertinite* and *liptinite*^{‡2} (Table 1.3).^{36,114,116,120}

^{‡2} Liptinite is the preferred term in place of Exinite. The term Exinite has generic connotations, associated with outer cell-wall material (exines), even though some macerals within this group (i.e. resinite, bituminite) are derived from fats, essential oils, resins and animal excretions.

TABLE 1.3 Maceral Terminology and Maceral Origins (Based Upon the I.C.C.P. and the Stopes-Heerlen System)

maceral group	maceral	origin
vitritine	telinite (lat. <i>tela</i> , tissue)	humified plant remains typically derived from woody, leaf or root tissue with well to poorly preserved cell structures
	vitrodetrinite	humified attrital or less commonly detrital plant tissue with particles typically being cell fragments
	collinite (grk. <i>kolla</i> , glue)	humified material showing no trace of cellular structure, probably colloidal in origin
liptinite (exinite)	sporinite	outer casing of spores and pollens
	cutinite	outer waxy coating from leaves, roots and some related tissues
	resinite	resin filling in cells and ducts in wood; resinous exudations from damaged wood
	fluorinite	essential oils in part; some fluorinite may be produced during physico-chemical coalification and represent non-migrated petroleum
	suberinite	cork cell and related tissues
	bituminite	uncertain but probable algal origin
	alginite	tests of some groups of green algae; material referred to alginite shows moderate to strong fluorescence
	exsudatinitite	veins of bitumen-related material expelled from organic matter during coalification
inertinitite	fusinite	fusinite originates from wood and leaf tissue oxidation
	semifusinite	wood or leaf tissue weakly altered by mouldering or by biochemical alteration
	inertodetrinitite	similar to fusinite or semifusinite but occurring as small fragments
	macrinitite	humic tissue probably first gelified and then oxidized by processes similar to those producing semifusinite
	sclerotinitite	moderately reflecting tissue of fungal origin - largely restricted to Tertiary coals
	micrinitite	largely of secondary origin formed by disproportionation of lipid or lipid-like compounds

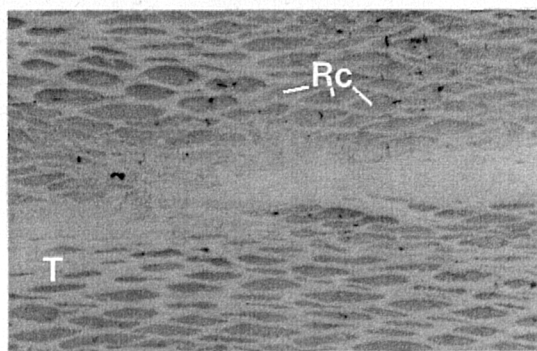
(adapted from Murchinson *et al* ⁸⁹)

The petrological distinction of macerals are based upon botanical affinities, morphological properties (shape and colour: Plate 2) and inferred mode of preservation.^{114,115,116}

1.7.2.1 The Vitrinites

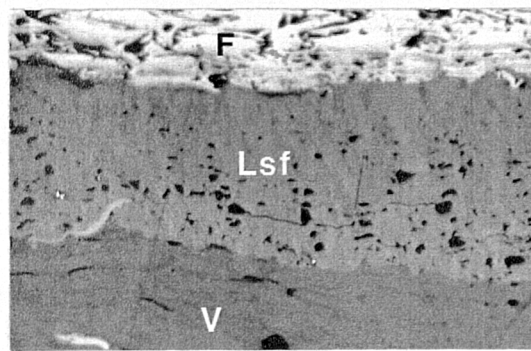
Vitrinite is the preponderant maceral in humic bituminous coals formed during the Carboniferous, Jurassic and Cretaceous periods, usually appearing medium grey in reflected light, in contrast to the darker liptinites and pale-grey to white inertinites.^{61,116}

Vitrinite macerals (Plate 2) are formed predominantly from the preservation or gelification of the secondary xylem or cortical tissue (woody cell-wall material) of stems, roots, branches and leaf mesophyll.^{11,33,61,114,115} The degree of botanical preservation is the main criteria for maceral differentiation. Those vitrinites that contain a distinct cellular structure (Plate 2a) are termed *telinites* (lat. *tela*, tissue),¹¹⁵ although this term is most usually reserved for the cell wall material only,^{61,114,115} whereas those vitrinites that contain no visible structure (Plate 2b & 2c) are called *collinites* (grk. *kola*, glue).¹¹⁴ Collinite is the structureless vitrinite that usually occupies former cell cavities and is thought to have formed from



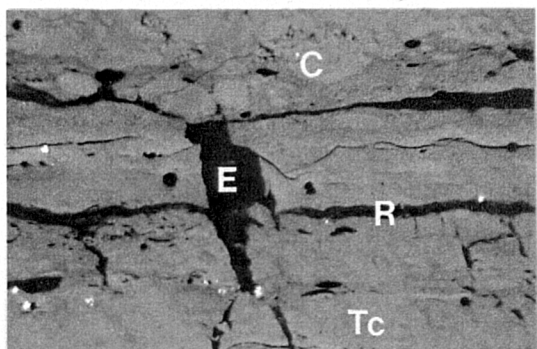
2a

50µm



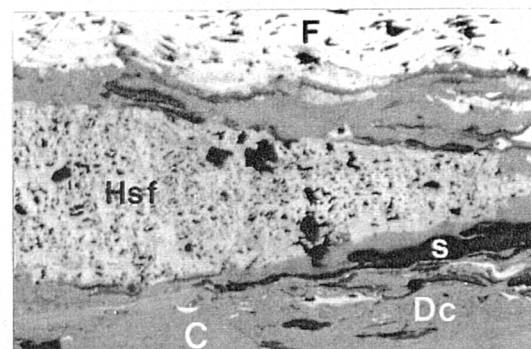
2e

50µm



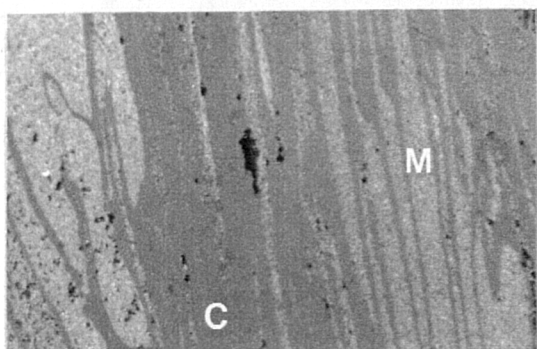
2b

50µm



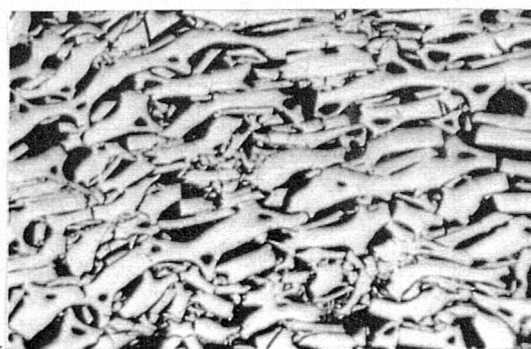
2f

50µm



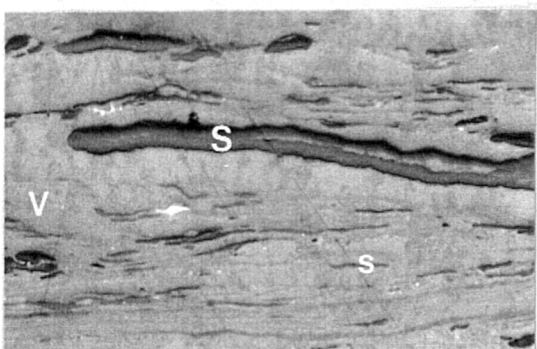
2c

50µm



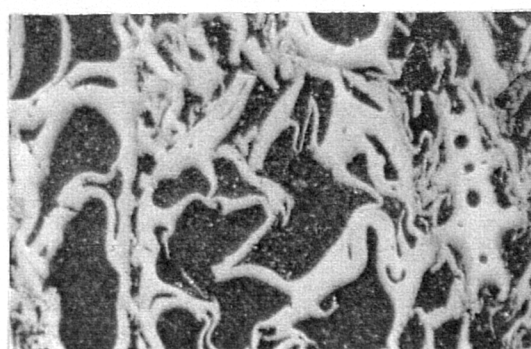
2g

50µm



2d

50µm



2h

25µm

Plate 2 The Macerals of Sub-Bituminous and Bituminous Coals

2a, Vitrinite showing Telinite (T), Resocollinite (Rc). 2b, Vitrinite and Resinite showing Telocollinite (Tc), Collinite (C), Resinite (R) and Exsudatinite (E). 2c, Collinite (C) and Micrinite (M). 2d, Sporinite with abundant Microspore and Megaspores within a vitrinite groundmass (V). 2e, Vitrinite (V), Low semi-fusinite (Lsf) and Fusinite (F). 2f, Desmocollinite (Dc), Collinite (C), Sporinite (S), High semi-fusinite (Hsf), Fusinite (F). 2g, Fusinite, showing typical 'bogen structure'. 2h, Fusinite showing preserved cell structure in-filled with clay (Leitz MPV3/Leica R4)



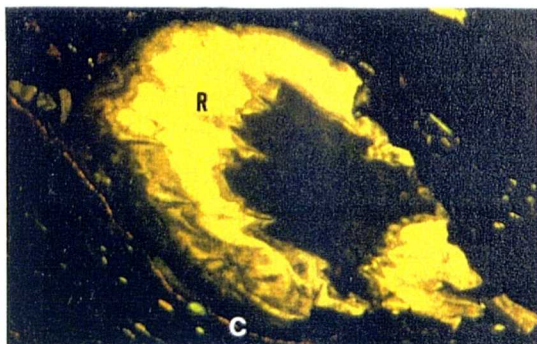
3a

50μm



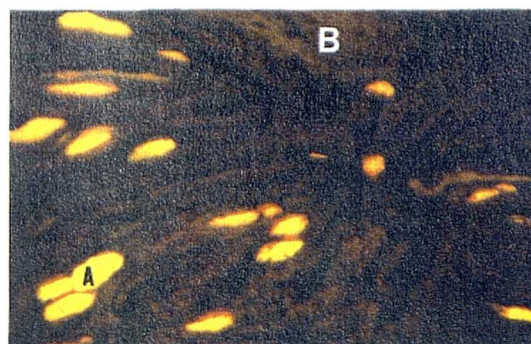
3e

50μm



3b

50μm



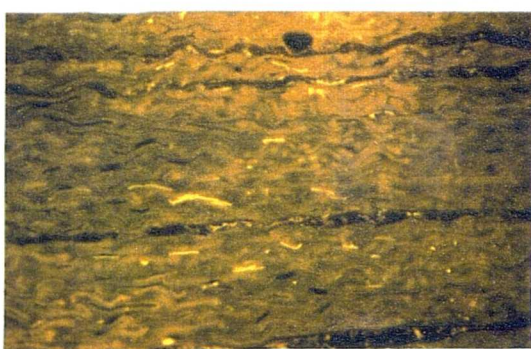
3f

50μm



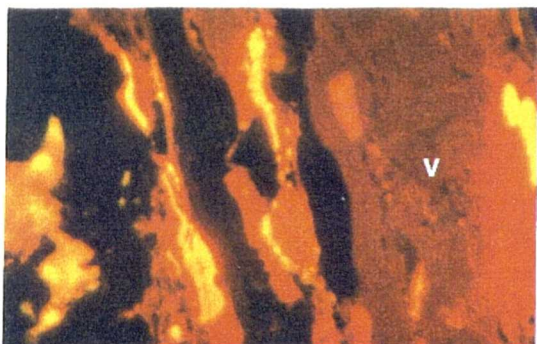
3c

50μm



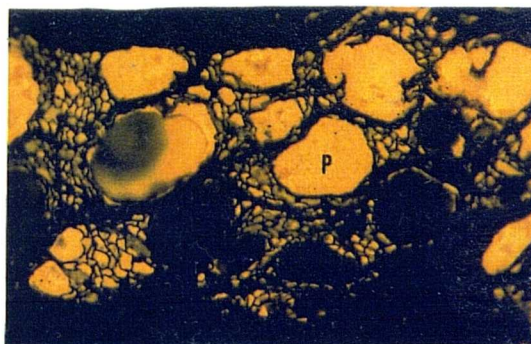
3g

50μm



3d

10μm



3h

50μm

Plate 3 Fluorescing Macerals of Sapropelic and Humic Coals

3a, Humic bituminous coal with Cutinite (C) and Resinite (R). 3b, Humic bituminous coal with Cutinite (C) and Resinite (R). 3c, Humic bituminous coal containing abundant Sporinite (S). 3d, Humic bituminous coal showing fluorescing Vitritine (V), Sporinite (S) and non-fluorescing Inertinite (I). 3e, Sapropelic algal canal containing Alginite (A) and Sporinite (S). 3f, Sapropelic 'Bog-head' coal containing Alginite (A) and Bituminite (B). 3g, A Sapropelic algal coal. 3h, Humic brown coal, a rootlet cross-section containing Phlobaphinite (P)

(Leitz MPV3/Leica R4)

humic-gels¹¹⁵ (Section 1.4.3). Vitrinites showing a telenitic structure with collinite occupying the former cell-cavities are referred to as *telocollinite*,^{114,115} (Plate 2b). In such instances, the telenite usually has a slightly higher reflectance than collinite.^{87,89} The vitrinite 'groundmass' in clarites or trimacerites is referred to as *desmocollinite* (Plate 2f), which is thought to have formed from dessicated humic-gels.¹¹⁵ A recent addition to the vitrinite group of macerals is *pseudovitrinite*¹²¹ which was first recognised as a material possessing poor fusibility properties during coking.^{61,121} Pseudovitrinite is structureless, often has serrated edges, a slightly higher reflectance than collinite⁶¹ and a lower fluorescence intensity (I_{650}) than collinite or telinite. Pseudovitrinite would appear to be more common in North American Carboniferous coals than those of Europe. The reflectance of the vitrinite macerals varies within a given low-rank coal, although such differences diminish with increasing rank.⁸⁹ Of the more common vitrinite macerals or sub-macerals, desmocollinite exhibits the lowest reflectance whereas telinite exhibits the highest.^{89,114,115,122}

1.7.2.2 The Lipinites

Liptinite,¹²⁰ also known as exinite,¹¹⁵ includes the macerals *sporinite*, *resinite*, *cutinite*, *alginite*, *suberinite*, *liptodetrinite*^{114,115} and, more recently, *fluorinite*, *bituminite* and *exudatinite*.^{122,123} The previous criterion for inclusion within the exinite group was botanical affinity, in that all exinite macerals were the 'exines' (plant organ coatings) of vascular plants.¹¹⁷ However, the inclusion of non-exines, such as resinite, alginite etc. renders that criterion invalid. Typically, lipinite macerals are associated with an auto-fluorescent property, a lower reflectance, a high hydrogen content and a higher proportion of volatile matter than the vitrinites.¹¹⁴ With increasing coal rank (up to medium volatile bituminous), the optical and chemical properties of the liptinites change rapidly. Above that rank, liptinites are optically indistinct from the vitrinite groundmass.⁸⁹ *Sporinite* (Plates 2d & 3c) is the term given to the remains of spore and pollen exines¹¹⁴ and are ubiquitous in Carboniferous coals.¹¹ *Cutinite* (Plates 3a & 3b) represents the outer cuticular material of epidermal tissues, such as leaves, stems and needles.^{4,11,114} Cutinite is easily recognised under the microscope by its long filamentous, saw-tooth appearance.¹¹⁵ *Suberinite*, with its distinctive cellular structure, is chemically related to sporinite and cutinite, which represents fragments of the outermost, secondary, corky tissue (periderm) produced by gymnosperms or angiosperms^{46,61} and is only recognised in Tertiary or Mesozoic coals.^{4,61} *Resinite* (Plates 2b, 3a & 3b) represents the solidified remains of tree-resins, waxes, balsam, copals, latex and essential oils.^{114,115,124} Resinite can appear as either cell in-fillings or as discrete spherical, oval or rod-like shaped bodies.¹¹⁵ *Alginite* (Plate 3) occurs only in *sapropelic* coals which consist predominantly of the hydrogen rich macerals sporinite and alginite, and clay, suggesting a lacustrine depositional environment.^{11,78} *Liptodetrinite* is the collective term for detrital forms of liptinite which cannot be differentiated on the basis of morphology because of their fragmentary nature and particle size.^{114,115} *Fluorinite*, *bituminite* (Plate 3f) and *exudatinite* (Plate 2b) are liptinites that are

not directly linked to any one single precursor material like cutinite. Fluorinite and bituminite are thought to be derived from the decomposition products of algae, bacterial lipids, animal secretions and plant lipids.^{122,123} Exudatinite is a secondary maceral formed from the 'mobilisation' of resinous or lipid material during coalification and often occurs as cell-cavity in-fillings or in micro-fissures.¹²²

1.7.2.3 The Inertinites

The term *inert-inite* was chosen to describe the infusible nature of certain highly reflecting macerals during carbonisation,¹¹⁵ thereby grouping the macerals *fusinite*, *semi-fusinite*, *micrinite*, *sclerotinite*, *macrinite* and *inertodetrinite* on the dual basis of technological property and morphology.^{4,61} All inertinite macerals have a higher reflectance than the vitrinites, although the differences diminish with increasing rank and all inertinites have a higher carbon and oxygen content than both vitrinite and liptinite.^{36,61,114,115} *Fusinite*¹¹⁷ is often associated with a well preserved cell-structure (Plate 2e - 2h),¹¹⁴ although this is no longer considered diagnostic.⁴ Often the cell structure is crushed generating a 'bogen structure' (Plate 2g),¹¹⁵ or the cell cavities may be in-filled, for example with clay (Plate 2h) or resinite. *Fusinite* has the highest reflectance of all macerals,^{61,87} which is considered to be related to its origin.⁶ Some regard *fusinite* to be the result of ancient forest fires,^{4,34,115} whereas others consider an origin that involves a process of aerobic oxidation during peatification more plausible.^{3,11,68,72} *Semi-fusinite* (Plate 2e & 2f) has a range of reflectance between that of vitrinite and *fusinite*, often showing a well preserved cell-structure;¹¹⁴ although this too is no longer considered diagnostic.⁶¹ *Macrinite* has a high reflectance and a massive, solid, homogeneous appearance.¹¹⁴ This maceral is thought to have been produced by the oxidation of humic-gels.⁶¹ *Micrinite* (Plate 2c) is another highly reflecting inertinite maceral, characterised by its small size (<c.a. 5µm) and high reflectance.¹¹⁵ *Sclerotinite* is considered to represent the highly reflecting coalified remains of fungal spores, sclerotia, hyphae and pterenchyme. It is also a common component of Tertiary coals^{61,114,115} and has often been mis-identified in Carboniferous coals.^{54,70} *Inertodetrinite* is composed of the fragmentary particles (<30µm) of the above inertinite macerals and can therefore be of variable origin.¹¹⁵

1.7.3 The Macerals: Physical and Chemical Characteristics

Using suitable separation techniques, it is possible to analyse the chemical and physical properties of the macerals; demonstrating that those micropetrologically distinct entities described above possess many distinct physical and chemical characteristics, such as refractive index, density, surface area, and elemental composition (Table 1.4).^{136,125,126} For a given rank of coal, up to medium volatile bituminous, the liptinite macerals are richer in hydrogen than the corresponding vitrinites and inertinites.⁶¹ Such bulk differences are due to variations in the proportion and type of aliphatic, aromatic and oxygen-bearing

Table 1.4 Chemical Composition and some Physical Properties of High Volatile A Bituminous Coal Maceral Components

Maceral	Elemental Composition (wt %)					Helium Density (g/cm ³)	Reflectance (oil, 546nm)	Refractive Index	Surface Area ^b
	S	N	O	C	H				
Exinite	0.7	1.1	5.5	86.2	6.5	1.21	0.32	1.68	2.5
Vitrinite	1.0	1.6	8.0	84.1	5.3	1.29	0.91	1.81	2.1
Fusinite	0.4	0.6	4.3	91.5	3.2	1.48	2.65	1.91	9.8

^bBET using nitrogen

(after Ergun³⁵)

functional groups.^{36,126} The early work of Dormans *et al*¹²⁷ clearly demonstrated the statistical distribution of the carbon atoms in each of the three maceral groups. More recent studies, using ¹³C cross-polarisation magic-angle-spinning solid-state nuclear magnetic resonance spectroscopy (¹³C CP/MAS NMR)^{111,128,129} and Fourier transform-infrared spectroscopy (FT-IR),¹²⁹ have only confirmed the aliphatic nature of liptinites and the highly aromatic content of the inertinites, with the fraction of protonated carbon decreasing in the order: liptinite → vitrinite → inertinite.¹²⁸ Both NMR and FT-IR studies indicate that the aliphatic components of vitrinite and liptinite consist of CH, CH₂ and CH₃ - carbons, with a greater proportion of CH and CH₂ within the liptinites.^{111,112,129} Alginite has the highest elemental hydrogen content consistent with its aliphatic polymeric structure,¹²⁶ whereas resinites are predominantly composed of terpenes.^{124,125} Analysis by pyrolysis gas-chromatography and pyrolysis mass-spectroscopy¹³⁰⁻¹³² has demonstrated that the maceral cutinite contains soluble waxes, poly-esters and non-hydrolysable polymethylenic biopolymers.^{131,132} Similarly, sporinite has been shown to contain a highly cross-linked aliphatic polymer with a small proportion of aromatic and phenolic components,^{125,132} and therefore sporinite is considered to be a molecular intermediate between vitrinite and more aliphatic-rich liptinites.¹³²

Hatcher *et al*¹³² consider the structure of vitrinite to be an 'alkylated benzene-like structure', that is derived primarily from lignin macromolecules (Section 1.4), although the concept that benzene-like structural units constitute the bulk of the 'vitrinite molecule' (>80%C) was originally incorporated in the model of Given in 1960 (Figure 1.22).¹³³ Given¹³³ based his polymeric model for vitrinite upon nuclear magnetic resonance data, upon the X-ray diffraction work of Hirsch,¹¹⁰ the infra-red studies of Brown.¹³⁴ Given¹³⁵ subsequently revised his model so that the aromatic nuclei were linked by a 1,4,-dihydrophenanthrene structures, instead of 9,10,-dihydroanthracene monomers. After twenty-five years, the aromatic/hydroaromatic model remains the most common structural basis for models of vitrinite (or coal)¹³⁶ and forms the basis of the models proposed by Ladner,¹³⁷ Pitt,¹³⁸ Wiser,¹³⁹ Shinn,¹⁴⁰ and Wender *et al*.¹⁴¹

Each 'molecule model' varies in structure through the differences in the spatial arrangement of aromatic nuclei, hydroaromatics, bridges and functional groups,^{141,142} although those

vitrinite molecular models share common features that vary with coal rank.

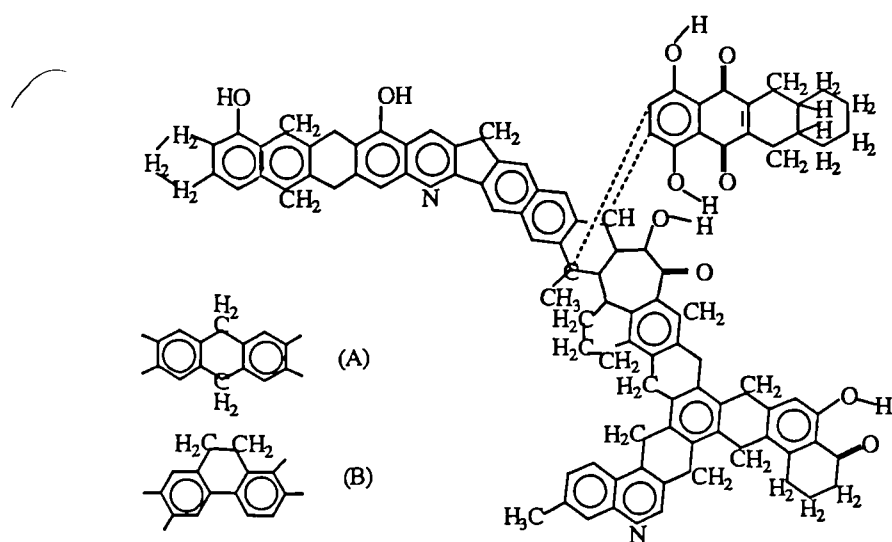


Figure 1.22 Given's proposed model for vitrinite with an empirical formula of $C_{102}H_{78}O_{10}N_2$, the dihydrophenanthrene structural unit (B) was later proposed as an alternative to the dihydroanthracene structural unit (A) used within the original model. (after Given^{133,135})

Table 1.5 Common Features of Vitrinite Models of Bituminous Rank

Feature	Molecular type or range
Functional groups	O - H, COOH, >O, C=O, >N:, >N - H
Bridges	ether, methylene, O - C, hydrogen bonds
Aromatic ring size	1 - 3
Hydroaromatics	dihydroanthracene, 9 - 10 dihydrophenanthrene

(after Thomas¹⁴²)

The models proposed by Given,^{133,135} Pitt¹³⁸ and Ladner¹³⁷ are generally based upon accepted chemical and physical properties, such as aromaticity (*f.a.*) derived by ^{13}C NMR,^{128,129,141,144} or by experimentation involving analysis by Fourier-transform infrared spectroscopy,^{112,129} chemical degradation,¹⁴³ pyrolysis-mass-spectroscopy^{130,144} and elemental analysis.^{36,141} However, such models are not predictive.^{142,145} That is, those models cited above do not necessarily predict behaviour upon utilisation in processes of liquefaction, combustion or pyrolysis.^{126,136,143} 'Coal models,' such as those proposed by Wiser¹³⁹ and Shinn,^{140,145} begin to meet those requirements in their non-planar, non-polymeric (not consisting of regular aromatic monomers) macromolecular systems consisting of aromatic units (1-5) interconnected by bonds of varying bond strengths,¹⁴² thereby enabling smaller units of various molecular size to be generated by selective bond scission. However, two comments regarding model representations of coal are worthy of note. Firstly, the experimental proofs of the so-called 'coal macromolecule' are obtained by either using vitrinite concentrates or high-purity vitrains so that the derived models more

aptly represent the molecular mix within vitrinite rather than a typical heterogeneous coal (i.e. clarain).¹²⁶ Secondly, Given and Drykacz¹²⁶ consider it very unlikely that pure samples of vitrinite macerals will ever be produced by density separation techniques due to similarities in density. Suggesting that attempts to represent a heterogeneous material by a single average molecule may well be an exercise in futility. This latter point is made all the more poignant when one considers the variety of lignin molecules within the peat-forming process (Section 1.4) and the probability that those various chemical precursors will form vitrinite (or coal) macromolecules, all containing the same average structure, when modified by the processes discussed above.

1.8 In Retrospect

Coal is an extremely complex material formed predominantly from plant material that reflects the conditions extant within a particular environment or geological time. There are coals (i.e. Gondwanaland) that owe their gross compositional differences to their respective peat-forming environments and flora.^{68,70} Other coals, such as the brown coals of West Germany,^{32,118} or the Jurassic coals of Russia,²⁷ owe their respective characteristics to their modes of preservation. There are other instances where coals show a variation (thickness, type) within a large basin (e.g. Pocahontas, USA) depending upon the location of the respective ancient peat deposited within the delta. Furthermore, simple vertical and lateral variations within a coal seam often reflect local variations in the hydrological regime within the peat-forming environment. From a simplistic point of view, the processes of plant debris accumulation, peatification and coalification represent phenomena that have changed little over time, or from place to place. However, in reality the interplay of variables is so complex and interdependent that a variation in one may affect other variables either directly or indirectly producing a variation in composition or rank even within the same basin. An attempt to illustrate this point is presented in Figure 1.23.

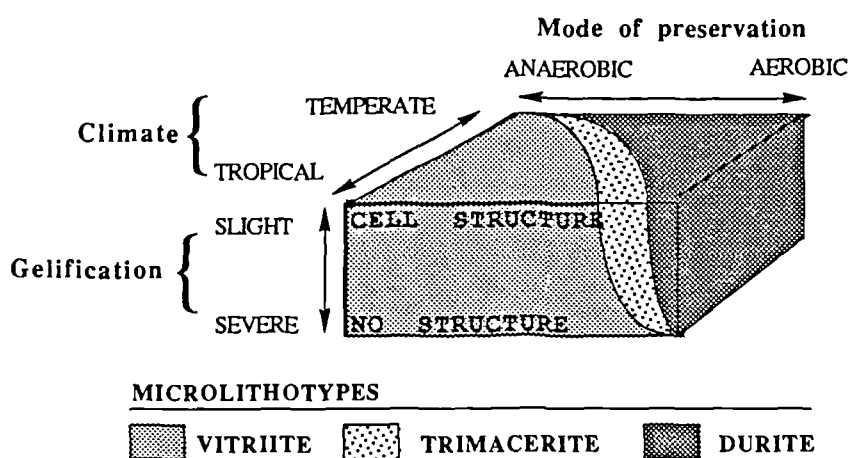


Figure 1.23 A schematic representation of the possible interplay of three variables important in determining the microlithotype content of a coal: variations in the climate (tropical-temperate), or hydrological regime (aerobic-anaerobic) and possibly the extent of gelification will lead to a difference in the gross composition of a coal.

References

1. Seyler, C.A. (1899). Proc. S. Wales Inst. Engrs. **21**, 483-526.
- Seyler, C.A. (1900). Proc. S. Wales Inst. Engrs. **22**, 112-120.
- Seyler, C.A. (1938). Proc. S. Wales Inst. Engrs. **53**, 254-327.
2. Mott, R.A. (1942). Fuel **21**, 126-135.
3. Berkowitz, N.L. (1979). 'An Introduction to Coal Technology'. Academic Press, New York.
4. Neavel, R.C. (1981) in: (Elliot, M.A. Ed.) 'Chemistry of Coal Utilisation'. 2nd Supplementary Volume, John Wiley and Sons, New York, 91-158.
5. Jones, J.M., Davis, A., Cook, A.C., Murchison, D.G., and Scott, E. (1984). Int. J. of Coal Geology **3**, 315-331
6. Given, P.H., Cronauer, D.C., Spackman, W., Lovell, H.L., Davis, A., and Biswas, B. (1975). Fuel **54**, 40-49.
7. Youtcheff, J.S., and Given, P.H. (1982). Fuel **61**, 980-987.
8. Price, J.T., Grandsen, J.F., Silverston, P.L., Readyhough, P.J., Newman, A., and Remachandran, P. (1985). Proceedings of the International Conference on Coal Science. Pergamon, Sydney, 969-972.
9. MacPhee, J.A., Price, J.T., and Grandsen, J.F. (1987). Proceedings of the International Conference on Coal Science. (Moulijn, J.A. et al Eds.), Elsevier, Amsterdam, 169-172.
10. Berkowitz, N., Fryer, D.F., Ignasiak, B.S., and Szladow, A.J. (1974). Fuel **53**, 141.
11. Falcon, R.M.S. (1986) in: 'Mineral deposits of S. Africa' No. 11 (Anbaeaurer, E.R. and Maske, S. Eds.) Geol. Soc. S. Africa, Johannesburg, 1899-1921.
12. Savage, W.H.D. (1977). Tech. Mem. Fuel Res. Inst. S. Africa, No. 10.
13. Sanyal, A. (1983). J. Inst. Energy, June, 92-95.
14. Nandi, B.N., Brown, T.D. and Lee, G.K. (1977). Fuel **56**, 125-130.
15. Cumming, J.W., Livingston, W.R., and Hesselmann, G.J. (1987). Conf. Papers of the 6th Int. Conf. and Exhibition on Coal Technology and Coal Economics, 9-11 June, London, 11-30.
16. Skorupska, N.M., Sanyal, A., Hesselmann, G.J., Crelling, J.C., Edwards, I.A.S., and Marsh, H. (1987). Proc. Int. Conf. on Coal Science (Moulijn, J.A. et al Eds.), Elsevier, Amsterdam, 827-832.
17. Bend, S.L., Edwards, I.A.S., and Marsh, H. (1989). Proc. Int. Conf. on Coal Science, Japan. 437-440.
18. Metcalf, G.S., Windig, W., Hill, G.R., and Meuzelar, H.L.C. (1987). Int. J. of Coal Geology **7**, 245-268.
19. Snyman, C.D. (1961). Publikasies van die Universiteit van Pretoria, No.15, Pretoria, S. Africa.
20. Hoffmann, H., and Hoehne, K. (1960). Brenstoff. Chemie **41**, 5-11.
21. Brown, H.R., and Taylor, G.H. (1961). Fuel **40**, 211-224.
22. Hobday, D.K. (1987) in: 'Coal and Coal Bearing Strata: Recent Advances', (Scott, A.C. Ed.), Geol. Soc., London, Sp. Publication, No. 32, Blackwell, Oxford, 219-314.
23. Cairncross, B., and Cadle, A.B. (1988). Int. J. Coal Geology **9**, 343-370.
24. Hagelskamp, H.H.B., Erikson, P.G., and Snyman, C.P. (1988). Int. J. Coal Geology **10**, 51-77.
25. Shiquing Zhao (1980). Unpub. report. Hvainan Coal College, Anhui, China.
26. Wang, Jie., and Jin Kui. li. (1980). Unpub. report. China Inst. of Mining, Beijing, China.
27. Lapo, A.V. (1974). Doklady Akad. Nauk USSR **221**, 210-213.
28. Lapo, A.V. (1978). Fuel **57**, 179-183.
29. Haquebard, P.A., and Donaldson, J.R. (1974). Geol. Soc. Amer. Sp. Paper 114, 14-191.
30. McCabe, P.J. (1978) in: 'Coal and Coal Bearing Strata: Recent Advances'. (Scott, A.C. Ed), Geol. Soc., London, Sp. Publication, No 32, Blackwell, Oxford, 51-66.
31. Newman, J. (1987). Coal Geology Reprint 3. Resource Management and Mining, Ministry of Energy, New Zealand.
32. Teichmüller, M. (1982) in: Stach's 'Textbook of Coal Petrology' 3rd Ed. Stach.E., Mackowsky, M-Th., Teichmüller, M., Taylor, G.H., Chandra, D. and Teichmüller, R. Gebrüder Borntraeger, Berlin, 5-86.
33. Given, P.H. (1988) in: 'New Trends in Coal Science' (Yürüm. Y, Ed.), Kluwer Academic Publishers, Dordecht, 1-52.
34. Scott, A.C. (1987) in: 'Coal and Coal Bearing Strata: Recent Advances', (Scott, A.C. Ed.), Geol. Soc., London, Sp. Publication, No 32, Blackwell, Oxford, 1-5.

35. Ergun, S. (1979) in: 'Coal Conversion Technology', (Wen, C.Y., and Stanley Lee, E. Eds.), Addison-Wesley, Reading, Massachusetts, 1-56.
36. van Krevelen, D.W., and Schuyer, J. (1957). 'Coal Science: Aspects of Coal Constitution', Elsevier, Amsterdam.
37. Barnsley, G.B. (1984). 'Coal Geology and Coal Technology' (Ward, C.R. Ed.) Blackwell, Oxford, 1-39.
38. Given, P.H. (1984) in: 'Coal Science', Vol 3, (Gorbaty, M.K., Larsen, J.W., and Wender, I. Eds.), Academic Press, San Diego, 63-252, 339-341.
39. Butler, J., Marsh, H. and Goodarzi, F. (1988). Fuel 67, 269-274.
40. Rowley, D.B., Raymond, A., Parrish, J.T., Loftes, A.L., Scotese, C.R., and Ziegler, A.M. (1985). Int. J. of Coal Geology 5, 7-42.
41. Newel, R.E. (1979). American Scientist 67, 405-416.
42. Dott, R.H., and Batten, R.H. (1988). 'Evolution of the Earth', 4th Edition, McGraw and Hill, New York.
43. Ziegler, A.M., Raymond, A.L., Gierlowski, T.C., Horrell, M.A., Rowley, D.B., and Lottes, A.L. (1987) in: 'Coal and Coal Bearing Strata: Recent Advances', (Scott, A.C. Ed.) Geol. Soc., London, Sp. Publication, No. 32, Blackwell, Oxford, 25-49.
44. DiMichele, W.A., Phillips, T.L., and Peppers, R.A. (1985) in: 'Geological Factors and the Evolution of Plants', (Tiffney, B.H. Ed.), Yale University Press, 223-256.
45. McAlester, A.L. (1977) 'The History of Life', Prentice Hall, New Jersey, 89-107.
46. Thomas, B.A., and Spicer, R.A. (1987) 'The Evolution and Palaeobiology of Land Plants', Croom Helm, London.
47. Raymond, A., Parker, W.C., and Parrish, J.T. (1985) in: 'Geological Factors and the Evolution of Plants', (Tiffney, B.H. Ed.), Yale University Press, 169-222.
48. Collinson, M.E., and Scott, A.C. (1987) in: 'Coal and Coal Bearing Strata: Recent Advances', (Scott, A.C. Ed.) Geol. Soc., London, Sp. Publication, No. 32, Blackwell, Oxford, 67-85.
49. Banks, H.P. (1970) 'Evolution and Plants of the Past', Macmillan, London.
50. Fulton, I.M. (1987) in: 'Coal and Coal Bearing Strata: Recent Advances', (Scott, A.C. Ed.) Geol. Soc., London, Sp. Publication, No. 32, Blackwell, Oxford, 201-218.
51. Saunders, W.B., and Ramsbottom, W.H.C. (1986). Geology 14, 208-212.
52. Plumstead, E.P. (1987). 'Coal in South Africa', Witwatersrand University Press, Johannesburg.
53. Schopf, J.M. (1952) J. Sedim. Petrol. 22, 61-69.
54. Cook, A.C. (1976) in: 'Australian Black Coal' (Cook, A.C. Ed.) Aust. Inst. Min. Metall. Illwarra Branch, A.B.C. Symposium, Melbourne, 68-84.
55. Creber, G.T., and Chaloner, W.G. (1985). Palaeogeography, Palaeoclimatology, Palaeoecology 52, 35-60.
56. Dobruskina, I.A. (1987). Palaeogeography, Palaeoclimatology, Palaeoecology 58, 75-86.
57. Khorasani, G.K. (1987) in: 'Coal and Coal Bearing Strata: Recent Advances', (Scott, A.C. Ed.), Geol. Soc., London, Sp. Publication, No. 32, Blackwell, Oxford, 303-310.
58. Moore, P.D. (1987) in: 'Coal and Coal Bearing Strata: Recent Advances', (Scott, A.C. Ed.) Geol. Soc., London, Sp. Publication, No. 32, Blackwell, Oxford, 7-16.
59. Ward, C.R. (1984). in: 'Coal Geology and Coal Technology', (Ward, C.R. Ed.) Blackwell, Oxford, 40-73.
60. Ferm, J.C. (1975) in: 'Palaeotectonic Investigations of the Pennsylvanian System in the United States Part II', U.S. Geol. Surv. Prof. Paper, No 853, 57-64.
61. Davis, A. (1984) in: 'Coal Geology and Coal Technology' (Ward C.R. Ed.) Blackwell, Oxford, 74-112.
62. Casagrande, D.J. (1987) in: 'Coal and Coal Bearing Strata: Recent Advances', (Scott, A.C. Ed.) Geol. Soc., London, Sp. Publication, No. 32, Blackwell, Oxford, 87-105.
63. Spackman, W. (1958). Trans. N.Y. Acad. Sci., Ser. II 20, 411-423.
64. Moore, P.D. (1984). 'European Mires', Academic Press, London.
65. Junk, W.J. (1984) in: 'The Amazon' (Sioli, H. Ed.) Monographiae Biologicae No. 56, 215-243.
66. Cohen, A.D., Spackman, W., and Raymond, R. (1987) in: 'Coal and Coal Bearing Strata: Recent Advances', (Scott, A.C. Ed.) Geol. Soc. London, Sp Publication, No. 32, Blackwell, Oxford, 107-125.
67. Clymo, R.S. (1987) in: 'Coal and Coal Bearing Strata: Recent Advances', (Scott, A.C. Ed.) Geol. Soc., London, Sp. Publication, No. 32, Blackwell, Oxford, 17-24.
68. Navale, G.K.B. (1979) in: 'Economic Geology: Coal Oil and Gas' (Cross, A.T. Ed.) Comptes Rendu No 4, Southern Illinois University Press, Carbondale, 258-270.

69. Jones, J.G., Conaghan, P.J., and McDonnell, K.L. (1987). *Palaeogeography, Palaeoclimatology, Palaeoecology* **58**, 203-219.
70. Chandra, D., and Taylor, G.H. (1982) in: *Stach's 'Textbook of Coal Petrology'* 3rd Ed., Stach, E., Mackowsky, M-Th., Teichmüller, M., Taylor, G.H., Chandra, D., and Teichmüller, R., Gebrüder Borntraeger, Berlin, 177-190.
71. Smith, A.H.V. (1962). *Proc. Yorkshire Geol. Soc.* **33**, 423-474.
72. Bartram, K.M. (1987) in: *'Coal and Coal Bearing Strata: Recent Advances'*, (Scott, A.C. Ed.) *Geol. Soc., London, Sp. Publication, No. 32*, Blackwell, Oxford, 187-199.
73. Stayan, W.B., and Bustin, R.M. (1983). *Int. J. Coal Geology* **2**, 321-370.
74. Given, P.H., Spackman, W., Painter, P.C., Rhoads, C.A., Ryan, N.J., Alemany, L., and Pugmire, R.J. (1984). *Org. Geochem.* **6**, 399-407.
75. Hayatsu, R., Winans, R.E., McBeth, R.L., Scott, R.G. Moor, L.P., and Studier, M.M. (1981) in: *'Coal Structure'* (Gorbaty, M.L. and Ouchi, K. Eds.) *Adv. In Chem. Series 192*, Washington D.C., 133-149.
76. Hatcher, P.G. (1987). *Org. Geochem.* **11**, 31-39.
77. Fischer, F., and Schrader, H. (1922). *Brennstoff-Chemie* **3**, 341, (1923) *Fuel* **2**, 93-94.
78. Cooper, B.S., and Murchison, D.G. (1969) in: *'Organic Geochemistry'* (Eglinton, G., and Murphy, M.T.J. Ed.), Longman, 699-726.
79. Hurst, H.M., and Burgess, N.A. (1967). in: *'Soil Biochemistry'* (McLaren, A.D. and Peterson, G.H. Eds.) Arnold, London, 260-286.
80. Crawford, R.L. (1981). *'Lignin Biodegradation and Transformation'*, John Wiley and Sons, New York, 38-108.
81. White, D. (1933). *Econ. Geol.* **28**, 556-570.
82. Clymo, R.S. (1965). *J. of Ecology* **53**, 747-758.
83. Dunbar, J., and Wilson, A.T. (1983). *Geochim. Cosmichim. Acta* **47**, 1541-1540.
84. Liu, S., Taylor, G.H. and Shiboaka, M. (1982) in: *'Proc. Symp. Coal Resources: Origins Exploration and Utilisation of Australian Coal'* (Malet, C.W. Ed.) *Geol. Soc. Australia, Melbourne*, 145-152.
85. Chaffee, A.L., Johns, R.B., Baerken, M.J., deLeeuw, J.W., Schenck, P.A. and Boon, J.J. (1984). *Org. Geochem* **6**, 409-416.
86. Hatcher, P.G., Romankiw, L.A., and Evans, J.R. (1985). *'Proc. Int. Conf. on Coal Science'*, Pergamon Press, Sydney, 616-619.
87. Smith, G.C. and Cook, A.C. (1980). *Fuel* **59**, 641-646.
88. Dulhunty, J.A. (1954). *Fuel* **33**, 145-152.
89. Murchison, D.G., Cook, A.C., and Raymond, A.C. (1985). *Phil. Trans. R. Soc, Lond. A* **315**, 157-186.
90. Erdmann, E. (1974). *Brennstof-Chem* **5**, 177-186.
91. Bergius, F. (1913). *J. Soc. Chem. Ind.* **32**, 462-467.
92. Briggs, H. (1931). *Chem. Ind.* **50**, 127-133.
93. Ivanov, T.A. (1967). *'Coal-Bearing Formations'*, Nauka, Leningrad, 351-366.
94. Huck, G., Patteisky, K. (1964). *Forstchr, Geol. Rheinld. Westfalen*, **12**, 551-558.
95. Jüntgen, H., and Karweil, J. (1966). *Erdöl u Kohle, Erdgas, Petrochem* **19**, 251-258, 339-344.
96. Bostick, N.H. (1974). *Geol. Soc. Amer. Sp. Paper., No. 153*, Boulder, Colorado, 1-17.
97. Karweil, J. (1956). *Z. Deutsch. Geol. Gesell* **107**, 132-139.
98. Lopatin (1971). *Izv, Akad. Nauk USSR, Ser. Geol.* **3**, 95-106.
99. Waples, D.W. (1984) in: *'Adv. Petroleum Geochemistry, Vol 1'* (Brooks, J., and Welte, D. Eds.), Academic Press, London, 7-67.
100. Toth, D.J., Lerche, I., Petroy, D.E., Meyer, R.J., and Kendall, C.G. St.C. (1981). *Adv. Org. Geochem.* **6**, 588-596.
101. Barker, C.E. (1979). Unpublished PhD Thesis, Dept. of Earth Sci. Univ. of California. California.
102. Windley, B.F. (1982). *'The Evolving Continents'* 2nd Ed., John Wiley and Sons, Chichester.
103. Dambeger, H.H. (1971). *Econ. Geol.* **66**, 488-494.
104. Hitchon, B. (1984). *A.A.P.G. Bull.* **68**, No. 6, 713-743.
105. Buntebarth, G., Koppe, I., and Teichmüller, M. (1982) in: *'Geothermics and Geothermal Energy'* (Cesmak, V. and Haenel, R. Eds.), Schweizerbart, Stuttgart, 45-53.
106. Creany, S. (1980). *Proc. Yorksh. Geol. Soc.* **42**, pt 4, 553-580.
107. Damberger, H.H. (1974). *Geol. Soc. Amer. Sp. Paper, No. 153*, Boulder, Colorado, 53-74.

108. Keen, C.E., Lewis, T. (1982). A.A.P.G. Bull. **66**, No. 9, 1402-1407.
109. Larsen, J.W. (1988) in 'New Trends in Coal Science', (Yarum, Y. Ed.), Klüwer Academic Publishers, Dordrecht, 73-84.
110. Hirsch, P.B. (1954). Prov. Roy. Soc. Lond. **226**, 143-169.
111. Kasuschke, I., Riepe, W., and Gerhards, R. Erdöl und Kohle, Erdgas Petrochem **42**, No. 5, 209-212.
112. Riesser, B., Starsinic, E., Squires, E., Davis, A. and Painter, P.C. (1984). Fuel **63**, 1253-1261
113. Wittehurst, D.D., Mitchell, T.O., and Farcasiu, M. (1980) 'Coal Liquefaction', Academic Press, New York, London, Toronto, Sydney, San Francisco.
114. International Handbook of Coal Petrography (1963) 1st Edition, plus 2nd Edition (1971) and 3rd Supplement (1973). International Committee for Coal Petrology, C.N.R.S., Paris.
115. Stach, E. (1982). in: Stach's 'Textbook of Coal Petrology' 3rd Ed. Stach, E., Mackowsky, M-Th., Teichmüller, M., Taylor, G.H., Chandra, D. and Teichmüller, R. Gebrüder Borntraeger, Berlin, 87-218.
116. Stopes, M.C. (1919). Proc. Roy. Soc. B. **20**, 470-487.
117. Stopes, M.C. (1935). Fuel **14**, 4-13.
118. Jacob, H. (1956). Freiburger Forschungsh A 45, Berlin.
119. Teichmüller, M. (1958) in: 'Die Niederrheinische Braunkohlen-formation' (Ahrens, W. Ed.) Geol. Rheinland, Westfalen, **2**, 599-612.
120. Ammosov, I.I. (1964). Cong. Intern. Strat. Geol. Carbonifere 3, Paris, 909-916.
121. Benedict, L.G., Thompson, R.R. and Shigo, J.J. (1968) Fuel **47**, 125-14.
122. Teichmüller, M., and Wolf, M. (1977). J. of Microsc. **109**, 49-73.
123. Teichmüller, M. (1974). Fortschr. Geol. Rheinld. Westfalen, **24**, 37-64.
124. Bend, S.L. (1986). MSc Dissertation. Unpub. Newcastle upon Tyne University, Newcastle upon Tyne.
125. Allen, J. (1975). PhD Thesis. Unpub. Newcastle upon Tyne University, Newcastle upon Tyne.
126. Given, P.H. and Drykacz, G. (1988) in: 'New Trends in Coal Science', (Yarum, Y. Ed.), Klüwer Academic Publishers, Dordrecht, 53-72.
127. Dormans, H.N.M., Huntjens, F.J. and van Krevelen, D.W. (1957). Fuel **36**, 321-335.
128. Pugmire, R.J., Soderquist, A., Burton, D.J., Beeler, A.L., and Grant, D.M. (1985). Int. Conf. on Coal Science, Sydney, 774-777.
129. Drykacz, G., Bloomquist, C.A.A. and Solomon, P.R. (1984). Fuel **63**, 536-542.
130. Nip, M., de Leeuw, J.W., and Schenck, P.A. (1987). Proc. Int. Coal Science. (Moulijn, J.A., Nater, K.A., and Chermin, H.A.G., Eds.), Elsevier, Amsterdam, 89-92.
131. Hayatsu, R., Botto, R.E., McBeth, R.L., Scott, R.G., and Winans, R.E. (1988). Energy and Fuels **2**, 843-847.
132. Hatcher, P.G., Lerch, H.E., Bates, A.L., and Verheyen, T.V. (1989). Org. Geochem **14**, No. 2, 145-155.
133. Given, P.H. (1960). Fuel **39**, 147-153.
134. Brown, J.K. (1955). J. Chem. Soc. 744-752
135. Given, P.H. (1961). Fuel. **40**, 427-431.
136. Davidson, R.M. (1980). 'Molecular Structure of Coal'. IEA Report No. ICTIS/TR 08. IEA Coal Research, London.
137. Ladner, W.R. cited in: Gibson, J. (1978). J. Inst. Fuel. **51**, 67-81.
138. Pitt, G.J. (1979) in: 'Coal and Modern Processing - An Introduction'. (Pitt, G.J., and Millward, G.R. Eds.) Academic Press, London.
139. Wiser, W.H. (1973). Proc. EPRI Conf. Coal Catalysis, Santa Monica, California.
140. Shinn, J.H. (1984). Fuel. **63**, 1187-1196.
141. Wender, I., Heredy, L.A., Neuworth, M.B., and Dryden, I.G.C. (1981) in: (Elliot, M.A. Ed.) 'Chemistry of Coal Utilisation'. 2nd Supplementary Volume, John Wiley and Sons Inc., New York, 425-521.
142. Thomas, M.K. (1986) in: 'Carbon and Coal Gasification - Science and Technology.' (Figueiredo, J.L. and Moulijn, J.A. Eds.) Martinus Nijhoff, Dordrecht, 57-92
143. Zilm, K.W., Pugmire, R.J., Larter, S.R., Allan, J., and Grant, D. (1981). Fuel. **60**, 536-542.
144. Hadicke, A., Schliephake, R.W. and Riepe, W. (1987). Proc. Int. Coal Science. (Moulijn, J.A., Nater, K.A., and Chermin, H.A.G., Eds.), Elsevier, Amsterdam, 123-126.
145. Shinn, J.H. (1985). 'Proc. Int. Conf. on Coal Science', Pergamon Press, Sydney, 738-741.

CHAPTER TWO

'Coal Characterisation and Classification'

2.1 Introduction

Coal is an important economic raw material, although any intrinsic value is based upon utilisation suitability. It is, therefore, necessary to characterize and classify coal according to a specific set of criteria related to utilisation and commercial value. The techniques used for characterisation range from the very simple, using a single variable, to the more complex, employing multivariate analyses, and tend to reflect either commercial or scientific interests.

This chapter discusses the most common commercial techniques used for characterisation, supplemented with some of the most simple 'scientific' techniques that have potential applications in commercial classification systems.

Coal Characterisation I: Petrographic Analysis

2.2 Sample Preparation

Difficulties in obtaining acceptable levels of precision and reproducibility are often attributable to the lack of instrument calibration¹ or poor sampling technique and subsequent sample preparation.² The adherence to set sampling procedures reduces the risk of obtaining a non-representative sample from either the coal-face (pillar or channel), drill core or stockpile.² There are written guidelines with set procedures for almost all aspects of coal sampling or sample preparation and a more detailed treatment of the subject can be found in: Ward,² the British Standards Document 1017 (Parts 1 and 2), American Society for Testing and Materials (ASTM) D2013 and D2234 and the International Standards Organisation (ISO) document 1988.

In addition to general guidelines for sampling and sample preparation, there are more specific guidelines relating to the petrographic analysis of coal and related preparative techniques; BS6127 (Parts 2 to 5), ASTM D2797-72, ISO/TC 27 N1255 (revised) supplemented by other internationally recognised guidelines.⁴

Whether conducting qualitative or quantitative microscopy, sample preparation involves one of three preparative techniques, which are: particulate (crushed) block-mounted samples, lump samples or thin sections.^{3,4,5} The universal use of incident light microscopy in coal

petrography coupled with the technical difficulties of preparing thin sections has precluded the continued usage of thin sections.^{5,6,7} Particulate blocks are required for the quantitative analysis of a coal, seam, pile or bulk sample which should be crushed and riffled to ensure that a statistically representative sample is prepared.^{2,3} Polished lumps are samples of coal that are cut in a desired plane (i.e. perpendicular to the bedding plane) from which the bireflectance, %R₀ max, or seam characteristics can be determined.^{2,3,6}

Samples can be polished either with or without relief, depending upon the lapping media used⁴ and the requirements of the analyst or mode of analysis. The correct standard of polish required for most applications is outlined in BS 6127 and the effects of over-polishing have been assessed and discussed by Murchison and Boulton.⁸

2.3 Maceral Analysis

The quantitative manual assessment of the relative proportions of macerals within a coal is referred to as petrographic analysis⁹ and is often determined on particulate blocks using the technique of modal analysis² based upon the point counting method of Glagolev¹⁰ and Barringer.¹¹ An integrated mechanical stage coupled to a counting device is used, in conjunction with a reflected light microscope equipped with oculars and an eye-piece reticule with cross-hairs, at an overall magnification of x 500.^{4,6} Unbiased sampling of the coal during analysis⁹ is achieved by using a predetermined interpoint and interline spacing that conforms to an imaginary grid over the surface of the particulate block.^{4,6,9} The prescribed criteria for selecting suitable interline and interpoint distances are the size of the particulate block and the size of the crushed particles of coal. Generally, a minimum distance of 50 µm is recommended⁴ or half the maximum particle diameter.¹²

The number of points counted is determined by the level of accuracy required. The Handbook of the ICCP⁴ states that the accuracy of analysis based upon 500 to 1000 points is ± 2 to 3%, to increase that value to ± 1% it is necessary to count at least 3000 points. To obtain a greater level of precision in the analysis, the ASTM 1981b Standard requires two separate analyses of 1000 points on two separate particulate blocks. The conversion of the analysed values from *per cent by volume* to *per cent by weight* is only possible if the mean density of the macerals is known.^{4,6,9}

Ward² discusses the relevance of conducting two sets of concurrent maceral analyses in both white-light and blue-light-fluorescence modes. Such a procedure discriminates between the various liptinite macerals and between liptinites and inorganics in low rank coals.^{2,3} As an additional aid in identifying specific sub-macerals (i.e. high/low semi-fusinite, vitrinite/semi-fusinite), the ICCP Standards Working Group¹³ recommend conducting all analyses with the microscope photometer system, thereby using maceral reflectance as an additional discriminant during the analysis.

2.4 Microlithotype Analysis

Macerals rarely occur coal without the presence of macerals or sub-macerals from the other maceral groups.² Therefore, a meaningful expression of the distribution of probable maceral associations can be of great use in certain technological situations (e.g. coking).^{2,6,9} Microlithotypes, as defined by Mackowsky and Kötter,¹⁴ are maceral assemblages⁴ or associations⁶ with macerals from the same or the other maceral groups. This rather vague definition requires set conventions to enable quantification of the associations, which are:

- i. a minimum band width of 50 μm , measured perpendicular to the bedding plane.
- ii. macerals occurring less than 5% within the defined measuring area (50 x 50 μm) are discounted from the analyses.⁴

Furthermore, all microlithotype names terminate with the suffix *-ite*, as a means of distinguishing between lithotypes (*-ain*), microlithotype (*-ite*) and macerals (*-inite*).

The samples are prepared in a similar way to those for maceral analysis and the microscope point-counting apparatus is similarly utilised as in maceral analysis⁴ with the exception that a special reticule is used within the ocular. The 20-point Kötter graticule¹⁴ (Figure 2.1)

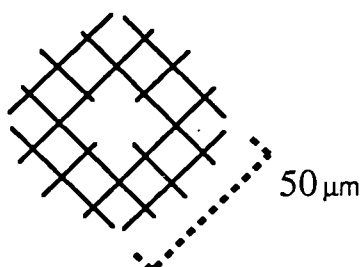


Figure 2.1 A graphical representation of the Kötter 20-point eyepiece reticule used for microlithotype analysis. (after Stach *et al*⁶)

should be scaled so that the indicated dimension covers 50 μm on a calibrated stage graticule at a magnification of x 400 to 500.⁴ During each analysis, the maceral group or maceral is identified at all intersections of the 20-point reticule, each intersection representing 5%. The sum of each maceral group under the measured area is then used to determine the overall microlithotype for that 50 μm area and recorded. The volumetric proportion of each microlithotype is obtained by conducting at least 500 such analyses on the coal sample.⁴

Unfortunately, this convention defines the microlithotype *Durite* as having between 5 to 90% inertinite. Therefore, the microlithotype terminology is often further subdivided to denote the relative proportions of any two or three maceral associations,^{15,16} the relevant criteria is given in Figure 2.2.

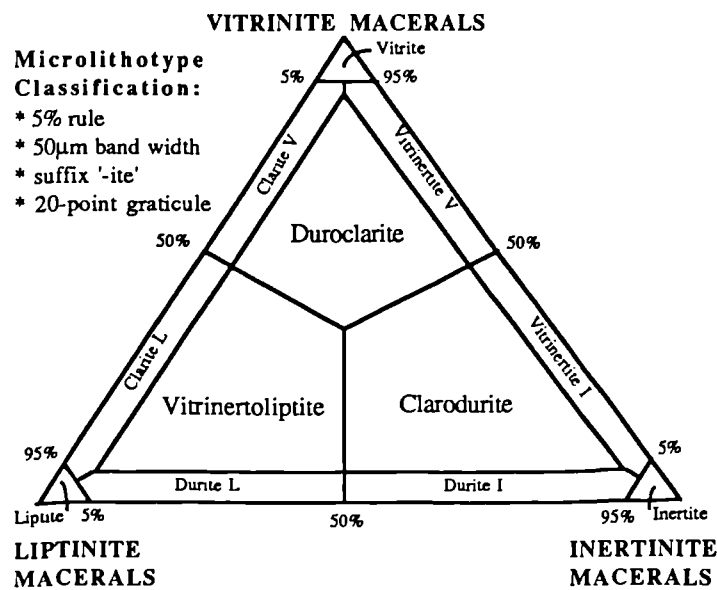


Figure 2.2 Specific criteria for microolithotype classification according to the proportion of the three maceral groups. (after Damberger *et al* ¹⁵)

Despite the vagueness of the above definitions, the different microolithotypes are considered to represent different palaeoenvironments, reflecting the hydrology of the peat-forming environment, the flora and conditions of preservation (Chapter 1).^{4,17,18}

2.5 Reflectance

2.5.1 The Theoretical Basis

The 'reflectance' of a maceral (or mineral) in coal petrography refers to the proportion of incident light that is reflected from a plane polished surface under specified conditions¹⁸ and is expressed as a percentage relative to some known absolute standard.^{2,4,6} The precise measurement of reflectance requires standard conditions and a properly adjusted and calibrated microscope-photometer system, equipped with a vertical illuminator.¹ Köhler illumination is the accepted mode of illumination for incident light microscopy.¹ (Figure 2.3) The relevant guides and standards are: BS 6127 (Part 5), ASTM D2798, ISO TC-27 and the Handbook of the ICCP.⁴

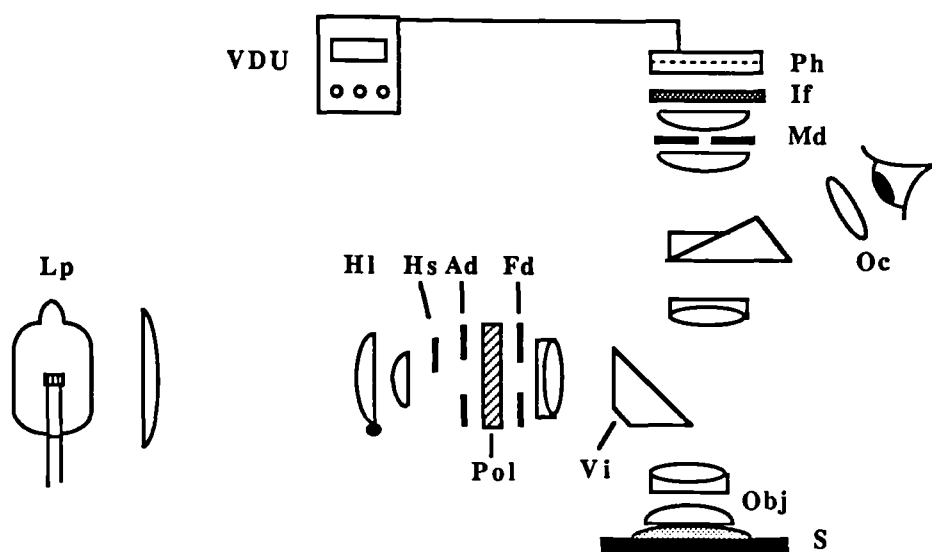


Figure 2.3 A schematic representation of the vertical illuminator within a Leitz Orthoplan-Pol MPV3 microscope-photometer, using a Berek prism reflector.
 Lp. Stabilized light., Hl. Hinged lens., Hs. Half-stop., Ad. Aperture diaphragm., Fd. Field diaphragm., Md. Measuring diaphragm., Pol. Polarizer., Vi. Berek prism., Obj. Objective (oil immersion)., S. Sample., Oc. ocular., If. Interference filter (i.e. 546nm)., Ph. Photomultiplier., VDU. Display panel / signal processor.

However, a cautionary note should be added regarding the suitability of various types of vertical illuminator for use in microscope photometry. Each type of vertical illuminator imparts a different set of characteristics upon the observed image and instrument. This is due to such factors as obliquity of illumination, control of glare, light loss at air/glass interfaces, etc. Therefore, care ought to be exercised when selecting the appropriate illuminator¹⁹ (Table 2.1).

Table 2.1 Characteristics and Properties of Vertical-illuminator Reflectors¹⁹

Characteristic	Reflector type		
	Plane-glass (45°)	Smith	Berek triple prism
Illumination	Usually at normal incidence		Oblique
Efficiency of illuminator	High light loss that varies with wavelength		Very efficient
Image brightness	Low	Low	High
Relief of object [†]	Low relief	Very low relief	Moderate-high
Troublesome reflections	Glare, back reflections and ghost images		No glare, no ghosting
Instrument linearity	Poor	Unknown	Generally linear

[†] This is also dependent upon the lapping media and technique used during sample preparation.

The reflectance of a polished maceral in monochromatic, plane polarized, light is a function of the refractive index of the maceral, the refractive index of the medium in which it is

measured and the absorptive index of the maceral^{3,19} which is expressed by the Fresnel-Beer equation:

$$- \%R = \frac{(n - n_o)^2 + n^2 K^2}{(n + n_o)^2 + n^2 K^2} \quad (2.1)$$

where: $\%R$ is the reflectance of the coal maceral
 n is the refractive index of the coal maceral
 K is the absorptive index of the coal maceral
 n_o is the refractive index of the measuring media

However, because the absorption index of a coal maceral is extremely difficult to obtain and requires the determination of reflectance in two media (e.g. air/oil), the reflectance of a maceral is directly obtained by a comparison with the reflectance of a standard that has known indices of refraction and an absorption index equal to zero.³ Furthermore, the measurements are usually conducted in an immersion media of known refractive index ($n_o = 1.518$) with a value of n_o coincident with the lowest value of n for coal macerals ($n = \text{c.a. } 1.5$); thereby, increasing the contrast between macerals but lowering the values of reflectance.¹⁹ Therefore, substituting the value of 1.518 for n_o , the Fresnel-Beer equation (2.1) can be expressed as:^{3,19}

$$\%R = \frac{(n_s - n_o)^2}{(n_s + n_o)^2} \times 100 \quad (2.2)$$

where: $\%R$ is the reflectance of the standard
 n_s is the refractive index of the standard
 n_o is the refractive index of the immersion media

The value of reflectance derived through the Fresnel equation will increase due to either an *increase* in the refractive index of the substance measured or due to a *decrease* in the refractive index of the immersion media.^{3,19} Changes in the refractive index may also occur due to changes in temperature and through the phenomenon of dispersion. For example, the refractive index of the immersion media has been shown to systematically decrease with an increase in temperature²⁰ and the refractive indices of the standard, immersion media and macerals vary with the wavelength of light (dispersion).²¹ Therefore, the refractive index of the immersion media (air, water, oil, etc.) is always given for a specified temperature (usually 23°C) and at a specified wavelength of light (546 nm).^{3,18,22}

Optical properties, such as the refractive and absorptive indices of vitrinite, are related to changes within the molecular structure during progressive coalification. McCartney and Ergun²¹ and later Murchison,¹² referring to the X-ray diffraction studies of Hirsch,²³ consider the refractive indices of vitrinite to be predominantly a function of the stacking order of the aromatic lamellae within the macromolecular structure of vitrinite. The rise in the absorptive indices, however, is considered to be due to the number of delocalized electrons within the structure which increase as the degree of aromaticity increases.¹²

2.5.2 Vitrinite Reflectance

Reflectance measurements are usually performed on vitrinite for the purpose of determining coal rank.⁶ Vitrinite is usually the most abundant coal maceral in humic coals²⁴ and exhibits a progressive increase in reflectance with increasing rank.²⁵ Vitrinite is also optically anisotropic and usually behaves as a uniaxial negative pseudo-crystalline substance with an orientation of the optic axis perpendicular to the bedding plane of the coal (Figure 2.4).

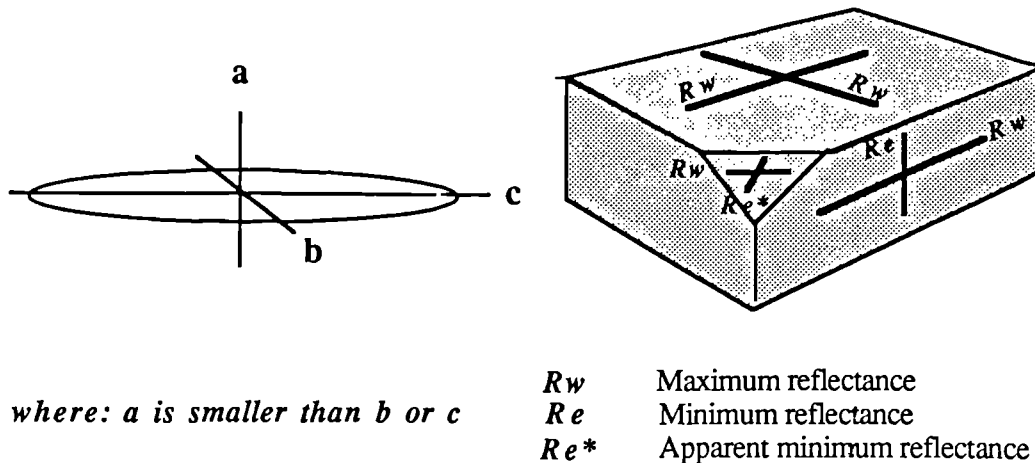


Figure 2.4 The anisotropic character of vitrinite schematically represented as a uniaxial negative optical indicatrix (a) and the relationship of vitrinite reflectance to the optic axes within an orientated sample of coal. (adapted from Davis²⁴)

The values for the maximum and minimum refractive and absorptive indices for a given coal rank depend upon the direction of polarized light with respect to the bedding plane.^{19,24} When viewed under plane polarized incident light, all sections within vitrinite (Figure 2.5), cut perpendicularly to the sedimentary bedding plane, will display a maximum ($\%R_{Omax}$) and a minimum ($\%R_{Omin}$) reflectance value. Cut sections orientated parallel to the plane of polarization will give true $\%R_{Omax}$ and cut sections orientated perpendicular to the plane of polarization will give values of $\%R_{Omin}$.^{4,24} Oblique sections will give true $\%R_{Omax}$ and an apparent $\%R_{Omin}$ that is intermediate between $\%R_{Omax}$ and $\%R_{Omin}$.³ Measurements conducted on randomly orientated crushed particles of coal will still provide values of $\%R_{Omax}$, because every vitrinite particle should exhibit the maximum reflectance in at least one position during the rotation of the microscope stage.³ All standards (i.e. BS, ASTM, etc.) require at least 100 measurements that involve a full rotation through 360° in plane polarized light at a wavelength of 546 nm to derive $\%R_{Omax}$. The arithmetic mean is called the mean maximum reflectance ($\%R_{Omax}$)⁴ which is used for the purpose of determining coal rank. The variance of the results is given by the standard deviation at the 95% confidence limit. Systematic and random errors in reflectance determinations are discussed in the ICCP Handbook⁴ and by Murchison.¹² The ICCP⁴ also discuss accuracy, concluding that beyond 100 measurements the gain in accuracy is negligible and that 10,000 such readings would be required for a ten-fold increase in accuracy.

There are many publications^{3,26,27,28} discussing variations in reflectance measurement techniques, some of which have subsequently been misunderstood²⁹ or misused partly due to the wider use of the technique within industries other than those concerned with coal. A comprehensive review of the various techniques and their applications is given by Davis.²⁴ One major advantage of vitrinite reflectance as a rank parameter is that it can be used on petrographically heterogeneous coals of various geological ages or chemical composition,^{6,2} although identical values of vitrinite reflectance from petrographically dissimilar coals does not ensure identical technological properties.³⁰ Fundamental work conducted during the late 1950's, 1960's and 1970's has established the relationship between vitrinite reflectance and other rank determinants such as calorific value, volatile matter and moisture content.^{27,31,32}

2.5.4 Automated Reflectance Techniques

Each maceral group has a characteristic range of reflectance values over the bituminous rank range (Figure 2.5).

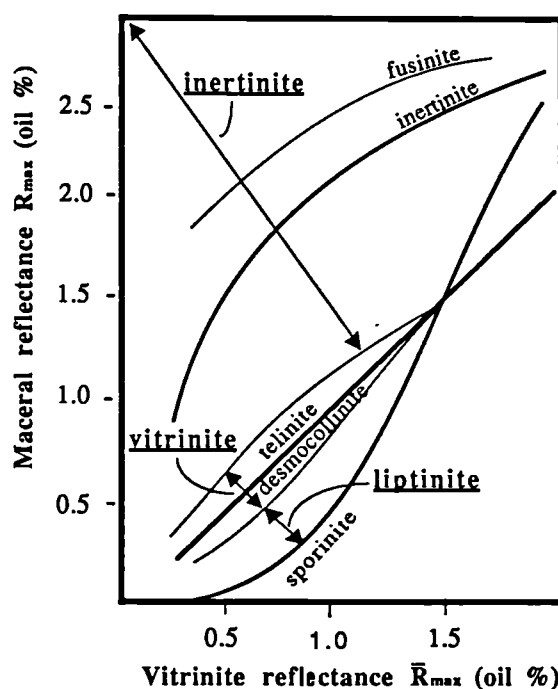


Figure 2.5 The reflectance curves of the maceral groups liptinite, vitrinite and inertinite versus coal rank (Vitrinite % $\bar{R}_{O,max}$). The diagram shows the relative changes in reflectance for the three maceral groups with progressive coalification. Specific lines for sporinite, telinite, desmocollinite and fusinite are included for comparison. (after Smith and Cook)³³

There have been many attempts to devise an automated technique using reflectance which can be applied to various types of petrographic analysis.^{3,24} Automated systems are designed to discriminate between coals and coal blends for utilisation purposes (maceral analysis), to determine coal rank or to perform a rudimentary form of mineral (pyrite) analysis^{3,24} and, occasionally, coal lithotype analysis.³⁴

Pioneering work by McCartney and Hofer, using a scanning microscope-photometer system, provided the impetus for more sophisticated systems that utilize the current 'state of the art' in microscope and data processing systems.^{3,24} The current 'third generation' of automated systems are designed to perform similar petrographic analyses to those outlined above, with the exception that processing times and the ability to discriminate between the different macerals and between macerals and artifacts are much improved.² Present systems are either based upon a scanning microphotometer,² a digitising image-analysis system^{35,36} or combinations of both techniques.³⁷ Microscope scanning microphotometer systems are currently considered to be more linear in their response over the reflectance range of bituminous coal¹² whereas the image analysis systems, using 'grey-levels' to discriminate between maceral groups,³⁵ provide the operator with the means to edit and select partial or whole fields of view. Furthermore, image analysis systems offer additional analytical techniques such as particle sizing, shape and porosity determinations that are unavailable with microscope photometer systems.³⁵

However, compromises must be made and technical problems are experienced by those using any automated technique.^{9,35} Coal rank, which uses $\%R_{Omax}$, must be derived from $\%R_{Orand}$ if using microscope photometers or $\%R_{Oav}$ for image analysis systems. The value $\%R_{Orand}$ has already been discussed (section 2.5.2.). $\%R_{Oav}$ is the reflectance derived in non-polarized light because image analysis cannot determine the optical anisotropy of vitrinite.⁹ The respective values are obtained using:

$$\%R_{Omax} = 1.061 \times R_{Orand}^{24} \quad (2.3)$$

or

$$\%R_{Omax} = 1.129 R_{Oav} + 0.092^{35} \quad (2.4)$$

where: $\%R_{Omax}$ = the mean of all maximum reflectance measurements
 $\%R_{Orand}$ = the mean of all random reflectance measurements
 $\%R_{Oav}$ = the mean of all average reflectance measurements

Problems include the recognition of maceral/binder or maceral/macerale boundaries and the discrimination of liptinites from binder material (both have low reflectance). Also, the requirement for defect and relief free highly polished blocks, and the inability to discriminate effectively between high rank vitrinite and inertinite macerals in coal blends of different rank are additional hazards yet to be overcome.⁹ The prospect of using image analysis and fluorometric techniques may obviate some of those problems.

2.6 Fluorescence Microscopy

Petrographic analytical techniques that utilize the auto-fluorescent properties of liptinites, vitrinites and some inertinites are used more often for scientific purposes and are not yet

incorporated in any domestic or international classification scheme. However, correlations have been established between the fluorescence of coal macerals and coal rank;³⁸ with further interest concentrating upon the relationship of vitrinite fluorescence to thermoplastic properties of vitrinite,³⁹ or coking propensity,^{40,41} or oxidation phenomena.^{42,43} Such studies indicate that fluorometric techniques have the potential to effectively discriminate between macerals and coals of differing technological properties.

The mechanism of fluorescence was not well understood by early proponents of the technique. Because emission spectra showed a pronounced shift to longer wavelengths with an associated decrease in hydrogen content (i.e. rank, or liptinite→vitrinite→inertinite), it was assumed that fluorescence was due to the presence of hydrogen-rich aliphatic material.^{44,45} This has subsequently been shown not to be the case. Coal maceral fluorescence is predominantly due to the promotion of electrons involving a $\pi \rightarrow \pi^*$ transition within aromatic systems.^{46,47,48} An increase in molecular conjugation, due to progressive coalification, shifts the first $\pi \rightarrow \pi^*$ absorption maxima towards longer wavelengths, with a concomitant red-shift in the emission spectra.⁴⁶ Aromatic ring rigidity, planarity, π electron delocalization and the presence of C=O groups, all affect the quantum efficiency or the excitation/emission wavelength maxima for polyatomic-polyaromatic systems.^{46,47}

Fluorescence microscopy is currently utilized in one of three techniques. Firstly, as an alternative to reflected mode white light microscopy, the liptinite macerals being best differentiated using their auto-fluorescence properties.⁶ Secondly, to derive and study the emission spectra of specific macerals which have been related to maceral type or coal rank.^{38,49} Thirdly, to measure the emission intensity at a specific wavelength (546 or 650 nm) and relate this to specific technological properties of coal or coal macerals.^{40,41,42,43} Single wavelength intensity measurements appear to have the greatest potential, to date, for incorporation in any domestic or international standard.

Coal Characterisation II: Standard Laboratory Tests

2.7 Introduction

The most common properties used within commercial classification schemes are proximate analysis, ultimate analysis and calorific value, petrographic analysis, ash fusibility, mechanical properties and behaviour on heating.^{2,5,15,50} These analytical techniques have become standardised methods of analysis and their stipulated procedures are contained within National or International Standards, for example: the American Society for Testing Materials (ASTM), German Normenansschuss (DIN), International Organisation for Standardisation (ISO), British Standards Institute (BS).^{51,52} In addition, there are other techniques that are either used as specifications to supplement the standard techniques or represent new methods of analyses that have not yet obtained the status of standard.^{2,51,53,54}

2.7.1 Analysis Report 'Bases'

Most analyses are conducted on 'air dried' samples and the percentages of the various elements or analyses are calculated in relation to the mass of that material.⁹ A more meaningful analytical report would, however, be corrected and expressed in relation to the organic fraction of the coal or 'pure coal' instead of the moist, mineral material.⁵⁵ There are several 'bases' that are currently used for reporting analyses, which are:⁹

- i. 'as received' (a.r.): the data is expressed as a percentage of the coal including surface moisture.
- ii 'air dried' in which a proportion of inherent but not surface moisture is included.
- iii 'dry' basis (d.b.) or 'moisture free': data is expressed as percentages of coal after the removal of moisture (surface and 'bed moisture').
- iv 'dry, ash-free' (d.a.f.) basis: the percentage volatile matter and fixed carbon is calculated with the moisture and ash removed.
- v 'dry, mineral matter-free' (d.m.m.f.) basis: this is given to represent the organic fraction of the coal only. The coal is assumed free of moisture and mineral matter.
- vi 'moist ash-free' (m.a.f.) basis: the coal is ash-free but still contains moisture.
- vii 'moist, mineral-matter-free' (m.m.m.f.) basis: mineral water free but still containing moisture.

The terms ash and mineral are not interchangeable.⁵³ Many classification schemes (i.e. ASTM) use the d.m.m.f. basis, the mineral content either measured directly⁹ or calculated using the Parr formula,⁷ whereas the ISO scheme uses the d.a.f. basis. Analyses given on the d.a.f. basis are easier to conduct, although d.m.m.f. is considered to be more representative of the organic fraction of a coal.⁵⁵

2.8 Proximate Analysis

'Proximate' analysis, derived from '*approximate analysis*' prior to standardisation,⁵⁶ provides a measure of the relative volatile and non-volatile organic compounds, water and non-combustible material² obtained by destructive thermal distillation.^{2,5,52} Proximate analysis determines the moisture content, volatile matter, ash and fixed carbon content of a coal.⁵⁶ The fixed carbon content is not measured directly but represents the difference in an air dried coal between the sum of the moisture, volatile matter, ash and 100%.² Because

volatile matter content, for example, is a function of sample size, particle size, the rate of heating and maximum temperature reached,⁵⁷ standardization is necessary and ought to be given in publications using data derived by this means⁵⁴ because there are several standards for proximate analysis (e.g. ASTM, BS, etc.), each with slight variations in maximum temperature that may effect the yield of volatile matter during analysis.⁵⁸

2.8.1 The Determination of Moisture

The ASTM methods are the most widely used and are outlined in the ASTM Standards D3173, D3302, D2013 and D1412-74.^{56,59} However, both the ASTM D 388 'Classification of coals by rank' and the ECE 'International classification of hard-coals by type' require the determination of the moisture holding capacity of the coal as a means of calculating the m.m.f. basis for calorific value.⁵⁶

The 'equilibrium moisture', 'moisture-holding capacity', 'bed moisture' and 'inherent moisture' are terms that relate to the moisture content of the coal in the coal seam.⁵⁶ The moisture in coal is considered to be retained as either:

- i. 'superficial water' or 'bulk water', present in cracks, capillaries and large pores,
- ii. physically absorbed water which is held in small pores and
- iii. chemisorbed water, produced by the thermal decomposition of hydrophilic functional groups.^{52,60}

In essence, both the ASTM D 1412 and the ISO 1018 Standards require that the sample is air dried at 105°C to a constant weight⁵⁶ whereas the British Standard includes three variations, but all with a common temperature of $107 \pm 2^\circ\text{C}$.⁵⁸

Bed moisture is often used as a rank parameter for low rank coals (e.g. lignites).^{2,52} Bed moisture decreases with increasing coal rank, with a small increase in coals greater than medium bituminous due to an increase in microporosity.^{54,60} However, the determination of moisture content is not without problems. The moisture content of coal is considered to be affected by the petrographic composition of a coal.⁵⁴ Also, there is some evidence that some moisture is retained as chemisorbed water beyond temperatures of 110°C and that the thermal decomposition of oxygen-bearing functional groups in low rank coals produces both water and CO₂ at temperatures below 100°C.⁶⁰

2.8.2 The Determination of Volatile Matter

The volatile matter content represents the loss of weight, corrected for moisture, when the coal is heated in specified apparatus under standardised conditions.⁵ The volatile matter evolved during heating consists of the gases, hydrogen, carbon monoxide, methane and

other low molecular weight hydrocarbons, carbon dioxide and water vapour.^{2,5}

The ASTM D 3175 Standard specifies a maximum temperature of $950 \pm 20^\circ\text{C}$ and the use of a platinum crucible with or without lid depending on whether the coal is 'sparking' or 'non-sparking'.^{2,56} The 'soak' period at $950 \pm 5^\circ\text{C}$ is exactly seven minutes. The ISO 562 Standard specifies a maximum temperature of $900 \pm 10^\circ\text{C}$ and a soak period of seven minutes. Only fused quartz crucibles and lids are permitted.⁵⁶ The BS 1016 Standard specifies a temperature of $900 \pm ^\circ\text{C}$ and a soak period of seven minutes using a cylindrical silica crucible.^{2,56,59}

However, volatile matter content is not a true physical entity⁵⁸ although it does represent the thermal distillation of hydrocarbons⁵ and the decomposition of oxygen-bearing functional groups.^{5,57} Volatile matter also represents a loss in weight due to the decomposition of inorganic material,^{2,54,59} especially carbonates which are known to decompose at temperatures in excess of 250°C .⁶¹ Other factors that affect the yield of volatile matter during proximate analysis include the rate of heating, the size of the furnace, the number of crucibles in an oven,⁵⁹ the size, shape and material from which the crucible is made,⁵⁶ the sample size and mean particle diameter and finally, the maximum temperature utilised by the technique.⁵⁴ It is evident that standardisation is crucial for an empirical technique so that accurate comparisons between coals can be made.

2.8.3 The Determination of Ash

Ash represents the residue remaining following the complete combustion of all organic material under controlled conditions^{1,56} and consists of oxides and sulphates.^{2,59} The ASTM D 3174 Standard provides two methods of deriving the ash content of coal, BS 1171 outlines a non-isothermal temperature programme, with a maximum temperature of 750°C and a two stage ashing programme, ambient to 500°C , and subsequently followed by final heating 500°C to 750°C over 2 hours.^{56,59} The BS specifies a final temperature of $815 \pm 10^\circ\text{C}$, heated from ambient until constant weight is maintained.²

The ASTM two stage method is considered² as a means of preventing the fixation of sulphur in the ash when analysing pyrite-rich coals. Alternatively, such ashing can be achieved by spreading the coal in thin layers.⁵⁷

There are several methods of deriving mineral matter content from the ash analysis when weight-percent mineral matter content analyses are not available. The most common formulae in use are those of Parr⁶² and the King *et al*⁶³ formulae. The Parr formula requires only ash and sulphur analyses:

$$M_m = 1.08A + 0.55S \quad (2.5)$$

where: M_m = the derived mineral matter content
 A = the ash content (wt%)
 S = the sulphur content (wt%)

The King *et al*⁶³ formula requires more complete initial analyses:

$$M_m = 1.09A + 0.5S_{pyr} + 0.8CO_2 - 1.1SO_3 \text{ ash} + 5SO_3 \text{ coal} + 0.5 Cl \quad (2.6)$$

where: A = the ash content (wt%)
 S_{pyr} = pyritic sulphur (wt%)
 CO_2 = mineral derived CO_2 (wt%)
 $SO_3 \text{ ash}$ = the SO_3 in the ash (wt%)
 $SO_3 \text{ coal}$ = the SO_3 in the coal (wt%)
 $Cl \text{ coal}$ = the Cl in coal

2.8.4. Fixed Carbon

The 'Fixed Carbon' content of a coal is considered to be the carbon remaining in the sample after the expulsion of volatile matter² and is determined by difference.^{2,7,54} Fixed Carbon content represents the sum of the other components (moisture, volatile matter and ash) subtracted from 100% and then corrected to whatever basis is being used.² However, as Given and Yarzab⁵⁷ note, the term 'Fixed Carbon' is an unfortunate misnomer because the term implies the existence of an entity within coal that has chemical meaning. Because the value representing 'Fixed Carbon' is dependent largely upon volatile matter content, which itself varies depending upon experimental conditions, the proportion of carbon remaining in the sample cannot truly be regarded as fixed or finite.⁵⁷ However, useful empirical correlations exist between fixed carbon content and other rank dependent parameters⁵⁴ and it is still the recognised ASTM procedure for determining the carbon content of coal as a means of defining coal rank.⁵⁴

2.9 Ultimate Analysis

'Ultimate analysis' essentially involves the determination of the elemental composition of the organic fraction of coal.^{2,5,7,52} The quantitative determination of the elements carbon (C), hydrogen (H), nitrogen (N) and sulphur (S) is achieved by standardized chemical procedures that involve oxidation, combustion and/or reduction techniques reported on a variety of analytical bases.^{5,52} Oxygen is traditionally determined by difference, subtracting $C + H + N + S$ from 100%,^{2,57} although there are techniques available for the direct determination of oxygen.

2.9.1 Carbon and Hydrogen Analysis

The determination of carbon and hydrogen involves the combustion of the coal sample in oxygen, in a closed system and collecting the gaseous products in absorption tubes and determining quantitatively the proportions of CO_2 and H_2O (Figure 2.6).²

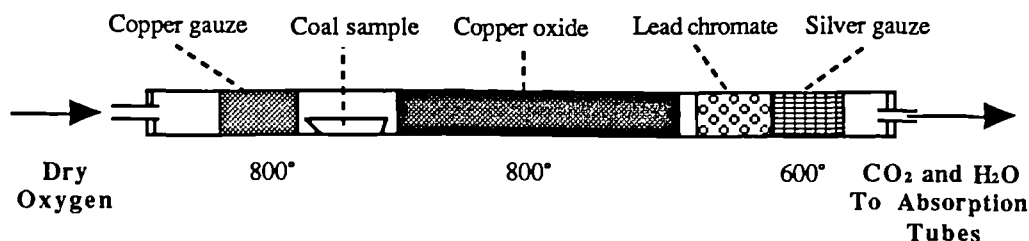


Figure 2.6 A schematic diagram of the Liebig apparatus used to derive CO_2 and H_2O .

The ASTM D 3176 Standard procedure recommends a combustion temperature of 800°C to 850°C and is based entirely upon the Liebig method (Figure 2.6).² In this process, the copper oxide converts the liberated CO to CO_2 and the oxides of sulphur and chlorine are retained by the lead chromate and silver gauze respectively.² The BS 1016 Standard, also using the Liebig method, recommends a temperature of 1350°C and is consequently faster.^{2,52}

2.9.2 Nitrogen Analysis

The most favoured method of nitrogen analysis is the Kjeldahl-Gunning procedure (ISO 333),⁵² in which nitrogen within the coal sample is converted to ammonia sulphate by catalytic digestion in sulphuric acid over a suitable catalyst (e.g. Mercury). The amount of ammonium sulphate formed by the reaction is then determined by back titration.^{2,52}

A technique favoured by commercial laboratories is the combustion of coal at temperatures similar to those used for carbon and hydrogen determinations and a process that converts the oxides of nitrogen to nitrogen by passing the gas over copper at 500°C . The separation of the gaseous products is achieved by chromatography; the detection and analysis of the gases is achieved by kathorimetry.⁶⁴

2.9.3 Sulphur Analysis

Sulphur may occur in coal either as organic sulphur, as sulphide minerals (i.e. pyrite) or as sulphate minerals (i.e. barytes).² In the ultimate analysis of sulphur, the total sulphur present within the coal is determined by a variety of possible methods.^{2,5,52,65} Of the three procedures contained within the ASTM D 3177 Standard, the Eschka procedure is the most widely used.⁶⁵

This procedure requires the combustion of the coal sample with a 1:2 ratio of coal and a mixture of sodium carbonate and calcined magnesium carbonate in air at $800 \pm 25^\circ\text{C}$. The sodium sulphate produced by this reaction is then precipitated as barium sulphate and determined by weighing.^{2,5,52}

2.9.4 Variation in Elemental Composition

The elemental composition of coal varies with both coal rank and type.^{2,9,32,52} The relative proportion of the elements carbon, hydrogen and oxygen vary for each of the three main coal maceral groups, inertinite, vitrinite and liptinite, and is incorporated in van Krevelen's H/C and O/C atomic ratio diagram (Figure 2.7).

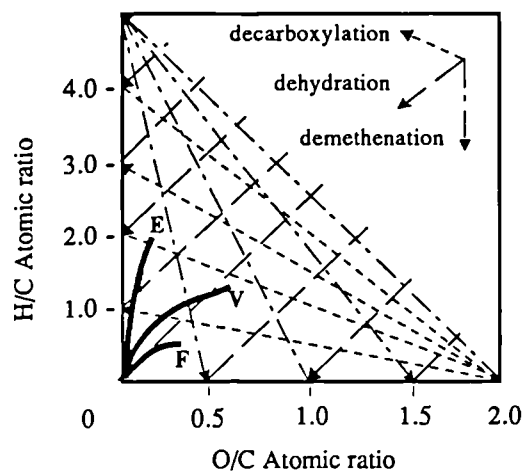


Figure 2.7 The H/C versus O/C atomic ratio diagram of van Krevelen, E. Exinite (Liptinite) macerals; V. Vitrinite macerals; F. Fusinite. (after van Krevelen and Schuyer⁷)

Because each maceral group is characterized chemically by different proportions of the three major elements, varying proportions of those macerals will strongly influence the overall bulk ultimate analysis of coal to such an extent that coals may be wrongfully assigned to a particular coal rank if using the elemental composition alone to determine rank,⁵³ properties or responses.⁶⁶

2.10 The Determination of Calorific Value

The calorific value of a coal, or specific energy,² is a direct measure of the chemical energy within coal and is therefore a valuable parameter for determining the suitability of a given coal as a fuel.⁵

Laboratory calorimetric determinations are conducted either under confined or open conditions.^{2,5,52} Under confined conditions the combustion products condense, causing the total amount of energy released by the coal to be increased due to the release of latent

heat during the analysis. This value represents the 'gross' calorific value;^{2,9,50} whereas, the heat given off during open combustion is known as the 'net calorific value'.^{2,50} The gross calorific value represents an over estimation of the actual specific energy during combustion and is subject to variation depending upon the moisture content of the coal sample.⁶⁷ The 'net calorific value' is determined from the gross value by subtracting 2.395 MJ kg⁻¹.^{50,56}

The most widely used type of calorimetric apparatus is the adiabatic bomb calorimeter.² The temperature of the water jacket surrounding the calorimeter is constantly adjusted during the reaction so that no corrections are required for heat loss.^{2,56} The ASTM D 2015 and 3286, ISO 1928 and BS 1016 (part 5) Standards contain detailed outlines governing the procedures. In addition, or as an alternative to direct analysis, the calorific value of a coal can be estimated using the Dulong formula:⁵

$$Q = 145.44 (C) + 620.28 (H - \frac{O}{8}) + 40.5 (S) \quad (2.7)$$

or the Mott and Spooner formula:⁵

$$Q = 145.4 (C) + 610 (H) - 62.5(O) + 40.5(S) \quad (2.8)$$

where: Q is the estimated calorific value.

C, H, O, S are the elements carbon, hydrogen, oxygen and sulphur (wt% d.a.f.).

Subject to the omnipresent problems of sampling in any coal analytical technique, the accumulation of errors or the influences of petrographic composition,^{5,54} the Mott and Spooner formula is claimed to be within ± 22 kJ⁻¹ of the measured value.⁵²

The calorific value of coal increases with increasing coal rank, largely due to the loss of oxygen within the organic fraction of coal.⁹ The ASTM classification of coals by rank (D 388-77) uses calorific value on a m.m.m.f. basis to differentiate low rank coals. Therefore, this parameter reflects both the increasing specific energy of the organic fraction and a decrease in the moisture-holding capacity of a coal.^{9,54}

2.11 The Determination of Grindability

The ability of a coal to undergo handling and transportation without excessive comminution and yet to be amenable to grinding during processing is an important property that is often determined in a standardized test.^{50,56} Grindability is a term that reflects the *ease* by which a coal may be crushed in comparison to a standard coal chosen to represent a grindability factor of 100.⁵⁶ The Hardgrove test, ASTM D 409, is the preferred method over the ball mill technique, because the operation is faster.⁵ The procedure specifies the required size fraction (1mm to 500µm), the equipment and methodology employed for the analysis. High Hardgrove indices are associated with coals that are soft and easy to grind² and there is a

claimed relationship between coal grindability and coal rank in that lignites and anthracites are more resistant to grinding.⁵ However, values derived for South African coals containing high proportions of inertinite suggest that grindability is influenced by petrographic composition.⁵³ Grindability is also influenced by the presence of cleats and microfractures in a coal.^{5,50} The mechanical properties of coals are apparently so loosely related to the characteristics of a coal, such as 'rank', that no justification for the inclusion of the parameter within a general classification scheme can be found.⁶⁸

2.12 Ash Fusibility

The ash fusibility test is an empirical test designed to provide an index of 'slagging potential'.^{56,59} The ASTM D 1857 Standard outlines a technique whereby coal ash is formed into cones (19 mm high) and heated to a temperature as high as possible. The profile shape of the ash pyramid at critical points is used to determine specific temperature indices. (Figure 2.8)^{2,56}

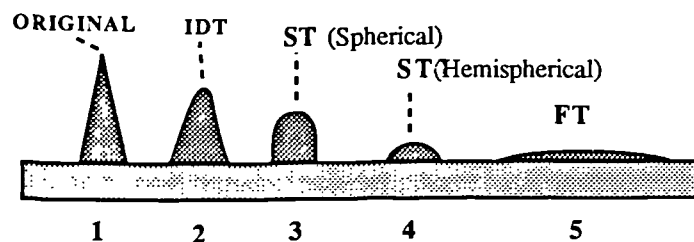


Figure 2.8 Profiles of ash pyramid specimens at critical points during ash fusion analysis.
1) original specimen., 2) the initial deformation temperature (IDT)., 3) the sphere temperature (ST)., 4) the hemispherical sphere temperature (ST)., 5) the flow temperature. (FT) (after Ward²)

The behaviour of the ash at high temperatures is related to chemical composition.⁵⁶ High proportions of alumina are considered to be the most refractory, whereas the presence of iron or potassium, for example, may reduce the ash fusion temperature.²

2.13 Behaviour upon Heating

2.13.1 General Considerations

The behaviour of the solid residue, after the release of moisture, gas and tar vapours, during (slow) heating is a means of classifying coals depending upon their agglomerating, caking and/or coking propensity.^{5,7,50} 'Caking' and 'coking' refer to the behaviour of a coal during rapid and slow rates of heating respectively,^{7,50} whereas 'agglomerating' refers to a coal's auto-binding ability⁵ when heated.

2.13.2 Free Swelling Index

The Free Swelling Index test (ASTM D720-67, BS 1016 pt 1 & 2) is based upon the volume change that takes place during heating at $400^{\circ}\text{C min}^{-1}$ up to a final temperature of 800°C , during which the coal is allowed to expand, unhindered, in a direction perpendicular to the heating surface.⁶⁰ Once the volatiles have been driven-off, the cross-sectional profile of the solid residue (button) is compared to a standard series of profiles. The swelling number is influenced by the particle size of the coal sample, the heating rate, petrographic composition and the extent of oxidation or weathering sustained by the coal.^{2,70}

2.13.3 Gray-King Assay

In this test (BS 1016, ISO 520-1982)), the proportion of solid, liquid and gaseous products that are released from the coal due to combustion are determined. The coal is heated in a sealed tube at a rate of $5^{\circ}\text{C min}^{-1}$ from 300 to 600°C , for low temperature carbonisation, or from 300 to 900°C for high temperature carbonisation. The solid residue is examined for coherence, fusibility and volume changes and related to standards of known behaviour. The volatiles are collected during carbonisation and the yield of each product determined.²

2.13.4 Gieseler Plastometer

The temperature range over which a coal remains fluid and the viscosity of that fluid mass are the two characteristics that are determined in this test.^{2,5,70} However, coal fluidity is dependent not only upon the inherent property of the coal but also upon the rate of heating, the final temperature and the duration of heating at that temperature. ASTM D 2639-74 outlines operating specifications for the Gieseler Plastometer.

2.13.4 Audibert-Arnu Dilatometer

The volume changes (contraction, swelling, dilatation) of a coal during carbonisation is the principle subject of this test (ISO R439).^{5,50,70} The unidirectional variation in length of a coal sample placed in a cylinder is monitored from 300°C up to 450° or 500°C at a heating rate of $3^{\circ}\text{C min}^{-1}$. Dilatometry is a test commonly used to determine the coking propensity of a coal and the swelling behaviour of a coke-charge at slow heating rates.⁷⁰

2.13.5 Roga Test

This is an East European test (ISO 335 1974) aimed at determining the caking propensity of a coal when mixed with standard anthracite, carbonised and tumbled in a drum-tumbler.^{2,7} There is a reasonable correlation between the free-swelling index parameter and the Roga index.²

Coal Characterisation Part III: Coal Classification

2.14 General Considerations

The diversity of organic source material, the condition during peat accumulation and peatification, followed by the subsequent processes of coalification, produce a fuel that is so heterogeneous that any expression or consideration concerning the composition or structure of coal has little meaning unless related to a scale.⁵² Because there is such a wide variation in the properties and composition of coal, attempts at detailed classification become very complex when full consideration is given to the wide range of uses of coal and the many analytical techniques available.⁵³ However, a classification scheme remains the standard means of communication between coal producers, users, engineers and scientists.^{2,53} A classification scheme is usually devised to serve a specific purpose and, therefore, the number of parameters employed to discriminate between a given range of coals will reflect the degree of complexity or simplicity of the scheme.^{52,53} In general terms, classification schemes may be subdivided into two categories:

- i. Those schemes that require a high degree of discrimination, with precision, between coals and utilize a wide range of properties and techniques such as: reflectance, ultimate, proximate, petrographic composition etc. Such schemes are often considered scientific and seek to discriminate between coals on the basis of composition, rank and origin.
- ii. Schemes that may be based upon legally defined parameters that are often straight forward and simple in use. Often those schemes have a tendency towards simplicity, usually using two discriminating parameters for commercial or technological purposes.

2.15 Domestic Commercial Classification Systems

At the most basic level, a classification system ought to be able to group together coals that are similar and distinguish between those that are not. Most of the European commercial classification systems (Figure 2.9) were based upon the results of proximate analysis, especially volatile matter.⁷ This is well illustrated by the Belgian classification system which is based upon volatile matter alone. The West German, French and Italian classification systems are all based upon volatile matter content plus one other parameter.^{2,7,52,54} All four classification systems are good examples of domestic commercial schemes designed specifically for domestic coals; empirically derived and correlated for use within their respective domestic markets.⁵³ They also reflect the heavy manufacturing base of those countries and their specific needs. The requirement for prime coking coals by the iron and steel industry and the understanding that European domestic coals are relatively consistent in ash content and reactivity negated any need to classify coals for combustion.^{53,71}

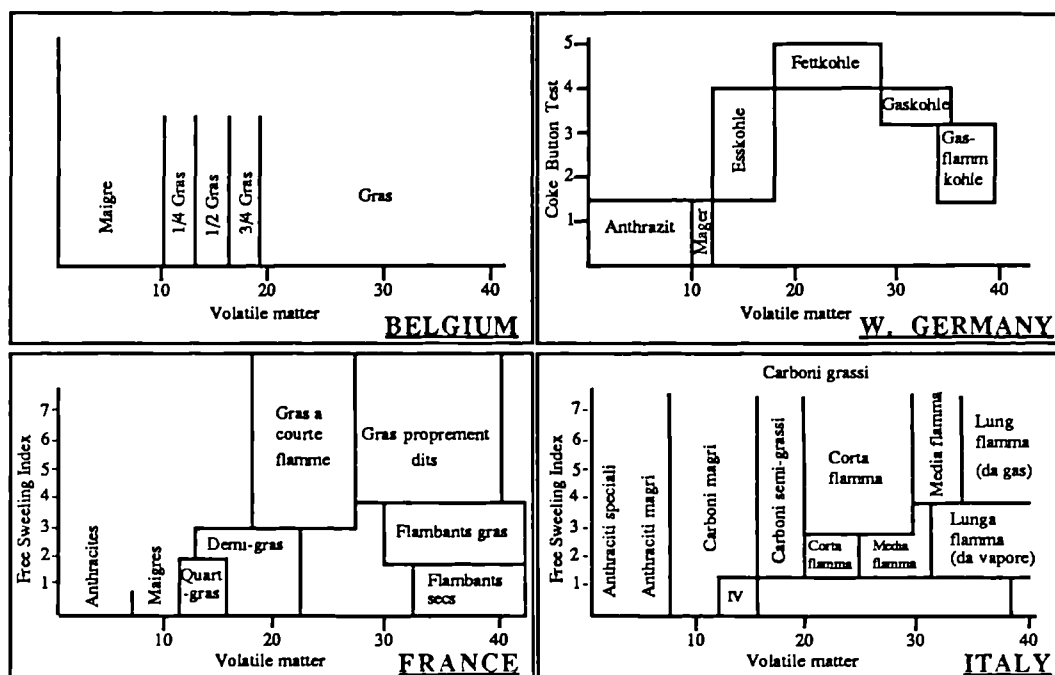


Figure 2.9 European commercial classification systems. (after Van Krevelen and Schuyer⁷)

The four European classification systems in Figure 2.9 and the British Gray-King system (Table 2.2) are schemes that seek to differentiate coals on their utilization characteristics, especially coking. The conditions used in the British Gray-King system are similar to those found in coke ovens.

Table 2.2 The British Gray King Classification Scheme (main classes only)

Coal rank code		Volatile matter (% d.m.m.f.)	Gray-King coke type	General description
Main class	Classes			
100 [†]	101-102	6.1- 9.0	A	Anthracites
200	201-204	9.1- 19.5	A-G8	Low-volatile steam coal
300	301-303	19.6-32.0	A-G9(and over)	Medium-volatile coals
400-900	401-902	Over 32.0	A-G9(and over)	High-volatile coals

† Anthracites can be sub-divided using hydrogen content $\pm 3.35\%$ (d.m.m.f.)
Notes: Heat affected coals would be distinguished by the suffix -H (e.g. 201H)
Weathered or oxidised coals are distinguished by using the suffix -W (e.g. 801W)
Coals with more than 10% ash must be washed prior to analysis

All five European classification systems outlined above are hierarchical, rank-based schemes. The use of volatile matter content is a valid empirical parameter for classifying domestic European hard coals, since those coals are predominantly vitrinite rich.^{9,51} However, misleading results occur when the same classification system is applied to Gondwanaland coals. For example, inertinite coals will have lower volatile matter yields

than comparable vitrinite-rich coals of the same rank^{3,54,67} and the reliability of that parameter has previously been discussed above. The ASTM classification system (Table 2.3) is also hierarchical, based upon proximate analysis, calorific value and agglomerating

Table 2.3 The ASTM Classification of Coal by Rank

Class	Group	Fixed Carbon		Volatile Matter		Calorific value		Agglomerating character
		≥ (% d.m.m.f.)	< (% d.m.m.f.)	> (% d.m.m.f.)	≤ (% d.m.m.f.)	≥ (Btu/lb m.m.f.)	< (Btu/lb m.m.f.)	
Anthracite	Semi-anthracite	86	92	8	14	Non-agglomerating
Bituminous	Low vol.	78	86	14	22	Commonly Agglomerating
	Med. vol.	69	78	22	31	
	High vol. A	...	69	31	...	14000	...	
	High vol. B	13000	14000	
	High vol. C	11500	13000	
						10500	11500	
Subbituminous		≤10500		Non-agglomerating

tendency. Above 69% fixed carbon, coals are classified by their volatile matter and fixed carbon values. Lower rank coals are differentiated on the basis of calorific value. The agglomerating characteristic is used to differentiate coals of similar rank.^{2,9,54} However, the classification system is seriously flawed in that it is specifically designed for homogeneous, vitrinite-rich coals.⁵⁴ Coals that are rich in exinite, inertinite or weathered are excluded. Only the British Gray-King system includes a designation for weathered coals using the suffix -w.^{2,9,54}

All classification systems discussed above reflect the markets (e.g. coking) and the coals for which the schemes were designed. There have been few attempts to cross-correlate different domestic classification schemes, although, such a comparison was conducted by the Teichmüllers during the 1950's,³² in which the German (DIN) and the American (ASTM) classification schemes were reproduced in one table (Table 2.4). The classification schemes are based upon the following standard analytical techniques: calorific value, bed moisture, carbon, volatile matter, and vitrinite reflectance. There are some important points regarding this work. Firstly, all analyses were conducted on vitrinite rich coals, as required by the ASTM system. Secondly, vitrinite reflectance is reported as % \bar{R}_O random, not % \bar{R}_O max. The former reflectance base is favoured in Germany, where optical anisotropy is comparatively small, whereas % \bar{R}_O max is preferred within Britain because optical anisotropy can significantly influence the measured values. Within the rank of anthracite the values may differ by 0.5% (\bar{R}_O max = 4.0%, \bar{R}_O random = 3.5%).

More recent processes, such as gasification, pulverised fuel combustion and liquefaction are not well served by present systems; for the more petrographically heterogeneous coals and coals from non-Carboniferous coalfields are difficult to classify.

Table 2.4 A comparison of the German (DIN) and North American (ASTM) Classification Systems and their distinction on the basis of different physical and chemical rank parameters.
(after Teichmüller & Teichmüller³²)

GERMAN	Rank	USA	%Rm	V.M.	C	Moist	C.V.	Applicability of Different Rank Parameters
			wt% d.a.f.	wt% d.a.f.	wt%	Btu/lb kcal/kg		
Weich- Matt- Glanz- Flamm- Gas- Fett- Löss- Mager- Anth.	Torf	Peat	0.2	68				
				64	60	75		
	Werk- kohle	Lignite	0.3	60			7200 4000	
						35		
	Sub- Bit		0.4	52	71	25	9900 5500	
			0.5					
	Bitum.	C	0.6		77	8-10	12600 7000	
	High Vol.	B	0.8					
		A	1.1	32				
Med. Vol. Bit.					87		15500 8650	
			1.5	22				
	Low Vol.							
	Bit.		1.9	8	91			
Anth.	Anth.		2.5					
			4.0					

%Rm represents the random reflectance of vitrinite in oil., VM, is the volatile matter., C represents elemental carbon, Moist. represents bed moisture, CV represents calorific value.

There would appear to be a real need for an international classification system applicable to all hard coals.^{9,54,67} However, it is doubtful that any one scheme would be suitable for all the gasification, liquefaction and combustion processes currently in use, but the need to have a common base through which vendors and buyers may communicate is the quest of the international classification systems.

2.16 International Classification Systems

2.16.1 The International Hard Coal Classification by Type

To facilitate the international exchange of coal on a standardized basis, a single unified classification system was sought. The Coal Committee of the Economic Commission for

Europe (ECE) was created for the purpose of devising a commercial system, based upon existing domestic systems, that would define the properties of all European coals and arrange them into classes or groups.^{2,53,54} In 1956, the International Classification of Hard Coal by Type⁷² was created. It is more elaborate than any European domestic system and it represents a commercial system, based upon coal rank, that utilizes a three-digit coding system to define each coal.^{2,4} Coals are assigned to classes 0 through to 5 on the basis of volatile matter (d.a.f.), whereas lower rank coals (VM = 33% d.a.f.) are ascribed to their respective classes (6 to 9 inclusive) by reference to their gross calorific value (m.a.f.).⁷² The class sub-division, representing the second digit, is a reflection of caking properties ('free-swelling index' or Roga index). The final sub-division and digit represent coking propensity, derived through either the Gray-King assay or Arnu-dilatometer tests.⁷⁰

The designation 'hard coal' indicates that coals (e.g. lignites) with gross calorific values less than 23.86 MJ kg⁻¹ are excluded from the system.^{2,70} The reference 'by type' is considered^{53,54} to be a misnomer because 'type' normally refers to petrographic composition. Volatile matter content is unsuitable as a basis for any international classification system; reflecting the dependency of that parameter upon heating rate, particle size, petrographic composition etc.⁵⁷ Furthermore, the system cannot be considered truly 'international' in that Gondwanaland coals are not adequately classified in that system; the classification system is only applicable to coals with a homogeneous maceral composition and low-inertinite composition.⁵³

2.16.2 The International Codification System for Medium and High Rank Coals

This system was endorsed by the Economic Commission for Europe in April 1988⁷³ and effectively superseded the older ECE Hard Coal classification system (Section 2.16.1). Eight parameters have been selected to specify a coal for various purposes and uses² with the intention that the codification system will enable producers, vendors and purchasers to communicate unambiguously with regard to coal quality and respective applications.⁷³ The eight parameters selected are:

- random reflectance of the vitrinite (%R_Orandom)
- reflectogram of the vitrinite (%R_Orandom)
- maceral composition (vol %)
- crucible swelling number
- volatile matter (d.a.f. wt%)
- ash (wt % d.b.)
- total sulphur (wt % d.b.)
- gross calorific value (d.a.f. MJ kg⁻¹)

The cut-off point for low and high rank coals is more satisfactorily defined than other

systems in that coals below 24 MJ kg⁻¹ with a mean random reflectance (%R_{0random}) of 0.6% are designated as low rank coals and excluded from the codification system. Also, unlike any other classification system, the ECE codification system (Table 2.5) is intended for use with run-of-mine, washed or blends of coal; therefore, rendering it much more flexible than existing classification systems. As a possible means of including non-Carboniferous coals, the proportion of inertinite within a coal is enumerated within the parameter of maceral composition. The inclusion of such a parameter may be prejudicial to vendors of Gondwanaland coals since there is no internationally accepted means of discriminating between reactive and un-reactive inertinite.

Table 2.5 The Economic Commission for Europe 'Codification of Hard Coals'

<u>Vitrinite Reflectance</u>		<u>Reflectogram</u>			<u>Maceral Composition</u>				<u>Swelling Number</u>		
(Mean Random)		Standard			Inertinite ^b		Liptinite				
Code	R _{random} %	Code	Deviation		Code	Vol. %	Code	Vol. %	Code	Number	
02	0.2 - 0.29	0	0.1	no gap	0	0 - 9	1	1 - 4	0	0	or 0.5
03	0.3 - 0.39	1	0.1/0.2	no gap	1	10 - 19	2	5 - 9	1	1	or 1.5
04	0.4 - 0.49	2	0.2	no gap	2	20 - 29	3	10 - 14	2	2	or 2.5
-	-	3	0.2	1 gap	-	-	-	-	-	-	-
49	4.9 - 4.99	4	0.2	2 gaps	-	-	-	-	-	-	-
50	5.0	5	0.2	2 gaps	8	80 - 89	8	35 - 39	8	8	or 8.5
					9	90+	9	40	9	9	or 9.5

<u>Volatile Matter^c</u>		<u>Ash</u>		<u>Total Sulphur</u>		<u>Gross Calorific Value</u>	
(d.a.f.)		(dry)		(dry)		(d.a.f.)	
Code	Percent	Code	wt%.	Code	wt.%	Code	MJ/kg ⁻¹
48	48	00	0 - 0.9	00	0.0 - 0.19	24	24 - 24.98
46	46 - 48	01	1 - 1.9	01	0.1 - 0.19	25	25 - 25.98
44	-	-	-	-	-	-	-
02	2 - 4	20	20 - 20.9	20	2.0 - 2.09	35	35 - 35.98
00	2	-	-	-	-	-	-

a) Classification does not include the lower rank coals: those coals with a mean random reflectance lower than 0.6% or a gross calorific value (m.a.f.) is greater 24MJ/kg⁻¹.

b) Part of the Inertinite maybe reactive.

c) Coals with ash content greater than 10% must be cleaned before analysis to give a maximum yield of coal.

Carpenter⁵⁴ in a discussion of the *draft* proposal, which consisted of six parameters, comments upon the validity of the analytical techniques used, most of which include the recognised inherent problems associated with the various techniques previously discussed in this Chapter. However, most of Carpenter's criticisms are facile. The review fails to recognise that the ECE Codification system recognises and recommends specific standard tests and procedures. Thereby attempting to standardise *both* assay and the classification process. The ECE Codification system is, without doubt, a compromise but all parameters are given equal weighting. Anomalous values, for example, an unexpected low volatile matter yield for a given coal may be cross-referenced to other parameters such as reflectance, calorific value and maceral composition. In this way, coals previously difficult to classify in domestic and previous international classification systems may be accommodated.

2.17 Scientific Classification Systems

Commercial classification systems arrange coals into 'classes' according to their suitability for some specific use. In the case of domestic systems, this usually involves one or two properties of technological interest selected on an empirical basis.⁹ Scientific classification systems, by comparison, combine several properties, presenting the user with alternative criteria with which to classify a coal.

The classification systems by Seyler^{74,75,76,77} and Mott are two of the most comprehensive systems in current usage.⁵² More recently, systems have been proposed by Alpern⁷⁹ and Falcon⁵³ that incorporate additional expressions of coal quality and consider coals from a much wider origin than the earlier systems.

2.17.1 Seyler's Classification System

The system devised by Seyler, originally in 1899⁷⁴ and subsequently perfected by him,⁷⁷ was based initially upon an extensive study of a wide range of coals from Great Britain⁷ and later extended to include a wider range of coals from Britain and Europe.⁵⁰ A plot of the elements carbon and hydrogen (percentages), for coals of various rank, defined a curved band that graphically represented the coalification tract of those coals. Low rank coals, containing the highest hydrogen and lowest carbon content, plot to the right of the coalification band. Seyler succeeded in correlating elemental composition (%C and %H) with both volatile matter and calorific value (d.m.m.f. basis). The relationships between elemental composition and technological properties were given as:⁷

$$Q = 388.12H + 123.92C - 4269 \quad (2.9)$$

$$VM = 10.61H - 1.24C + 84.15 \quad (2.10)$$

$$H = 0.069 (Q/100 + VM) - 2.86 \quad (2.11)$$

$$C = 0.59 (Q/100 - 0.367 VM) + 43.4 \quad (2.12)$$

where: Q = the calorific value
VM = the volatile matter content
H and C = the wt% of the hydrogen and carbon

The relationships of the four properties outlined above formed the basis of the renowned 'coal chart' (Figure 2.10). Coals were classed in four groups or 'species' according to carbon content. Each species of coal was subsequently sub-divided into varieties of general according to hydrogen content.^{7,76} Coals considered 'normal' were given the prefix *ortho*-; such coals were typically vitrains.⁵⁴ Coals that contained more carbon than the norm for a given rank were given the prefix *meta*-, whereas carbon-lean coals were denoted

by the prefix *para*-.⁷⁶

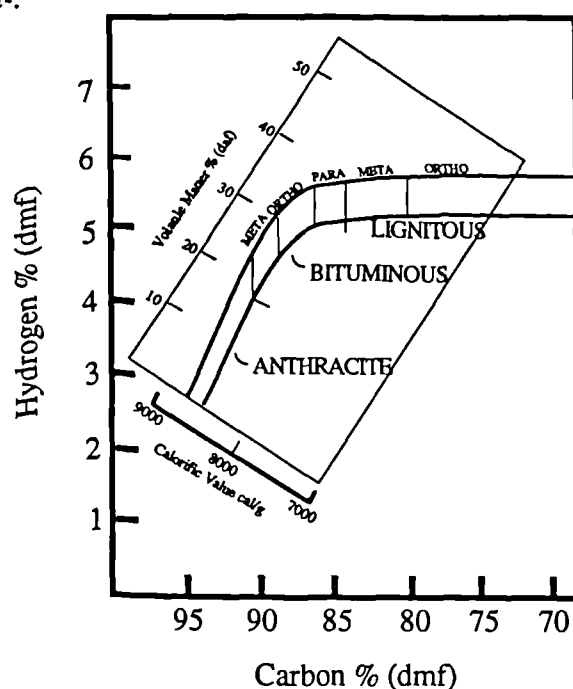


Figure 2.10 Seyler's coal chart showing the relationship between the elemental composition, volatile matter content and calorific value of coal. (after van Krevelen and Schuyer⁷)

Similarly, hydrogen-rich coals were differentiated by the prefix *per*- (perhydrous) and hydrogen-lean coals were given the prefix *sub*- (subhydrous).⁷⁶ In this way, Seyler sought to accommodate within his system, variations in chemical composition. The *para*- and *per*-types were coals rich in liptinites (clarains), whereas the *meta*- or *sub*- types were coals containing a higher proportion of inertinites (durains).

The main criticism of the Seyler classification system was its alleged restrictive applicability.^{52,77,78} Because the system was based upon British and European coals, the system did not perform well when used in conjunction with North American coals⁷⁸ or other non-Carboniferous coals.⁵⁴ Other limitations or criticisms cited concerning this system included:

- the limited rank range of coals used to derive the relationships and equations given above (2.9 to 2.12),^{7,52}
- the classification was too complex for use as a commercial system,⁵²
- ultimate analysis was too time consuming for regular usage by a commercial laboratory, and
- the terminology was considered to be too complex and confusing.⁵⁰

However, viewed in a historical context, Seyler's classification system demonstrates that inter-relationships exist between various coal properties. It also inspired other graphical representations depicting coal properties or behaviour, such as those by van Krevelen⁷ and Mott⁷⁷ and it is probably still the most favoured scientific classification scheme.

2.17.2 Mott's Classification System

Mott's⁷⁷ coal classification chart bears an initial resemblance to that of Seyler's classification chart. However, the basic rectangular co-ordinates are different in that Mott used volatile matter content (d.m.m.f.) and calorific value (d.m.m.f.) with a superimposed grid representing carbon and hydrogen (% d.m.m.f.) to differentiate between lignites of differing composition. Another distinction between the two classification systems is that Mott based his coalification band and correlations upon a wide range of coals from different countries. As with Seyler's chart, Berkowitz⁵² doubts the statistical validity of the coal band on Mott's chart for coals with a carbon content of 80% or less, due to the great scatter in analyses. Van Krevelen and Schuyer⁷ are more critical, commenting that the system is too complicated both in the number of sub-divisions incorporated within the system and in the selected nomenclature. Furthermore, van Krevelen and Schuyer⁷ comment on the lack of consideration given by Mott to coals differing in petrographic composition. They consider this a serious limitation, stating that it would be difficult to assess a coal's coking propensity by referring specifically to its volatile matter and calorific value. In a slightly earlier publication, Mott⁷⁸ discussed the relationships between %hydrogen and %carbon (Parr basis) and the caking and swelling properties of coal. Neither Seyler nor Mott give any consideration to coal grade, i.e. the mineral (inorganic) contaminants within coal.⁵³ This is one of the main features of the more recent 'scientific' type of classification such as those proposed by Alpern⁷⁹ and Falcon.⁵³

2.17.3 Recent Scientific Classification Systems

Both Alpern⁷⁹ and Falcon⁵³ employ a three dimensional diagrammatic representation of their systems. They are clearly much more complex and intricate than those of Seyler or Mott. Alpern⁷⁹ uses nomenclature for the various classes, whereas Falcon⁵³ offers the user the option of a coding system or nomenclature. The two systems differ from all previous scientific and commercial systems in that they:

- offer a descriptive terminology for use in coal seam characterisation and, in the case of Falcon's system, offer a coding system for technological and legal use.
- use a hierarchical system (rank) based upon vitrinite reflectance with subdivisions achieved by considering coal type (compositional parameter) and coal grade (mineral content).
- the systems utilize a three-dimensional framework.
- avoid the problem concerning the inertinite content of Gondwanaland coals by creating a new term 'total reactives' (liptinite + vitrinite + reactive semi-fusinite) that is given a scale (0 -100).

It is difficult to comment upon possible international reaction to such systems. They are unlikely to find favour with the protagonists of simple domestic systems like that of the Belgian system. However, it is possible that vendors of Gondwanaland coals would support the new term 'total reactives', therefore avoiding the inert = 'unreactive label' implicit in present maceral terminology. Just how 'reactive' those coals are under certain utilisation conditions, such as pulverised fuel combustion, is still undergoing investigation. Certainly, coals from different geographical regions do not behave in the same way and some means of classification is required that incorporates a means of indicating or 'predicting' utilisation characteristics.

2.18 In Retrospect

All existing commercial classification schemes were originally devised for a specific purpose; that is, to classify coals depending upon specific properties, empirically related to a particular process (i.e. coke making). It is evident that the success of new or existing classification schemes depends upon the suitability of the classification parameters to a particular process or utility. The parameters required for the selection of suitable feedstock for utilities such as carbonisation or liquefaction are not necessarily the most applicable in the case of pulverised fuel combustion. This thesis describes investigations of coal devolatilisation, char formation, char type and burn-out under conditions (i.e. heating rate), relevant to those encountered in an industrial pulverised coal boiler, as a means of understanding the process involved with a view to suggesting ways in which coal feedstock may be characterised and classified.

References

1. Pillar, H. (1977). 'Microscope Photometry', Springer-Verlag, Berlin.
2. Ward, C.R. (1984). 'Coal Geology and Coal Technology', Blackwell, Oxford, 1-39.
3. Davis, A. (1975). *Microstructural Science* **3**, 973-990.
4. International Handbook of Coal Petrography (1963) 1st Edition, plus 2nd Edition (1971) and 3rd Supplement (1973). International Committee for Coal Petrology, C.N.R.S., Paris.
5. Ergun, S. (1979) in: 'Coal Conversion Technology', (Wen, C.Y., and Stanley Lee, E. Eds.), Addison-Wesley, Reading, Massachusetts, 1-56.
6. Stach, E. (1982) in: Stach's 'Textbook of Coal Petrology' 3rd Ed. Stach, E., Mackowsky, M-Th., Teichmüller, M., Taylor, G.H., Chandra, D. and Teichmüller, R. Gebrüder Börntraeger, Berlin, 87-218.
7. van Krevelen, D.W., and Schuyer, J. (1957). 'Coal Science: Aspects of Coal Constitution', Elsevier, Amsterdam.
8. Murchison, D.G., and Boulton, E.H. (1961). *Fuel* **40**, 389-406.
9. Neavel, R.C. (1981) in: 'Chemistry of Coal Utilisation' (Elliot, M.A. Ed.). 2nd Supplementary Volume, John Wiley and Sons Inc., New York, 91-158.
10. Glagolev, A.A. (1934). *Engng. Min. J.* **135**, 399-400.
11. Barringer, A.R. (1953). *Trans. Inst. Min. Metall.* **63**, 21-41.
12. Murchison, D.G. (1978) in: 'Analytical Methods for Coal and Coal Products', (Karr, C. Ed.) Academic Press, New York, 415-464.
13. International Committee for Coal Petrology, Standards Working Group. Aachen, September, 1988.
14. Mackowsky, M-Th., and Kötter, K. (1960). *Rev. Industr. Minér.* **42**, 1-16.
15. Damberger, H.H., Harvey, R.D., Ruch, R.D., and Thomas, J. (1984) in: 'The Science and Technology of Coal and Coal Utilization', (Cooper, B.R. and Ellingson, W.A. Ed.). Plenum Press, New York, London, 7-45.
16. Bend, S.L. Edwards, I.A.S., and Marsh, H. (1989). *Proc. Int. Conf. on Coal Science, Japan*, 437-440.
17. Given, P.H., and Drykacz, G. (1988) in: 'New Trends in Coal Science', (Yurum, Y. Ed.), Kluwer Academic Publishers, Dordrecht, 53-72.
18. Styan, W.B., and Bustin, R.M. (1983). *Int. J. of Coal Geol.* **2**, 321-370.
19. Jones, J.M., and Murchison, D.G. (1981). 'You can pick it up in afternoon: Principles of Petrology' Unpublished. Dept. of Geology, Newcastle upon Tyne University, Newcastle upon Tyne.
20. Alpern, B. (1971). *Bull. Soc. fr. Minéral Cristallogr.* **24**, 179-180.
21. McCartney, J.T., and Ergun, S. (1958). *Fuel* **37**, 272-282.
22. British Standards Institute, BS 6127.
23. Hirsch, P.B. (1954). *Proc. Roy. Soc. Lond.* **226**, 143-169.
24. Davis, A. (1978) in: 'Analytical Methods for Coal and Coal Products', (Karr, C. Ed.) Academic Press, New York, 27-81.
25. Hoffman, E., and Jenkner, A. (1932). *Glückauf* **68**, 31-88.
26. Hevia, V., and Virgos, J.M. (1976). *J. of Microscopy* **109**, 23-28.
27. McCartney, J.T., and Teichmüller, M. (1972). *Fuel* **51**, 64-68.
28. Ting, F.C. (1978) in: 'Analytical Methods for Coal and Coal Products' (Karr, C. Ed.), Academic Press, London, 3-26.
29. McCartney, J.T., and Teichmüller, M. (1972). *Fuel* **53**, 63.
30. Hoffman, E., and Jenkner, A. (1932). *Glückauf* **68**, 61-88.
31. Patteisky, K., and Teichmüller, M. (1960). *Brennst. Chem.* **41**, 97-104.
32. Teichmüller, M. (1982) in: Stach's 'Textbook of Coal Petrology' 3rd Ed. Stach, E., Mackowsky, M-Th., Teichmüller, M., Taylor, G.H., Chandra, D. and Teichmüller, R., Gebrüder Börntraeger, Berlin.
33. Smith, G.C., and Cook, A.C. (1980). *Fuel* **59**, 641-646.
34. Crelling, J.C. (1983). *J. Microsc.* **132**, 251-266.
35. Lee, J.B. (1985). *J. of Microscopy* **137**, 145-154.
36. Chao, B.C.T., Minkin, J.A., and Thompson, C.L. (1982). *Int. J. of Coal Geol.* **2**, 113-150.
37. Kuili, J., Jian, X., and Duohu, H. (1988). *Int. J. of Coal Geol.* **2**, 385-395.
38. Ottenjan, K., Teichmüller, M., and Woolf, M. (1974). *Fortsch. Rheinld. Westfalen*, **24**, 49-64.
39. Lin, R., Davis, A., Bensley, D.F., and Derbyshire, F.J. (1985). *Int. J. of Coal Geol.* **6**, 215-228.

41. Hagemann, H.W., Ottenjann, K., Puttnamm, W., Wolff, M., and Wolf-Fischer, E. (1988). Erdöl und Kohle Erdgas **42**, 99-10.
42. Quick, J.C., Davis, A., and Lin, R. (1988). Ironmaking Conference Proc. **47**, 331-337.
43. Bend, S.L., Edwards, I.A.S. and Marsh, H. (1989). Extended Abstract. 19th Biennial Conf. on Carbon, June 25-30th, 1989 Penn State University, Pennsylvania, USA.
44. Teichmüller, M., and Wolf M. (1977). J. of Microscopy **109**, 49-73.
45. Teichmüller, M., and Durand, B. (1983). Int. J. of Coal Geology **2**, 197-230.
46. Wayne, R.P. (1970). 'Photochemistry', Butterworths, London.
47. Lin, R. and Davis, A. (1988). Org. Geochem. **12**, 363-374.
48. Khorasani G.K. (1987). Org. Geochem. **11**, 157-168.
49. Stout, S.A., and Bensley, D.F. (1987). Int. J. of Coal Geol. **7**, 119-133.
50. Elliot, M.A., and Yohe, G.R. (1981) in: 'Chemistry of Coal Utilisation' 2nd Edn. (Elliot, M.A. Ed.) Wiley-Interscience, New York, 1-54.
51. Karr, C. (1978) in: 'Analytical Methods for Coal and Coal Products' Vol I. (Karr, C. Ed.) Academic Press, New York, Preface.
52. Berkowitz, N.L. (1979) 'An Introduction to Coal Technology' Academic Press, New York.
53. Falcon, R.M.S. (1986) in: 'Mineral Deposits of S. Africa', No. 11. (Anbaeaurer, E.R. and Maske, S. Eds.), Geol. Soc. S. Africa, Johannesburg, 1899-1921.
54. Carpenter, A.M. (1987). 'Geochemistry of Coal Classification', Draft Discussion Paper, IEA Coal Research.
55. Given, P.H (1984) in: 'Coal Science', Vol. 3 (Gorbaty, M.K., Larsen, J.W. and Wender, I. Eds.) Academic Press, San Diego, 63-252, 339-341.
56. Montgomery, W.J. (1978) in: 'Analytical Methods for Coal and Coal Products' Vol. I. (Karr, C. Ed.) Academic Press, New York, 192-246.
57. Given, P.H., and Yarzab, R.F. (1978) in 'Analytical Methods for Coal and Coal Products' Vol. II. (Karr, C. Ed.) Academic Press, New York, 3-42.
58. Cumming, J. (1987). M.Sc. Thesis, Unpublished, University of Salford, Salford, UK.
59. Gulskotter, H.J., Shimp, N.F., and Ruch, R.R. (1981) in: 'Chemistry of Coal Utilisation' Vol. II (Elliot, M.A. Ed.) Wiley-Interscience, 369-424.
60. Allardice, D.J., and Evans, D.G. (1978) in: 'Analytical Methods for Coal and Coal Products' Vol. I (Karr, C. Ed.) Academic Press, New York, 247-262.
61. Horsfield, B., Denbicki, H., and Ho, T.T.Y. (1983). J. Geol. Soc. London **140**, 431-443.
62. Parr, S.W., and Wheeler, W.F. (1909). Univ. Illinois Eng. Exp. Sta. Bull. No. 37.
63. King, J.G., Maries, M.B., and Crossley, H.E. (1936). J. Soc. Chem. Ind. **55**, 277-281.
64. Durand, B., and Monin J.C. (1980) in: 'Kerogen' (Durand, B. Ed.) Editions Technip, Paris, 113-142.
65. Shimp, N.F., Kuhn, S.K., and Helfinstine, R.J. (1977) Energy Sources **3**, 93-109.
66. Neavel, R.C., Smith, S.E., Hippo, E.J., and Miller, R.N. (1986). Fuel **65**, 312-320.
67. Cook, A.C. (1976) in: 'Australian Black Coal' (Cook, A.C. Ed.) Aust. Min. Metall. Illwarra Branch., A.B.C., Symposium, Melbourne. 68-84.
68. Pearson, D.E. (1985) in: 'Coal in Canada' (Patching, T.H. Ed.) C.I.M. and M., Montreal, Can., 21-30.
69. Brewer, R.E. (1945) in: 'Chemistry of Coal Utilisation' Vol I. (Lowry, H.H. Ed.) John Wiley and Sons, New York, 160-309.
70. Habermehl, D., Orywal, F., and Beyer, H.D. (1981) in: 'Chemistry of Coal Utilisation' Vol II (Elliot, M.A. Ed.) Wiley-Interscience, New York, 317-368.
71. Economic Commision for Europe. (1956). 'International Classification of Hard Coal by Type'. ECE, United Nations. E/ECE/247; E/ECECoal/110, Geneva, Switzerland.
72. Economic Commision for Europe. (1988) International Codification System for Medium and High Rank Coals. ECE, United Nations. E.88IIE.15, Geneva, Switzerland.
73. Seyler, C.A. (1899). Proc. S. Wales Inst, Engrs. **21**, 483-526.
74. Seyler, C.A. (1900). Proc. S. Wales Inst, Engrs. **22**, 112-120.
75. Seyler, C.A. (1924). Fuel **3**, 15-26, 41-49, 79-83.
76. Seyler, C.A. (1938). Proc. S. Wales Inst, Engrs **53**, 254-327.
77. Mott, R.A. (1942). Fuel **21**, 126-135.
78. Mott, R.A. (1942). Fuel **22**, 20-26.
79. Alpern, B. (1981). Bull. Rech. Explor. Prod., Elf Aquitaine, Pau., **5**, (2) 271-290.

CHAPTER THREE

'Pulverised Coal Combustion'

3.1 Introduction

Between 1953 and 1983 the consumption of electricity in the United Kingdom more than doubled.¹ Such an increase in demand for cheap electrical power by industry and the domestic market requires economies of scale. Over the same thirty-year period, power generation sets have grown within the United Kingdom from 30 MW, with thermal efficiencies of approximately 28%, up to 660 MW units with associated thermal efficiencies of 38%.^{2,3} Small, multi-engine electrical generation units, based upon the internal combustion engine seldom exceed a total capacity of 100 MW; and, at present, maximum thermal efficiencies are only possible through the use of large, fossil-fuel, steam turbine generation sets,² typified by the large 500 and 660 MW generating sets used in the UK and the very large 1300 MW generating sets used in the USA.⁴ The majority of the large base-load steam generating sets rely upon pulverised fuel as the main source of energy due to the relatively high efficiencies gained through pulverised fuel combustion and the favourable price and availability of coal.^{2,3}

3.2 Pulverised Coal Utility Boilers

3.2.1 Utility Boiler and Burner Configurations

There are a variety of utility boiler types and burner configurations used throughout the world, which depend upon the generating capacity of the system (which determines the size of the utility boiler), the rank and type of coal to be burned and whether the utility boiler is designed for the removal of ash in the dry or molten state.^{3,4} Utility boiler and burner configurations 'a' to 'e' in Figure 3.1 represent 'dry-bottom' utility boilers.⁴ Such boilers are designed to ensure that no contact occurs between the flame and water-wall,^{3,4} with the lowest incidence of ash fouling and slagging possible.⁴ Utility boiler type 'f' (Figure 3.1) contains a 'cyclone' burner in which a greater proportion of the ash produced during combustion collects as molten slag at the base of the boiler and represents one of the many variants of 'wet-bottom' utility boilers in use.^{4,5} 'Dry-bottom' units represent the greatest proportion of utility boilers currently in use outside the Soviet Union.⁴ They are generally larger, have a higher steam capacity and are more adaptable to varying loads than 'wet bottom' utility boilers,^{3,4} which are discussed and reviewed by Ceely and Daman.⁴ Burners that produce a long narrow flame, colloquially known as 'single-shot burners',⁵ (Figure 3.1a) are used in cement kilns and are inappropriate for use in modern utility boilers,^{3,4,5} either because combustion still occurs beyond the region of the steam re-heaters or because

those burners are incapable of reducing the production of NO_x .³ Early boiler designs adapted the long-flame design in a downward firing burner configuration (Figure 3.1b) known as 'U-flame' boilers; a 'w-flame' configuration is a back-to-back version of the single burner variant.⁴

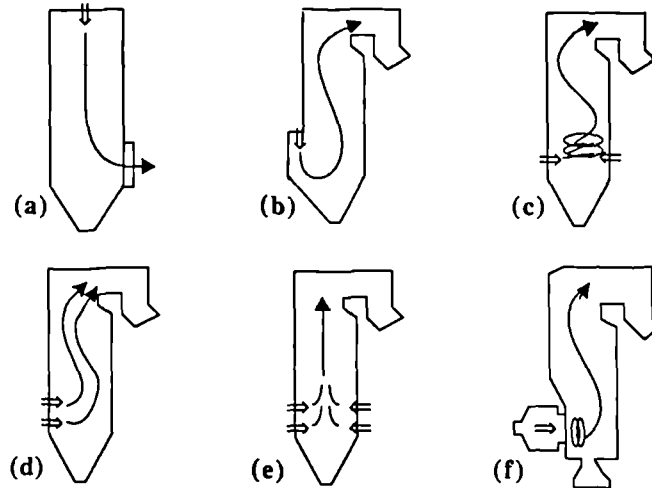


Figure 3.1 Utility boiler and burner configurations used in pulverised fuel combustion: (a) vertical, (b) single U-flame, (c) tangential, (d) horizontal [front or rear], (e) horizontal [opposed], (f) horizontal cyclone. (adapted from Ceely and Daman,⁴ and Essenhigh⁷)

'U-flame' utility boilers typically fired anthracites or coke; material that burned slowly, therefore, requiring longer residence times for complete combustion within the utility boiler.⁴ Few such units remain in service.⁵ A tangential burner configuration (Figure 3.1c and Figure 3.2) reduces flame turbulence at the mouth of the burner almost completely, the

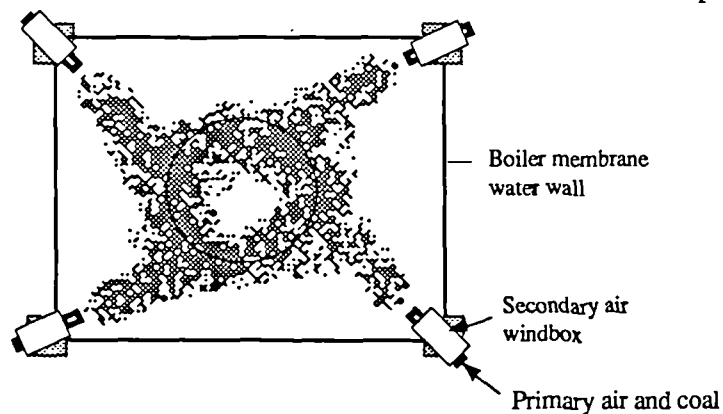


Figure 3.2 Schematic cross-section of a tangential-burner furnace configuration showing a typical burner 'off-set' and the location of the 'fire-ball'. (after Essenhigh⁵)

utility boiler effectively acts like a large burner.⁴ In this configuration, where the burning material is fired from the corner of the utility boiler (Figure 3.2), a single swirling-flame is created, enveloping the central portion of the utility boiler.^{4,5} Such configurations apparently favour low levels of NO_x formation.⁴ A tilt and swivel facility for each burner provides the necessary control of combustion residence times and superheater temperatures.^{4,7}

Horizontal and opposed burner configurations (Figure 3.1d and e) represent the more typical, modern, large, high capacity utility boiler and burner arrangement used to raise steam for electricity generation.³ The circular, turbulent burners utilise either single or double register secondary air ports;^{3,5} the dual register type representing a recent development for use as a low NO_x burner.³ The short 'bushy' flame (Figure 3.3) is generated by the rotation of

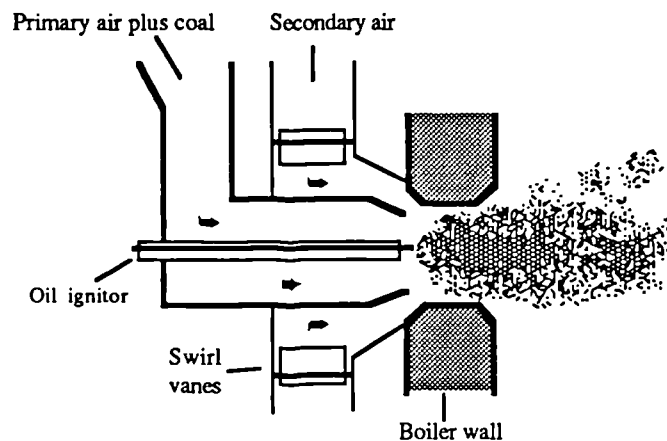


Figure 3.3 A schematic cross-sectional representation of a single register low NO_x pulverised coal burner. (adapted from Essenhigh⁵)

the secondary air through an arrangement of 'swirl vanes' within the burner wind-box. The rotating mass of air within the flame envelope creates an aerodynamic back-mix of combusting gases and solids, generating a short 'turbulent' and 'bushy' flame that has good flame stability characteristics capable of self sustained ignition.^{3,5} Circular turbulent burners are fixed. They are therefore, incapable of superheater temperature regulation by inclining the burner, unlike the tangential-burner (Figure 3.2).⁵ Changes in utility boiler residence times and the control of superheater temperature is usually achieved by varying the number (up to 60) and the configuration of burners used, by varying the amount of excess air used for combustion, or by the attemperation of the high temperature steam.³

3.2.2 The Modern Utility Boiler

During the combustion of pulverised coal, a mixture of air and finely ground coal is injected into the utility boiler⁵ in which 90 to 98% of all particles are below 100 μm ⁶ although, the actual particle size distribution is usually regulated according to the rank of the coal.² A small proportion of the air required for combustion (15 to 20%) is used to transport the pulverised fuel into the region of the burner and this is known as the primary air. The remainder of the air required for combustion is introduced at the mouth of the burner and is known as the secondary air.³ The entrainment of the coal through the coal-feed equipment requires velocities of 20 to 28 m s^{-1} ,² producing a typical firing density of 30 $\text{kg hr}^{-1} \text{m}^3$.^{3,4} Combustion times for pulverised coal are in the order of 1 s with heating rates of 10^4 to

$10^5 \text{ }^\circ\text{C s}^{-1}$ and during optimal combustion conditions, the flame typically occupies one half to two thirds of the combustion volume within the utility boiler.^{3,4,5}

The modern, high pressure, high temperature 660 MW pulverised coal utility boiler (Figure 3.4) consists of a tall vertical fire box (up to 55 m) with the following features:^{2,3,5}

- membrane-type water walls
- contains up to 60 pulverised fuel burners
- uses platen type superheaters and re-heaters
- uses forced and induced draught air-blowers
- is supplied by adjustable coal pulverising mills and feed system
- is provided with grit and ash collectors
- is able to burn a wide variety of coals
- is capable of operating at less than full load
- is designed to completely combust the pulverised coal, with residual carbon-carry over levels within the fly-ash, of less-than 2%

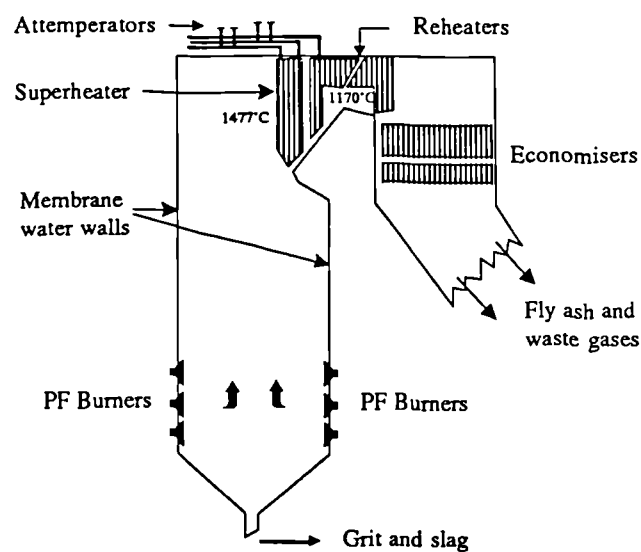


Figure 3.4 A schematic diagram of a radiant, high pressure, high temperature water-wall pulverised coal utility boiler. (adapted from Babcock and Wilcox,³ and Essenhigh⁵)

The conversion of water into steam is achieved by the radiative and convective transfer of heat from the flames to the boiler tubes³ with an optimisation of maximum temperatures within the region of the superheaters.^{3,4} Combustion temperatures for a 660 MW utility boiler are typically 1477°C (1750K) within the superheaters (Figure 3.4) and 1170°C (1443K) within the re-heater.² This translates into a superheated steam temperature of 568°C (841K) at a pressure of 166.5 bar and a steam flow of 561 kg s^{-1} under normal operating load.^{2,3}

3.2.3 Coal Feed System

To achieve the fine particle size ($< 100 \mu\text{m}$) required for pulverised coal combustion, high capacity pneumatic coal feeders and pulverisers are required, capable of rapid response to changes in generation load.^{2,3} In the larger 660 MW generating units, 10 coal mills supply 60 circular turbulent-flow burners. Each mill supplies a horizontal row of burners.³ The coal is transported from the coal feeder into the pulverising mill by hot air (removing any bed or inherent moisture^{3,5}) to each pressurised pulverising mill which contains a ball and ring type of grinding surface. The circulating air flow through the pulverised mill is controlled in relation to the velocity required for transporting the fuel to the burners (air-fuel ratio, Section 3.3.2).^{3,5} Oversize coal is separated by the classifier and returned to the grinding zone.³ The provision for varying the grinding force applied during the milling of the coal and the use of a classifier enables a variety of coals of different Grindability indices (Chapter 2) to be pulverised using the same coal feed and milling equipment.^{3,6} The use of Hardgrove indices assists in pre-determining the required settings for coal pulverisation,³ anthracites and semi-anthracites being harder than bituminous coals, whereas lignites have an added complication for milling due to their very high moisture content.^{2,6}

3.2.4 Fly Ash Collection

The combustion of pulverised coal generates extremely fine particles of ash (*fly ash*) due to the ashing of mineral matter that is incorporated within coal, a 500 MW boiler operating at full load can produce up to 1500 t (1.5×10^6 kg) of fly ash per day.⁶ Therefore, the efficient removal of entrained fly ash from flue gases is a necessary feature of any pulverised coal utility boiler and requires the selection of a coal with known ash fusion characteristics (e.g. ash fusion temperature, slagging temperature, Chapter 2.12).^{3,6} The removal of entrained 'fly ash' is achieved by passing the fly ash and waste gases through electrostatic precipitators that have a claimed efficiency of up to 99.5%.² Slag and larger grit particles fall to the bottom of the utility boiler into the water-cooled, hopper-shaped bottom from which the grit and slag is removed hydraulically or pneumatically.^{2,6}

3.3 Coal Combustion: An Overview

3.3.1 Background

Most coals are considered to be suitable for combustion,⁹ although their suitability for use in pulverised fuel combustion depends not only upon the nature (type/rank) of the coal but also upon the required power output of the generating equipment and the design of the utility boiler, plus ancillary equipment.³ Essenhigh⁵ notes that a qualitative assessment of the heating and combustion characteristics of different coals suggests similarities in behaviour during combustion, although he qualifies that statement by adding that any discussion

concerned with coal combustion or heating phenomena must carry the qualification: 'governed by coal type, and/or experimental conditions such as particle size, heating rate, particle density and reaction temperature'. It is well documented in the literature⁷⁻¹⁵ that all of the above factors are important in determining the rates of devolatilisation and char gasification, although there is no consensus of opinion as to which 'factor' predominates during the process of combustion. In fact, no single factor would appear to predominate due to the interdependent and associated relationships between all factors during the various stages of coal combustion. However, recent experiences concerning the combustion of widely different coals have indicated the importance of considering coal type as a major factor in pulverised fuel combustion (Section 3.7).

3.3.2 The Classical View of Coal Combustion

Entrained coal particles entering a flame during pulverised coal combustion undergo rapid heating, at rates of 10^4 to 10^5 °C s⁻¹, attaining temperatures in the range of 1400° to 1600°C (1670 to 1870°K) within 10 ms to 50 ms of the total time required for complete combustion (≈ 1 s).^{10,11} The very rapid temperature increase within small coal particles (<100 μ m) is the result of an energy transfer, in the form of thermal radiation, from the existing flame to the dark-coloured coal particles.¹⁰ The rapid rates of heating have a marked effect upon the coal particles (Figure 3.5), initially inducing a thermal degradation (*pyrolysis*) of the coal macromolecule,^{5,7,16,17} accompanied by a pronounced swelling in bituminous coal particles and rapidly followed by the release of volatile material (CO, CO₂, light hydrocarbons and 'tars').^{5,11,18,19,20}

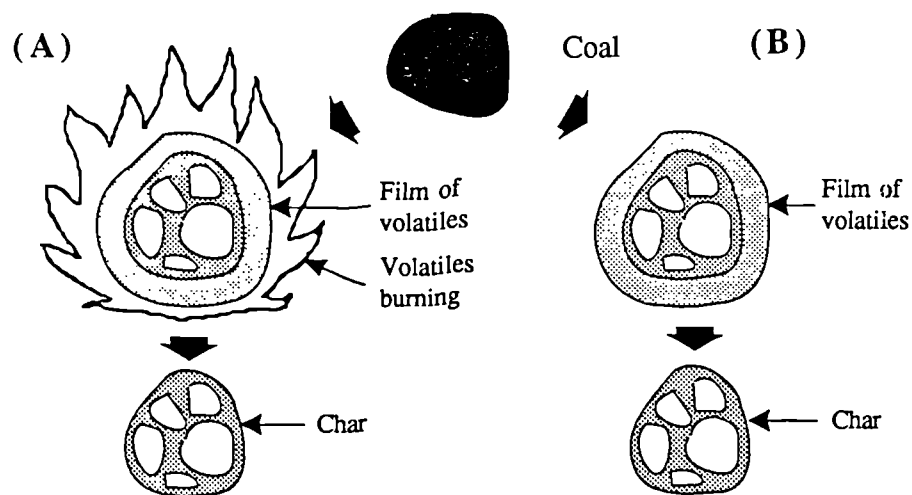


Figure 3.5 A schematic representation of a single coal particle undergoing pyrolysis in either the presence (A) or absence (B) of oxygen. (modified from Wen, C.Y. and Dutta, S.²¹)

The duration of *pyrolysis*, during which devolatilisation of the coal particle occurs, is considered to take place within 10 to 50 ms of the total time required for complete combustion^{10,16,18} and is accompanied by homogeneous gas/gas and heterogeneous

liquid/gas reactions involving the oxidation of reactants and volatiles.¹⁸ The combustion of the volatile material is considered to account for 70 to 80% of the total heat released during the entire combustion process.²² The ignition of volatile material generates a 'flame sheet' that surrounds the coal particle,^{23,24} feeding radiant energy back to the coal particle, the surrounding gaseous environment⁷ and the boiler membrane water-walls.²⁵ During the combustion of volatiles, very little oxidation (gasification) of the solid carbonaceous residue (char) is thought to occur.^{16,22} However, during the pyrolysis of the coal particle, the characteristics of the residual char (pore structure, size, shape, density, reactivity) are determined due to the generation of vacuols resulting from rapid devolatilisation. Which is considered to be controlled by coal type and rank, temperature, pressure (internal/external to the char) and particle size.¹¹ Residual char gasification (heterogeneous solid/gas reactions) - 'char burnout', occurs within and down stream of the flame envelope;²² over a period of time ranging from 30 ms⁻¹ to over 1 s⁻¹, depending upon the characteristics of the char.^{11,26,27} Char gasification is considered to be dependent upon the characteristics of the char that are formed during devolatilisation, such as: optical texture, active surface area, porosity and permeability. In addition the variations in temperature and pressure, presence of inorganics, and the constraints placed upon the mass transport of the gaseous reactants all play important roles in char gasification.^{11,13,18,19,26,27}

The classical concept of pulverised coal combustion is, therefore, one of initial rapid pyrolysis, ignition and the combustion of the volatiles, followed by the relatively slower process of heterogeneous char gasification.^{19,27} The various stages involved during the combustion of pulverised coal will be discussed in more detail below.

3.3.3 Laboratory Based Studies, the Techniques and Rationale

The assessment of coal behaviour and the reactions that occur during combustion is difficult without the use of laboratory based reactors that simulate the phenomenon of combustion and the *typical environment under which it occurs*. Carefully controlled laboratory based experiments provide both qualitative and quantitative data concerning the behaviour of coal during pyrolysis and the subsequent slower stage of char oxidation.^{6,13,16,21} When studying coal combustion phenomena, it is usual to treat the combustion process as consisting of two separate and distinct stages, mirroring the classical concept of combustion outlined above (Section 3.3.2) consisting initially of pyrolysis, followed by a separate subsequent char gasification process.^{13,28,29} The mechanisms of pyrolysis and char gasification represent different phenomena. Pyrolysis involves the thermal decomposition of coal accompanied by homogeneous gas/gas and heterogeneous liquid/gas reactions, whereas char gasification represents a heterogeneous solid/gas reaction.^{16,19,21,26}

There are a variety of techniques available for the study of pyrolysis and/or combustion phenomena that can be subdivided into two broad areas: those techniques that utilize slow heating rates (>1 °C s⁻¹) and densely packed samples and those employing high heating rates

($10^3 - 10^4$ °C s⁻¹) and dispersed coal samples.²⁸ The former is of interest particularly to those studying coking and carbonisation phenomena and will not be discussed further. A review of such techniques is given by Howard.³⁰ Techniques utilising high heating rates create realistic conditions applicable to pulverised fuel combustion and pyrolysis phenomena. Common features to all types of apparatus are:^{16,21,28,30}

- high temperatures, up to 1600 °C (1850 K+)
- high heating rates, up to 10^5 °C s⁻¹, typically 10^4 °C s⁻¹
- dilute sample loadings
- short reaction times
- a minimisation of secondary reactions
- small coal particles, typically <100 µm
- variable atmospheres (depending upon phenomenon studied)

Howard³⁰ distinguishes between two general classes of fast pyrolysis techniques; *captive techniques* in which the sample is fixed or stationary during heating (i.e. heated grid,^{31,32} 'pyro-probe'³³ and more recently curie-point pyrolysis^{29,34,35}), or *continuous flow techniques* in which the coal is continuously fed into and removed from the 'hot-zone' during the experiment (e.g. entrained flow reactor apparatus^{12,13,16,23,24} and laminar flame techniques^{25,37}). Captive techniques are suitable for both qualitative and quantitative forms of analysis using on-line detection equipment such as: pyrolysis-gas chromatography,^{25,37} pyrolysis-mass spectroscopy,^{38,39} pyrolysis-elemental analysis⁴⁰ and pyrolysis-Fourier transform-infra red techniques.⁴¹ The advent of absolute quantization, using 'internal standards' (e.g. poly- α -methylstyrene)^{42,43} during *flash pyrolysis* (i.e. captive techniques), offers the potential for the absolute quantization of pyrolysates rather than determining relative proportions.

However, no technique is without its limitations or faults. Captive pyrolysis techniques are micro-analytical tools and demand small sample sizes, usually <200 mg, but typically 5 mg.^{28,30} Because the proportion of char generated by such techniques is extremely low, they are therefore excluded as char preparation techniques. Furthermore, there is the inherent problem of obtaining a representative sample from a given large sample of coal. Experimental techniques using heated screens or ribbons require continuous purging through the reactor with a suitable carrier gas (e.g. N₂, He) to prevent secondary reactions, either on the heated surface or on the walls of the reactor. Thermal inertia is cited³⁰ as a potential problem area when using a captive pyrolysis technique, because the heating surface could be 2000 times the mass of the sample, thereby complicating residence times and increasing the prospect of secondary reactions occurring.

The most widely used apparatus to study pyrolysis and char oxidation processes, typical of combustion, is the entrained flow reactor (Figure 3.6).

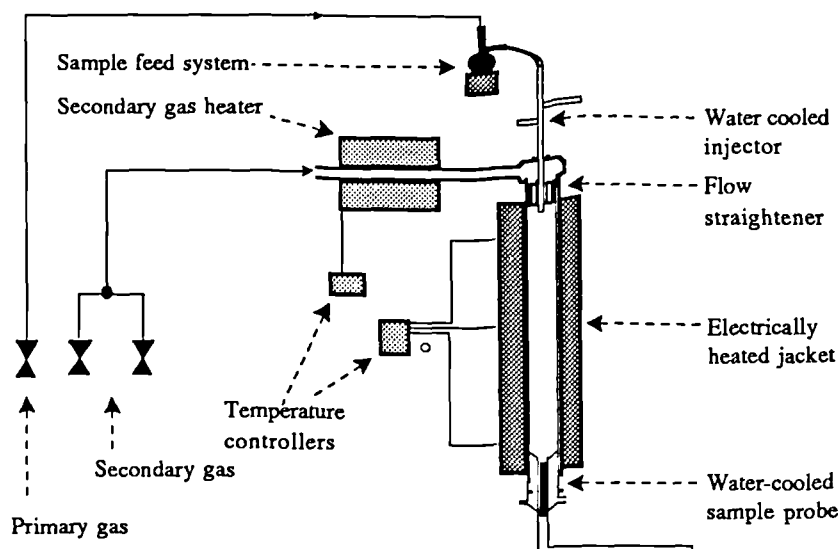


Figure 3.6 A schematic representation of an electrically heated entrained flow apparatus.

Coal particles ($<100\ \mu\text{m}$) are swept into the hot reaction zone using a primary gas supply (N_2 , He, Ar) through a water cooled injector and supplemented by a much larger, pre-heated, secondary gas supply. The entrainment of the coal particles, under laminar flow conditions within the reactor reduces the incidence of particle dispersion, thereby maintaining theoretical residence times. Collection of the products is achieved by using a water cooled probe and/or cyclone, thereby reducing the prospect of secondary reactions. Residence times are adjusted either by regulating the secondary gas flow or by varying the distance between the sample injector and collection probe. Typical residence times are less than 1 second with reported heating rates of 10^4 to $10^5\ ^\circ\text{C s}^{-1}$, giving heating times of $5\text{--}200\ \text{ms}$.^{6,12,13,16,22,28,30,36} Residence times are calculated using either gas or particle velocity models.^{27,36} Unlike captive heating techniques, the attraction of continuous flow techniques is in the homogeneous and even heating of the coal particle.³⁰ Furthermore, the design, geometry and behaviour of continuous flow apparatus simulates the conditions within the utility boiler during combustion.²⁹ This is regarded to be a very important consideration.

3.4 Coal Combustion: Devolatilisation and Char Formation

The term pyrolysis is derived from the Greek $\piυρoς$ (fire) and $\lambdaυειν$ (loose, untie), therefore, reactions involving some form of pyrolysis mechanism are those that involve the thermal decomposition of material at high temperatures.²⁸ However, the pyrolysis of coal is complex and consists of both parallel and consecutive reactions in a free radical environment.^{21,29} To understand the mechanisms, reactions and nature of the products that occur during pyrolysis, the laboratory based techniques outlined above are used over a wide range of temperatures and heating rates, in an attempt to understand the complex behaviour of 'coal' during the initial stages of pulverised coal combustion; which encompass the processes

of devolatilisation and char formation.

One facet of rapid pyrolysis that is commonly reported^{8,30} is that the weight loss at high heating rates, is greater than the weight loss that occurs at slower heating rates, typical of volatile matter determinations during proximate analysis. Essenhigh⁶ estimates that the ratio of observed weight loss, resulting from high temperature rapid pyrolysis (HTRP), to that estimated from the volatile matter content derived from proximate analysis is 1.5 to 2.0. However, in reality the situation is more complex. Suuberg *et al.*,⁴⁴ and more recently Solomon *et al.*,⁴¹ studying the effects of HTRP on lignite and bituminous coal demonstrated that an increase in weight loss during pyrolysis can be obtained not only by higher heating rates but also by increasing the final temperature of pyrolysis. Furthermore, both the yield of volatiles and the range of volatile species vary with both coal type and rank,^{15,17,31,32,37,41,44} considered to be related to the thermoplastic behaviour of the metaplast during char formation.⁴⁵ Studies involving the flash pyrolysis of coal macerals and coals of differing petrographic composition indicate that the total yield of volatiles decreases in the order liptinite → vitrinite → inertinite.^{30,44} The volatiles derived from macerals of the liptinite group generally contain a higher proportion of hydrocarbons (alkanes, alkenes, alkadienes, hydroaromatics, etc.) whereas vitrinites generally yield volatiles with higher proportions of phenolic and aromatic compounds.^{30,38} The range of volatile species also varies as a function of rank during HTRP.²⁹ Volatiles obtained from lignites are dominated by oxygen-bearing volatile species, such as H₂O, CO₂ and CO and only minor amounts of tar and hydrocarbons (Figure 3.7). In contrast coals of bituminous rank yield volatiles containing a greater proportion of tar and hydrocarbons.^{41,44}

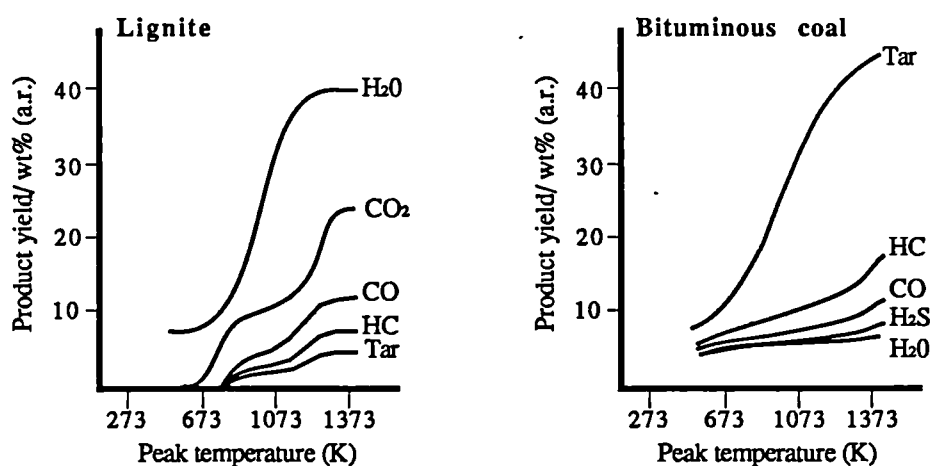
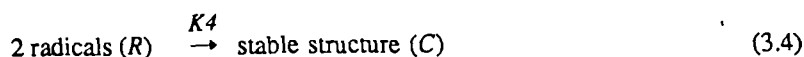
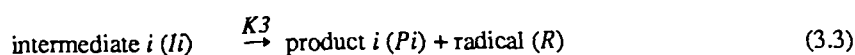
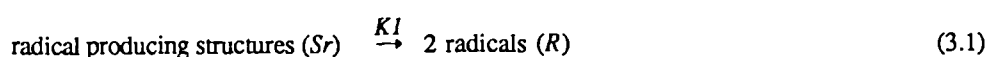


Figure 3.7 Pyrolysis product distributions from a Lignite and Bituminous coal rapidly heated to different temperatures (after Suuberg *et al.*⁴⁴)

Such differences reflect not only the experimental conditions (temperature, heating rate, etc.) but, more significantly, changes at the molecular level within coal due to coalification. As discussed in Chapter One, a consequence of coalification is the progressive removal of

oxygen-bearing functional groups from the structure of coal.⁴⁶ The presence of oxygen-bearing functional groups within lignites has been shown to influence tar yields during HTRP, in that lignites with high O/C-ratios are associated with lower tar yields compared to lignites of the same rank with lower O/C-ratios.¹⁸ During HTRP, the coal structure is thought to depolymerise by the scission of the least stable bonds considered to be the weak bridges (functional groups, methylene structures) that form the linkages between the aromatic and hydroaromatic clusters.^{17,18,28,41,47,48,49} The topic of bond scission and radical interaction, within complex structures like coal, has received much attention.^{19,30,50} A proposed sequence for the cracking of polyaromatics (such as coal) is: (a) generation of hydrogen radicals by the scission of weak alkyl bridges, (b) hydrogen attack on outer aromatic rings, (c) successive naphthenic ring openings, and (d) side chain cracking.³⁰ The sequence is outlined in the following general scheme:³⁰



The chemical nature of the radicals (*R*), interacting structure (*Si*), radical producing structure (*Sr*), intermediate (*Ii*), and stable structures (*C*) are intentionally general in this model. The major feature of the radical producing structure (*Sr*) is the production of radicals (step 3.1) that can interact either directly or via some chain reaction within a given structure (*i*) ultimately yielding a pyrolysate product.³⁰ The retention of volatile species, especially the larger molecular weight material (tars), within the softened particle (metaplast) promotes the occurrence of secondary reactions, such as cracking, re-polymerisation (cross-linking) and condensation reactions.^{28,41,47,48,49} Mass transfer limitations,^{31,51} representing the inability of volatile species to escape from the metaplast either by diffusion or by bubble transport,^{48,52} promotes the cracking of volatile species through the enhancement of secondary reactions involving the trapped 'tar-like' larger molecular weight material within the metaplast.^{21,32,50} Secondary reactions are considered to represent either cracking reactions or condensation / polymerisation reactions.²⁷ Cracking reactions are considered to generate stable, low molecular weight material (i.e. gases), that escape to the flame envelope,²⁴ and a carbon residue which is deposited on the char surface.^{18,27} Alternatively, condensation / polymerisation reactions form high molecular weight material which is incorporated as char material.²⁷ The formation of gaseous material, generating higher pressures within a particle, is regarded by Gray⁵³ as the mechanism for the explosive release of volatiles in some bituminous coals during HTRP.

Solomon *et al*^{48,49} discuss their rank independent Functional Group-Depolymerisation,

Vapourisation and Cross-linking model (FG-DVC) that encompasses coal devolatilisation, char formation (Figure 3.8) and mass transport effects in conjunction with the concept of

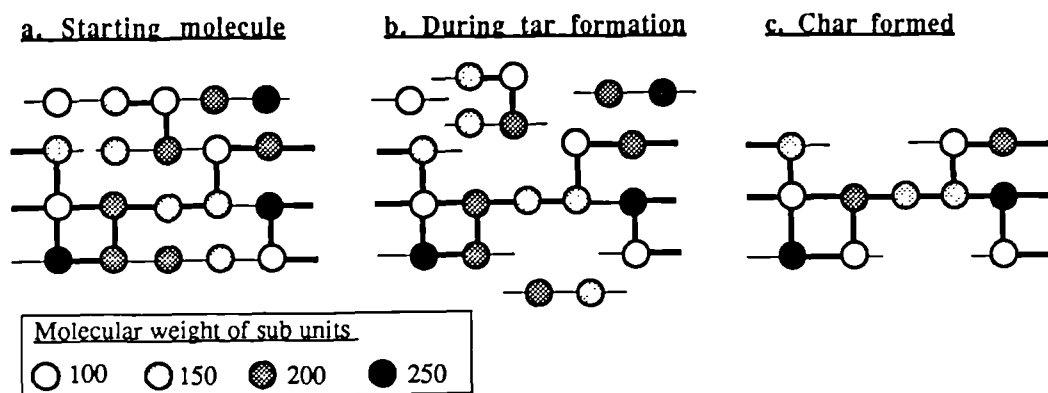


Figure 3.8 A representation of tar and char formation due to the selective scission of bridges between aromatic ring clusters. (after Solomon *et al*⁴⁹)
In the FG-DVC model the circles represent monomers (ring clusters and peripheral groups). The molecular weights, as indicated, represent the molecular weight of each monomer including the attached bridges. The thin line-bridges are breakable and can donate hydrogen whereas the thickened lines are considered unbreakable and do not donate hydrogen. 1a, the parent coal is represented by a two dimensional network of oligomers, consisting of 'n' condensed ring clusters linked by breakable and un-breakable bridges. 1b, during pyrolysis selective bond scission occurs, some bonds have been converted to unbreakable bonds by the abstraction of hydrogen (to stabilise the free radicals) with the creation of new cross-links. 1c, a char is formed.

competing reactions. The essential feature of the FG-DVC model is that all pyrolysis products compete for donateable hydrogen for stabilisation. The relative proportions of functional groups and methylene bridges (the aromatisation of hydroaromatics is not considered) within the parent coal determine metaplast viscosity, the extent of cross-linking, the proportion and molecular weight of tar and the species of gaseous products during HTRP. The amount and molecular size of macromolecular sub-units within the char determines the char viscosity which, in turn, control the transport of volatile species through the particle during pyrolysis.⁴⁸ The model has merit in that the model provides a useful qualitative and descriptive view of a complex process. However, the model, faithfully represented in Figure 3.8, implies that the distribution and molecular weight of monomers within the char is determined by a pre-arranged and fixed number of monomers and bridge structures within the parent coal. The plastic or 'fluid' transformations of coal to char during pyrolysis and increases in volatile matter yield with increasing rates of heating⁶ demonstrate that this is not so. In this respect the FG-DVC model contrasts with the thinking behind the models of Niksa and Kerstein.

The prediction of volatile products and rates of char formation evolution during pyrolysis was the aim of the Distributed Energy Chain Model (DISCHAIN) of Niksa and Kerstein,⁵⁴ which they later developed into two mathematical renderings of rapid pyrolysis: DISARAY

(Distributed Energy Array Model) and DISKIN (Distributed Energy Reaction Kinetics Model).⁵⁵ All models essentially treat coal as a macromolecular structure and devolatilisation as a complex polymer degradation. The liberation of aromatic nuclei, by bridge dissociation, forms free monomers which are consumed by either recombination reactions and form char or escape as volatile species. The difference between DISKIN and DISRAY is that DISKIN assumes stoichiometric proportions between monomers and chain segments and is purely a chemical-kinetic formulation, whereas DISRAY using network statistics is able to account for higher tar yields at faster heating rates due to the higher activation energy of tar formation. From the DISRAY model Niksa and Kerstein estimate that upper limits exist for the number of bound aromatic units that are converted to monomers during pyrolysis; representing an upper theoretical limit on volatile yields, which are given as 82% at 10^2 K s^{-1} and 93% at 10^5 K s^{-1} . To accommodate the network statistics used in the DISRAY model, the macromolecular structure of coal is simplified by adopting a BETHE lattice (Figure 3.9) in which the number of links at each node is four ($z = 4$).

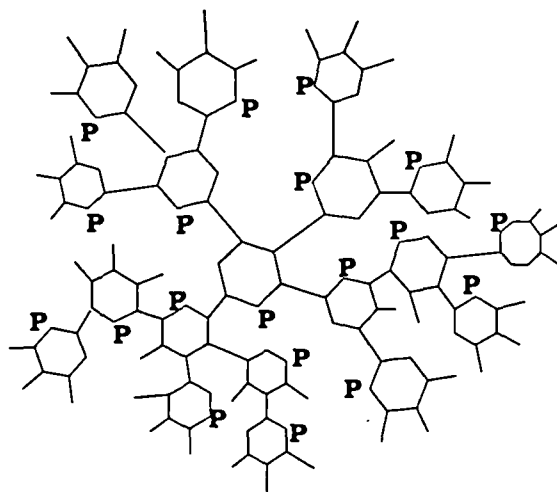


Figure 3.9 A model representation of the macromolecular structure of coal according to Niksa and Kerstein⁵⁵ based upon the Bethe lattice with a coordination number of $z = 4$. A typical lattice consists of node points and links; nodes correspond to aromatic units, links to bridges and each node is given one peripheral group (P).

3.5 Coal Combustion: The Combustion of Volatiles

Hüttinger¹⁹ considers the combustion of volatiles to involve homogeneous gas/gas and heterogeneous liquid/gas reactions. Unfortunately, information on the former is scant and non-existent relating to the latter.^{2,8,19} Due to the complex nature of volatile species (tar and gases), little attention has been given to oxidation reactions involving volatiles.¹⁹ Early approximations were borrowed from oil drop combustion theory in which the volatiles were assumed to form a spherical film around the particle and burnt at a rate controlled by boundary layer diffusion,⁷ later known as 'flame sheet' models.²³ The Diffusion Limited Volatile Model (DVLC) (Figure 3.10), which is a more recent variant of the 'flame sheet'

model, assumes that the combustion of volatiles proceeds via a homogeneous gas/gas reaction and largely ignores possible heterogeneous liquid/gas reactions as postulated by Hüttinger.¹⁹ Furthermore, there is the implicit assumption within the model that the homogeneous gas/gas reaction rate is greater than the rate of mass transport of reacting species; therefore, oxidation of volatiles takes place on a thin stoichiometric surface (Figure 3.10a), represented as a flame sheet, in which the mass flux of volatiles to oxygen is equal to

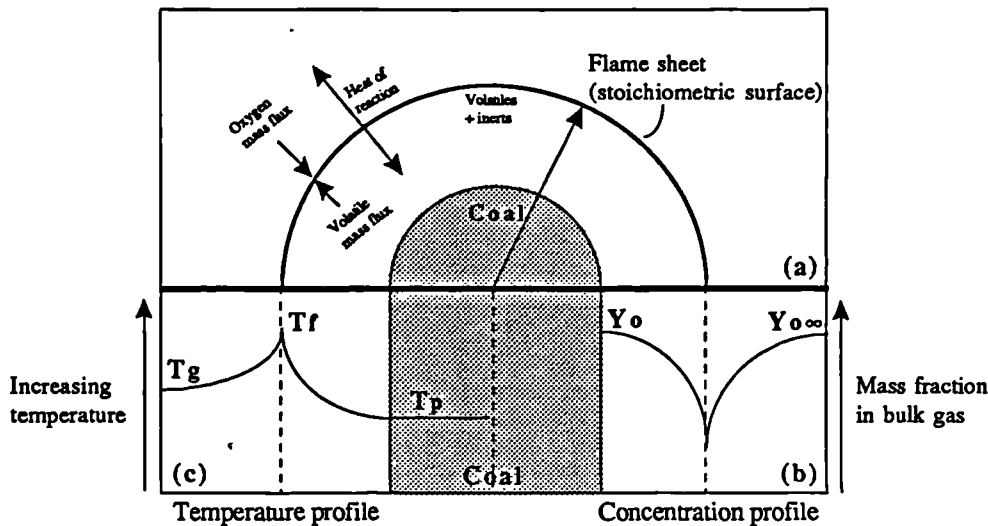
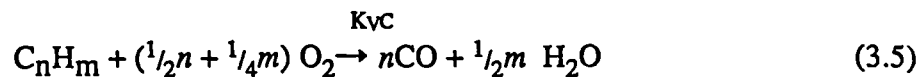


Figure 3.10 A diagrammatic representation of the Diffusion Limited Volatile Model (DVLC) utilising the 'flame sheet' concept. (after Gururajan *et al.*²⁴)
In the above diagram T_p represents the Particle temperature ($^{\circ}\text{K}$), T_f is the flame temperature ($^{\circ}\text{K}$), T_g is the ambient gas temperature ($^{\circ}\text{K}$), $Y_{O\infty}$ is the concentration of oxygen and Y_O is the concentration of gaseous volatiles.

the stoichiometric ratio (Figure 3.10 b). The model also assumes that within the flame sheet, volatiles are partially oxidised to CO and H_2O , whereas CO is oxidised to CO_2 outside that stoichiometric surface.²⁴ Therefore, the combustion of volatiles in the DVLC model consists of two stages: firstly, the oxidation of volatiles to CO and H_2O and, secondly, the subsequent oxidation of $\text{CO} \rightarrow \text{CO}_2$.²⁴ The volatile combustion rate (K_{VC}) for the conversion of volatiles to CO and H_2O has been estimated by Hampartsoumian *et al.*⁵⁶ in which:



where: K_{VC} represents the reaction rate for volatiles combustion
 n is the apparent order of reaction ($n = m + 1/2$)
 m true order of reaction
 C_nH_m a generalised formula for hydrocarbon volatile species
 O_2 reactant species, oxygen (mole/m^3)

A variation of this oxidation scheme is also discussed by Essenhigh,⁷ in which volatiles react initially to produce CO and H_2 , with the oxidation of CO as the final process.

3.6 Coal Combustion: Char Oxidation

Following the process of coal devolatilisation and the combustion of volatiles, the slower process ($>1 \text{ sec}^{-1}$) of char combustion or oxidation occurs. The rate of oxidation is considered to be controlled by chemical kinetics, mass transport limitations, or a combination of the two, depending upon the temperature under which the reactions occur and the size, and the porosity of the particle undergoing oxidation.^{6,8,27,56,57,58} Despite extensive research into char oxidation phenomena at high temperatures ($>1000^\circ\text{C}$), the char-oxygen (carbon-oxygen) reaction is still not completely understood partly due to the complex nature of the reacting surface and the interplay of factors during combustion.^{56,58} The overall reaction scheme involving char combustion can be simply stated thus:^{9,27,59}

- the diffusion of mass (reactant and product species) and heat across the char particle boundary layer (gas/solid interface)
- the diffusion of mass and heat through the char particle structure
- the heterogeneous gas/solid reaction

Which ever of the three processes outlined above determines the overall reaction rate is considered to be the rate controlling step. For example, diffusion of mass is likely to become the rate controlling step if the chemical reaction (heterogeneous gas/solid reaction) is very fast and/or the particle is very large (c.a. $1000 \mu\text{m}$).²¹

Three general scenarios plus two intermediates (Figure 3.11) are considered by Walker *et al*⁵⁷ to represent plausible mass transport situations; indicated by apparent activation energies that are functions of temperature, pressure, O_2 concentration, particle size and porosity.^{8,19,21,27,57} Zone I (Figure 3.11) represents situations in which low temperatures predominate and the chemical reaction rate is slow.^{27,57} The concentration of reactant gas

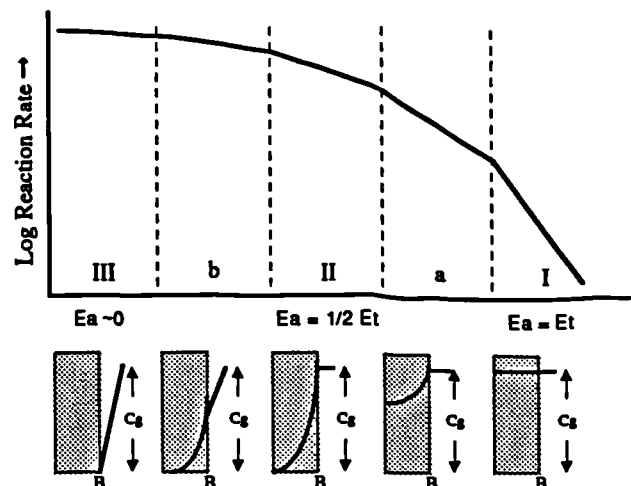


Figure 3.11

The three idealised zones (III - I), plus intermediaries (a & b), representing the change of reaction rate of a porous char in response to changes in temperature and the concentration of reactant gas (C_g) across the 'boundary layer' or the gas/solid interface (B) and within the char (stippled area). (after Walker *et al*⁵⁷ and Hüttinger¹⁹)

(Cg) within the particle is similar to that of the bulk gas outside the 'boundary layer' (gas/solid interface), because the reactant gas is able to diffuse across the solid/gas interface (Sb) and through the pore network of the particle without instantly reacting. When reactions do occur the reactant gas is replaced easily and quickly from outside the boundary layer.^{56,57} Because the chemical reaction rate is slow, char oxidation under such conditions have (high) apparent activation energies (E_a) equal to the true activation energy (E_t). This implies that true activation energies may only be experimentally determined under chemically controlled conditions.²⁷ At very high temperatures, represented by Zone III, the rapid reaction rate diminishes the reactant gas (Cg) concentration to zero at the boundary layer (B). In this situation the diffusion of reactant gas is the rate limiting step and the apparent activation energy approaches zero due to mass transport limitations. The intermediate situation, Zone II, represents control by chemical reaction kinetics plus the rate of gaseous diffusion; the apparent activation energy is half the true activation energy and the consumption of reactant gas is such that the gas concentration is zero at the centre of the particle.^{27,56,57} The intermediaries 'a' and 'b' (Figure 3.11) represent transitions between the idealized cases represented by the three zones.⁵⁷ Under the normal operating conditions within a utility boiler Zone II conditions are regarded most probable due to pore size effects and the range of particle sizes.^{8,27} Similar conditions using entrained flow reactor equipment are also report the existence of Zone II conditions for particles between 22 and 90 μm .^{8,9}

The 'zone-concept' of Walker *et al*⁵⁷ was adopted by Wen and Dutta²¹ to illustrate the behaviour of 'Volumetric' and 'Shrinking un-reacted core' models (Figure 3.12).

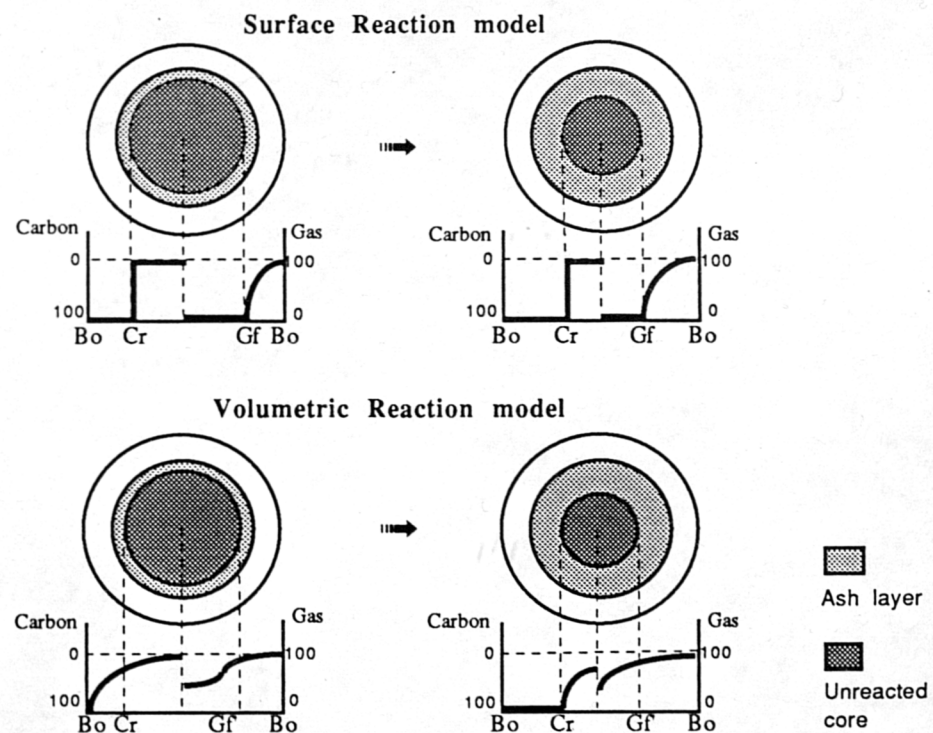


Figure 3.12 Carbon and reactant gas profiles for the Surface Reaction and Volumetric models. (modified after Wen and Dutta²¹) Bo. Boundary layer., Cr. Carbon-oxygen reaction zone., Gf. Gas front.

In either model (Figure 3.12) the burning particle is surrounded by a stoichiometric surface. In the case of the surface reaction model the reactant gas cannot diffuse into the interior of the reacting particle and as the reacting zone spreads throughout the particle, an ash layer may build-up on the outer rim of the particle as the unreacted carbon core shrinks. In the volumetric model, the reactant gas is able to penetrate into the particle interior and the reaction zone penetrates the body of the solid. At high temperatures (i.e. Zone III), in which diffusion is the rate limiting step, Wen and Dutta²¹ demonstrated that the two models, the volumetric reaction model and the shrinking core model, are essentially identical.²¹ Laurendeau²⁷ also discusses the 'unreacted shrinking core' and volumetric models. Laurendeau²⁷ using different terminology renames the volumetric type model a 'progressive conversion' model. This is subdivided into two sub-categories, depending whether an outer layer of ash or unreacted carbon is (Type I) or is not (Type II) present within the reacting particle. The 'progressive conversion model: Type I' of Laurendeau²⁷ and the volumetric model of Wen and Dutta²¹ are considered to apply to porous particles combusted within entrained flow reactor systems, whereas non-porous solids are best represented by the unreacted shrinking core model.²⁷

Other models such as the 'crackling' core model,⁶⁰ based upon the grain model of Szekely *et al.*,⁶¹ describe systems in which an initially non-porous particle develops a grain-like structure during combustion. Carbon-oxygen reactions are considered to occur only on the surface of the spherical grains. However, such models are not applicable to situations involving porous char particles but may apply to the combustion of dense non-porous char (e.g. anthracite).

A recent model (Figure 3.13), that incorporates the concepts of progressive conversion and char fragmentation, has been proposed by Kerstein and Edwards.⁶² The model attempts to predict particle combustion as a function of the type and distribution of bonds within the char structure and the onset of particle fragmentation and disintegration.

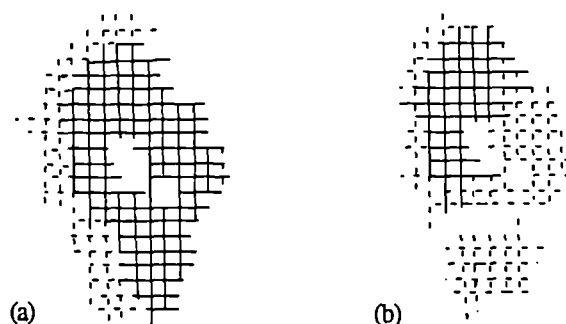
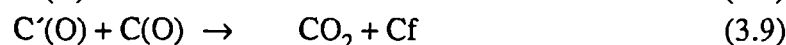
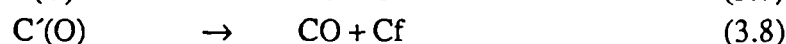
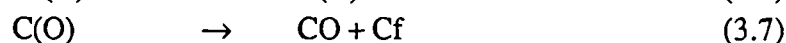
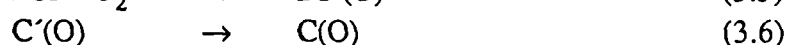
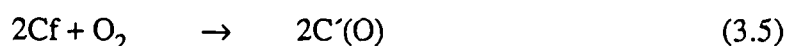


Figure 3.13 A two-dimensional simulation of char burnout, in which (a) the broken lines represent carbons undergoing oxidation leading to fragmentation (b). (after Kerstein and Edwards⁶²)

The model of Kerstein and Edwards⁶² is more descriptive than predictive, since the exact molecular structure of char is not known, neither is it readily amenable to precise

characterisation. The variety of different char types, reflecting the highly variable nature of coal, cannot be represented by such a simple scheme. However, the model has merit in that it does not assume that a char possesses a regular and spherical surface. Furthermore, the incorporation of a fragmentation process within the model more faithfully replicates the irregular decomposition of the more complex char structures during char burn-out.

Similarly, the carbon-oxygen reaction during char combustion is complex and not yet fully understood.⁵⁸ However, at the temperatures typical of combustion (c.a. 1000 to 1500°C) the currently accepted oxidation mechanism for a 'non-homogeneous interacting surface' such as char is:^{9,56}



where:

Cf	is a free 'active site' in the char structure
C(O)	is an immobile, covalent, bond
C'(O)	is a mobile, ionic, bond

The carbon-oxygen reaction scheme, given above, incorporates the concepts of: reactant absorption at an 'active site' such as carbon edges (Figure 3.14), the effects of inorganic impurities and functional groups, the surface migration of an intermediate to a new site (3.6) and the desorption of products.^{9,56}

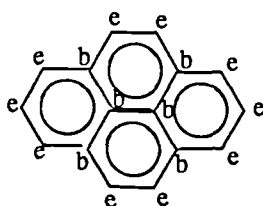


Figure 3.14 A representation of a polynuclear aromatic structure showing basal carbons (b) and edge carbons (e). (after Laurendeau²⁷)

3.7 Coal Combustion: The Effect of Coal Type and Rank

The pyrolysis and oxidation models discussed above (sections 3.4 to 3.6) all contain major assumptions concerning the nature of the materials and their characteristics. Coal is assumed to be essentially macromolecular. Particles are usually assumed to be regular in shape or spherical and most attempts at modelling combustion phenomena (pyrolysis and solid/gas

oxidation reactions) seek to construct a single universal model of coal combustion, largely ignoring the highly variable nature of coal and associated char. However, coal is a highly complex material and behaves as such during combustion. Recent investigations demonstrated that coal rank and the petrographic composition have a marked influence upon the combustion characteristics of pulverised coal combustion. Pilot and industrial scale studies^{63–67} have indicated that combustion efficiencies are inversely related to the proportion of *inertinite* macerals (Chapter 1) present in a given coal, deduced from higher incidences of unburnt carbon ('carbon carry-over') within the fly-ash than normally observed for vitrinite-rich coals. Lightman and Street⁶⁸ demonstrated, in an early laboratory study, that a range of char morphologies are produced during the high temperature pyrolysis of coal. It was subsequently shown^{67,68,69} that the highly vesiculated and porous *cenosphere* chars (Plate 4) were associated with vitrinite-rich coals, whereas the solid chars, showing very little vesiculation, were associated with macerals of the inertinite group. A variation in char morphology with coal rank was also noted.^{67,69,70,71} Vitrains were shown to produce chars with increasing structural complexity with decreasing rank, attributed to the high oxygen content and crosslinked nature of low-rank coals.⁶⁷ Subsequent investigations^{72,73,74,75} extensively developed those early relationships between coal rank, petrographic composition, char type and combustion efficiency. To accomplish this task, complex and intricate classification systems have been created. The most comprehensive, to date, is that of Bailey⁷⁶ which forms the basis of the system used in this thesis (see Experimental). Oka *et al*⁷² using a six-fold char classification scheme related the physical structure and shape of the respective char type to char reactivity and produced a ranking for bituminous coals (Figure 3.15).

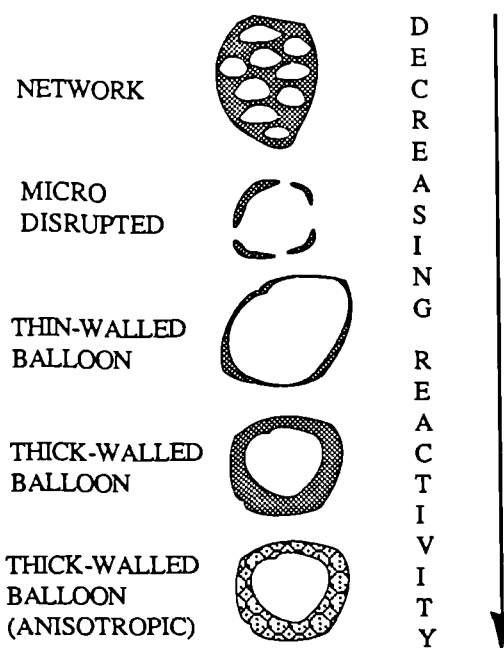
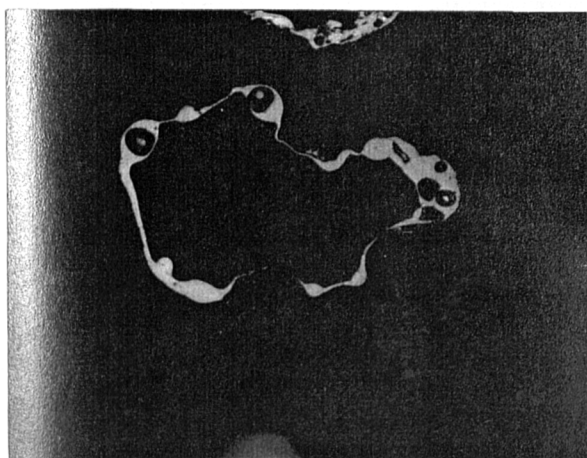
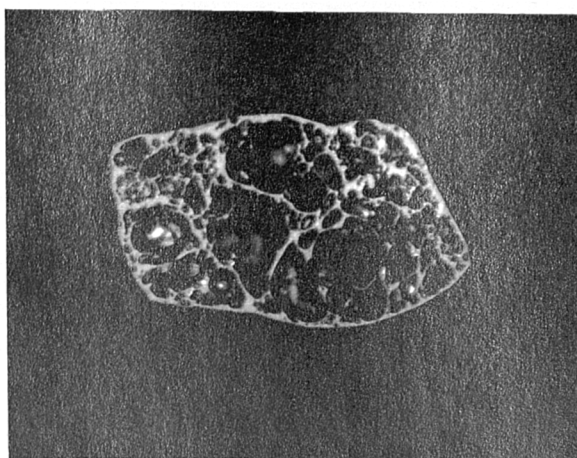


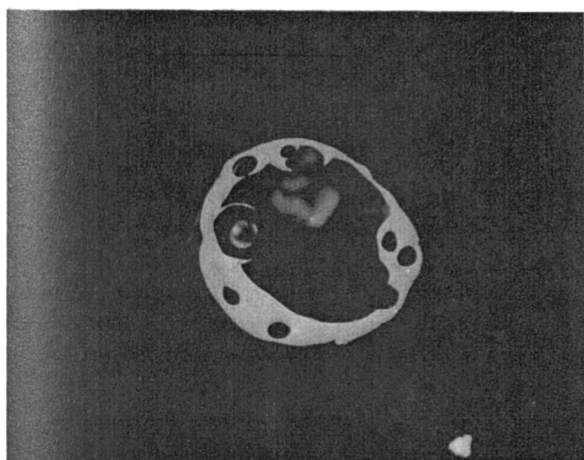
Figure 3.15 The reactivity order for five of the six chars studied by Oka *et al*.⁷² they also determined that SOLID char types (not shown) had the lowest reactivity.



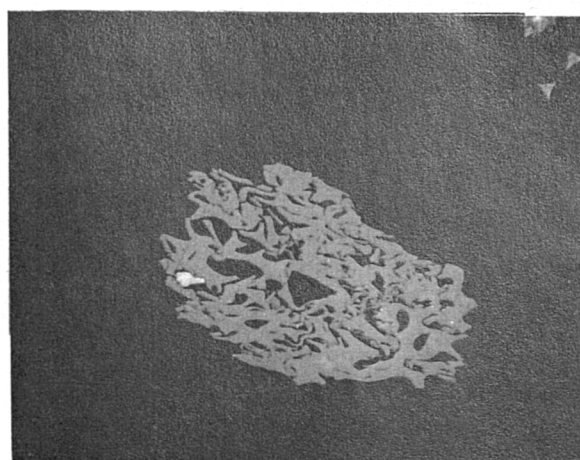
4a
Balloon⁶⁷ Cenosphere⁷²
Thin-walled Balloon⁷¹ 25μm



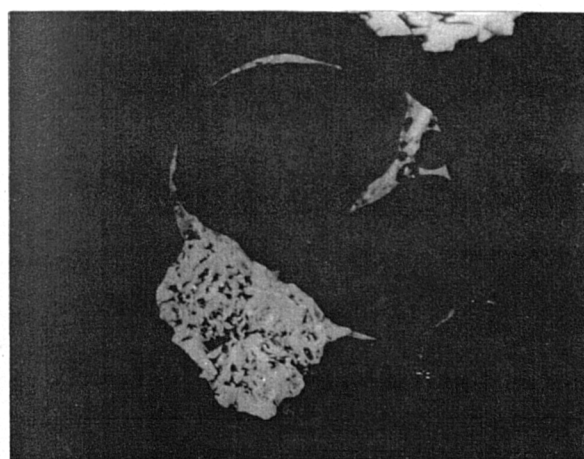
4e
Lacy⁶⁷ Honeycomb⁷²
Network⁷¹ 25μm



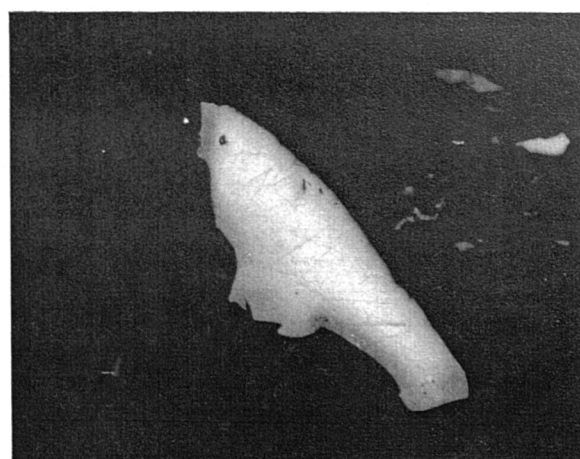
4b
Balloon⁶⁷ Cenosphere⁷²
Thick-walled Balloon⁷¹ 25μm



4f
Unfused⁷² Skeleton⁷¹ 25μm



4c
Lacy/Balloon⁶⁷ Cenosphere⁷² 25μm



4g
Solid⁶⁷ Unfused^{71, 72} 25μm

Plate 4 Char morphology and nomenclature pre-1987

(photographs taken by J. Bailey)

Oka *et al*⁷² also noted that a low rank (Sub-bituminous to high volatile C bituminous) inertinite rich coal produced char that was more reactive than the anisotropic cenospheres (balloon structure) derived from higher rank vitrinite rich coals. They also noted the occurrence of anisotropic char fragments within industrial plant fly ash due to incomplete combustion. The topic of inertinite reactivity and associated char morphology has been investigated using maceral concentrates.^{74,75} In which it was determined that the char forming properties of certain sub-macerals of inertinite also varied due to coal rank during pyrolysis. It was speculated⁷⁴ that the behaviour of vitrinite and inertinite during pyrolysis (vesiculation and plasticity) would converge with increasing rank, or due to oxidation.⁶⁴ But this was not investigated further. Interest in relating char characteristics to combustion rates and in turn relating the various char morphologies to precursor material continues. It is the goal of most researchers, who are engaged in the laboratory based behavioural study of coals of differing rank, composition and origin, to relate coal characteristics to pulverised fuel combustion, ultimately for the prediction of combustion phenomena. The recent increase in the world trade of steam coal⁷⁷ and the availability of coals with unproven combustion characteristics necessitates the development of analytical techniques that are able to assess the suitability of a given coal for use as a pulverised fuel. The conventional evaluative techniques currently used for coal selection purposes (proximate and ultimate analysis, calorific value) are not always reliable. Reports^{63,64,65} of diminished combustion efficiencies, poor flame stability and the requirement to utilise coal in an environmentally unacceptable manner,⁶³ highlights the problem. There is the requirement by industry for improved coal characterisation techniques related to coal combustion.

References

1. Schaffer, I.R. (1986). 'Combined Heat and Power and Electricity Generation in British Industry, 1983-1988'. Energy Efficiency Office, Dept. of Energy, HMSO, London.
2. Clarke, G.H. (1988). 'Industrial Marine Fuels Reference Book'. Butterworths, London.
3. Babcock and Wilcox Co. (1978). 'Steam, Its Generation and Use' 39th Edn., The Babcock and Wilcox Co., USA.
4. Ceely, F.J., and Daman, E.L. (1981) in: 'Chemistry of Coal Utilisation', 2nd Sup. Edn. (Elliot, M.A., Ed.). Wiley Interscience New York, Chichester, Brisbane, Toronto, 1313-1387.
5. Ward, C.R. (1984) in: 'Coal Geology and Coal Technology', (Ward, C.R. Ed.), Blackwell Scientific, Melbourne, Oxford, London, 113-150.
6. Essenhigh, R.H. (1981) in: 'Chemistry of Coal Utilisation' 2nd Sup. Edn. (Elliot, M.A. Ed.), Wiley Interscience, New York, Chichester, Brisbane, Toronto, 1153-1312.
7. Essenhigh, R.H. (1979) in: 'Coal Conversion Technology' (Wen, C.Y. and Lee, E.S. Eds.) Addison-Wesley, Massachusetts, 171-312.
8. Morrison, G.F. (1986). 'Understanding Pulverised Coal Combustion'. IEA Coal Research ICTIS/TR34, London.
9. Smith, I.W. (1982). 19th Symp. (Int.) Combust, The Combustion Inst, Pittsburgh, PA, 1054-1065.
10. Singer, S. (1983). 'Pulverised Coal Combustion', Dept. of Energy, Report DOE/ET/10679-T17. P.E.T.C. Pittsburgh, PA, USA.
11. Smoot, L.D. (1981), 18th Symp. (Int.) Combust. 'The Combustion Inst'. Pittsburgh, PA, 1185-1202.
12. Field, M.A. (1970). Combust. Flame **14**, 237-248.
13. Smith, I.W. (1971). Combust. Flame **17**, 303-314.
14. Brown, B.W., Smoot, L.D. and Hedman, P.O. (1986). Fuel **65**, 673-679.
15. Fu, W., Zhang, Y., Han, H. and Wang, D. (1989). Fuel **68**, 505-510.
16. Morgan, M.F. and Dekkar, J.S.A. (1988). 'Characterisation of the Combustion Performance of a Suite of Pulverised Coals'. I.F.R.F. Research Report. Doc.No. F188/a/4. Ijmuiden.
17. Given, P.H. (1984). Prog. Energy Combust. Sci. **10**, 149-158.
18. Jüntgen, H. (1981). Erdöl und Kohle Erdgas, Pt. 1. **40**, No. 4, 153-165.
19. Hüttinger, K.J. (1988) in: 'New Trends in Coal Science' (Yürüm, Y. Ed.). Klüwer Academic Press, Dordrecht, Boston, London, 433-480.
20. Haussmann, G.J. and Kruger, C.H. (1987). in: 'Int. Conf. on Coal Science' (Moulijn, J.A., Nater, K.A. and Chermin, H.A.G. Eds.), Elsevier Science Pubs. B.V., Amsterdam, 809-812.
21. Wen, C.Y. and Dutta, S. (1979). in: 'Coal Conversion Technology' (Wen, C.Y. and Lee, E.S. Ed.) Addison-Wesley, Massachusetts. 57-170.
22. Morgan, M.E. (1987). in: 'Int. Conf. on Coal Science' (Moulijn, J.A., Nater, K.A. and Chermin, H.A.G. Eds.), Elsevier Science Pubs, B.V. Amsterdam, 823-826.
23. Jost, M., Leslie, I and Kruger, C. (1984). 20th Symp. (Int.) Combust. 'The Combustion Inst', Pittsburgh, P.A., 1531-1537.
24. Gururajan, V.A., Wall, T.F. and Truelove, J.S. (1988). Combust. Flame **72**, 1-12.
25. Mitchell, R.E. and McLean, W.J. (1982). 20th Symp. (Int.) Combust. 'The Combustion Inst'. Pittsburgh P.A., 1113-1122.
26. Smoot, L.J. (1984). Prog. in Energy and Combustion Science **10**, 229-272.
27. Laurendeau, N.M. (1978). Prog. in Energy and Combustion Science **4**, 221-270.
28. Moulijn, J.A. and Tromp P.J.J. (1988), in: 'New Trends in Coal Science' (Yürüm, Y. Ed.), Klüwer Academic Press Dordrecht, Boston, London, 433-480.
29. Moulijn, J.A. and Tromp, P.J.J. (1986) in: 'Carbon and Coal Gasification' (Figueiredo, J.L. and Moulijn, J.A. Eds.) Martinus Nijhoff, Dordrecht. Boston, Lancaster, 455-484.
30. Howard, J.B. (1981) in: 'Chemistry of Coal Utilisation' 2nd Sup. Edn. (Elliot, M.A. Ed.), Wiley Interscience, New York, Chichester, Brisbane, Toronto, 665-784.
31. Jüntgen, H. and van Heek, K.H. (1968). Fuel **47**, 103-117.

32. Suuberg, E.M., Unger, P.F. and Lilly, W.D. (1985). *Fuel* **64**, 956-962.
33. Chaffee, A.L., Perry, G.J. and Johns, R.B. (1983). *Fuel* **62**, 303-316.
34. van Graas, G., de Leeuw, J.E. and Schenck, P.A. (1979). in: 'Advances in Organic Geochemistry' (Douglas, A.G. and Maxwell, J.R. Eds.), Pergamon Press, London, 485
35. Tromp, P.J.J., Moulijn, J.A. and Boon, J.J. (1988). in: 'New Trends in Coal Science' (Yürüm, Y. Ed.), Kluwer Academic Press, Dordrecht, Boston, London, 241-270.
36. Kobayashi, H., Howard, J.B. and Sarofim, A.F. (1977). 16th Symp. (Int.) Combust. 'The Combustion Inst', Pittsburgh, P.A., 411-425.
37. Hargrave, G., Pourkashanian, M. and Williams, A. (1986). 20th Symp. (Int.) Combust. 'The Combustion Inst', Pittsburgh, P.A., 221-230.
38. Nip, M., de Leeuw, J.W. and Schenck, P.A., (1987). in: 'Int. Conf. on Coal Science' (Moulijn, J.A., Nater, K.A. and Chermin, H.A.G. Eds.), Elsevier Science Pubs. B.V., Amsterdam, 89-92.
39. Hädicke, A., Schliephake, R.W. and Riepe, W. (1987). in: 'Int. Conf. on Coal Science' (Moulijn, J.A., Nater, K.A. and Chermin, H.A.G. Eds.), Elsevier Science Pubs. B.V., Amsterdam, 123-126.
40. Bruinsma, O.S.L., Geertsma, R.S., Oudhuis, A.B.J. and Moulijn, J.A. (1987). in: 'Int. Conf. on Coal Science' (Moulijn, J.A., Nater, K.A. and Chermin, H.A.G. Eds.), Elsevier Science Pubs. B.V., Amsterdam, 663-666.
41. Solomon, P.R., Serio, M.A., Carangelo, R.M. and Markham, J.R. (1989). *Fuel*, **65**, 182-194.
42. Larter, S.R. and Senftle, J. (1985). *Nature* **318**, 277-280.
43. Eglington, T. I. (1988), 'An Investigation of Kerogens using Pyrolysis Methods'. PhD Thesis (Unpub.), Dept. Geology, Newcastle upon Tyne University, Newcastle upon Tyne.
44. Suuberg, E.M., Peters, W.A. and Howard, J.B. (1979). 17th Symp. (Int.) Combust. 'The Combustion Inst', Pittsburgh, P.A., 117-130.
45. Tsai, C.Y. and Scaroni, A.W. (1985). 20th Symp. (Int.) Combust. 'The Combustion Inst', Pittsburgh, P.A., 1455-1462.
46. Wender, I., Heredy, L.A., Neuworth, M.B. and Dryden, I.G.C. (1981) in: 'Chemistry of Coal Utilisation', 2nd Sup. Ed. (Elliot, M.A. Ed.), Wiley Interscience, New York, Chichester, Brisbane, Toronto, 425-521.
47. Deshpande, G.V., Solomon, P.R. and Serio, M.A. (1988). *ACS Preprints* **33**, No 2, 310-321.
48. Solomon, P.R., Hamblen, D.G., Deshpande, G.V. and Serio, M.A. (1987). in: 'Int. Conf. on Coal Science' (Moulijn, J.A., Nater, K.A. and Chermin, H.A.G. Eds.), Elsevier Science Pubs. B.V., Amsterdam, 601-604.
49. Solomon, P.R., Hamblen, D.G., Carangelo, R.M., Serio, M.A. and Deshpande, G.V. (1988). *Combust. Flame* **71**, 137-146.
50. McMillen, D.F., Malhotra, R. and Nigenda, S.E. (1989). *Fuel* **68**, 380-386.
51. Unger, P.E. and Suuberg, E.M. (1984). *Fuel* **63**, 606-615.
52. Klose, W. and Polte, D. (1987). in: 'Int. Conf. on Coal Science' (Moulijn, J.A., Nater, K.A. and Chermin, H.A.G. Eds.), Elsevier Science Pubs. B.V., Amsterdam, 621-624.
53. Gray, R.V. (1988). *Fuel*, **67**, 1298-1304.
54. Niksa, S. and Kerstein, A.R. (1986). *Combust. Flame*, **66**, 95-110, 111-120.
55. Niksa, S. and Kerstein, A.R. (1987). *Fuel*, **66**, 1389-1399.
56. Hampartsoumian, E., Pourkashanian, M. and Williams (1988). *J. Inst. Energy*, March, 48-56.
57. Walker, P.L. Jr., Pusinko, F. Jr., and Austin, L.G. (1959). in: 'Advances in Catalysis, Vol II' (Eley, D.D., Selwood, P.W. and Weisz, P.B. Eds.), Academic Press, New York, 133-221.
58. Young, B.C. and Smith, I.W. (1987). in: 'Int. Conf. on Coal Science' (Moulijn, J.A., Nater, K.A. and Chermin, H.A.G. Eds.), Elsevier Science Pubs. B.V., Amsterdam, 793-796.
59. Skorupska, N.M. (1987) Ph.D. Thesis (Unpub.) Dept. of Chemistry, Newcastle upon Tyne University, Newcastle upon Tyne.
60. Park, J.Y. and Levenspiel, O. (1975). *Chem. Eng. Science*, **30**, 1207-1214.
61. Szekely, J. and Propster, M. (1975). *Chem. Eng. Science*, **30**, 1049-1055.
62. Kerstein, A.R. and Edwards, (1987). in: 'Int. Conf. on Coal Science' (Moulijn, J.A., Nater, K.A. and Chermin, H.A.G. Eds.), Elsevier Science Pubs. B.V., Amsterdam, 785-788.

63. Yavorskii, I.A., Alaev, G.P., Pugach, L.I. and Talankin, L.P. (1968). *Teploenergetika*, **15**, No.9, 69-72.
64. Nandi, B.N., Brown, T.D. and Lee, G.K. (1977). *Fuel* **56**, 125-130.
65. Sanyal, A. (1983). *J. Inst. Energy*, June, 92-95.
66. Lee, G.K. and Whaley, H. (1983). *J. Inst. Energy*, **56**, 190-197.
67. Shibaoka, M. (1985). *Fuel* **64**, 263-269.
68. Lightman, P. and Street, P.J. (1968). *Fuel* **47**, 7-28.
69. Street, P.J., Weight, R.P. and Lightman, P. (1969). *Fuel* **48**, 343-365.
70. Hamilton, L.H. (1981). *Fuel* **60**, 909-913.
71. Shibaoka, M., Thomas, C.G., Oka, N., Matsuoka, H., Murayama K. and Tamaru K. (1968). *Inst. Conf. on Coal Science*, Pergamon, Sydney 665-668.
72. Oka, N., Murayama, T., Matsuoka, H., Yamada, S., Yamada, T., Shinozaki, S., Shibaoka M. and Thomas, C.G. (1987). *Fuel Proc. Technol.* **15**, 213-224.
74. Jones, R.B., McCourt, C.B., Morley, C. and King, K. (1985). *Fuel* **64**, 1460-1467.
75. Skorupska, N.M., Sanyal, A., Hesselman, G.J., Crelling, J.C., Edwards, I.A.S. and Marsh H. (1987). in: 'Int. Conf. on Coal Science' (Moulijn, J.A., Nater, K.A. and Chermin, H.A.G. Eds.), Elsevier Science Pubs. B.V., Amsterdam, 827-837.
76. Bailey, J. pers. comm.
77. McCloskey, G. (1987). 6th Int. Conf. and Exhb. on Coal Technol. and Coal Econ, Unpub. Conf. Notes, 9-11th June, London U.K.

CHAPTER FOUR

Objectives

4.1 Overall Objectives

The overall objective of this research is to characterise a range of coals of different origin, rank and petrographic composition, using a variety of petrographic and standard analytical techniques. Furthermore, to investigate, using a laboratory based Entrained Flow Reactor (EFR) that simulates the rapid rates of heating (10^4 to 10^5 °C s⁻¹) typical of a pulverised fuel boiler, the relationships between the morphology of chars produced during pyrolysis, char characteristics, standard coal analytical techniques and coal petrography. To identify those relationships that may be used in the assessment of coal feedstock for use within a pulverised fuel boiler.

For the purpose of satisfying the above overall objective, the research is subdivided into three studies:

1. The influence of coal rank upon char morphology and combustion.
2. Coal and char characterisation and correlations.
3. The effects of coal oxidation and weathering upon coal properties, char morphology and combustion.

4.2 Specific Objectives

4.2.1 The Influence of Coal Rank upon Char Morphology and Combustion

- 4.2.1.1 To investigate the influence that coal rank has upon char morphology and the respective physical and structural characteristics of those chars using a suite of vitrinite rich coals of differing rank.
- 4.2.1.2 To examine the relationships between coal properties and the generation of specific types of char during rapid pyrolysis using a suite of vitrinite rich coals of differing rank.
- 4.2.1.3 To relate the combustion characteristics of chars, produced from a suite of vitrinite rich coals of different rank, to the physical and structural properties of the char.

4.2.2 Coal and Char Characterisation and Correlations

- 4.2.2.1 To investigate the possible use of whole-coal reflectograms as a means of characterising coal feedstock, using a suite of coals of different rank and petrographic composition.
- 4.2.2.2 To examine the relationships between standard coal analytical techniques and the morphology of associated chars using a laboratory based EFR and a suite of Cretaceous/Tertiary and Carboniferous coals.
- 4.2.2.3 To investigate the relationships between char morphology and coal petrographic techniques using the same suite of Cretaceous/Tertiary and Carboniferous coals.
- 4.2.2.4 To explore possible interrelationships between petrographic composition, standard analytical techniques and char morphology, and to investigate possible relationships that could be used as a means of characterising and discriminating between coals of different rank, composition and age.

4.2.3 The Effects of Coal Oxidation and Weathering upon Coal Properties, Char Morphology and Combustion

- 4.2.3.1 Using fresh coal samples, investigate and assess the effects of both oxidation (100°C/air) and weathering (ambient) upon standard coal characterisation techniques.
- 4.2.3.2 To examine the effects of oxidation (100°C/air) and weathering upon vitrinite fluorescence using a fluorescence microphotometer and to examine the relationship between fluorescence intensity and the duration of oxidation or weathering.
- 4.2.3.3 To explore and assess possible new techniques capable of assessing the extent of oxidation (100°C/air) and/or natural weathering (ambient) that maybe sustained by coal feedstock.
- 4.2.3.4 To study and examine the effects of both oxidation (100°C/air) and weathering (ambient) upon the morphology of associated chars and their physical and structural characteristics, and their effects upon subsequent combustion using the EFR.

CHAPTER FIVE

Experimental

5.1 Coal Samples Used

5.1.1 Origin of Samples

A total of 26 coal samples have been used in this thesis (Table 5.1) which consists of three distinct but related studies. The coal samples were kindly donated from several sources:

Dr A. Cameron, I.S.P.G., Geological Survey of Canada., Dr R. Neavel, Exxon., Babcock Energy (UK) Ltd., Mr J. Pearson, British Coal Ltd.

The original laboratory coding used during experimentation has been retained through this thesis as an aid to those working within the laboratory.

Table 5.1 The Origin, Coal Sample Code, Rank, Vitrinite Reflectance, Proximate Analysis and Calorific Value For all Coals used within this Study.

<u>Country</u>	<u>Mine</u>	<u>Coal</u> (code)	<u>Rank</u> (ASTM)	<u>Reflectance</u> (%Romax)	<u>Proximate analysis</u>		<u>Calorific Value</u>	
					Volatile Matter (wt% d.a.f.)	Fixed Carbon	Mj/kg ⁻¹ (d.a.f.)	Btu/lb (d.a.f.)
Canada	Luscar 4	86/001	hV Bc	0.58	42.3	57.7	27.929	12,641
Canada	Luscar 4	86/002	hV Bc	0.61	33.7	66.2	29.578	12,716
Canada	Luscar 4	86/003	hV Bc	0.55	24.3	75.7	22.161	9,527
Canada	Luscar 4	86/004	hV Bc	0.57	33.2	66.8	29.805	12,814
Canada	High Vale 4	86/005	sub a	0.50	24.8	75.2	13.822	5,942
Canada	High Vale 4	86/006	sub a	0.48	33.2	66.8	24.998	10,747
Canada	High Vale 4	86/007	sub a	0.52	31.9	68.1	23.729	10,202
Canada	High Vale 3	86/008	sub a	0.49	31.6	68.4	22.902	9,846
Canada	High Vale 3	86/009	sub a	0.52	29.8	70.2	24.802	10,663
Canada	High Vale 3	86/010	sub a	0.52	24.3	75.7	26.862	11,548
Canada	Fording R. 3	86/011	mvb	1.33	23.0	77.0	36.271	15,544
Canada	Fording R. 3	86/012	mvb	1.33	17.2	82.8	35.169	15,119
Canada	Fording R. 3	86/013	mvb	1.27	18.2	81.8	35.203	15,134
Canada	Fording R.4	86/014	hV Ba	0.96	31.8	68.2	35.821	15,400
Canada	Fording R.4	86/015	hV Ba	0.93	30.4	69.6	34.115	14,667
Canada	Fording R.4	86/016	hV Ba	0.93	30.5	69.5	33.618	14,453
Britain	Unknown	87/017	hV Ba	0.87	26.6	73.4	35.117	15,097
Poland	Unknown	87/018	hV Ba	0.88	26.7	73.3	36.210	15,567
USA	Unknown	87/019	hV Ba	0.90	22.9	77.1	34.190	14,699
Columbia	Cerrejon	87/021	hV Bb	0.67	31.1	68.9	31.474	13,531
Columbia	Cerrejon	87/022	hV Bb	0.67	40.5	59.5	32.807	14,104
Canada	Sydney	87/023	hV Ba	1.08	25.1	74.9	33.301	14,316
Britain	Wearmouth	88/024	hV Ba	0.93	37.5	62.5	35.150	15,111
Britain	Lynemouth	88/025	hV Bb	0.76	39.0	61.0	33.800	14,530
Britain	Taff Merthyr	88/027	s-anth	2.06	7.6	92.3	-	-
Britain	Cynheidre	88/028	anth	4.29	3.0	98.0	-	-

5.1.2 Sample Preparation

Coals 86/001 to 86/016 and 88/024 to 88/028 were received as lumps whereas all other samples were pre-crushed to a top size of 2.5 mm and sealed in air-tight containers. Samples in lump-form were crushed to a top size of 2.5 mm using a mechanical jaw crusher, quartered using a rotary riffler, from which a portion was removed for immediate analysis and the remainder stored under an atmosphere of nitrogen at -5°C . The material required for immediate analysis was crushed using a mortar and pestle and sieved to a top size of $212\text{ }\mu\text{m}$. An aliquot was removed for petrographic analysis by 'cone and quartering' and the remainder crushed and sieved to the required 38 to $75\text{ }\mu\text{m}$ size fraction. All (coal) petrographic analyses were conducted on the $212\text{ }\mu\text{m}$ size fraction whereas, all other analyses (except calorific value) including rapid pyrolysis were conducted on the 38 to $75\text{ }\mu\text{m}$ size fraction. The removal of fine material ($< 38\text{ }\mu\text{m}$) was considered desirable to ensure that pyrolysis and combustion characteristics were a function of the inherent properties of the coals used, rather than due to inconsistencies of particle size. The oxidation of coals 88/024 and 88/025 was achieved using a large thermostatically controlled oven ($100 \pm 2.5^{\circ}\text{C}$) in static air with a mono layer of coal ($<2.5\text{ mm}$). The weathering was achieved by exposing the evenly distributed coal ($<2.5\text{ mm}$) to the atmosphere in an enclosed (but ventilated) container. Samples were removed periodically for analysis, sieved to a top size of 1.18 mm and ground in a glove box under an atmosphere of nitrogen.

5.2 Petrographic Characterization Techniques

5.2.1 Sample Preparation

The coal, crushed to $< 212\text{ }\mu\text{m}$, was bound in a cold-setting polyester resin in plastic moulds (25 mm diameter). The block-mounted sample was successively ground on 5 grades of Silicon-carbide paper (220, 320, 400, 600 and 1200 grits) and polished successively with three different grades of alumina (5/20, 3/50 and gamma) on selvyt-covered stationary laps, well lubricated with distilled water. At each stage on the selvyt-laps, the number of rotations was counted and reduced from 120 (5/20) through 80 (3/50) to finally 40 rotations (gamma). Thereby ensuring that samples were not excessively polished in an attempt to minimize the formation of differential relief due to differences in 'hardness' between macerals and between macerals and binder.

After each grinding and polishing stage, the blocks were immersed in distilled water and cleaned in an ultrasonic bath to remove surplus alumina and debris. With the exception of those blocks required for fluorescence microphotometry work, the blocks were finally rinsed with distilled water and the surface water drawn off. Blocks required for fluorescence microphotometry work were immersed in distilled water.

5.2.2 Maceral Analysis

5.2.2.1 Description of Apparatus

Petrographic (maceral) analysis was conducted on each sample using a Leitz MPV3 microscope photometer (Plate 5) in conjunction with a Swift automatic point-counter (Model F). The microscope was equipped with an adjustable ocular (10 x) fitted with a cross-hair graticule, a oil-immersion strain-free infinity corrected objective (50 x) providing a total magnification of 800 x.

5.2.2.2 Procedure

The analysis of each coal involved the recognition of the macerals and/or sub-macerals described in Chapter 1 (pages 20-22) located at the intersection of the graticule cross-hair. Quantification was achieved by recording 500 individual maceral determinations per coal using an interpoint and interline distances of 0.5 mm. The number of counts recorded was converted to a proportion by volume of the total.

5.2.2.3 Reproducibility of Data

The criterion for the accuracy of the analyses were given by the reproducibility and the comparability of the results. The reproducibility of two analyses made by a single operator on the same polished surface is given to be $\pm 1.5\%$, based on a 500 point-count.

5.2.3 Microlithotype Analysis

5.2.3.1 Description of Apparatus

The equipment required for microlithotype analysis was identical to that used for maceral analysis with the exception that a Kötter graticule, imprinted with a 20-point intersecting cross-hair pattern (Figure 5.1), was used in place of the simple cross-hair graticule within the ocular.¹

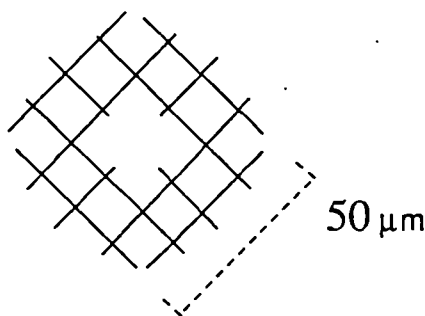


Figure 5.1 A schematic representation of the Kötter 20-point eyepiece graticule used for microlithotype analysis (adapted from Stach *et al* ¹)

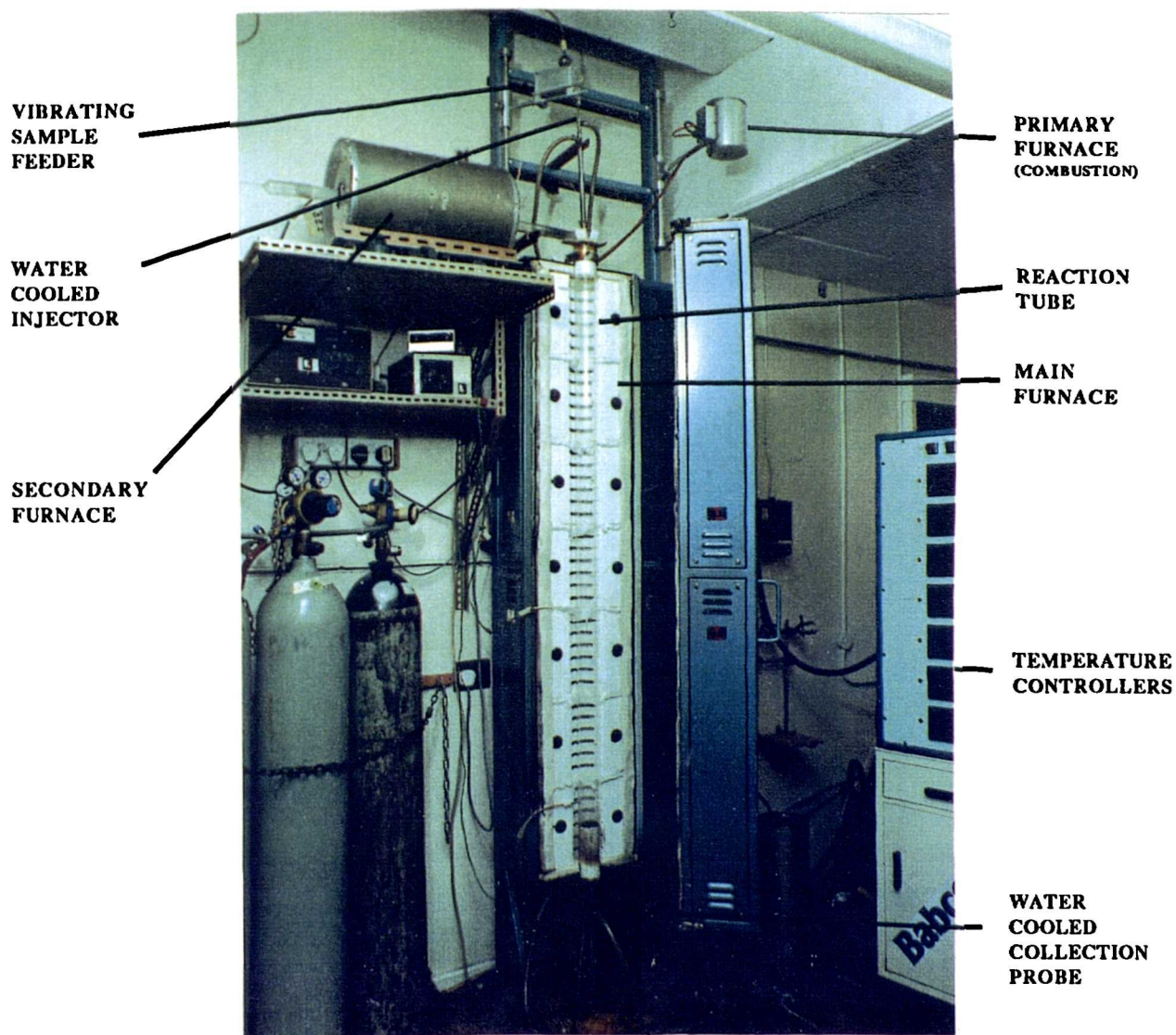
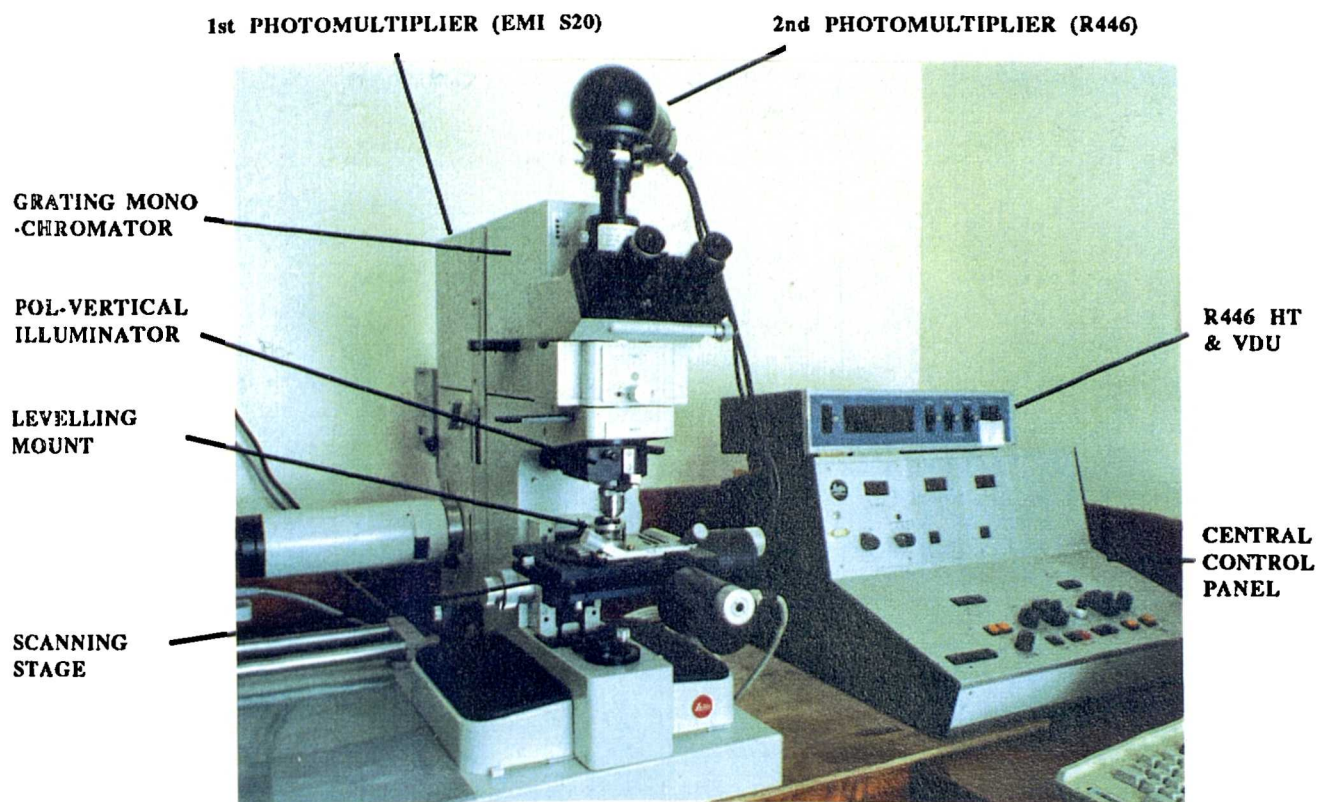


Plate 5. The EFR and the Leitz MPV3 Microscope Photometer

5.2.3.2 Procedure

The convention governing this type of analysis is documented in Chapter 2 (page 33). Essentially, during the analysis, each observation on a group of 20 intersections was considered as a point. The allocation of an individual observation to a particular microlithotype was governed solely by the type and number of macerals present at all 20 intersections. A total of 500 points were recorded for each coal sample and the microlithotype content was expressed as proportion (volume %) of the total points recorded.

5.2.3.3 Reproducibility of Data

The repeatability for analyses was ± 2.5 % by volume based on a 500 point-count.

5.2.4 Vitrinite Reflectance

5.2.4.1 Description of Apparatus

The equipment used for the measurement of the mean maximum reflectance of vitrinite (%R₀ max) was the Leitz MPV3 microscope photometer (Plate 5) correctly adjusted for Köhler illumination and equipped with the following: an EMI 9558B 11 dynode (CsSb) S20/B photomultiplier tube, a Pol-vertical illuminator fitted with a Berek triple-prism and polarizer, a 12v/100W tungsten lamp and stabilized power supply, a monochromising (546 nm) interference line-filter (HW <15 nm), a rotating microscope stage and a recording device (Hewlet Packard 9826A computer).

Initially the blocks were fixed and levelled on a glass microscope slide using Blu-Tack™ and a mounting press. However, this technique was found to be unsatisfactory for maximum reflectance, reflectance scanning (reflectogram) and fluorescence microphotometry analyses due to the poor co-planarity of the polished sample surface when placed on the microscope stage. Therefore, small three-point levelling sample holders were designed and manufactured to overcome that problem (see line drawings, Appendix B).

5.2.4.2 Procedure and Calculations

Vitrinite reflectance is a comparative technique which relates the intensity of the monochromatic plane-polarised light, reflected at near normal incidence from a specified sub-maceral of vitrinite using an oil-immersion media, to that of a known standard measured under identical conditions. When determining the rank (the degree of coalification) of a coal, a total of fifty measurements were conducted in plane-polarized light at a wavelength of 546 nm on the submaceral desmocollinite during which the microscope stage was rotated through 360° and the maximum (and minimum) values recorded. Because the digital display of the microscope

photometer was set to the nominal value of the standards used, reflectance values pertaining to vitrinite were read straight from the display (Section 5.2.5). The mean maximum reflectance (%R₀max) and the standard deviation (σ) of the distribution were calculated using the following formulae in accordance with British Standard 6127:

$$\%R_{0\max} = \frac{\sum \%R_i}{n} \quad (5.1)$$

$$\sigma = \sqrt{\left(\frac{n \sum R_i^2 - (\sum R_i)^2}{n(n-1)} \right)} \quad (5.2)$$

where: %R₀max = mean reflectance
 %R_i = individual reflectance value
 n = number of measurements
 σ = standard deviation

5.2.4.3 Calibration of the Microscope Photometer

A correction for photo cathode dark current and parasitic reflections within the optical system was initially achieved by placing a black cavity cell filled with immersion oil on the stage and adjusting the photocathode dark-current compensator until the digital display indicated zero. The appropriate specular reflectance standard was then placed on the stage and the high tension voltage adjusted until a value corresponding to the nominal value of the standard was indicated. The procedure was then repeated using a suitable range of specular standards. Subsequent measurements on polished samples were then read directly from the digital display. The calibration of the photometer system was subsequently checked every 25 measurements, a variation of ±0.02% was the maximum deviation allowed on subsequent calibration checks. The specular standards used and their respective nominal reflectivities for oil and water immersion media were calculated using the Fresnel-Beer equation (2.2, page 36) and are given in Table 5.2

Table 5.2 Specular Reflectance Standards: Percent Reflectance at Normal Incidence

Standard	Reflectance in Water (%R _w @ 20°C)		Reflectance in Oil (%R _{oil} @ 23°C)	
	λ546	λ650	λ546	λ650
Spinel	1.69	1.68	0.44	0.43
Y.A.G.	2.52	2.49	0.92	0.91
Cubic Zirconia	5.93	5.78	3.32	3.22

5.2.4.4 Reproducibility of Data

The repeatability of *all reflectance* determinations is influenced by a variety of factors which

includes: instrument drift during the analyses, non-linearity of photomultiplier, non-coplanarity of the polished surface, inconsistent polish, sampling errors and poor sub-maceral recognition. All analyses have a repeatability of 0.06 % and a reproducibility between different blocks of the same sample better than 0.08 %.

5.2.5 Reflectance Scanning

5.2.5.1 Description of Apparatus

The investigation of automated petrographic analysis was achieved using the Leitz MPV3 microscope photometer correctly adjusted for Köhler illumination and configured as for vitrinite reflectance with the exception that the polarizer was removed. The Swift point-counting apparatus and the Leitz fine-scanning stage provided the means by which the sample block could be moved relative to the measurement point at regular intervals. The polished blocks were levelled using three-point levelling sample holders (see line drawing, Appendix B).

5.2.5.2 Procedure

Measurements were conducted using the point-counter to generate an interpoint and interline distance of 40 μm , with the necessary smaller incremental distances provided by the fine-scanning stage. A total of 1500 manually recorded reflectance measurements were conducted on each polished sample block using non-polarized light (random reflectance) with a measuring aperture of 3.6 μm at $\times 800$. During the calibration of the microscope photometer attention was paid to photomultiplier linearity using the whole range of specular standards: only the Berek vertical illuminator was found to generate linearity over the reflectance range used. At each sample point the material being measured could be both visually assessed and evaluated for particle homogeneity by incrementing the stage 1 μm using the fine-scanning stage (Figure 5.2). In this way it was possible to discriminate *objectively* between macerals, boundaries and

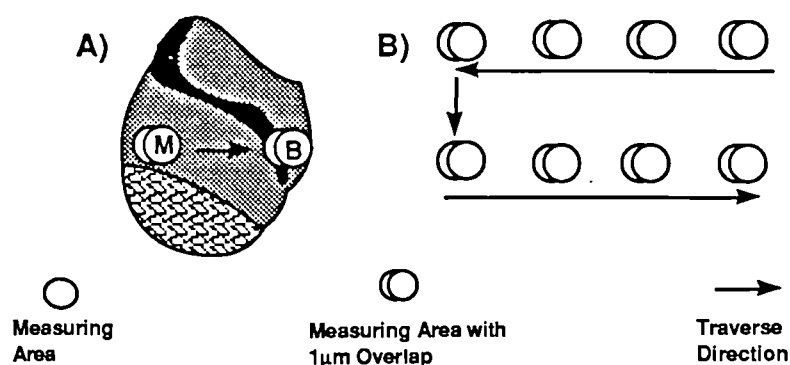


Figure 5.2 A representation of the measuring tract employed during reflectance scanning (5.2B) as a means of discriminating (5.2A) between measurements on macerals (M) or those associated with boundaries (B) and the binder. The overlap is a schematic representation of the method employed to discriminate *objectively* between macerals, boundaries and binder.

binder. During the analysis it was noted that changes in reflectance greater than 10 percent coincided with either inter- and intra-particle boundaries and were recorded as such. Reflectance values less than 0.2% ($\%R_{0\text{random}}$) typified those measurements associated with the epoxy binder material.

5.2.6 Fluorescence Microphotometry

5.2.6.1 Description of Apparatus

The investigation of fluorescence microscopy as a quantitative technique was explored using the Leitz MPV3 microscope photometer fitted with an HBO 100 mercury lamp and a XBO xenon lamp, an EMI S20 11-stage photomultiplier tube, the Ploemopak rotating filter turret, a Zeiss Plan Neofluoar x 40 (n.a.0.9) water immersion objective giving an overall magnification of x 640, a masked uranyl glass standard and the filter block combinations Tu (BP 280-410 nm) and I2 (BP 450-490 nm, RKP 510 nm, LP 515 nm). A second photometer unit (Plate 5) comprised of a Hamamatsu R446 9-stage side window photomultiplier tube (PMT), a Vickers digital microphotometry unit and high tension supply, focusing lens, adjustable diaphragm and fitted with a 546 nm line filter. The polished blocks were levelled using three-point levelling sample holders (see line drawing, Appendix B).

The relationship between fluorescence intensity measurements at 650 nm and maceral reflectance at 546 nm in reflected white light was achieved by constructing a second photometer on the microscope, located on the phototube exit point of the binocular eyepiece (Figure 5.3). The location of the photocathode was positioned conjugate to the plane of the real image. The Hamamatsu (PMT) and Vickers digital microphotometry unit was calibrated using water as the immersion media and the specular reflectance standards outlined in Table 5.2.

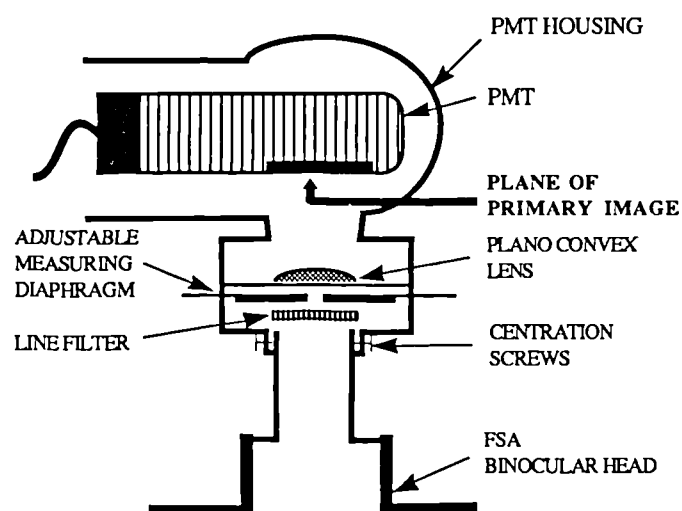


Figure 5.3 A representation of the Hamamatsu PMT, and the location of measuring diaphragm, lens and line filter.

This assembly provided the means by which quantitative determinations at two wavelengths, calibrated to different standards could be conducted on exactly the same field of view (not simultaneously). The relationship between fluorescence intensity measurements at I_{650} and $\%R_{w \text{ random}}$ (546 nm) in white light and calculated to $\%R_{o \text{ random}}$ is given in Figure 5.4.

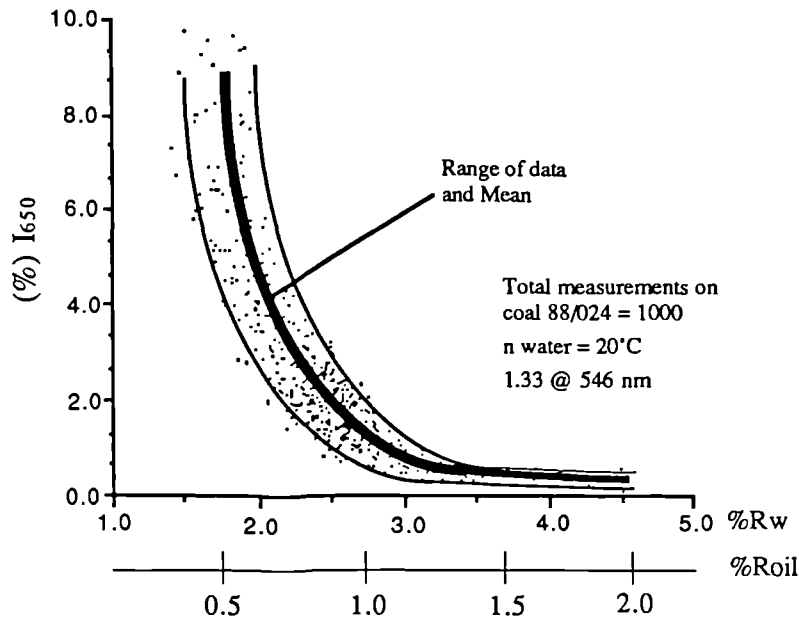


Figure 5.4 The relationship of Fluorescence intensity (I_{650}) to random reflectance of coal using water as the immersion medium for coal 88/024, calculating the equivalent reflectance for oil.

5.2.6.2 Procedure

Fluorescence intensity measurements were conducted at 650 nm using a 20 μm square measuring spot, the I2 filter block combination, the grating monochromator set to 650 nm and the EMI S20 PMT. A black cavity cell was used to compensate for parasitic reflections and for zeroing the photometer. The calibration of the photometer was achieved using the uranyl glass standard to which the response of the photometer was set to 100%. Fluorescence intensity measurements scanned across coal particle surfaces were measured using an interpoint distance of 20 μm using a stepping stage, with a procedure that involved examining the field-of-view using the Tu filter block, then focusing, measuring the random reflectance at 546 nm ($\%R_{w \text{ random}}$, $n = 1.3$ @ 23°C) using the stabilised tungsten lamp and the Hamamatsu PMT, rotating the filter block turret to the I2 filter block and opening the synchro-compur shutter, positioned in front of the mercury lamp, for the duration of the fluorescence intensity measurement (2 s) and measuring the response at I_{650} using the EMI S20 PMT. A new measuring area was then selected using the stepping stage and the process repeated.

5.3 Proximate Analysis

5.3.1 Introduction

The determination of the moisture, volatile matter, ash and fixed carbon content of coal or char was achieved through the use of thermogravimetry² using a Stanton Redcroft STA 780 thermobalance. The use of thermogravimetry, rather than the traditional muffle furnace technique (B.S. 1016),³ was chosen for several reasons:

- There is a reduction in analysis time.
- The technique is less labour intensive, offering a simplified procedure.
- Less sample is required (<50 mg compared to 4 x 1 g).
- A continuous recording of weight loss as a function of time and temperature is produced.

5.3.2 Description of Apparatus

The instrument consisted of an electronic microbalance, nichrome wound furnace, a solid state temperature controller and a Linseis Type 2041 multipen recorder. The sintered platinum crucible (8mm high x 12 mm top diameter x 10 mm bottom diameter) was suspended from the balance assembly by a 'hangdown' system into the centre of a hermetically sealed furnace. The furnace was lowered and raised around the 'hangdown' assembly for the removal of ash and the placement of fresh sample.

5.3.3 Procedure

For the analysis of coal, 50 mg (± 0.5 mg) of sample was weighed into the platinum crucible. However, when analysing char or combustion products the sample weight was reduced to typically 20 mg (± 0.3 mg) due to the reduction in available material.

The sample was heated from room temperature to $105\text{ }^{\circ}\text{C} \pm 3\text{ }^{\circ}\text{C}$ (furnace temperature: $127\text{ }^{\circ}\text{C}$) at a rate of $99\text{ }^{\circ}\text{C min}^{-1}$, in an upward flowing stream of nitrogen (50 ml min^{-1}) held at $105\text{ }^{\circ}\text{C}$ ($\pm 3\text{ }^{\circ}\text{C}$) until constant weight was achieved. The weight loss up to this point represented the moisture content. From $105\text{ }^{\circ}\text{C}$, the sample was heated to $900\text{ }^{\circ}\text{C} \pm 5\text{ }^{\circ}\text{C}$ (furnace temperature $927\text{ }^{\circ}\text{C}$). The temperature was then held for 3 minutes, at which point the weight was noted. The weight loss recorded between $105\text{ }^{\circ}\text{C}$ and $900\text{ }^{\circ}\text{C}$ represented the volatile matter content. The furnace was subsequently cooled to $800\text{ }^{\circ}\text{C} \pm 5\text{ }^{\circ}\text{C}$ (furnace temperature = $824\text{ }^{\circ}\text{C}$) and maintained at that temperature. Once the sample weight and temperature stabilized, the gas supply was switched to air, maintained at 50 ml min^{-1} . The weight remaining at the end of the analysis represented the ash content and the fixed carbon content was derived by difference. The temperature and weight loss were recorded simultaneously on a multipen chart recorder. The weights derived from the chart were subsequently corrected for 'bouyancy effects' due to

the upward flowing gas. This phenomenon was previously studied using inert materials and the following correction factors applied:

Moisture	add 0.2 wt.%
Volatile matter	subtract 0.2 wt.% from the total value, then subtract the corrected moisture content value.
Ash content	add 0.1 wt.%

The wt.% fixed carbon, determined on a dry volatile matter free basis (D.V.M.F.), was calculated using the following equation:

$$\text{wt.\% fixed carbon (D.V.M.F.)} = \frac{(100 - y) \times 100}{(100 - x)} \quad (5.3)$$

where: y = wt.% ash + wt.% moisture + wt.% volatile matter,
 x = wt.% moisture + wt.% volatile matter

5.3.4 Reproducibility of Data

Reproducibility tests have been conducted and values compared between the TGA used in N.C.R.L. with those values derived on the TGA at Babcock Energy Ltd (BE), Renfrew, Scotland. The results are given in Table 5.3.⁴

Table 5.3 Repeatability and Reproducibility Values for the Stanton and Redcroft STA 780 TGA used for Proximate Analyses

Parameter	Range of Values (wt.%)	Repeatability within NCRL	Reproducibility NCRL & BE
Moisture	< 5.0	0.10	-
	> 5.0	0.15	-
Volatile matter	<10.0	0.2	0.5
	>10.0	0.3	1.0
Ash	<10.0	0.15	0.3
	10.0 - 20.0	0.20	0.4
	>20.0	0.25	0.5

5.4 Elemental Analysis

5.4.1 Description of Apparatus

Determinations of the elements carbon, hydrogen and nitrogen were achieved using a Carlo Erba model 1106 Elemental analyser coupled to a Shimadzu Chromatopac C-E1B integrator and single channel chart recorder. The instrument consisted of an auto-sampling head in the form of a carousel, a combustion furnace, a reduction furnace and a combined gas chromatograph/detector unit.

5.4.2 Procedure

A small amount of sample (1 to 2 mg) was carefully weighed into a tin crucible, placed into the carousel, along with additional samples, standards and blanks. During each analysis a crucible was dropped into the combustion furnace, maintained at a temperature of 1020 °C. The reaction produces CO₂, H₂O and NO_x. The oxides of nitrogen were subsequently reduced to nitrogen, and both excess oxygen and halogens were removed by passing the evolved gases over copper within the reduction furnace, which was maintained at 650 °C. The gases CO₂ and H₂O were unchanged during this stage of the analysis. Separation of the gases, N₂, CO₂ and H₂ was achieved by chromatography using a 2 m x 5.0 mm (ID) Porapak 'S' column. Detection was by kathorimetry and both the detector and column were maintained at a temperature of 103 °C. The carrier gas was helium and the flow maintained at 20 ml min⁻¹.

Determinations of the elements carbon, hydrogen and nitrogen were achieved by a comparison of the integrals derived during each analysis with those obtained for a standard of known composition. The standard used was Alanine giving carbon 40.4 wt.%, hydrogen 7.85 wt.% and nitrogen 15.72 wt.%. The following equations are used to calculate the K factor and the percentage of each element.

$$K = \frac{\%std \times wt.std}{I.std - B} \quad (5.4)$$

where: %std = % of element in standard
 wt.std = weight of standard (in mg)
 I.std = standard integral values
 B = the mean of blank integrals

The percentage elemental composition for each element is calculated by:

$$\text{Percentage of element} = \frac{K \times (I-B)}{wt} \quad (5.5)$$

where: K = K factor
 I = sample integral value
 B = mean of blank integrals
 wt = weight of the sample (in mg).

5.4.3 Reproducibility of Data

The reproducibility of analyses varied with the element analysed. From analyses conducted in duplicate the following values are applicable: Carbon ± 0.5 wt.%, Hydrogen ± 0.1 wt.%, Nitrogen ± 0.1 wt.%.

5.5 Calorific Value

5.5.1 Description of Apparatus

The equipment used was a Gallenkamp Automatic Adiabatic Bomb Calorimeter in which the internal calorimeter vessel was completely surrounded by two water jackets maintaining the system at approximately uniform temperature. A pair of matched thermistors were immersed in both the outer jacket and inner vessel respectively, forming the arms of a bridge circuit control. The outer jacket was fitted with a quick acting electrode heater and a cooling coil. By maintaining the system at a uniform temperature no heat was lost from the calorimeter vessel and no cooling corrections were necessary. The thermometer used was a solid stem, mercury in glass type, conforming to BS 791 (range: 18 - 24 °C with 0.5 °C intervals) calibrated by NPL to an accuracy of 0.002 °C. The target weight for each analysis was 0.8 g (± 0.05 g), providing an adequate temperature rise of 1.8 to 2.5 °C for most coals.

5.5.2 Procedure

The total heat liberated, measured in joules, was given by the product of the corrected temperature rise and the total water equivalent of the system, which was constant at a value of 2400 g. The total heat liberated was corrected by subtracting the heat of formation for the sulphuric and nitric acids with an additional correction for the ignition cotton and wire. The sulphur correction was obtained by titration with 0.1N sodium hydroxide to a neutral end point using screened methyl orange indicator. The quantity of sulphuric acid was given by:

$$V = T - 0.17 \times N \quad (5.6)$$

V = the sulphuric acid content in ml of 0.1N H₂SO₄

T = the 0.1N sodium hydroxide titration (ml)

N = the empirically derived nitric acid correction in joules (28 joules).

The sulphuric acid correction to be subtracted = 15.1 x V. The empirically derived correction for the cotton and wire is 74.5 joules. The gross calorific value of the fuel is given by the total heat released minus the given corrections, divided by the mass of fuel burnt:

$$G_v = \frac{(T \times 2400 \times 4.1818) - e_1 - e_2 - e_3}{M} \quad (5.7)$$

where: G_v = the gross calorific value at constant volume
T = the recorded temperature rise (K)
e₁ = the correction for the cotton + fuse wire
e₂ = the correction for nitric acid
e₃ = the correction for sulphuric acid
M = the mass of the fuel, as analysed.

5.5.3 Reproducibility of Data

From duplicate analyses the calorific values are reproducible to within $\pm 160 \text{ kJ kg}^{-1}$

5.6 Fourier Transform Infrared Spectroscopy

5.6.1 Description of Apparatus

Fourier transform infrared spectroscopy (FT-IR) was performed on the crushed coals using the KBr pellet technique and a Nicolet 20 SXB single-beam Fourier transform infrared spectrometer equipped with a liquid nitrogen cooled mercury-cadmium-telluride detector.

5.6.2 Procedure

Between 0.5 to 1.0 mg of dry crushed coal (38 - 75 μm) was mixed with $\approx 100 \text{ mg}$ of dry KBr, ground and pressed into a disc using a die. The spectra of coals were constructed from a total of 64 scans over a spectra range of 400 to 4000 cm^{-1} with a resolution 4 cm^{-1} .

5.7 Nuclear Magnetic Resonance Spectroscopy

5.7.1 Description of Apparatus

All ^{13}C CP/MAS NMR analyses were conducted by ARCO Inc. of the United States. The ^{13}C CP/MAS NMR spectra were obtained at 50.3 MHz on Bruker AC-E 200 NMR spectrometer operating at 4.7 tesla. The contact time was 10 ms and the number of scans per spectra varied from 240 to 670.

5.8 Entrained Flow Reactor

5.8.1 Description of Apparatus

The Northern Carbon Research Laboratories *Entrained Flow Reactor* (EFR) was developed⁴ to provide a laboratory facility capable of generating the high heating rates encountered in a commercial pulverized fuel boiler. Depending upon the size of the carbonaceous particle, the maximum heating rates encountered within the EFR at temperatures greater than 850 $^{\circ}\text{C}$, was 10^4 - $10^5 \text{ }^{\circ}\text{C s}^{-1}$ which are comparable to those encountered in a commercial pulverized fuel boiler.^{5,6} The design of the EFR was based upon existing models, operated by other workers,^{5,6} which consists of a furnace system and several component accessories.

The EFR consists of a main, 7-zone, vertical split tube furnace and temperature controllers, a

166 cm silica reaction tube, primary and secondary gas heaters, primary and secondary gas feeders, a flow straightener, sample feed system and product collection (Figure 5.4, Plate 5).

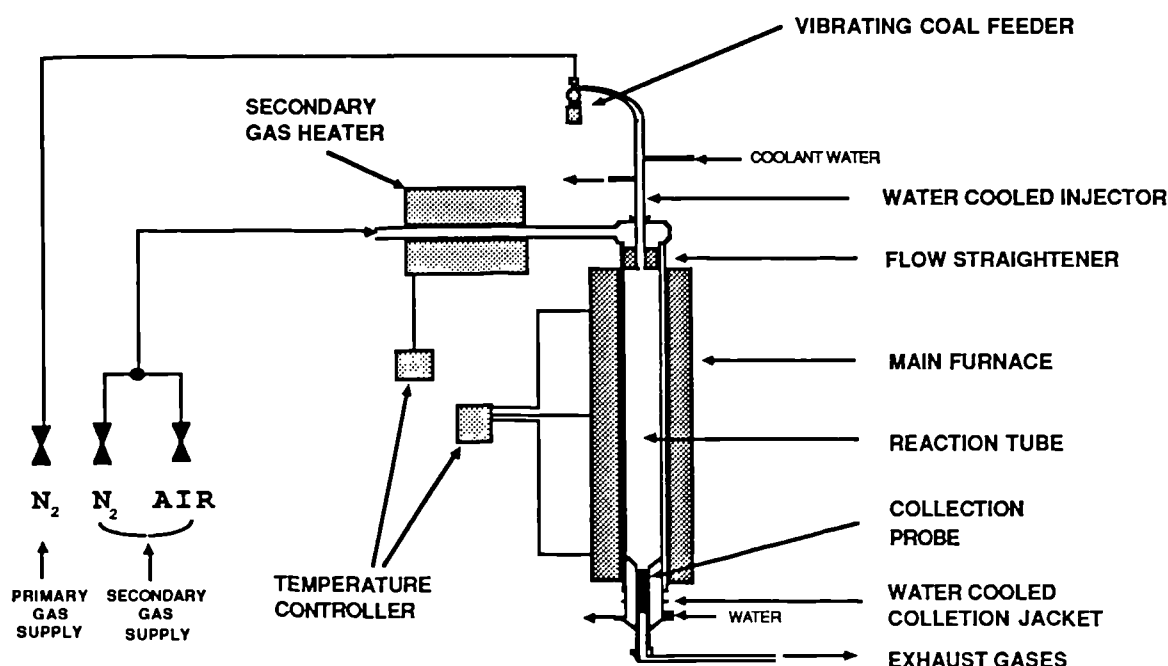


Figure 5.4 A schematic representation of the EFR configured for coal pyrolysis.

The essential features of the EFR are:

- operating temperature for all pyrolysis and combustion experiments was 1000 °C
- reaction zone length = 1.66m
- residence time ≈ 1 s
- heating rate 10^4 - 10^5 °C s⁻¹
- the water cooled injection probe allows the injection of *coal* particles into the reaction zone without pre-heating
- the silica injector conducts pre-heated primary gas and *char* into the reaction zone
- the flow straightener removes turbulence within the secondary gas on entering the reaction zone
- the water cooled collecting jacket is used to cool the collection probe and bronze filter positioned along the furnace axis
- the collection filters are sintered bronze with a mesh size of 3 - 6 μ m
- coal or char sample feeders fluidized the sample, promoting the creation of an aerosol
- the primary gas used was N₂ (oxygen free)
- the secondary gas used was N₂ (pyrolysis) or air (combustion).

The *efficiency* of the entrained flow reactor *feeder system* was greatly improved with the development and subsequent utilization of a vibrating unit (see line drawing, Appendix B). The

action of the vibrating head against the underside of the glass fuel feeder produced a flocculation of the pulverized coal, which is then swept into the sample feeder pipe, producing a greater efficiency of sample introduction. With the aid of the vibrator unit, the percentage of material lost during the pyrolysis of pulverized coal, to form char, has been reduced from 25% to 6%.

To enable comparisons of pyrolysis and combustion behaviour between coals of differing characteristics it was essential that the residence time of particles within the reaction zone was known.

The residence time of particles within the reaction zone was governed by the gas flow rate and flow regime (laminar or turbulent). Under laminar flow conditions particles travel down the centreline along a parabolic velocity profile...

$$\frac{V_{\text{centreline}}}{V_{\text{mean}}} = 2.0 \quad (5.8)$$

where:

reaction zone length	=	1.66 m
diameter	=	0.065 m
residence time required	=	1 s

therefore:

$$V_{\text{centreline}} = \frac{1.66 \text{ m s}^{-1}}{1} = 1.66 \text{ m s}^{-1} \quad (5.9)$$

and hence:

$$V_{\text{mean}} = \frac{1.66}{2} = 0.83 \text{ m s}^{-1} \quad (5.10)$$

To achieve the desired residence time of 1 s during the pyrolysis of coal particles in N₂ the required gas flow was calculated as follows:⁴

$$\text{Total gas flow} = \left(\frac{\text{Fluid}}{\text{density}} \right) \times \left(\frac{\text{Reaction zone}}{\text{cross sectional area}} \right) \times (\text{Mean velocity}) \quad (5.11)$$

$$\begin{aligned} \text{For N}_2 &= 0.2695 \times \frac{\pi \times 0.065^2}{4} \times 0.83 \text{ kg s}^{-1} \\ &= 7.4225 \times 10^{-4} \text{ kg s}^{-1} \\ &= 7.4225 \times 10^{-4} / 1.1709 \text{ m}^3 \text{ s}^{-1} \text{ (N.T.P.)} \\ &= 6.339 \times 10^{-4} \text{ m}^3 \text{ s}^{-1} \text{ (N.T.P.)} \\ &= 0.0634 \text{ l s}^{-1} \text{ (N.T.P.)} = 38.0 \text{ l min}^{-1} \text{ (N.T.P.)} \\ &\quad \text{(N.T.P. = 20 °C and 1 atmosphere pressure.)} \end{aligned}$$

The total gas flow rates for air were calculated as above using 0.2772 kg m^{-3} as the gas density for air.

Secondary gas flow: $V_{\text{primary gas}} = V_{\text{centreline}}$

$$\text{Secondary gas} = 1.66 \text{ m s}^{-1}$$

Earlier systems^{5,6} used 0.05 - 1.4 percentage fractions of the total gas flow for the primary gas. It was decided⁴ that the primary gas flow would be maintained at 1.5% of the total flow rate to maintain the primary gas velocity below that of the secondary gas.

To determine whether the gas velocities described above would be sufficient to produce laminar flow the Reynolds number (Re) was calculated. For Reynolds numbers below 2300 flow is normally laminar and turbulent above 3200, with intermediary states between those values.⁷ The Reynolds number was calculated using:

$$Re = \frac{Vdl}{\gamma} \quad (5.12)$$

where: V = fluid density (kg m^{-3})
 d = tube diameter (m)
 l = gas velocity (m s^{-1})
 γ = gas viscosity ($\text{g m}^{-1} \text{ s}^{-1}$)

using equation 5.12, substituting $Re = 312$ for air (304 for N_2) laminar flow conditions were achieved.

5.8.2 Procedure

5.8.2.1 Coal Pyrolysis Using N_2

To produce $\approx 1 \text{ g}$ of char approximately 1.5 g of coal ($38\text{-}75 \mu\text{m}$) was used. Using a clean sample injection and collection probes, with the furnace stabilized at 1000°C , the procedure for the pyrolysis of coal using the E.F.R. system was:-

- The sample was weighed into the fuel feeder.
- The secondary gas supply was set to the correct flow-rate (37.5 l min^{-1}).
- The primary gas supply was switched on and set to 0.55 l min^{-1} .
- The coal was swept into the reaction zone and the char collected dry within the bronze filter located within the water cooled collecting probe.
- All coal pyrolysis were conducted in duplicate after cleaning all probes, feeder and injector apparatus.
- All samples were weighed prior to and following pyrolysis.

5.8.2.2 Char Combustion Using Air

To produce 10-50 mg of combustion product 1.0 - 1.5 g of coal char was used. The procedure employed for the combustion of char was similar to that for pyrolysis; air was used as the primary gas which was pre-heated to reaction zone temperature using the silica injector/primary gas heater. Furthermore, the combustion product was collected within the bronze filter using quench water (8 l h^{-1}) within the collection probe.

The char and combustion product proximate analyses, conducted as outlined in section 5.3.2, were used inconjunction with the following formulae to calculate the proportion of un-burnt carbon within the combustion product:

$$W = \frac{100 \times A_o}{100 - A_o} \times \frac{C^1}{A^1} \quad (5.13)$$

where: W = the proportion of un-burnt carbon within the combustion product
 C^1 = remaining carbon within the combustion product (wt.%, DVMF)
 A^1 = remaining ash content of the combustion product (wt.%, DVMF)
 A_o = the ash content of the char (wt.%, DVMF)

5.9 Optical Char Characterisation (Morphology)

5.9.1 Sample Preparation

The char was bound in a cold-setting polyester resin in small (10 mm diameter) plastic moulds. Once set, the small blocks were re-mounted in a larger mould (25 mm) to provide a larger block for grinding and polishing. The block-mounted char was successively ground and polished as outlined in section 5.2.1.

5.9.2 Description of Apparatus

Char morphology analysis was conducted on each sample using a Leitz MPV3 microscope photometer in conjunction with a Swift automatic point-counter (Model F). The microscope was equipped with an ocular (10 x) fitted with a cross-hair graticule, an oil-immersion strain-free, infinity corrected, objective (50 x) providing a total magnification of 800 x. Cross-polars with $\frac{1}{4} \lambda$ retarder plate were employed to differentiate between optically isotropic or anisotropic char-wall material. The limit of resolution at x 800, using an oil immersion objective is $\leq 1 \mu\text{m}$.

5.9.3 Procedure

The analysis involved the identification of the char located at the intersection of the graticule

cross-hair using and the recording of 500 individual determinations per polished char block using an interpoint and interline distances of 0.5 mm. The number of counts recorded was converted to a proportion (in %) by volume of the total. Char analysis required cross-sectional morphological recognition of the char type outlined in Table 5.5 (Plate 6) using specific criteria outlined below. The nomenclature was based on a modified Bailey/Diessel classification system⁸ and all chars produced within the EFR were characterized in terms of cross-sectional morphology, optical texture (isotropic/anisotropic), macro porosity and mean maximum char diameter.

Table 5.5. Char Morphology Classification and Nomenclature⁸

Class	Sub-class	Optical Texture
Coal Particle (unchanged)		
Coal particle (with pore development)		
Cenosphere	Mono-	Isotropic Anisotropic
	Tenui-	Isotropic Anisotropic
	Crassi-	Isotropic Anisotropic
Cenospheropore		Isotropic Anisotropic
Network	Tenui-	Isotropic Anisotropic
	Crassi-	Isotropic Anisotropic
	Mixed-	Isotropic Anisotropic
Solid	Inertoid	Isotropic Anisotropic
	Fusinoid	
Fragment	< 10 mm	(no equivalent)
Mineral Matter		

5.9.4 Char Classification Criteria

Please refer to accompanying plate (Plate 6)

- Unchanged coal particle: no softening, no vesiculation
- Coal with pore development: softening, some vesiculation but recognisable as coal
- Mono-cenosphere: spherical - subspherical in shape, single pore, no secondary or tertiary vesiculation within the char wall, porosity $\geq 70\%$
- Tenui-cenosphere: spherical - subspherical in shape, one large pore, some secondary or tertiary vesiculation within the char wall, char wall thickness $\leq 5\mu\text{m}$, porosity $\geq 65\%$
- Crassi-cenosphere: spherical - subspherical in shape, one large pore with pronounced secondary or tertiary vesiculation within the char wall, char wall thickness $\geq 5\mu\text{m}$, porosity $\geq 65\%$

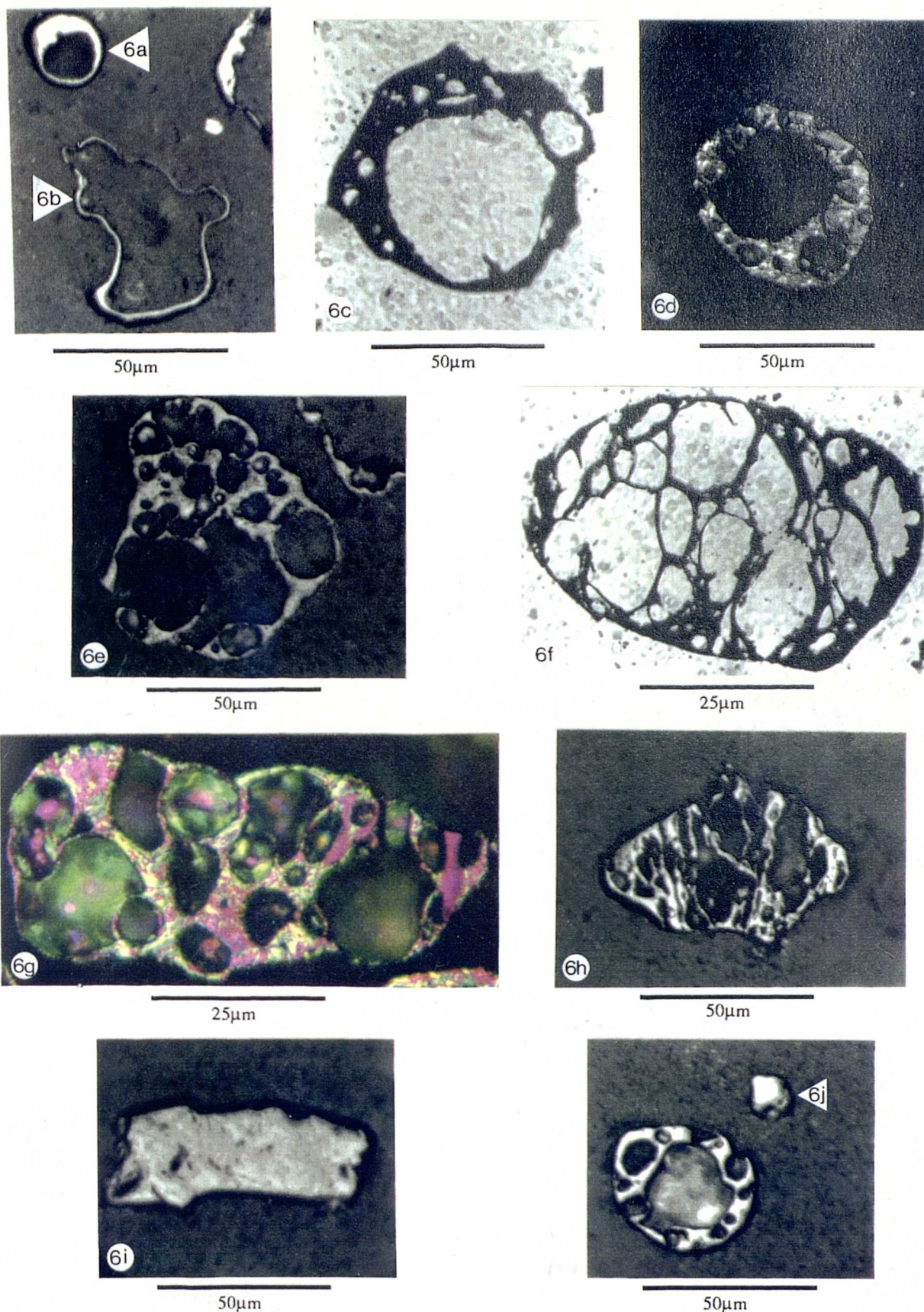


Plate 6 Char Morphologies and Nomenclature Used

Cenospheres. (6a) Monocenosphere, reflected light. (6b) Tenuicenosphere, reflected light. (6c) Crassicenosphere, transmitted light. (6d) Crassicenosphere, reflected light [crossed-polars].

Cenospheropore. (6e) reflected light [crossed-polars]

Network. (6f) Tenuinetwork, transmitted light. (6g) Crassinetwork, reflected light [crossed-polars + $\frac{1}{4}\lambda$ plate]. (6h) Mixed-network, reflected light.

Inertoid. (6i) Solid, reflected light. (6j) Fragment, reflected light

- Cenospheropore subspherical to elongate, consisting of more than one large rounded pore, char wall thickness $\geq 5\mu\text{m}$, porosity $\geq 65\%$
- Tenui-network elongate to oblong, consisting of many sub-parallel elongate pores, char wall thickness $\leq 5\mu\text{m}$, porosity $\geq 65\%$
- Crassi-network elongate to oblong, consisting of many sub-parallel elongate pores, char wall thickness $\geq 5\mu\text{m}$, porosity $\leq 65\%$
- Mixed-network variety of shapes, an admixture of porosities, char wall thickness and/or optical texture
- Solid (Inertoid) Solid, massive particle with no vesiculation, coal precursor material not recognisable, high reflectance
- Solid (Fusinoid) Solid, massive particle with no vesiculation, coal precursor material recognisable as fusinite, high reflectance

5.9.5 Reproducibility of Data

The criterion for the accuracy of the char morphology analyses were given by the reproducibility and the comparablilty of the results. The reproducibility of two analyses made by a single operator on the same polished surface is $\pm 1.5 \%$, based on a 500 point-count.

5.10 Macro Porosity Determinations

5.10.1 Description of Apparatus

The mean porosity of a char was determined using the *AMS Optomax V Image Analyser*, a Vickers M17 transmitted light microscope (50 x oil immersion objective) and an AST 286 Premium computer with data processing software and interface card.

5.10.2 Procedure

Polished thin sections of char were prepared for use on the image analyser. The use of thin sections (thickness $\approx 3 - 5 \mu\text{m}$) and transmitted light was used in preference to polished blocks and reflected light. This technique produced an image with higher contrast, no scattering of light due from within the char pores or due to trapped bubbles of air within the pores, producing a much more objective technique than that obtained through the use of a graphics pad and reflected light. The porosities of the chars were determined by the image analyser through an assessment of gray levels which were used to differentiate between pore and char, relating the porosity of the char by determining the 'x' and 'y' ferets through number of pixels detected.

5.10.3 Reproducibility of Data

Due to the technical difficulties encountered with such a technique, the variation for mean maximum (macro) porosity analyses was $\pm 2.5\%$.

5.11 Scanning Electron Microscopy of Chars

5.11.1 Description of Apparatus

A Jeol JSM T-20 scanning electron microscope was used to examine the gold sputter-coated outer surfaces of chars, mounted on 1 cm diameter aluminium stubs, between magnifications of $\times 200$ to 10,000.

5.12 Transmission Electron Microscopy of Chars

5.12.1 Description of Apparatus

A Jeol Cx-100 transmission electron microscope was used to examine microtomed sections of char wall material in bright field⁹ with an electron wavelength of 0.0037 nm at 100KV and a camera constant of 77.4 cm.

5.13 TGA Reactivity Measurements of Coal

5.13.1 Description of Apparatus

Reactivity analyses of all the coal samples were carried out using a technique similar to that described by Jenkins *et al.*¹⁰ The successive charring and gasification of samples were conducted in a Stanton Redcroft STA 780 Thermal Gravimetric Analyser (TGA). The instrument consisted of an electronic microbalance, nichrome wound furnace, a solid state temperature controller and a Linseis Type 2041 multipen recorder. The sintered platinum crucible (8mm high \times 12 mm top diameter \times 10 mm bottom diameter) was suspended from the balance assembly by a 'hangdown' system into the center of a hermetically sealed furnace. The furnace was lowered and raised around the 'hangdown' assembly for the removal of ash and the placement of fresh sample. This equipment enabled continuous weight measurements to be made during the reactivity determination.

5.13.2 Procedure

The reactivity test technique involved heating 15 mg \pm 0.5 mg sample of 38-75 μ m coal in a stream of dry nitrogen in the TGA apparatus up to 700 °C maximum temperature at a constant

heating rate of 99 °C min⁻¹. It was held at that temperature until no further weight loss was recorded. The newly-formed char was then cooled to 500 °C ± 5 °C and its weight noted. The gaseous environment was changed to air and the sample was allowed to burn-off isothermally to completion.

Under the conditions used, the charts recording the gasification have a rectilinear portion which is indicative of the region of maximum reactivity. The reactivity parameter was calculated using the following formula:

$$R_T = \frac{-1}{W_o} \frac{dw}{dt} \quad (5.14)$$

where:

- R_T = the maximum reactivity at a temperature, T °C (mg h⁻¹ mg⁻¹).
- W_o = the initial mass of the char on an 'ash free' basis (mg).
- $\frac{dw}{dt}$ = the maximum rectilinear weight loss rate (mg h⁻¹).

The parameter, R_T , gives an indication of the chemical reactivity of the in-situ prepared char.

5.13.3 Reproducibility of Data

From analyses run in triplicate the standard error for all TGA based reactivity determinations was ± 4.5%.

5.14 Surface Area Measurements of the Chars

5.14.1 Description of Apparatus

The surface areas of the chars produced by rapid pyrolysis in the EFR at 1000 °C were determined from the adsorption of carbon dioxide at 273 K using a McBain Spring Apparatus and the single point method.

5.14.2 Procedure

About 150 mg of char was outgassed overnight at 373 K and 10 Pa. The extension of the spring was measured and recorded. Carbon dioxide was then admitted to the system and the adsorption determined by the measuring the extension of the spring and formulating a ratio (Equation 5.15). The adsorption of CO₂ was conducted at atmospheric pressure.

5.14.3 Calculations

The adsorption of CO₂ was calculated from the spring extensions using the following equation:

$$n = \frac{E_a \times 1000}{E_o \times 44} \quad (5.15)$$

where:

n	=	the CO ₂ adsorbed at 1 atmosphere 273 K (m mols g ⁻¹)
E_a	=	the extension of the spring due to CO ₂ adsorbed
E_o	=	the extension of the spring due to clean sample

A value for the minimum surface area was calculated using n in the following equation:-

$$S_a = n \ L \times 10^{-3} \times a \quad (5.16)$$

where:

S_a	=	the CO ₂ minimum surface area (m ² g ⁻¹)
L	=	the Avogadro number (6.023 x 10 ²³)
a	=	the area of a physisorbed CO ₂ molecule (2 x 10 ⁻¹⁹ m ²)

5.14.4 Reproducibility of Data

Due to the limitations of the apparatus minimum CO₂ surface area determinations have an accuracy of within 10 m² mg⁻¹.

References

1. Stach, E. (1982) in: Stachs 'Textbook of Coal Petrology' 3rd Ed. Stach. E., Mackowsky, M-Th., Teichmüller, M., Taylor, G.H., Chandra, D. and Teichmüller, R. Gebrüder Borntraeger, Berlin.
2. Ottaway, M. (1982). Fuel **61**, 713-716.
3. British Standards Institute, BS 1016.
4. Skorupska, N.M. (1987). Ph.D. Thesis (Unpub.) University of Newcastle upon Tyne. Newcastle upon Tyne.
5. Street, P.J., Weight, R.P. and Lightman, P. (1960). Fuel **48**, 343-365.
6. Kobayashi, H., Howard, J.B. and Sarofim, A.F. (1977). Sixteenth Symp. (Int.) Combust., The Combust. Inst., Pittsburg., P.A., 411-425.
7. Bradley, J.N. (1969) in: 'Flame and Combustion Phenomena', Methuen., London.
8. Bailey. J. and Diessel, C.F.K. (1987). Presented at the ICCP Combustion Working Group, Heerlen.
9. Rymer, T.B. (1970). 'Electron Diffraction', Methuen.
10. Jenkins, R.G., Nandi, S.P. and Walker, Jr. P.L. (1973). Fuel **52**, 288-293.

CHAPTER SIX

Results

6.1 The Influence of Coal Rank upon Char Morphology and Combustion

The laboratory code number, the rank (ASTM nomenclature) and vitrinite reflectance data for the nine coals used in the *coal rank, char morphology and combustion study* is given in Table 6.1.

The volatile matter and fixed carbon analyses (ash is given in Table 6.4), the percentage of the elements hydrogen, carbon, nitrogen and oxygen (by difference) and the atomic H/C and O/C ratios for the coals used, are also contained within Table 6.1. The aromaticity (f.a.) derived by ^{13}C CP/MAS NMR is given in Table 6.2, with the exception that there are no f.a. values for coals 88/026 and 88/027, which were included too late in the study for analysis by ^{13}C CP/MAS NMR.

The optical texture of the associated chars, the TGA reactivity values, plus the volatile matter yields during pyrolysis within the EFR (by difference) and the proportion of unburnt carbon within the char combustion product is given in Table 6.2

A tabulation of all char morphological types pertaining to the coal rank, char and combustion study is given in Table 6.3

6.2 Coal and Char Characterisation and Correlations

The country of origin, laboratory sample code number, coal rank, vitrinite reflectance and proximate analysis for the coals used in this study is given in Table 6.4, in order of coal rank.

The proportion of the elements hydrogen, carbon, nitrogen and oxygen (by difference), atomic H/C and O/C ratios and calorific value determinations are given in Table 6.5, in order of rank.

The petrographic (maceral) analyses derived by the point-counting technique are given in Table 6.6, in order of rank.

The petrographic (microlithotype) analyses derived by the point-counting technique (using the 20-point Kötter graticule) are given in Table 6.7, in order of rank.

The proportion of char types, generated by rapid pyrolysis, for all coals is given in Table 6.8. The mean porosity determinations derived through image analysis is given in Table 6.9.

Reflectogram data, expressed as the proportion of occurrences within a $1/2$ -V class for those coals included within that study is given in Table 6.10. A $1/2$ -V class represents reflectance values within a 0.5 reflectance range (e.g. 0.55 to 0.599, 0.6 to 0.649).

6.3 The Effects of Coal Oxidation and Weathering upon Coal Properties, Char Morphology and Combustion

The laboratory sample code number and duration of oxidation or weathering for the coals used in this study are listed in Tables 6.11 through to 6.14. The petrographic analyses (maceral) for the coals in this study are contained within Table 6.6.

The changes in volatile matter content, fixed carbon (plus ash), the elements hydrogen, carbon, nitrogen and oxygen (by difference) plus their respective H/C and O/C atomic ratios are given for each coal/oxidation or coal/weathering series in Tables 6.11 through to 6.14.

The changes in vitrinite reflectance, fluorescence intensity and corresponding oxidation quotients for each coal/oxidation or coal/weathering series are given in Tables 6.15 through to 6.18.

The char analyses are given as four tables, corresponding to the individual coal/oxidation or coal/weathering series and listed in Tables 6.19 through to 6.22.

Data relating to changes in char optical texture, CO₂ surface area, intrinsic reactivity and the efficiency of char combustion expressed as the unburnt carbon within the combustion product, are contained within four tables, Tables 6.23 to 6.26.

Table 6.1 Coal rank, Vitrinite Reflectance, Proximate and Elemental Analyses, and Atomic Ratios for the Rank Series of Coals

Coal (Code)	Rank R _o max (ASTM)	Proximate analysis			Elemental analysis				Atomic Ratio	
		Volatile matter (%)	Fixed Carbon (wt% d.b.)	Carbon (wt% d.b.)	Hydrogen (wt% a.r.)	Carbon (wt% a.r.)	Nitrogen (wt% a.r.)	Oxygen (wt% a.r.)	H/C	O/C
86/006	sub a	0.48	33.1	66.8	5.1	71.0	0.7	23.2	0.85	0.25
86/008	sub a	0.49	31.6	68.4	4.9	69.3	0.8	25.0	0.85	0.27
86/001	hvBc	0.58	42.3	57.7	4.9	77.1	1.0	17.0	0.76	0.16
87/022	hvBb	0.67	40.5	59.5	5.6	83.3	1.5	9.6	0.81	0.09
86/016	hvBa	0.93	30.5	69.5	5.2	84.2	1.7	8.8	0.74	0.08
86/014	hvBa	0.96	31.8	68.2	5.3	86.9	1.6	6.2	0.74	0.05
86/011	mvb	1.33	23.0	77.0	4.7	89.5	1.3	4.4	0.63	0.04
88/026	s-anth	2.06	7.5	90.3	4.2	92.0	1.5	1.6	0.55	0.01
88/027	anth	4.29	2.8	95.3	2.9	95.2	1.0	0.9	0.37	0.01

Table 6.2 Aromaticity, Reactivity, Weight Loss and Unburnt Carbon Levels for the Rank Series of Coals

Coal (Code)	Char Optical Texture		Coal Aromaticity ³ (f.a.)	Reactivity (mg h ⁻¹)	Vm ⁴ (%)	Uc ⁵ (%)
	Anisotropic (%)	Isotropic (%)				
86/006	0.0	100.0	0.64	1.260	45	0.5
86/008	1.3	98.7	0.67	1.039	46	0.8
86/001	0.0	100.0	0.72	0.857	56	1.4
87/022	31.1	68.8	0.72	0.308	57	2.3
86/016	88.9	11.0	0.76	0.282	62	8.9
86/014	90.5	9.5	0.78	0.275	61	10.2
86/011	100.0	0.0	0.85	0.137	60	15.9
88/026	95.7	4.3	-	1.377	34	13.8
88/027	0.0	100.0	-	2.187	23	62.3

Table 6.3 Char Types related to the Rank Series of Coals

Coal (Code)	Cenospheres								Network				Solid			Mineral		
	Mono-		Tenui-		Crassi-		Ceno'pore		Tenui-		Crassi-		Mixed-	Inertoid	Fusinoid		Fragment	
	i ⁶	a	i	a	i	a	i	a	i	a	i	a	i					a
86/006	0.6	0.0	1.4	0.8	0.4	0.0	28.6	0.4	47.0	0.0	11.2	0.0	3.4	0.0	1.4	0.0	0.2	1.4
86/008	0.8	0.0	1.8	0.0	2.8	0.0	24.2	0.0	43.4	0.0	19.2	0.0	1.6	0.0	4.6	0.6	0.2	0.8
86/001	4.8	0.0	24.8	0.0	10.0	0.0	32.8	0.0	12.0	0.0	10.8	0.0	2.4	0.0	0.6	0.0	0.8	1.0
87/022	3.2	0.4	19.4	9.2	11.4	8.4	21.6	8.8	3.2	0.0	3.2	1.2	0.8	0.4	0.4	3.2	4.0	1.2
86/016	0.8	4.0	4.2	44.4	2.0	11.2	0.6	12.2	0.0	0.6	0.0	5.6	0.6	2.0	3.6	1.0	0.2	7.0
86/014	1.8	14.8	2.0	40.0	2.0	9.4	2.6	10.0	0.8	1.2	0.2	0.0	0.0	0.0	3.0	0.2	9.8	2.2
86/011	0.0	28.0	0.0	40.8	0.0	14.2	0.0	8.8	0.0	0.0	0.0	0.0	0.0	0.0	0.0	0.6	7.6	0.0
88/027	0.0	2.2	0.0	31.8	0.2	30.8	1.2	15.4	0.0	3.8	0.8	4.4	2.0	2.8	3.6	0.6	0.2	0.2
88/028	0.0	0.0	0.0	0.0	0.0	0.0	0.0	0.0	0.0	0.0	0.0	0.0	0.0	0.0	100.0 ⁷	0.0	0.0	0.0

³ Determined by Nuclear Magnetic Resonance

⁴ Material lost as volatile material during pyrolysis in the EFR

⁵ Unburnt carbon within the combustion product of the char

⁶ Where: i = optical isotropy, a = optical anisotropy

⁷ The anthracite does not form a vesiculated char.

Table 6.4 The Country of Origin, Coal Sample Code, Rank, Vitrinite Reflectance, Proximate Analysis and Reactivity Data for the 22 Coals, within this Study in Order of Rank

Country	Coal (code) ⁹	Rank (ASTM)	Reflectance ⁸ (%R _o max)	Proximate analysis			Reactivity	
				Volatile Matter (wt% d.a.f.)	Fixed Carbon (wt% d.a.f.)	Ash (wt% d.b.)	(mg h ⁻¹)	(mg h ⁻¹ d.a.f.)
Canada	86/005	sub a	0.50	24.8	75.2	46.7	2.525	0.700
Canada	86/006	sub a	0.48	33.2	66.8	9.0	1.260	1.073
Canada	86/007	sub a	0.52	31.9	68.1	17.5	1.348	0.942
Canada	86/008	sub a	0.49	31.6	68.4	11.6	1.039	1.081
Canada	86/009	sub a	0.52	29.8	70.2	16.5	4.253	0.623
Canada	86/010	sub a	0.52	24.3	75.7	15.0	1.265	1.014
Canada	86/001	hvBc	0.58	42.3	57.7	5.3	0.857	0.740
Canada	86/002	hvBc	0.61	33.7	66.2	8.3	0.969	0.827
Canada	86/003	hvBc	0.55	24.3	75.7	15.0	1.064	0.564
Canada	86/004	hvBc	0.57	33.2	66.8	9.4	1.171	1.026
Columbia	87/021	hvBb	0.67	31.1	68.9	9.1	0.377	0.377
Columbia	87/022	hvBb	0.67	40.5	59.5	2.5	0.308	0.279
Britain	88/025	hvBb	0.76	39.1	60.9	4.8	0.695	0.686
Britain	88/024	hvBa	0.93	37.5	62.5	5.1	0.448	0.435
Canada	86/014	hvBa	0.96	31.8	68.2	3.5	0.275	0.218
Canada	86/015	hvBa	0.93	30.4	69.6	21.1	2.268	0.317
Canada	86/016	hvBa	0.93	30.5	69.5	23.1	0.282	0.209
Britain	87/017	hvBa	0.87	26.6	73.4	11.2	0.275	0.279
Poland	87/018	hvBa	0.88	26.7	73.3	11.3	0.306	0.312
USA	87/019	hvBa	0.90	22.9	77.1	15.9	0.176	0.179
Canada	87/023	hvBa	1.08	25.1	74.9	15.5	0.146	0.149
Canada	86/011	mvb	1.33	23.0	77.0	2.5	0.137	0.134
Canada	86/012	mvb	1.33	17.2	82.8	9.2	0.215	0.076
Canada	86/013	mvb	1.27	18.2	81.8	10.7	0.103	0.094

Table 6.5 The Elemental Analysis, Atomic Ratio and Calorific Values for the 22 Coals Used within the Study, in Order of Rank.

Coal (code)	Elemental analysis				Atomic ratios		Calorific value		
	Hydrogen (% a.r.)	Carbon (% a.r.)	Nitrogen (% a.r.)	Oxygen (% a.r.)	H/C	O/C	(gross)	Mj/kg ⁻¹ (dry)	(d.a.f.)
86/005	3.6	41.9	0.5	53.9	1.03	0.96	8.959	9.420	13.822
86/006	5.1	71.0	0.7	23.2	0.85	0.25	21.277	22.926	24.998
86/007	4.6	65.2	1.0	29.2	0.85	0.34	19.136	20.204	23.729
86/008	4.9	69.3	0.8	25.0	0.85	0.27	19.342	20.518	22.902
86/009	4.5	73.3	0.8	21.4	0.74	0.22	19.029	21.286	24.802
86/010	5.2	74.0	0.9	19.9	0.85	0.20	20.917	23.354	26.862
86/001	4.9	77.1	1.0	17.0	0.76	0.16	26.393	27.929	29.403
86/002	4.8	77.7	1.1	16.4	0.74	0.16	26.006	27.316	29.578
86/003	3.4	58.1	0.7	37.8	0.70	0.49	18.487	19.267	22.161
86/004	4.6	79.4	1.1	14.9	0.70	0.14	25.391	27.237	29.805
87/021	5.7	82.2	1.5	10.6	0.83	0.10	27.927	28.859	31.474
87/022	5.6	83.3	1.5	9.6	0.81	0.09	31.169	32.017	32.807
88/025	5.3	80.5	1.7	12.5	0.79	0.12	31.354	32.076	33.800
88/024	5.2	81.0	1.9	12.4	0.78	0.10	33.587	34.463	35.150
86/014	5.3	86.9	1.6	6.2	0.74	0.05	34.128	34.613	35.821
86/015	5.2	82.8	1.6	10.4	0.75	0.09	27.929	28.166	34.115
86/016	5.2	84.2	1.7	8.9	0.74	0.08	27.033	27.311	33.618
87/017	5.6	88.6	1.6	4.2	0.75	0.04	30.972	31.595	35.117
87/018	5.6	89.6	1.7	3.1	0.75	0.03	31.704	32.522	36.210
87/019	5.0	87.4	1.3	6.3	0.68	0.05	29.051	29.51	34.190
87/023	4.8	85.7	1.3	8.2	0.67	0.07	28.385	28.842	33.301
86/011	4.7	89.5	1.4	4.4	0.63	0.04	35.099	35.373	36.271
86/012	4.3	88.5	1.0	6.2	0.58	0.05	32.031	32.197	35.169
86/013	4.4	88.1	1.1	6.4	0.60	0.05	31.629	31.803	35.203

⁸ Vitrinite reflectance

⁹ The laboratory coding has been retained throughout this thesis to aid other researchers working in NCRL within the area of coal combustion.

Table 6.6 Petrographic (maceral) Analyses for the 22 Coals used within the Coal and Char Characterisation and Correlations Study

Coal (code)	Petrographic (maceral) Analysis						
	Vitrinite (vol %)	Liptinite (vol %)	Semi-fusinite ¹⁰ (vol %)	Semi-fusinite ¹¹ (vol %)	Fusinite (vol %)	Mineral (vol %)	Other (vol %)
86/005	5.4	1.0	6.8	23.6	20.2	42.8	0.2
86/006	82.8	3.2	2.0	0.8	4.9	4.2	2.1
86/007	38.7	5.8	7.3	14.7	15.1	15.1	3.3
86/008	84.6	1.2	3.2	1.4	3.4	6.2	0.0
86/009	24.8	8.4	19.0	19.2	26.2	2.4	0.0
86/010	49.0	7.4	13.4	11.0	8.8	9.0	1.4
86/001	85.2	11.6	0.2	0.2	1.8	1.0	0.0
86/002	54.0	6.4	11.2	13.2	9.2	4.8	1.2
86/003	7.8	2.0	4.0	18.6	41.2	26.4	0.0
86/004	63.0	4.2	15.6	8.4	6.0	2.8	0.0
87/021	75.8	4.6	4.8	4.4	4.0	6.4	0.0
87/022	82.4	5.0	5.2	3.2	3.0	1.2	0.0
86/014	95.2	1.8	0.4	1.4	1.2	0.0	0.0
86/015	59.2	2.6	8.0	3.0	1.8	25.4	0.0
86/016	65.8	5.4	5.2	1.8	2.4	19.4	0.0
86/017	49.8	14.0	12.2	12.6	5.2	5.0	1.2
86/018	55.6	16.0	9.2	7.0	3.8	1.4	7.0
86/019	46.0	16.4	15.2	8.8	6.4	2.2	5.0
88/023	53.6	3.6	21.2	9.2	6.4	6.0	0.0
86/011	94.2	0.0	0.4	2.0	3.2	0.2	0.0
86/012	28.0	0.4	29.2	19.0	22.0	1.4	0.0
86/013	41.8	0.8	25.6	18.0	10.4	2.6	0.8

Table 6.7 Microlithotype Analyses for the 22 Coals used within the Coal and Char Characterisation and Correlations Study

Coal (Code)	Monomacerite			Bimacerite				Trimacerite			Carbominerite (vol %)
	Vitrite (vol %)	Inertite ¹²		Clarite (vol %)	Durite (vol %)	Vitrinerite ¹³		Trimacerite ¹³			
		sf (vol %)	f (vol %)			v (vol %)	i (vol %)	v (vol %)	i (vol %)	l (vol %)	
86/005	1.6	17.2	35.0	0.0	0.0	2.4	1.6	0.0	0.0	0.0	42.2
86/006	67.8	3.4	4.4	9.0	0.6	2.8	2.2	3.2	2.2	0.0	4.4
86/007	16.0	16.8	17.0	1.6	3.6	9.6	4.4	8.0	6.4	0.0	16.6
86/008	62.8	2.2	0.2	4.8	0.0	4.0	0.2	5.8	0.4	0.0	19.6
86/009	10.8	34.6	8.0	0.2	7.6	7.0	13.8	2.8	7.6	0.2	7.4
86/010	30.2	14.4	4.6	6.4	4.0	9.4	5.4	4.0	9.2	0.0	12.4
86/001	73.2	0.2	0.8	12.2	0.0	3.8	0.2	4.4	0.0	0.0	5.2
86/002	22.8	11.0	9.6	5.8	1.0	13.0	7.6	14.8	9.6	0.4	4.4
89/003	1.4	23.2	55.2	0.0	0.2	5.6	4.8	0.4	0.4	0.0	8.8
86/004	20.4	9.8	11.0	4.4	0.6	11.6	9.2	19.8	6.8	0.0	6.4
87/021	36.6	2.0	0.8	11.2	0.0	7.2	3.0	29.2	3.8	0.0	6.2
87/022	39.2	4.2	3.4	5.8	0.0	11.6	5.8	26.8	2.4	0.0	0.8
86/014	85.6	2.0	0.0	5.0	0.2	3.0	0.4	3.0	0.4	0.0	0.4
86/015	44.8	0.8	0.4	7.6	0.0	4.0	0.8	4.0	0.4	0.0	37.2
86/016	49.6	6.4	2.6	12.0	0.6	1.4	0.4	7.4	0.4	0.0	19.2
86/017	18.2	13.4	0.8	2.8	7.2	7.0	0.2	28.2	12.6	4.8	4.8
86/018	14.4	5.4	5.0	4.0	6.0	7.8	1.2	34.2	13.8	1.8	6.4
86/019	31.6	21.6	2.8	3.4	1.8	4.0	2.4	14.2	3.6	0.6	14.0
87/023	21.8	22.0	2.4	1.2	2.8	14.6	9.8	11.2	6.2	0.2	7.8
86/011	86.6	2.0	0.2	1.8	0.0	6.4	1.8	0.8	0.0	0.0	0.4
86/012	24.4	18.6	10.0	0.0	0.6	15.2	27.8	1.4	1.8	0.0	0.2
86/013	25.0	15.6	13.6	0.4	0.0	25.6	15.0	4.2	0.2	0.0	0.4

¹⁰ Low semi-fusinite, a lower reflecting, 'reactive', fusible semi-fusinite especially relating to carbonisation

¹¹ High semi-fusinite, a higher reflecting, 'non-reactive' and infusible semi-fusinite

¹² Where sf indicates a predominance of Semi-fusinite macerals; f indicates that the maceral Fusinite predominates

¹³ In which the following maceral predominates: v = vitrinite; l = liptinite; i = inertinite

Table 6.8 Char Analyses for All Coals used within the Coal and Char Characterisation and Correlations Study (in volume %)

Coal (Code)	Cenospheres								Network						Solid			Mineral (%)
	Mono-		Tenui-		Crassi-		Ceno'pore		Tenui-		Crassi-		Mixed-		Inertoid	Fusoid	Fragment	
	i ¹⁴ (%)	a (%)	i (%)	a (%)	i (%)	a (%)	i (%)	a (%)	i (%)	a (%)	i (%)	a (%)	i (%)	a (%)	(%)	(%)	(%)	
86/005	0.0	0.0	1.0	0.0	0.2	0.0	0.8	0.0	8.6	0.0	33.4	0.0	15.2	0.0	24.4	4.0	0.4	12.0
86/006	0.6	0.0	1.4	0.8	0.4	0.0	28.6	0.4	47.0	0.0	11.2	0.0	3.4	0.0	1.4	0.0	0.2	1.4
86/007	0.0	0.0	0.8	0.0	0.4	0.0	4.6	0.0	11.4	0.0	43.2	0.0	8.6	0.0	19.6	6.6	1.8	3.0
86/008	0.8	0.0	1.8	0.0	2.8	0.0	24.2	0.0	43.4	0.0	19.2	0.0	1.6	0.0	4.6	0.6	0.2	0.8
86/009	0.0	0.0	0.0	0.0	0.0	0.0	0.4	0.0	6.6	0.0	53.6	0.0	4.4	0.0	22.6	6.8	2.8	2.8
86/010	0.0	0.0	0.8	0.0	0.2	0.0	5.4	0.0	16.0	0.0	48.6	0.0	8.6	0.0	12.2	2.2	4.0	2.0
86/001	4.8	0.0	24.8	0.0	10.0	0.0	32.8	0.0	12.0	0.0	10.8	0.0	2.4	0.0	0.6	0.0	0.8	1.0
86/002	2.3	0.0	12.6	0.0	3.9	0.0	32.2	0.0	10.8	0.0	14.0	0.0	7.8	0.0	14.0	1.6	0.8	1.8
86/003	0.0	0.0	0.6	0.0	0.8	0.0	6.2	0.2	7.2	0.0	23.6	0.0	17.0	0.0	34.4	2.0	0.0	8.0
86/004	3.8	0.0	7.4	0.0	5.2	0.2	27.4	0.0	16.0	0.0	20.4	0.0	6.6	0.0	4.6	3.0	4.6	0.8
87/021	3.8	0.0	18.2	5.0	9.8	3.4	20.0	2.6	8.6	0.0	7.8	0.8	2.2	0.0	1.2	4.8	5.0	6.8
87/022	3.2	0.4	19.4	9.2	11.4	8.4	21.6	8.8	3.2	0.0	3.2	1.2	0.8	0.4	0.4	3.2	4.0	1.2
86/014	1.8	14.8	2.0	40.0	2.0	9.4	2.6	10.0	0.8	1.2	0.2	0.0	0.0	0.0	3.0	0.2	9.8	2.2
86/015	0.4	0.0	14.2	0.0	12.0	0.0	19.6	0.0	6.4	0.0	17.4	0.0	3.4	0.0	4.4	2.0	3.8	16.4
86/016	0.8	4.0	4.2	44.4	2.0	11.2	0.6	12.2	0.0	0.6	0.0	5.6	0.6	2.0	3.6	1.0	0.2	7.0
88/025	1.8	0.0	16.6	26.2	10.6	8.4	8.4	6.4	0.4	4.4	2.2	0.8	2.8	0.8	3.6	1.8	0.2	4.0
86/017	4.0	4.2	11.0	32.4	3.8	14.4	3.8	7.8	1.8	0.6	1.6	2.2	1.2	0.2	2.2	0.8	6.2	1.8
86/018	1.0	10.8	3.4	37.6	4.2	10.8	8.2	10.4	0.6	1.2	0.2	0.0	0.2	0.0	3.0	0.0	7.8	0.6
86/019	0.4	1.8	6.4	24.6	4.8	8.2	12.8	15.2	2.0	2.0	2.4	1.0	0.6	0.2	5.2	1.0	6.4	4.0
88/024	1.0	9.4	2.2	77.0	0.8	2.6	0.6	1.6	0.0	0.0	0.0	1.2	0.6	0.6	1.0	0.2	0.6	0.6
87/023	0.0	5.0	0.6	18.2	0.8	10.6	2.6	18.2	2.6	1.8	8.6	4.8	1.0	3.0	3.0	8.0	4.8	6.4
86/011	0.0	28.0	0.0	40.8	0.0	14.2	0.0	8.8	0.0	0.0	0.0	0.0	0.0	0.0	0.0	0.6	7.6	0.0
86/012	0.0	4.0	0.2	6.8	0.2	9.2	0.6	19.0	5.0	6.4	12.0	7.8	3.8	3.8	5.0	10.8	3.2	2.0
86/013	0.0	2.4	0.0	24.6	0.0	17.8	1.8	19.4	0.0	0.8	9.4	1.8	4.0	1.6	6.2	2.0	6.2	3.0
88/027	0.0	2.2	0.0	31.8	0.2	30.8	1.2	15.4	0.0	3.8	0.8	4.4	2.0	2.8	3.6	0.6	0.2	0.2
88/028	0.0	0.0	0.0	0.0	0.0	0.0	0.0	0.0	0.0	0.0	0.0	0.0	0.0	0.0	100.0†	0.0	0.0	0.0

† The anthracite does not form a vesiculated char

Table 6.9 Mean Porosity Determinations for the main classes of Char Types used in the Study

	Cenospheres				Network			Solid		
	Mono- (%)	Tenui- (%)	Crassi- (%)	Ceno'pore (%)	Tenui- (%)	Crassi- (%)	Mixed- (%)	Inertoid (%)	Fusoid (%)	Fragment (%)
Porosity	79.8	83.5	63.7	61.6	65.6	42.8	45.6	14.9	21.1	-
δ	7.8	5.9	5.3	6.0	6.7	7.3	5.8	4.9	6.8	-

δ Standard Deviation

¹⁴ Where i = optical isotropy, a = optical anisotropy

Table 6.10 Reflectogram Data as a Proportion (in %) : Listing reflectance Values Recorded between 0.1% and 3.0% R_0 random (n_{oil} 1.518 : 546nm @ 23°C)

Reflectance	Reflectogram data as a proportion (in vol %) per total reflectance measurements for coals listed [†]																					
Interval ¹⁵	1	2	3	4	5	6	7	8	9	10	11	12	13	14	15	16	17	18	19	21	22	
0.10			0.2		11.6	0.5	0.5	0.4		0.9						0.7						
0.15	0.4	0.5	12.4		20.6	0.3	5.9	1.3		1.8						1.6				1.0		
0.20	0.4	0.3	9.4	2.7	9.9	1.0	4.6	1.1	2.9	4.0						1.4	0.9	0.5	1.0	1.2	1.1	
0.25	0.6	1.0	2.4	0.9	4.2	0.2	2.4	0.9	2.9	0.2					0.4	0.8	1.3	0.5	1.2	1.2	1.6	
0.30	0.6	0.5	2.0	0.3	1.4	0.2	2.4	1.7	3.5	2.7					0.4	1.8	1.4	2.6	0.6	2.7	0.8	
0.35	1.2	0.5	1.4	1.2	0.6	2.3	1.8	4.8	5.9	3.0					0.7	0.4	2.1	1.0	1.0	0.9	3.2	
0.40	2.3	0.8	1.9	0.3	0.8	6.5	5.6	13.2	8.2	11.6					0.7	0.4	1.6	0.9	0.4	0.3	2.7	
0.45	5.0	1.1	2.1	4.8	2.3	16.5	11.8	22.6	16.5	15.4					1.0	1.6	1.8	1.6	0.4	1.2		
0.50	10.3	6.6	2.1	6.9	2.1	27.0	19.3	33.4	18.2	16.6					1.4	0.7	1.4	0.9	0.8	0.3	1.6	
0.55	26.8	15.0	3.4	16.6	2.2	22.3	6.1	13.9	5.9	5.9					0.7	0.4	0.4	1.4	1.2	4.8	2.7	
0.60	29.8	17.9	3.8	23.2	2.1	8.0	2.0	4.1	0.6	3.4					0.7	0.2	3.2	1.0	1.0	6.9	16.5	
0.65	19.4	18.0	1.7	15.1	1.0	5.5	1.1	0.4	1.2	1.7					0.7	1.1	3.8	2.6	1.8	16.6	28.2	
0.70	2.0	6.3	1.7	6.3	2.6	0.5	1.4	0.4	0.6	2.6				0.1	1.8	1.8	5.9	4.9	3.4	23.2	26.4	
0.75	0.4	2.8	1.0	2.4	1.8	3.7	1.4		1.20	0.9				2.7	3.9	6.5	7.7	9.0	6.5	15.1	9.0	
0.80		0.8	3.8	0.9	1.6	0.8	2.5		2.9	1.5				5.2	7.6	19.6	13.2	14.9	8.1	6.3	2.1	
0.85	0.4	1.5	3.2	3.3	3.2	1.0	2.7	0.4	1.8	1.9				10.4	12.7	21.4	11.1	18.9	10.3	2.4	1.6	
0.90		2.5	1.5	0.9	2.2	0.5	1.8		4.1	2.0				24.3	18.1	19.8	8.5	10.9	8.7	0.9		
0.95		1.3	3.6	1.2	3.8	0.5	3.2	0.2	4.7	1.9				30.2	20.6	10.1	3.8	5.7	7.7	3.3		
1.00		2.0	3.8	0.9	3.2	0.2	3.6		5.3	2.4	1.4	0.1	0.6	22.5	12.1	1.3	2.5	3.6	3.0	0.9	0.5	
1.05		1.6	2.7	0.6	3.1	0.3	3.2	0.2	5.3	1.8	4.2	0.8	0.6	4.0	8.3	1.1	1.1	1.6	1.4	1.2	0.5	
1.10		0.6	4.6	1.2	2.3	0.5	2.9		5.3	1.6	13.0	0.4	3.8	0.3	1.8	0.7	2.0	0.9	2.8	0.9	0.5	
1.15		1.2	2.3	1.5	3.2	0.8	2.0		5.3	1.2	22.0	1.8	6.3	0.1	0.7	0.2	0.4	0.7	2.0	0.6		
1.20	0.2	1.5	2.7	0.9	2.3	0.3	1.4		7.1	2.1	29.2	3.6	14.5		0.4	0.4	1.3	0.7	1.9	1.2	0.5	
1.25		1.7	3.4	0.6	1.6		1.1		7.7	1.6	18.6	5.9	13.2	0.1		0.4	2.0	0.5	1.5	1.5		
1.30		0.3	2.7	0.6	1.6	0.3	1.7	0.2	4.1	1.9	6.7	5.5	3.8		0.4	0.9	1.4	0.7	1.2	0.9		
1.35	0.2	0.5	2.1	1.2	2.3	0.3	1.4		1.8	1.4	2.5	5.2	5.7			0.7	1.1	0.7	1.0	0.6		
1.40		1.6	3.2	0.3	0.8		0.9	0.2	2.3	0.9	0.6	5.7	4.4	0.1		0.4	2.0	0.5	2.0	0.6	0.5	
1.45		0.8	1.3		1.0		0.5	0.2	1.2	1.2	0.4	5.2	2.3			0.5	2.0	0.9	2.0	1.2		
1.50	0.2	1.2	2.5	1.2	0.8		0.5		2.4	0.7	0.2	4.1	8.1			0.7	1.2	0.7	1.2	0.3		
1.55		1.2	1.3		0.8		0.9		2.4	1.2		6.4	3.1			0.5	1.6	1.4	0.4			
1.60		0.3	1.3	0.6	0.4				0.6	0.4	0.2	5.5	3.8			0.7	0.6	1.2	1.8	1.2		
1.65		1.5	1.0		0.8			0.2	1.2	0.5		4.5	4.4			0.4	1.4	0.9	1.0			
1.70		0.6	2.3		0.2			0.2	0.6	0.4	0.2	5.0	5.0					2.0	0.9	1.6	0.6	
1.75		1.0	2.0		0.6		0.9		0.6	0.5		4.6	1.3					2.1	0.4	1.8		
1.80		1.0	0.4		0.4		0.5		0.6			3.8	1.3			0.5	0.5	0.2	2.0			
1.85		0.1	0.4		0.6		0.5					4.4	3.8			0.2	1.6	1.0	2.6			
1.90		1.0	0.4		0.2					0.4		2.2	0.6	0.1			1.3	0.5	2.4			
1.95		0.3	0.2				0.5			0.2		2.9	2.5				0.9	0.9	1.2			
2.00		0.5	0.4				0.5			0.2	0.2	3.0	2.5	0.1			0.9	1.0	1.4			
2.05		0.3	1.0				0.5			0.4		2.5	1.0				0.2	0.2	0.4			
2.10		0.3	0.2								0.2	2.2	1.3				0.2	0.4	1.0			
2.15		0.3	0.2									2.7	0.6				0.2	0.2	1.6			
2.20		0.3										1.6	1.2				0.2	0.4	1.4	0.6		
2.25		0.3										1.4	1.2									
2.30		0.1									0.4					0.4	0.2	0.2	0.4			
2.35		0.5										1.2					0.2		0.6			
2.40												1.5	1.3									
2.45												1.2					0.2	0.2	0.2			
2.50												0.5						0.2	0.4			
2.55												0.5	0.6						0.6			
2.60												0.1	0.6				0.2	0.2	0.6			
2.65												0.5					0.2		0.6			
2.70												0.4							0.2			
2.75												0.1							0.2			
2.80												0.1							0.6			
2.85												0.4							0.2			
2.90												0.2							0.5			
2.95												0.1	0.6						0.8			
3.00+												0.8							0.6			

¹⁵ The 1/2 V-steps shown represent all values recorded within a reflectance class of 0.05%, e.g. 0.2% - 0.249% = 0.25

[†] Coals 86/001 to 87/022

Table 6.11 Duration of Oxidation, Proximate and Elemental Analyses for the Oxidised A24 Coal Series (100°C/static air)

Coal (Code)	Oxidation Duration (days)	Proximate Analysis			Elemental Analysis				Atomic Ratios	
		Volatile Matter (wt% d.b.)	Fixed Carbon (wt% d.b.)	Ash (wt% d.b.)	Hydrogen (wt% a.r.)	Carbon (wt% a.r.)	Nitrogen (wt% a.r.)	Oxygen (wt% a.r.)	H/C	O/C
A24-0	Fresh	35.6	59.3	5.1	5.3	81.0	1.7	12.5	0.79	0.12
A24-1	1	32.7	61.8	5.5	4.7	77.6	1.7	16.0	0.73	0.15
A24-2	7	32.7	61.9	5.4	4.2	73.9	1.6	20.3	0.68	0.21
A24-3	17	31.6	62.8	5.6	3.7	71.0	1.6	23.7	0.63	0.25
A24-4	30	31.3	62.1	6.6	3.4	69.3	1.6	25.7	0.59	0.28
A24-5	112	31.3	63.5	5.2	2.9	65.0	1.6	30.5	0.54	0.35

Table 6.12 Duration of Oxidation, Proximate and Elemental Analyses for the Laboratory Oxidised A25 Coal Series (100°C/Static Air)

Coal (Code)	Oxidation Duration (days)	Proximate Analysis			Elemental Analysis				Atomic Ratios	
		Volatile Matter (wt% d.b.)	Fixed Carbon (wt% d.b.)	Ash (wt% d.b.)	Hydrogen (wt% a.r.)	Carbon (wt% a.r.)	Nitrogen (wt% a.r.)	Oxygen (wt% a.r.)	H/C	O/C
A25-0	Fresh	37.2	58.0	4.8	5.2	80.5	1.9	12.4	0.78	0.10
A25-1	1	37.2	57.7	5.1	4.5	75.5	1.7	18.3	0.72	0.17
A25-2	7	33.4	62.6	4.0	4.0	74.6	1.5	19.9	0.64	0.20
A25-3	17	32.6	63.1	4.3	3.4	66.2	1.5	28.9	0.62	0.33
A25-4	30	31.4	64.0	4.6	3.1	64.2	1.5	31.0	0.58	0.36
A25-5	112	31.0	65.6	3.4	2.8	61.8	1.6	33.8	0.54	0.41

Table 6.13 Duration of Oxidation, Proximate and Elemental Analyses for the Weathered W24 Coal Series

Coal (Code)	Duration (weeks)	Proximate Analysis			Elemental Analysis				Atomic Ratios	
		Volatile Matter (wt% d.b.)	Fixed Carbon (wt% d.b.)	Ash (wt% d.b.)	Hydrogen (wt% a.r.)	Carbon (wt% a.r.)	Nitrogen (wt% a.r.)	Oxygen (wt% a.r.)	H/C	O/C
W24-0	Fresh	35.6	59.3	5.1	5.3	81.0	1.7	12.5	0.79	0.12
W24-1	1	35.5	58.7	5.8	5.1	80.1	1.8	13.0	0.79	0.12
W24-2	4	35.2	58.6	6.2	5.3	80.6	1.7	12.4	0.79	0.12
W24-3	19	33.0	60.5	6.5	4.9	78.6	1.6	14.9	0.75	0.14
W24-4	32	32.9	62.6	4.5	4.9	78.4	1.7	15.0	0.75	0.14
W24-5	52	31.7	61.1	7.2	4.9	78.0	1.7	15.4	0.75	0.15

Table 6.14 Duration of Oxidation, Proximate and Elemental Analyses for the Weathered W25 Coal Series

Coal (Code)	Duration (weeks)	Proximate Analysis			Elemental Analysis				Atomic Ratios	
		Volatile Matter (wt% d.b.)	Fixed Carbon (wt% d.b.)	Ash (wt% d.b.)	Hydrogen (wt% a.r.)	Carbon (wt% a.r.)	Nitrogen (wt% a.r.)	Oxygen (wt% a.r.)	H/C	O/C
W25-0	FRESH	37.2	58.0	4.8	5.2	80.5	1.9	12.4	0.78	0.12
W25-1	1	36.8	60.0	3.2	4.9	75.6	1.7	17.8	0.77	0.18
W25-2	4	35.4	61.4	3.2	4.9	75.7	1.7	17.7	0.78	0.18
W25-3	19	32.9	63.5	3.6	4.9	74.0	1.7	19.4	0.79	0.20
W25-4	32	32.1	63.0	4.9	4.9	73.2	1.7	20.2	0.80	0.21
W25-5	52	31.9	62.4	5.7	4.7	73.0	1.7	20.6	0.77	0.21

Table 6.15 Petrographic (Vitrinite Reflectance, Fluorescence Intensity) Data for the Oxidised A24 Coal Series (100°C/static air)

Coal (Code)	Oxidation (days)	Petrographic Analysis				
		R _{oil} (%random)	Standard Deviation	I ₆₅₀ ¹⁶ (max/min)	Standard Deviation	Oxidation Quotient
A24-0	FRESH	0.93	0.03	2.7	0.4	2.9
A24-1	1	0.94	0.03	1.7/0.8	0.32/0.51	1.8
A24-2	7	0.99	0.05	0.9/0.4	0.06/0.03	0.9
A24-3	17	1.04	0.04	0.4	-	0.4
A24-4	30	1.09	0.06	0.4	-	0.4
A24-5	112	1.16	0.07	0.4	-	0.3

Table 6.16 Petrographic (Vitrinite Reflectance, Fluorescence Intensity) Data for the Oxidised A25 Coal Series (100°C/static air)

Coal (Code)	Oxidation (days)	Petrographic Analysis				
		R _{oil} (%random)	Standard Deviation	I ₆₅₀ ¹⁶ (max/min)	Standard Deviation	Oxidation Quotient
A25-0	FRESH	0.76	0.03	2.3	0.39	3.0
A25-1	1	0.78	0.03	1.5/0.9	0.35/0.14	1.9
A25-2	7	0.8	0.04	0.8/0.4	0.09	1.0
A25-3	17	0.83	0.04	0.5/0.4	0.05	0.6
A25-4	30	0.86	0.05	0.4	-	0.5
A25-5	112	0.93	0.03	0.4	-	0.4

Table 6.17 Petrographic (Vitrinite Reflectance, Fluorescence Intensity) Data for the Weathered A24 Coal Series

Coal (Code)	Weathered weeks)	Petrographic Analysis				
		R _{oil} (%random)	Standard Deviation	I ₆₅₀ ¹⁶ (max/min)	Standard Deviation	Oxidation Quotient
W24-0	FRESH	0.93	0.03	2.6	0.21	2.8
W24-1	1	0.91	0.04	2.4/1.6	0.22/0.13	2.6
W24-2	4	0.89	0.04	1.7/1.0	0.28/0.13	1.9
W24-3	19	0.86	0.04	1.2/0.9	0.41/0.62	1.3
W24-4	32	0.84	0.05	1.1/0.8	0.53/0.66	1.3
W24-5	52	0.81	0.06	0.8	0.76	0.9

Table 6.18 Petrographic (Vitrinite Reflectance, Fluorescence Intensity) Data for the Weathered W25 Coal Series

Coal (Code)	Weathered (weeks)	Petrographic Analysis				
		R _{oil} (%random)	Standard Deviation	I ₆₅₀ ¹⁶ (max/min)	Standard Deviation	Oxidation Quotient
W25-0	FRESH	0.76	0.03	2.29	0.21	3.0
W25-1	1	0.72	0.04	2.1/1.4	0.31/0.25	2.9
W25-2	4	0.69	0.03	1.6/1.2	0.39/0.31	2.3
W25-3	19	0.68	0.03	1.1/0.8	0.56	1.6
W25-4	32	0.66	0.03	0.9/0.8	0.78	1.3
W25-5	52	0.65	0.04	0.6	-	0.9

¹⁶ Fluorescence Intensity measured at 650 nm, values are for the particle centre/rim, single values indicate uniformity

Table 6.19 Char Analyses for the Oxidised A24 Coal Series (100°C/static air)

Sample (Code)	Cenospheres								Network						Solid			Mineral
	Mono-		Tenui-		Crassi-		Ceno'pore		Tenui-		Crassi-		Mixed-		Inertoid	Fusinoid	Fragment	
	i ¹⁷	a	i	a	i	a	i	a	i	a	i	a	i	a				
	(%)	(%)	(%)	(%)	(%)	(%)	(%)	(%)	(%)	(%)	(%)	(%)	(%)	(%)				
A24-0	1.0	9.4	2.2	77.0	0.8	2.6	0.6	1.6	0.0	0.0	0.0	1.2	0.6	0.6	1.0	0.2	0.6	0.6
A24-1	0.0	1.6	32.2	30.0	12.4	1.8	10.8	0.6	2.4	0.0	2.4	0.2	0.8	0.0	2.8	0.0	0.4	1.6
A24-2	0.0	0.0	11.8	0.8	10.0	0.2	18.8	0.4	34.6	0.6	8.6	0.2	3.4	0.0	6.0	0.6	0.8	3.2
A24-3	0.0	0.0	0.0	0.0	2.8	0.0	2.8	0.0	2.6	0.0	50.8	0.0	10.6	0.0	27.8	0.0	0.6	2.0
A24-4	0.0	0.0	0.4	0.0	2.4	0.0	3.4	0.0	0.0	0.0	54.0	0.0	7.6	0.0	28.6	0.0	1.8	1.8
A24-5	0.0	0.0	0.4	0.0	2.2	0.0	1.2	0.0	0.0	0.0	38.0	0.0	4.6	0.0	47.8	0.0	2.8	3.0

Table 6.20 Char Analyses for the Oxidised A25 Coal Series (100°C/static air)

Sample (Code)	Cenospheres								Network						Solid			Mineral
	Mono-		Tenui-		Crassi-		Ceno'pore		Tenui-		Crassi-		Mixed-		Inertoid	Fusinoid	Fragment	
	i	a	i	a	i	a	i	a	i	a	i	a	i	a				
	(%)	(%)	(%)	(%)	(%)	(%)	(%)	(%)	(%)	(%)	(%)	(%)	(%)	(%)	(%)	(%)	(%)	(%)
A25-0	1.8	0.0	16.6	26.2	10.6	8.4	8.4	6.4	0.4	1.4	2.2	0.8	2.8	0.8	3.6	1.8	3.2	4.6
A25-1	0.6	0.2	28.4	17.6	10.4	3.8	18.2	6.0	0.8	0.2	1.6	0.0	1.8	0.0	3.8	1.4	2.4	2.8
A25-2	0.4	0.0	3.8	0.8	5.2	0.2	18.6	0.4	44.4	0.0	13.0	0.0	4.6	0.0	5.2	1.4	0.6	1.6
A25-3	0.0	0.0	1.8	0.2	4.4	0.2	6.6	0.4	12.2	0.0	51.6	0.0	7.0	0.0	11.8	1.2	1.0	1.6
A25-4	0.0	0.0	1.2	0.0	1.2	0.0	2.4	0.0	1.0	0.0	41.2	0.0	7.2	0.0	41.4	1.4	1.2	1.6
A25-5	0.0	0.0	0.0	0.0	0.2	0.0	0.8	0.0	0.0	0.0	23.0	0.0	1.4	0.0	68.6	1.2	0.0	4.2

Table 6.21 Char Analyses for the Weathered W24 Coal Series

Sample (Code)	Cenospheres								Network						Solid			Mineral
	Mono-		Tenui-		Crassi-		Ceno'pore		Tenui-		Crassi-		Mixed-		Inertoid	Fusinoid	Fragment	
	i	a	i	a	i	a	i	a	i	a	i	a	i	a				
	(%)	(%)	(%)	(%)	(%)	(%)	(%)	(%)	(%)	(%)	(%)	(%)	(%)	(%)	(%)	(%)	(%)	
W24-0	1.0	9.4	2.2	77.0	0.8	2.6	0.6	1.6	0.0	0.0	0.0	1.2	0.6	0.6	1.0	0.2	0.6	0.6
W24-1	0.2	5.6	19.0	66.4	0.6	2.2	0.6	2.6	0.0	0.0	0.0	0.2	0.0	0.2	0.4	0.2	0.8	1.0
W24-2	2.6	5.2	17.6	63.8	2.0	2.8	1.0	3.4	0.4	0.0	0.0	0.0	0.0	0.0	0.4	0.4	0.2	0.2
W24-3	0.6	2.2	31.8	35.8	5.6	8.6	2.8	6.4	0.2	0.2	0.0	0.0	0.8	1.2	1.2	0.8	0.8	1.0
W24-4	0.8	0.2	41.8	19.0	10.2	1.8	12.2	1.8	4.2	1.2	0.6	0.8	1.0	0.4	1.4	0.6	1.2	0.8
W24-5	0.0	0.0	22.4	1.2	18.4	0.4	28.8	0.4	11.6	3.6	1.6	1.6	2.4	0.8	2.0	1.6	0.4	2.8

Table 6.22 Char Analyses for the Weathered W25 Coal Series

Sample (Code)	Cenospheres								Network						Solid			Mineral
	Mono-		Tenui-		Crassi-		Ceno'pore		Tenui-		Crassi-		Mixed-		Inertoid	Fusinoid	Fragment	
	i	a	i	a	i	a	i	a	i	a	i	a	i	a				
	(%)	(%)	(%)	(%)	(%)	(%)	(%)	(%)	(%)	(%)	(%)	(%)	(%)	(%)	(%)	(%)	(%)	
W25-0	1.8	0.0	16.6	26.2	10.6	8.4	8.4	6.4	0.4	4.4	2.2	0.8	2.8	0.8	3.6	1.8	0.2	4.0
W25-1	2.4	0.0	32.6	11.6	13.0	4.4	6.6	3.0	2.6	2.4	2.8	0.8	6.0	2.0	3.8	2.2	0.2	3.6
W25-2	0.6	0.0	26.4	4.6	22.4	2.4	14.2	2.8	4.8	2.4	2.8	1.2	2.8	0.8	4.4	1.6	3.0	2.8
W25-3	0.0	0.0	31.2	5.4	14.2	3.2	19.2	6.2	2.2	1.8	2.6	0.4	3.2	1.2	4.6	1.8	0.6	2.2
W25-4	0.4	0.0	20.4	5.2	18.8	2.8	28.4	7.2	2.4	3.6	1.6	1.6	2.4	0.4	2.0	0.8	0.4	1.6
W25-5	0.0	0.0	8.4	2.8	17.8	0.2	36.2	2.8	9.2	0.2	6.4	0.0	5.6	0.2	4.6	1.6	1.8	2.2

¹⁷ Where: i = optical isotropy, a = optical anisotropy

Table 6.23 Optical Texture, Reactivity, Char and Burn-Out Product Proximate Analyses, and Fractional Conversion Data for the Oxidised A24 Coal Series

<u>Coal</u> (Code)	<u>Surface Area</u> CO ₂ (m ² g ⁻¹)	<u>Optical Texture</u>		<u>Reactivity</u> (mg h ⁻¹)	<u>Uc¹⁸</u> (%)
		Isotropic (vol%)	Anisotropic (vol%)		
A24-0	60	7.6	92.4	2.687	28.9
A24-1	-	65.8	34.2	3.144	14.3
A24-2	-	97.8	2.2	3.517	16.0
A24-3	-	100.0	0.0	3.805	0.5
A24-4	-	100.0	0.0	3.792	1.2
A24-5	250	100.0	0.0	4.004	1.6

Table 6.24 Optical Texture, Reactivity, Char and Burn-Out Product Proximate Analyses, and Fractional Conversion Data for the Oxidised A25 Coal Series

<u>Coal</u> (Code)	<u>Surface Area</u> CO ₂ (m ² g ⁻¹)	<u>Optical Texture</u>		<u>Reactivity</u> (mg h ⁻¹)	<u>Uc¹⁸</u> (%)
		Isotropic (vol%)	Anisotropic (vol%)		
A25-0	120	56.0	44.0	4.172	2.2
A25-1	-	72.2	27.8	5.964	1.6
A25-2	-	98.6	1.4	6.048	0.3
A25-3	200	99.2	0.8	5.907	7.5
A25-4	-	100.0	0.0	5.784	7.8
A25-5	270	100.0	0.0	5.550	10.1

Table 6.25 Optical Texture, Reactivity, Char and Burn-Out Product Proximate Analyses, and Fractional Conversion Data for the Weathered W24 Coal Series

<u>Coal</u> (Code)	<u>Surface Area</u> CO ₂ (m ² g ⁻¹)	<u>Optical Texture</u>		<u>Reactivity</u> (mg h ⁻¹)	<u>Uc¹⁸</u> (%)
		Isotropic (vol%)	Anisotropic (vol%)		
W24-0	60	5.3	94.7	2.687	28.9
W24-1	-	21.4	78.6	2.856	22.4
W24-2	-	23.8	75.2	2.985	6.9
W24-3	-	43.0	57.0	2.950	3.6
W24-4	-	74.5	25.5	3.104	2.8
W24-5	100	91.4	8.6	3.256	1.7

Table 6.26 Optical Texture, Reactivity, Char and Burn-Out Product Proximate Analyses, and Fractional Conversion Data for the Weathered W25 Coal Series

<u>Coal</u> (Code)	<u>Surface Area</u> CO ₂ (m ² g ⁻¹)	<u>Optical Texture</u>		<u>Reactivity</u> (mg h ⁻¹)	<u>Uc¹⁸</u> (%)
		Isotropic (vol%)	Anisotropic (vol%)		
W25-0	120	56.0	44.0	4.172	2.2
W25-1	-	73.7	26.3	4.360	1.9
W25-2	-	80.3	19.7	4.369	1.8
W25-3	-	79.9	20.1	4.667	1.7
W25-4	-	81.1	18.9	4.952	0.8
W25-5	110	93.1	6.9	5.268	0.4

¹⁸ Unburnt carbon as residue remaining after the combustion of the char

CHAPTER SEVEN

Discussion

7.1 The Influence of Coal Rank upon Char Morphology and Combustion

7.1.1 Introduction

There are several publications discussing relationships between aspects of combustion (e.g. char formation, morphology and burn-out) and a number of coal characterisation techniques.¹⁻⁹ However, due to the diverse and complex nature of coal, conclusions concerning char formation and morphology in relation to coal rank and petrographic composition are equivocal. Essentially, all investigations concerning the relationships between the char, char combustion and the properties of the parent coal seek to identify those key coal characteristics that may be used for classification purposes. Interest in the char morphology seeks to assess the relative importance and effect that the structure, density and optical texture of the char has upon the heterogeneous gas/solid reaction during char combustion and char burn-out. For example, the porosity and permeability of the char control the diffusion of gaseous reactants through the char material.

Studies by Street *et al.*,¹ Oka *et al.*⁶ and Shiboaka *et al.*¹⁰ using entrained flow reactor (EFR) apparatus and a study by Hamilton⁵ using heated grid experiments focused upon the morphological differences in chars produced from coals of different rank. Other workers^{3,4,8,12} have concentrated upon the influence of petrographic composition in determining specific char morphologies (Plate 6). Investigations of the relative behaviour of inertinite macerals during pulverised fuel combustion using laboratory based equipment or pilot and full-scale plant,^{3,4,9,11} led some workers to conclude that specific char morphologies were generated during the combustion, or during the pyrolysis of specific macerals (e.g. cenospheres from vitrinite).^{12,13} Such persuasive work detracted from rank related studies to the extent that some workers have assumed that an inextricable link exists between specific char types and certain macerals or sub-macerals, therefore largely ignoring the effects of rank.

An attempt to relate specific macerals or sub-macerals to specific types of char, using twenty two coals of different petrographic composition and rank, is given in Figures 7.1 and 7.2. There is a poor relationship between the vitrinite content and the proportion of cenospheres present in the EFR pyrolysis product for those coals studied (Figure 7.1). This is especially noticeable concerning the vitrinite rich coals 86/006 (82.8% vitrinite), 86/008 (84.6% vitrinite) and coal 86/004 (63.0 % vitrinite), which are associated with low yields of cenospheres compared to other vitrinite rich coals within the same sample set (e.g. compare

86/008 to 86/011: Table 6.8). A poor relationship also exists between network chars and the proportion of semi-fusinite present within each coal (Figure 7.2).

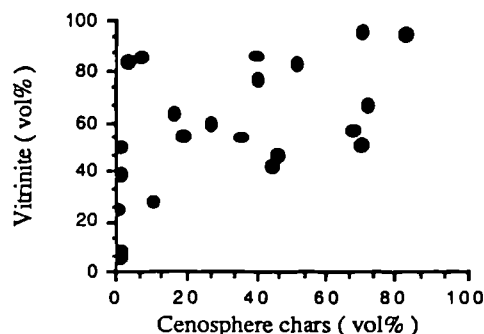


Figure 7.1 The proportion of cenosphere chars against the vitrinite content of coal feedstock.

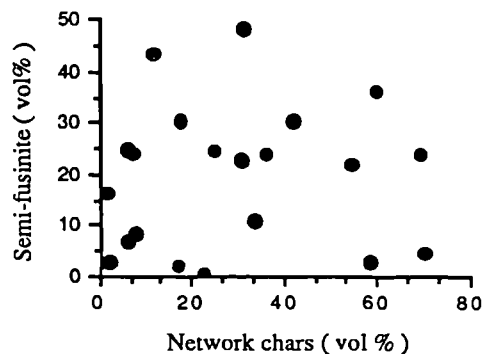


Figure 7.2 The proportion of network chars against the semi-fusinite content of coal feedstock.

The absence of satisfactory correlations in either case suggests that the proposed maceral and char morphology relationships of Jones *et al*⁴ are too simplistic and that of Skorupska¹² requires a more detailed examination.

7.1.2 The Relationship between Coal Rank and Char Morphology

This study is based upon a suite of six vitrinite rich coals from Western Canada (Cretaceous) encompassing a range in rank from sub-bituminous (sub A) to medium volatile bituminous (mvb), supplemented by a high volatile bituminous (hvB) coal from Columbia (Tertiary) and a semi-anthracite (s-anth) and anthracite from Wales (U.K., Carboniferous). The latter two coals were selected because no anthracites or semi-anthracites were made available from Western Canada. The rank, vitrinite content and sample codes for the nine coals used is given in Table 7.1.

Table 7.1 The Coal Rank, Vitrinite Content and Sample Code for the Coals used in the Char Morphology, Combustion and Coal Rank Study.

	Coal Samples								
	88/006	86/008	86/001	87/022	86/016	86/014	86/011	88/026	88/027
Coal Rank	sub A	sub A	hvBc	hvBb	hvBa	hvBa	mvb	s-anth	anth
Vitrinite Content	82.8%	84.6%	85.2%	82.4%	65.8%	95.2%	94.2%	78.2%	88.4%

An examination of the chars generated (Figure 7.3) during rapid pyrolysis, for those coals studied, reveals that it is impossible to ascribe any one char type to vitrinite rich coals.

Clearly, vitrinite generates a wide range of chars dependent upon the rank of the coal.

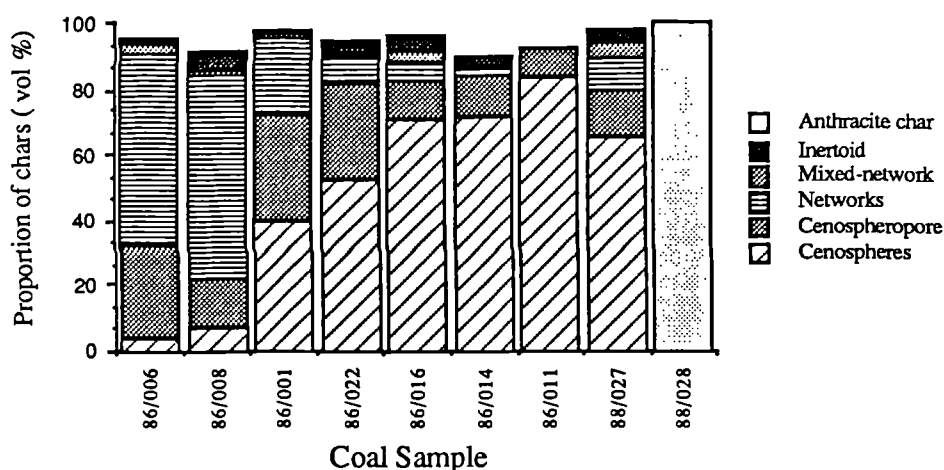


Figure 7.3 Stacked histograms showing the changes in char population for vitrinite rich coals due to differences in rank.

The role of rank is demonstrated by plotting (Figure 7.4) the proportion of cenospheres generated from each coal, against coal rank. The implication is that the proportion of cenospheres generated during pyrolysis was dependent upon rank. The distribution of network chars over rank (Figure 7.5) also indicates a rank dependency.

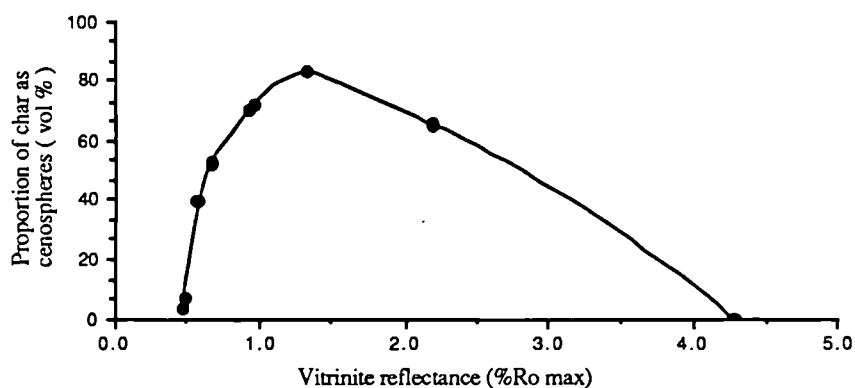


Figure 7.4 The relationship between coal rank and the proportion of cenosphere.

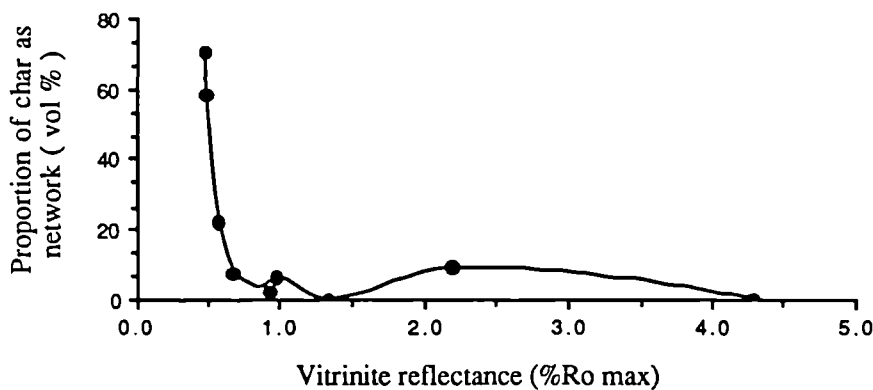


Figure 7.5 The relationship between coal rank and the proportion of network chars.

The development of optical anisotropy within the char walls is also dependent upon the rank of the coal used (Figure 7.6) and follows the cenosphere/coal rank distribution.

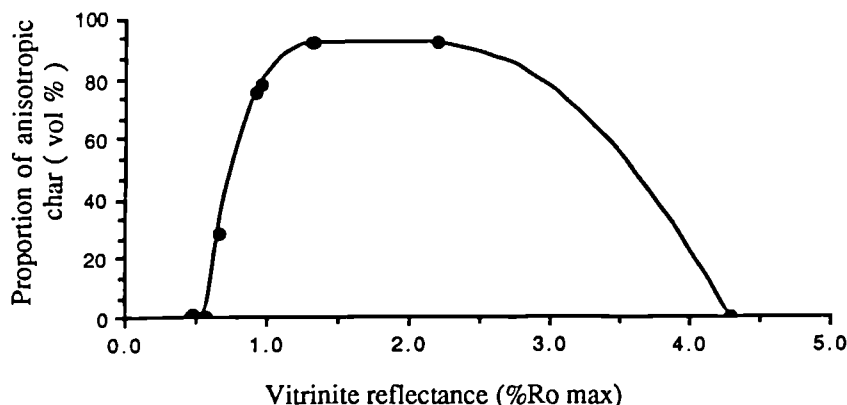
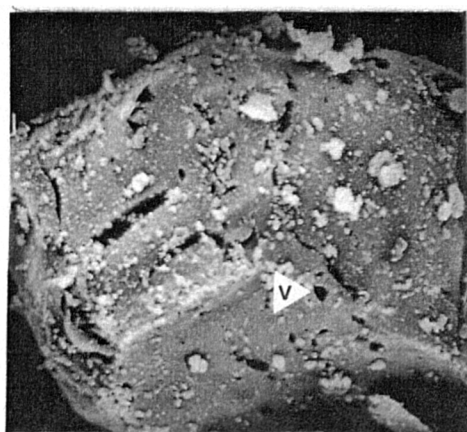


Figure 7.6 Char optical anisotropy against the rank of the coal feedstock.

Network chars are predominantly optically isotropic at the magnification employed (x800) using a polarised light microscope, whereas the cenospheres exhibit either optical isotropy or anisotropy, depending upon the rank of the parent coal.

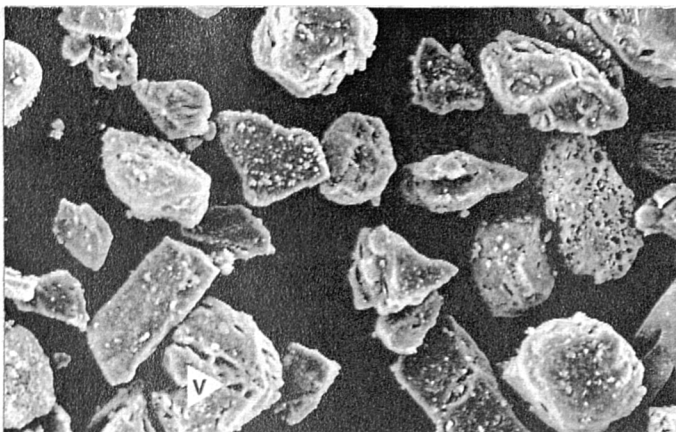
The external appearance of a char, when viewed by scanning electron microscopy (SEM), can be related to the rank of the parent coal (Plate 7). The chars shown in Plate 7a, which are derived from a sub-bituminous coal (86/006), have a sub-angular to oblate appearance which is typical of the network chars. Their fenestrated appearance is due to the existence of small vents (V) that range in size from 1 μm to 5 μm . The close proximity of the small vents to each other suggests either in-situ vesiculation or that the escaping volatiles from within the devolatilising metaplast are able to access a number of permeable channels through the thermo-setting viscous mass during devolatilisation. The existence of permeable channels within the char wall is verified by viewing microtomed sections (Plate 8a) of char with a transmitted electron microscope (TEM) in bright field. The char wall has a highly perturbed appearance in which inter-connected pores (P) are visible, ranging in size from approximately 5 to 50 nm in diameter. However, mechanical damage during the microtoming of such a brittle material may have contributed to the texture the char wall material depicted in TEM micrograph. The existence of a micro-porosity (≤ 2 nm), inferred from CO_2 surface area analysis ($200 \text{ m}^2 \text{ g}^{-1}$) also suggests that network chars have a highly disordered (and micro-porous) structure, thereby complimenting the porosity shown in the TEM and SEM micrographs. The retention of visible porosity within the char walls is significant because an inter-connected pore structure enables reactant gases to penetrate the char material during gasification.^{16,17}

The external appearance of the chars derived from a medium volatile bituminous vitrinite rich coal (86/011) have a rounded, sub-rounded to oblate appearance, considered typical of cenospheres or 'collapsed' cenospheres (Plate 7b). This contrasts with the char derived from sub-bituminous coals (Plate 7a). The cenospheres have fewer devolatilisation vents, although

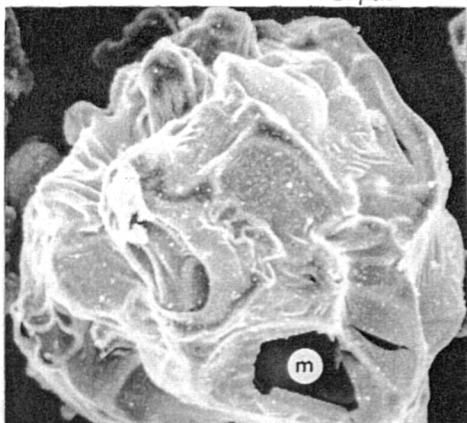


7a

25µm

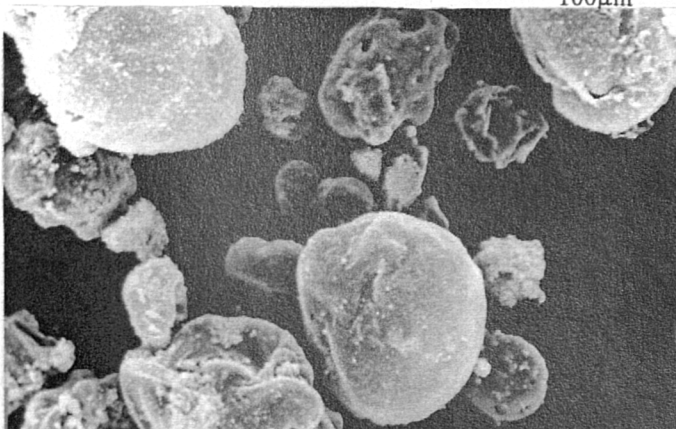


100µm

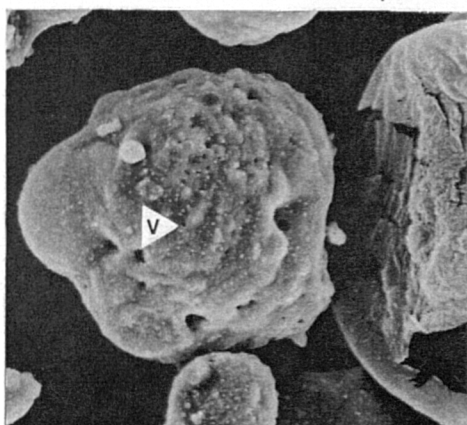


7b

100µm

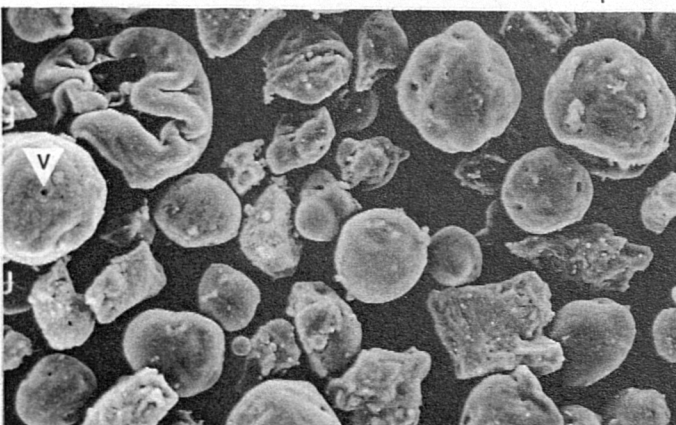


100µm

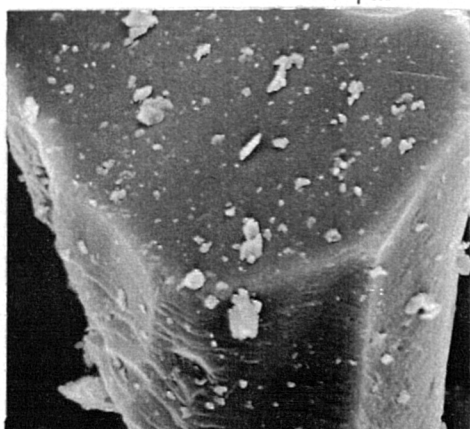


7c

50µm

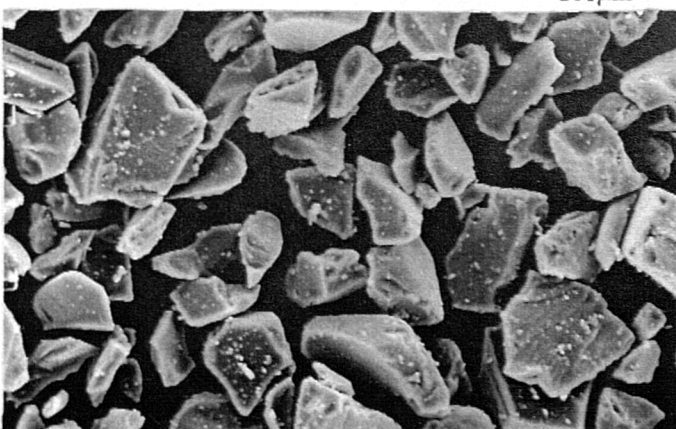


100µm



7d

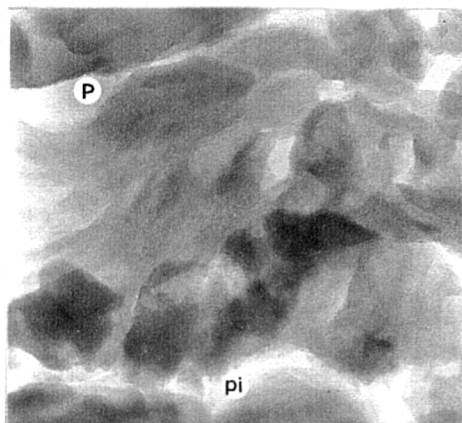
25µm



100µm

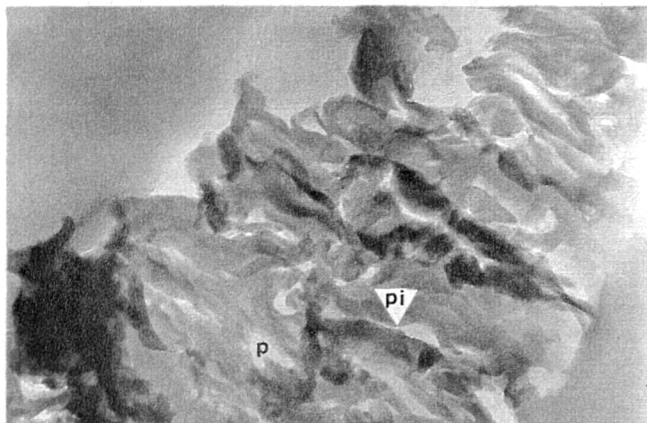
Plate 7 Scanning Electron Micrographs of Char

7a, Char derived from a sub-bituminous coal. 7b, Cenospheres and collapsed cenospheres derived from a medium volatile bituminous coal. 7c, Cenospheres derived from a semi-anthracite coal. 7d, 'Unchanged coal', anthracite rank. (v), devolatilisation vents. (m), mechanical damage. (JEOL JSMT20)

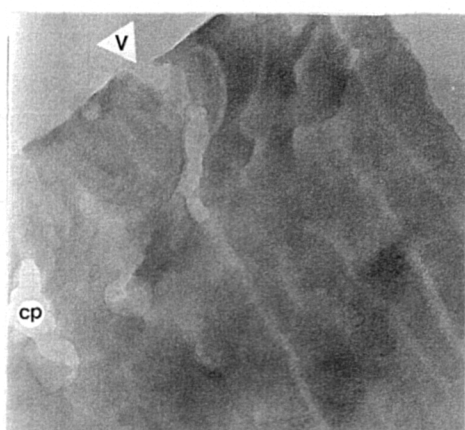


8a

100nm

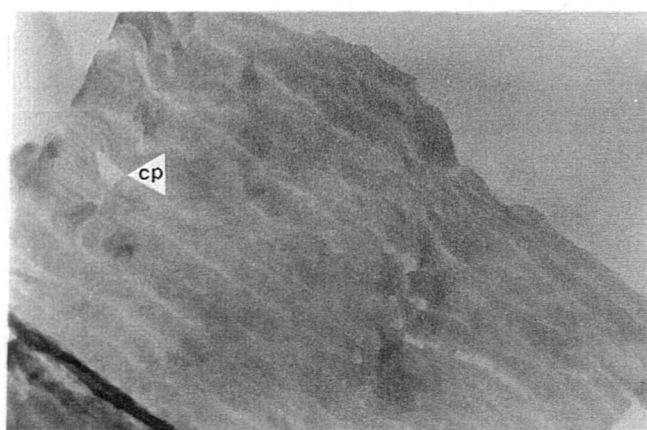


600nm

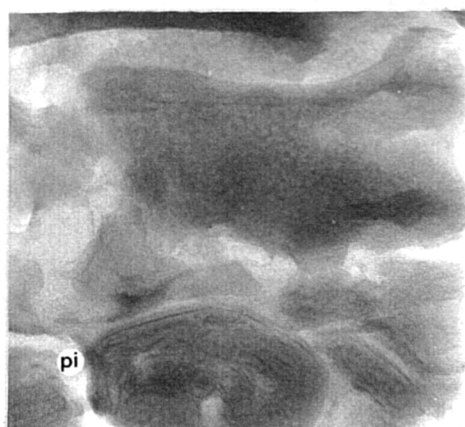


8b

100nm

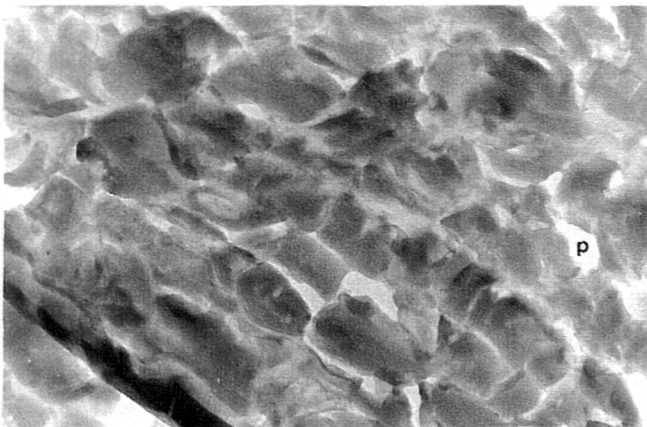


600nm



8c

100nm



600nm

Plate 8 Transmitted Electron Micrographs of Char

8a, Micrographs of char wall material derived from a sub-bituminous coal. 8b, Micrographs of char wall material derived from a medium volatile bituminous coal. 8c, Micrographs of char wall material derived from a semi-anthracite coal. (p), pore. (cp), enclosed pore. (pi), interconnecting channel. (v), devolatilisation vents. (JOEL C-100)

large (i.e. $>10\ \mu\text{m}$) vents are occasionally visible, attributed¹⁸ to a volatile matter 'jet-release' phenomenon. The TEM micrograph (Plate 8b) also contrasts with that of the sub-bituminous char (Plate 8a). The possibility that the striated appearance is an artifact, created during microtoming, cannot be discounted; however, the texture of the char wall differs greatly from that shown in Plate 8a. The appearance of 'blind' (i.e. not inter-connected) and inaccessible (i.e. closed) pores (P) within the cenosphere char wall (within the resolution of TEM) is also evident within the SEM micrographs (Plate 7b) by the paucity of vents on the external surface of the char wall material. In particular the existence of 'thermally-annealed' vents within the surface of the char are possible indications of metaplast 'fluidity' during the formation of the char. The absence of significant micro-porosity is suggested by a very low CO_2 surface area of $20\ \text{m}^2\ \text{g}^{-1}$.

The external appearance (Plate 7c) of the semi-anthracite char, ranges from oblate to angular. Devolatilisation vents are visible and vary in both size and number from char to char. Open and accessible porosity is visible within the char wall material in the TEM micrograph (Plate 8c). The porous nature of this char wall material is similar to that of the sub-bituminous char (Plate 8a), with pores ranging in size from 5 to 25 nm within the TEM micrograph and a CO_2 single isotherm surface area of $160\ \text{m}^2\ \text{g}^{-1}$.

The char derived from the anthracite showed no visible signs of softening or appreciable devolatilisation during pyrolysis, essentially passing through the EFR as 'apparent unchanged coal' producing a material with a low CO_2 surface area $60\ \text{m}^2\ \text{g}^{-1}$.

The occurrence of specific types of char for coals of differing rank within this study can be illustrated thus:-

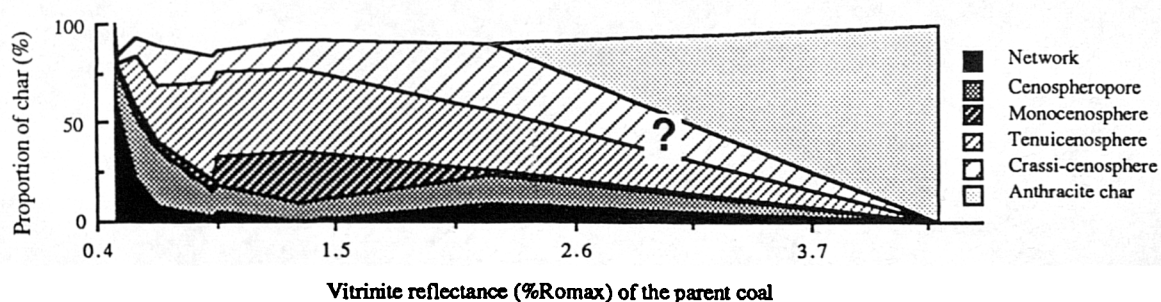


Figure 7.7 A illustration of the observed occurrence of specific types of char, due to rank, for vitrinite rich coals pyrolysed at 1000°C in an EFR.

With respect to the coals used and the experimental conditions employed in this study the following conclusions can be drawn (Figure 7.7). Network chars (Plate 6) are generated predominantly from the sub-bituminous coals, with a small proportion of anisotropic network char derived from the semi-anthracite. Above the rank of sub-bituminous, network chars are systematically replaced by the occurrence of cenospheropores and finally cenospheres, with sub-classes of cenospheres in-turn exhibiting a general rank dependence (Tenui-, \rightarrow Mono-, \rightarrow Crassi-cenosphere). Beyond the rank of semi-anthracite and up to that of anthracite, the trend

remains uncertain. However, the anthracite coal did not form a 'vesiculated char' and probably represents an end-point on the above char/coal rank relationship. The development of optical anisotropy within the chars parallels the formation of cenospheres.

Chars derived from the sub-bituminous and semi-anthracite coals have a higher, visible, char wall porosity, whereas char derived from the medium volatile bituminous coal have the least. A similar trend exists for CO₂ surface area analyses.

7.1.3 Relationships Between Char Morphology and Coal Structure

An excellent correlation coefficient ($R^2 = 0.89$) was obtained between the aromaticity (f.a.) of the coals, as determined by ¹³C CP/MAS NMR, and the proportion of cenosphere chars over the high volatile to medium volatile bituminous rank range (Figure 7.8).

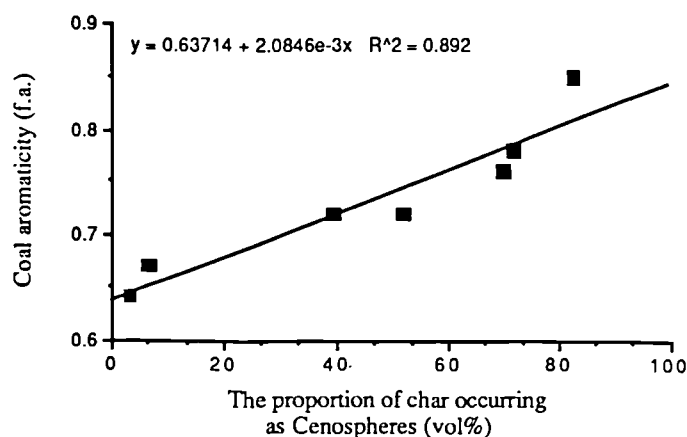


Figure 7.8 Coal aromaticity (f.a.) and the proportion of cenospheres generated during rapid pyrolysis.

However, the relationship between coal aromaticity and the proportion of char occurring as cenospheres (Figure 7.8) is considered to be a reiteration of the coal rank/cenosphere relationship presented in Figure 7.4 (up to semi-anthracite). The increase in aromaticity (f.a.), within vitrinite, represents one of the many structural responses to progressive coalification and is not considered to be the significant aspect of the coal structure (physical or chemical) that influences the generation of specific char types during pyrolysis.

A more plausible causal relationship is represented in Figures 7.9 and 7.10 in which the elemental oxygen content (by difference, wt% d.b.) for each coal (excluding the semi-anthracite and anthracite) is correlated with the corresponding proportion of associated cenosphere or network char generated during pyrolysis. Correlation coefficients of $R^2 = 0.97$ and $R^2 = 0.95$ respectively, indicate that the relationships are good.

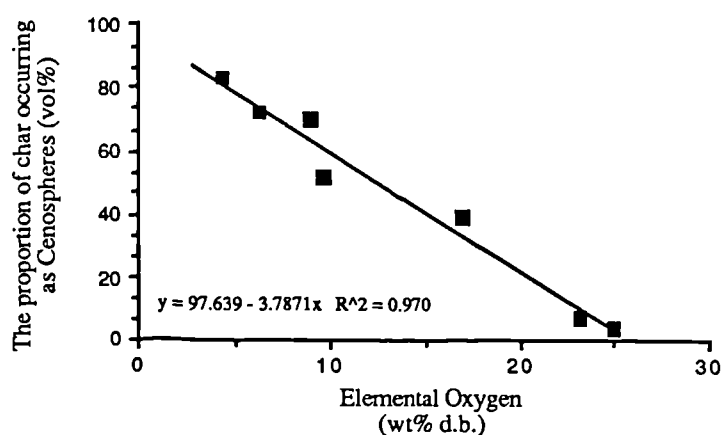


Figure 7.9 The relationship between the elemental oxygen content of coal (sub-A to mvb) and the corresponding proportion of cenosphere chars.

However, better correlations exist between the O/C atomic ratio and the proportion of cenosphere chars ($R^2 = 0.97$), and also between the O/C atomic ratio and the proportion of network chars ($R^2 = 0.98$) generated during pyrolysis. The elemental oxygen content of a coal diminishes with increasing coal rank (Chapter 1), although it is believed that the *char / elemental oxygen* and *char / atomic O/C* relationships outlined above are much more than alternative expressions of the char/ rank relationship presented in Figures 7.4, 7.5 and 7.8.

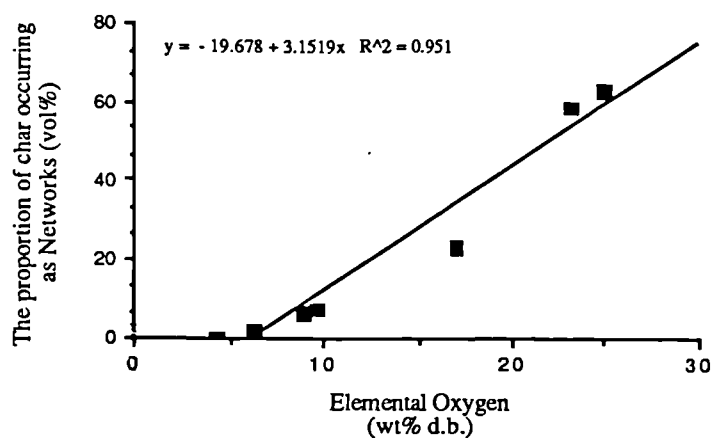


Figure 7.10 The relationship between the elemental oxygen content of coal (sub-A to mvb) and the corresponding proportion of network chars.

The existence (or absence) of oxygen-bearing functional groups within the molecular structure of the coal (\leq mvb) probably represents one of the main factors determining char morphology during rapid pyrolysis at 1000°C. Qualitative Fourier transform-infra red (FT-IR) analysis of the coals up to the rank of medium volatile bituminous, presented as a stacked annotated diagram (Figure 7.11), allows interpretations of the molecular nature of those oxygen-bearing functional groups.

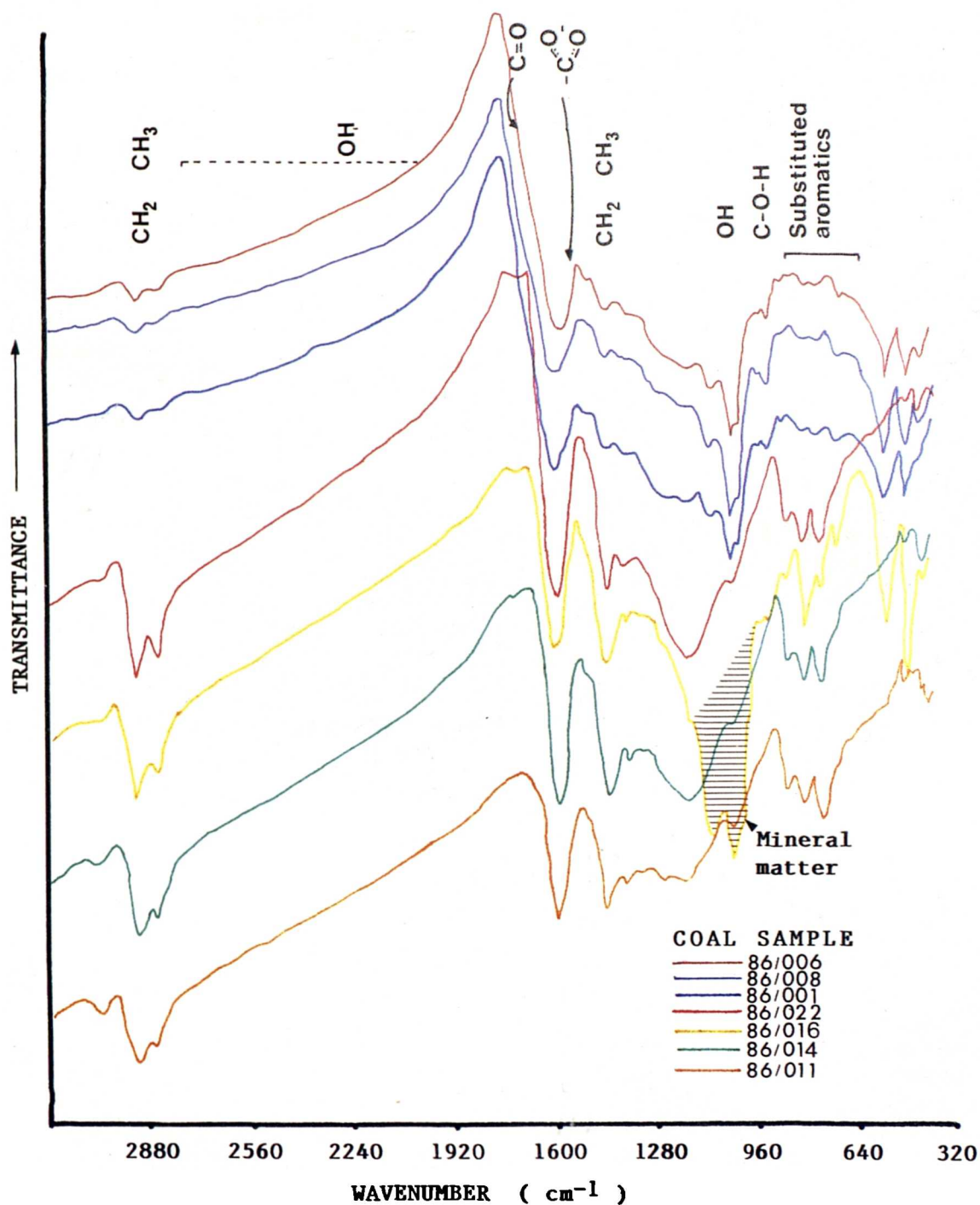
In general terms, the FT-IR spectra (Figure 7.11) indicate that, within the suite of coals

studied, and with increasing rank, there is a decrease in oxygen-bearing functional groups and a waxing and waning in intensity of the various aliphatic absorption bands. The use of absorption intensity ratios between various bands^{19,21,22} has been avoided because the application of curve fitting techniques²² to these spectra was not possible. Also the resolution of the spectra is considered insufficient to derive unequivocal ratios of aromatic/aliphatic absorption integrals^{20,21} and, furthermore, the 1580 cm⁻¹ to 1600 cm⁻¹ absorption band favoured by some^{19,23} as an 'internal standard of the 'bulk' coal',¹⁹ is considered possibly inaccurate and potentially misleading since the intensity of this fairly broad band varies with rank (and also due to oxidation: Section 7.3).

In detail, there is an initial increase within the sub-bituminous to high volatile bituminous A rank range in aliphatic CH₃, CH₂ and CH- groups associated with the 2910-2920 cm⁻¹, 2850-2860 cm⁻¹ (CH- stretching vibrations) absorption bands,^{22,24,25,26} the 1430-1440 cm⁻¹ and 1370-1380 cm⁻¹ CH- deformation band.^{19,24,27,28,29} This is accompanied by a possible decrease in the intensity of those bands for the medium volatile bituminous coal and a possible increase in the out-of-plane deformation vibrations associated with isolated (740 - 750 cm⁻¹), two adjacent (802 - 804 cm⁻¹) and four adjacent CH- groups (850 cm⁻¹).^{24-27,29,30} Furthermore, within the high volatile bituminous A and medium volatile bituminous coals, there is a marked increase in aromatic C-H (2990-3100 cm⁻¹)^{22,27,29} and aromatic ring vibrations occurring at 1030 cm⁻¹.²⁹ Although possible contributions from mineral matter (e.g. 86/016) make interpretations concerning absorptions within 1000 - 1100 cm⁻¹ difficult.

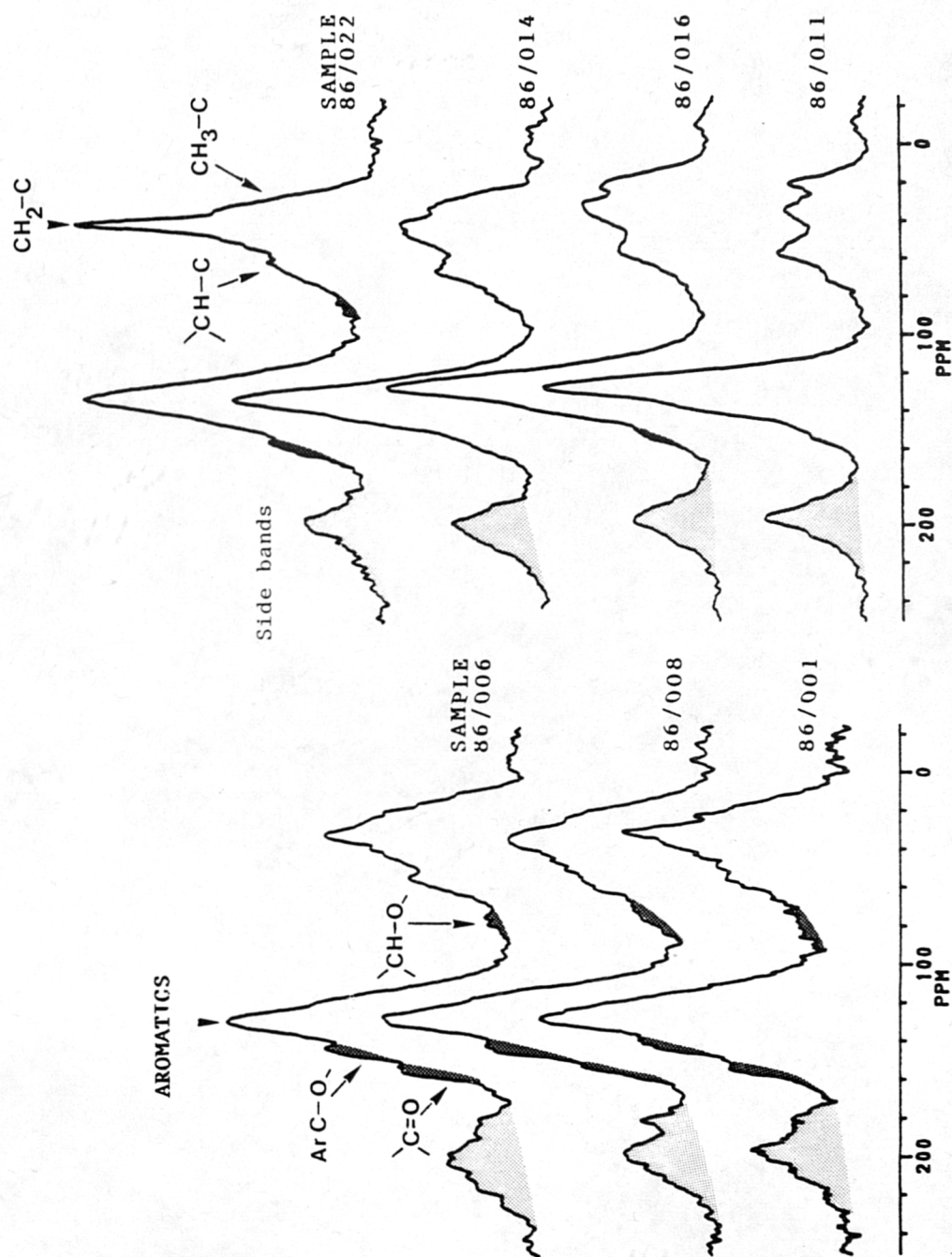
The presence of oxygen-bearing functional groups is suggested within the sub-bituminous and high volatile bituminous B and C coals through the appearance of the following possible absorption bands. A 'shoulder' occurring at 1590 cm⁻¹ possibly represents the antisymmetrical stretching vibrations of carboxylic acids.^{19,20,23} A broadening of the 1430 cm⁻¹ band has been attributed to C-O stretching and/or -OH out-of-plane stretching vibrations,²⁹ although no such firm assignments can be made with the present spectra. Ethers are also thought to give rise to an absorption band that occurs within the low-rank coals at 1010-1035 cm⁻¹ (coals 86/006 - 86/022), although the possible contribution from mineral matter (e.g. 86/016) once again could not be discounted.

However, the presence of oxygen-bearing functional groups, especially within the high volatile bituminous coals, is supported by the appearance of 'shoulders' on the aromatic and aliphatic spectral regions of the ¹³C CP/MAS N.M.R. spectra (Figure 7.12). The tentative assignments to the chemical shifts occurring at 150 ppm, 145 ppm and 75-80 ppm to C=O, (Ar)C-O and CH-O groups respectively,³¹ lends support to the FT-IR spectra interpretations and the estimations of the elemental oxygen content of those coals.



STACKED FT-IR SPECTRA FOR THE RANK SERIES 86/006 - 86/011

Figure 7.11 Stacked spectra of the rank series of coals (except the semi-anthracite and anthracite).



A STACKED PLOT OF SOLID STATE ^{13}C CP/MAS N.M.R. OBTAINED AT 50.0 MHz WITH A CONTACT TIME OF $10\mu\text{s}$, FOR TERTIARY AND CRETACEOUS BITUMINOUS AND SUB-BITUMINOUS COALS. CARBON NUCLEI ASSIGNMENTS ARE INDICATED.

Figure 7.12 The solid state ^{13}C CP/MAS NMR spectra, showing the presence of 'shoulders'.

7.1.4 Mechanism of Char Formation During Pyrolysis Related to the Influence of Coal Rank

Devolatilisation and the proportion of material lost as volatiles during rapid pyrolysis is dependent upon bond breaking and char formation reactions.^{32,33} The coal structure decomposes (depolymerisation) through the thermal dissociation of weak bridges, such as methylene structures and oxygen-bearing functional groups, creating radicals that either recombine to form stable volatile species or char.^{34,35,36}

Since the pyrolysis of coal is considered to involve the scission of the least stable bonds, the proportion and molecular nature of such bonds within a structure would also be expected to influence the pyrolysate characteristics (i.e. light gases or 'tar'). The type and proportion of pyrolysate produced during devolatilisation has been shown to be rank dependent¹⁸ (Figure 7.13).

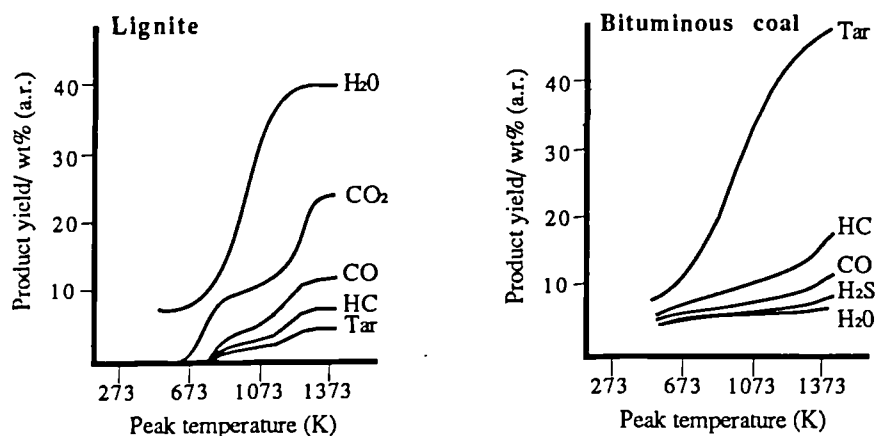


Figure 7.13 Pyrolysis product distribution as a function of temperature for a lignite and a bituminous coal heated to various temperatures at a rate of 10^4 °C s⁻¹. (after Suuberg *et al*¹⁸)

The formation of various specific char types, during rapid pyrolysis, from vitrinite rich coals of differing rank can similarly be explained by the same radical-driven mechanism. The presence of oxygen-bearing functional groups within the low rank, sub-bituminous and high volatile C bituminous coals is suggested in this study by FT-IR and ¹³C CP/MAS NMR spectra and is well known from many previous structural studies (Chapter 1).

The thermal decomposition of oxygen-bearing functional groups would generate a high proportion of hydrogen-scavenging radical (i.e. transient) species of low molecular weight during pyrolysis (Figure 7.14).³⁴⁻³⁶ A lower proportion of aliphatic material within the low rank coals, especially CH₂ and CH₃ groups, would generate insufficient hydrogen, upon pyrolysis, to saturate those radicals thereby promoting the re-combination (repolymerisation) of the higher molecular weight material to form a cross-linked char of limited 'fluidity' rather than generating stable volatile species³⁷ (Figure 7.14).

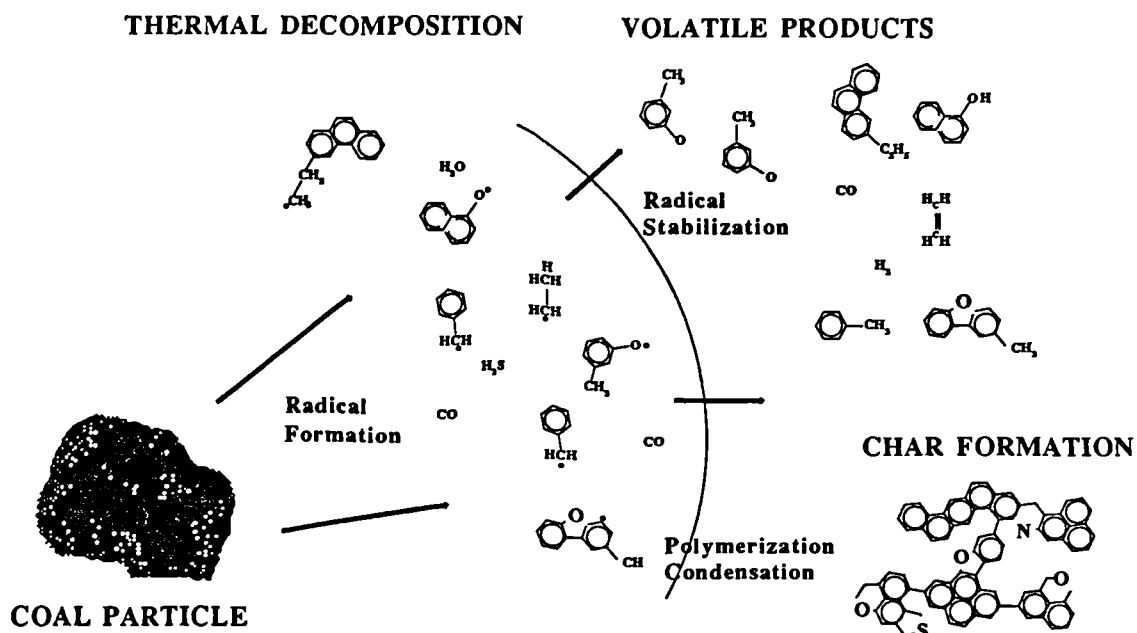


Figure 7.14 The formation of radicals, volatiles and char during pyrolysis. (after Moujlin and Tromp³⁶)

It is proposed that the correlation between the elemental oxygen content of the coals ($\leq m\text{vb}$) used within this study (Figure 7.11) and the generation of specific types of char is related through a radical-driven pyrolysis mechanism that determines both the type and the characteristics of the char. A coal with an O/C atomic ratio of 0.25 - 0.2 or greater generates network char structures during pyrolysis (1000°C) due to the promotion of re-condensation reactions, whereas a coal with a lower O/C atomic ratio contains insufficient proportions of oxygen-bearing functional groups to restrict metaplast 'fluidity' and cenosphere formation.

The relative abundance of radical-capping hydrogen, generated by the cleavage of alkyl (CH_2 and CH_3) groups present within the high volatile A and B bituminous and medium volatile bituminous coals (indicated by FT-IR, ^{13}C CP MAS/NMR), would possibly provide the means through which metaplast 'fluidity' was maintained, in contrast to the char-promoting condensation reactions during the pyrolysis of the low rank coal, resulting in the generation of higher volatile yields during pyrolysis (Figure 7.15).

In contrast, an elemental hydrogen content *lower* than 3.0 % (as analysed), a high carbon content (+ 95.0%) and very low (< 3.0%) volatile matter content (Table 6.1) and a generally acknowledged higher aromaticity and lower aliphatic content within the anthracite are probable factors responsible for the inability for that coal to form a char and devolatilise.

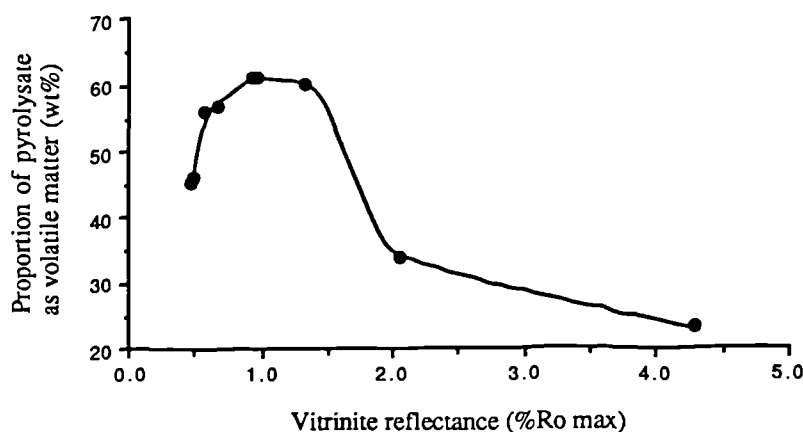


Figure 7.15 The variation of volatile material generated during pyrolysis against the corresponding rank of the coal feedstock.

The mass transport of volatile material through the soft metaplast walls during pyrolysis is considered to occur as an *evaporative process*, rather than by pore diffusion, which promotes char swelling and occasionally the 'jet' release of volatiles.^{36,38} Either an *evaporative* mechanism or pore 'thermal annealing' could explain the relative absence of pores and vents on the external surface and within the char walls of the cenospheres, as shown in the SEM and TEM micrographs (Plates 7b & 8b).

However, an *evaporative* mechanism does not necessarily account for the formation of pores within the network char walls or those of the semi-anthracite char. The localised release of volatiles through a number of pores within a viscous, *thermosetting*, metaplast would possibly preserve the pores and vents, producing a char with a highly porous and permeable outer char wall; the lack of metaplast '*fluidity*' prevents pore thermal annealing from occurring.

7.1.5 Char Reactivity and Burn-out

The efficiency of char combustion in the EFR, at 1000°C using air, is measured by the proportion of 'carbon carry-over' within the combustion product residue. The proportion of unburnt carbon varies with the rank of the corresponding coal (Figure 7.16) and can be related to the char characteristics outlined above.

Char combustion can be related to a complex interaction of the char optical texture, surface area and the presence of accessible porosity within the wall of the char. There is an apparent relationship between the proportion of unburnt carbon remaining in the ash and the proportion of char exhibiting optical anisotropy (Figure 7.17), which concurs with the findings of Oka *et al*⁶ who report the occurrence of optically anisotropic fragments within pilot plant fly ash.

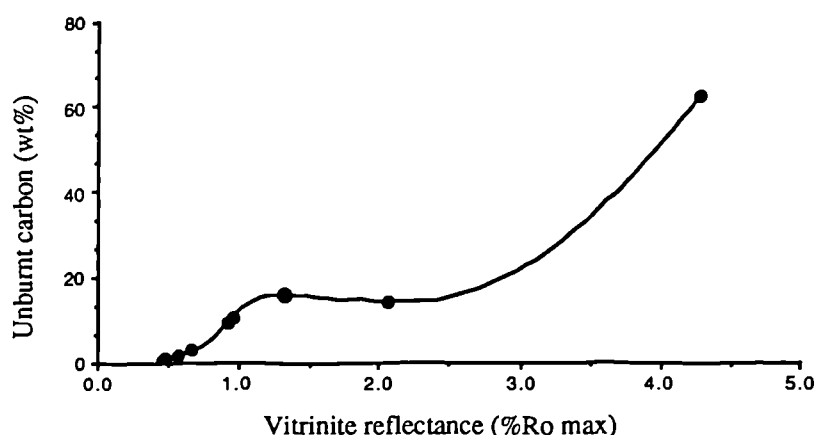


Figure 7.16 The proportion of unburnt carbon remaining within the residue after combustion in air at 1000°C in the EFR.

Char burn-out is probably related to basic char characteristics, in that chars derived from low rank vitrinite rich coals are characterised by hollow, multi-chambered interior, an optical isotropic texture, an accessible inter-connected macro porosity within the char walls and a higher (CO₂) surface area. Chars derived from higher rank coals (\leq mvb) are characterised by hollow, single-chambered interiors, an optical anisotropy, a paucity of visible porosity within the char walls (using TEM) and a low (CO₂) surface area. The semi-anthracite chars are characterised by hollow, single to multi-chambered interiors, an optical anisotropy, an accessible inter-connected macro porosity within the char walls and a higher (CO₂) surface area. In contrast the anthracite generates material that does not vesiculate, remains solid and dense, has an optical isotropic texture, no visible porosity and a low surface area.

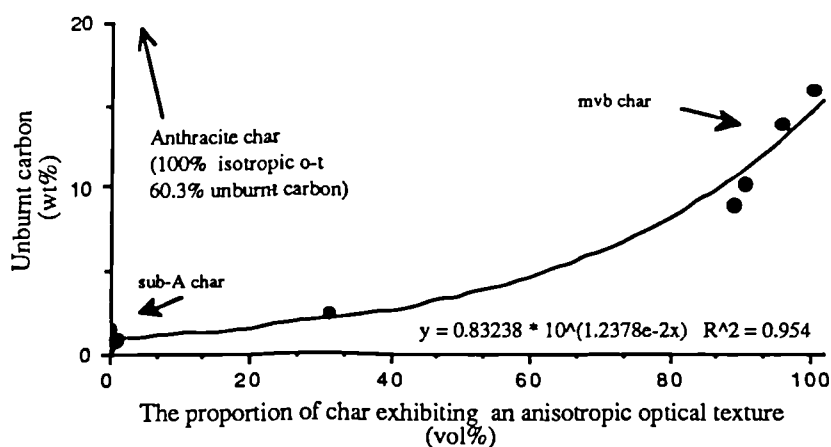
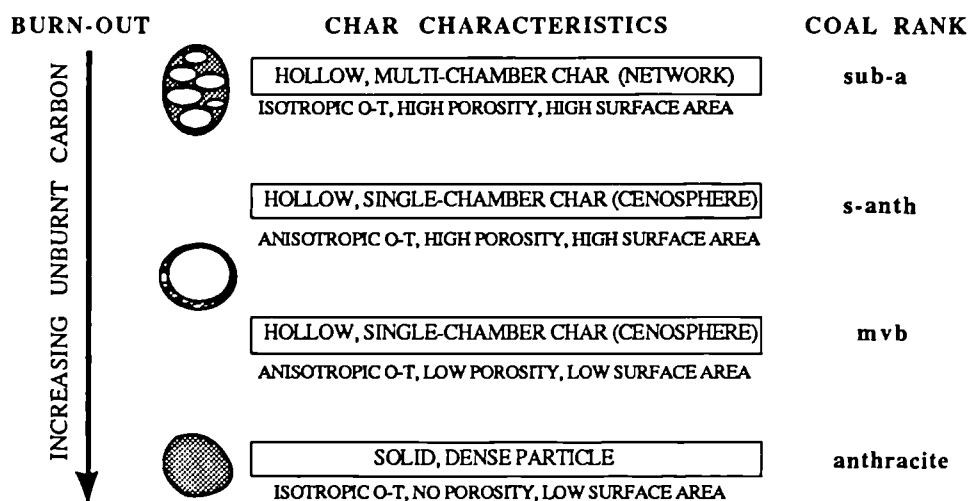


Figure 7.17 The apparent relationship between char optical anisotropy and unburnt carbon remaining in the combustion product.

The reactivity of chars possessing a lower structural order, a higher surface area and a greater degree of inter-connected porosity is acknowledged to be higher than for those chars that do not possess such characteristics.^{16,17} The unburnt carbon levels probably reflects a complex

interplay of the char optical texture, surface area and the presence of accessible porosity within the wall of the char. The relationship between char characteristics and unburnt carbon levels for those coals studied is given in the following summary :-



The proposed relationship between char burn-out and char characteristics, outlined in the above summary, concurs with the char/reactivity relationship of Oka *et al*⁶ given in Chapter 3. The major influence over char burn-out in the EFR at 1000°C would appear to be char/particle density and the presence or absence of an accessible porosity that probably controls the diffusion of the oxidising gaseous reactant during char burn-out.

7.1.6 Review

The respective characteristics of chars derived from vitrinite rich coals vary in their response to the rank of the parent coal. Several correlations were shown to exist between char morphology and coal rank, showing that low rank, vitrinite rich, coals (sub- to high volatile C bituminous) generate highly vesiculated fenestrated isotropic chars (network variety) which are systematically replaced by single-hollow chambered anisotropic chars (cenospheres) as coal rank approaches that of medium volatile bituminous. Beyond that rank, the chars show a reduction in porosity until very little vesiculation occurs during pyrolysis. The generation of specific char types, under the experimental conditions used, is shown to correlate well with the elemental oxygen content of the parent coal. Below an atomic O/C ratio of 0.25/0.2 the predominant char is network, whereas a vitrinite rich coal with an O/C ratio between 0.25/0.2 and 0.01 would appear to generate cenospheres. During the pyrolysis of the sub-bituminous coals, the formation of network char is ascribed to the production of hydrogen scavenging-radicals by the thermal decomposition of oxygen-bearing functional groups and the sparsity of hydrogen capping moieties associated with coals of low rank. Char characteristics such as, optical texture, molecular ordering and porosity appear to be determined during devolatilisation and char formation.

Those characteristics in turn would appear to strongly influence char burn-out (i.e. mass

transport effects) during combustion at 1000°C in air using an entrained flow reactor. The results and interpretations within this study confirm those early findings of Street *et al.*,¹ Oka *et al.*,⁶ Shiboaka *et al.*,¹⁰ and Hamilton,⁵ but has identified a possible causal link between coal chemical structure (elemental oxygen) and the formation of specific types of char.

7.2 Coal and Char Characterisation and Correlations

7.2.1 Introduction

The volatile matter content of a coal and coal calorific value are two standard analytical techniques that form the basis of the North American and many European domestic coal classification schemes and form the main criteria upon which pulverised coal is assessed for use as a fuel in a commercial utility boiler. However, the determination of coal rank in this study was difficult using those standard analytical techniques. For example, coals from the Luscar 4 Mine represent a vitrinite rich coal (86/001), two 3' channel samples (86/002 and 86/004) and a durain (86/003), all from the same seam. There are slight differences in their respective vitrinite reflectance values (Table 6.6). However, the differences in volatile matter, fixed carbon and calorific value are even greater due to the relative influence of petrographic composition. On the basis of calorific value alone, the durain (Fusinite = 41.2 %) would be classified as a sub-bituminous B rather than a high volatile C bituminous coal. The fixed carbon value for the durain (86/003) is 24% *greater* than the vitrinite rich coal (86/001), whereas the calorific value is 24% *lower*. In contrast, the vitrinite reflectance values are 0.55% and 0.58% respectively. Therefore, vitrinite reflectance (%R_Omax) has been used as the rank determinant for all coals used within this study. Cross-references to other standard analytical methods, using a comparative scheme such as that in Table 2.4 (page 53), have been conducted where appropriate. This demonstrates one of the major problems regarding coal classification systems and their application (Chapter 2). Not only is it necessary to consider the utility in which the coals will be used, but also the combined influences of petrographic composition and rank.

7.2.2 Coal Characterisation using Whole-Coal Reflectograms

A possible technique for characterising petrographically heterogeneous coals of differing rank is to systematically measure the reflectance of the whole coal. The three maceral groups have different reflectivities that vary with rank (Chapter 2, Figure 2.5). Therefore, the prospect of deriving whole-coal reflectograms by an automated means for the purpose of characterising coal (rank/composition) has been the subject of much interest over the last 30 years.⁴⁰⁻⁴⁴ The application of an automated or semi-automated reflectance technique warrants investigating with respect to various aspects of pulverised coal combustion.

A necessary prerequisite for any automated data gathering technique, involving the robotic use

of instrumentation, is suitable computer software and hardware. Compiling such a computer program was beyond the scope of the present study or expertise of the author. However, the applicability of the technique and the potential of using reflectograms was investigated using a semi-automated technique with manual data recording.

Automated reflectance techniques require a systematic approach to data acquisition to avoid the incorporation of spurious data or imparting bias during the analysis. An 'unprocessed' reflectogram is shown in Figure 7.18. The total area within the histogram has been demarcated into three broad areas: maceral measurements, spurious measurements due to maceral/maceral or maceral/epoxy boundaries and measurements that fall on the epoxy resin.

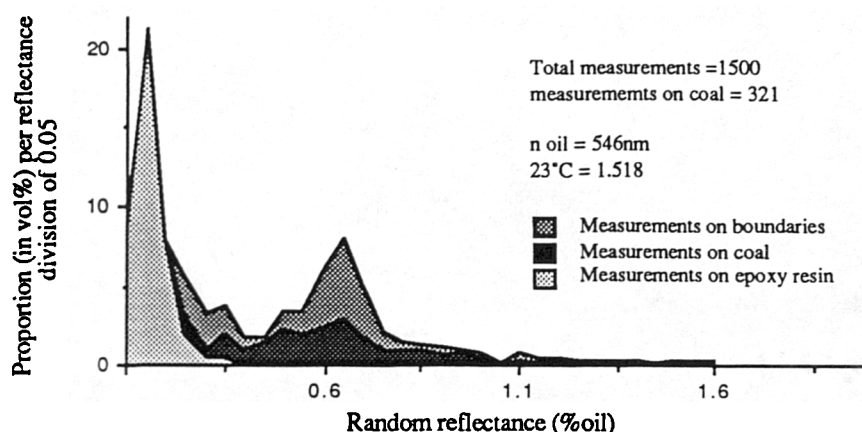


Figure 7.18 A whole-coal reflectogram showing the distribution of measurements that represent measurements on macerals, spurious measurements on maceral/maceral or maceral/epoxy boundaries and measurements that represent the epoxy resin.

The subtraction of maceral measurements from the total generates typical whole-coal reflectogram profiles as shown in Figure 7.19.

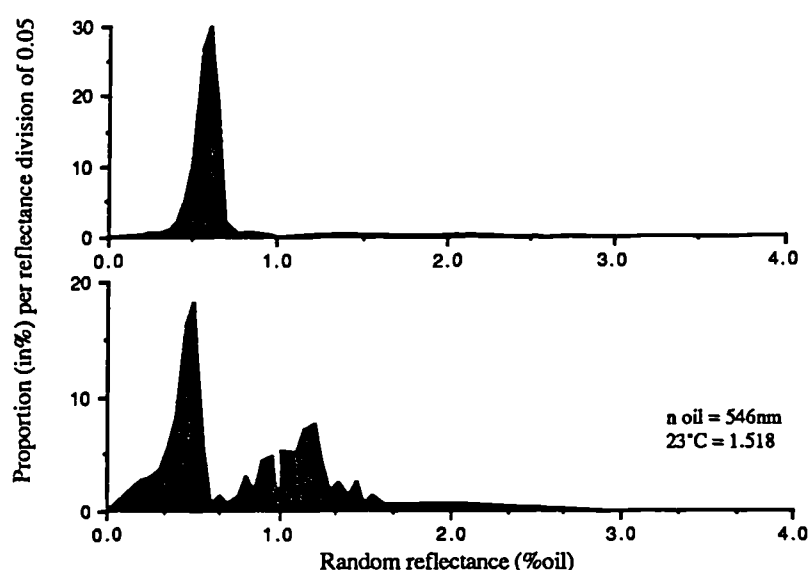


Figure 7.19 Whole-coal reflectograms for a low rank vitrinite rich coal (upper) and a low rank inertinite rich coal (lower), stacked for comparison.

However, the data embodied within a reflectogram must be amenable to statistical treatment. Furthermore, a meaningful relationship must be established between the technique and the utility for which the coal characterisation technique is aimed to serve. Jones *et al*⁴⁵ discuss the char forming behaviour of the sub-maceral *low-reflecting semi-fusinite* (Plate 2e), which is a member of the inertinite group of macerals, and consider 'low-semi-fusinite' to be 'reactive' during pyrolysis and combustion. They determined that a reflectance cut-off point between 'reactive' and 'un-reactive' inertinite varied with coal rank, from 1.2% for a high volatile C bituminous coal to 1.8% for a medium volatile bituminous coal. Macerals, or more particularly, portions of the coal reflectogram could therefore be simply differentiated into 'reactives' (liptinite+vitrinite+low-semi-fusinite) and 'un-reactives' (remainder) by reference to the frequency distribution of measurements within whole-coal reflectograms (Figure 7.20).

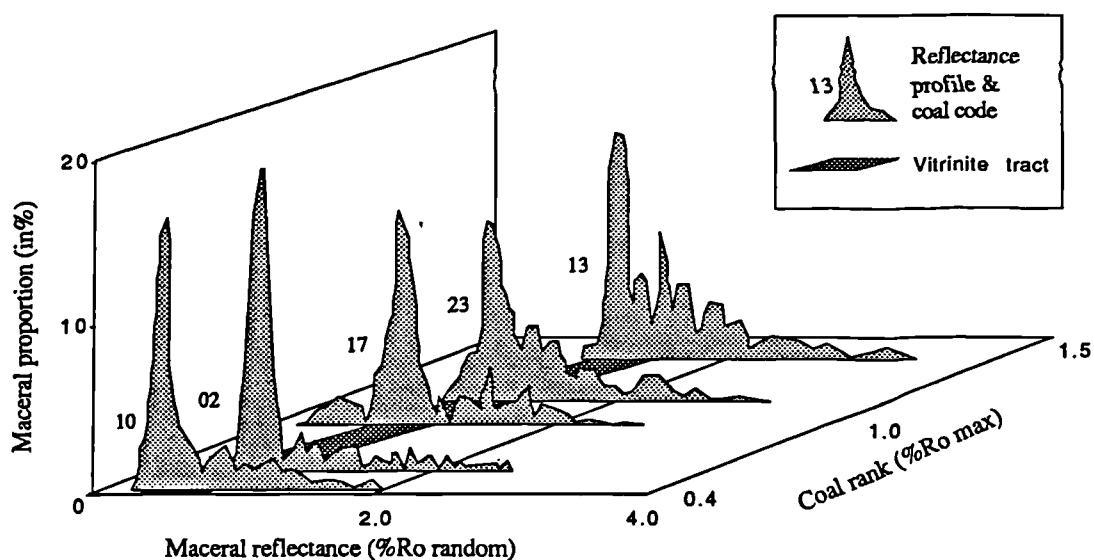


Figure 7.20 A three-dimensional array of reflectograms representing petrographically heterogeneous coals of differing rank.

Within the array of reflectograms above, the reflectance band corresponding to that of vitrinite, which was determined on vitrinite rich coals (not shown), has been included. Using the low/high reflecting semi-fusinite delineation points proposed by Jones *et al*⁴⁵ and the number of measurements per reflectance division within each reflectogram, an attempt was made to ascertain the proportion of 'reactive' and 'un-reactive' maceral components for each coal and compare those values with the pyrolysis products (char + volatiles). This was also compared to the values for macerals derived by the traditional point-counting technique (Table 7.2).

Although some analyses (i.e. 86/016, 86/023) would appear to give a reasonable agreement between the proportion of 'reactive' material and the char + volatile material, the relatively high mineral matter and ash contents for coals 86/002 and 86/016 indicate a significant problem yet to be resolved concerning the use of reflectance profiles as a coal characterising tool.

Table 7.2 A comparison of petrographic and char analyses

Coal	Petrographic Analyses [†]		Char and Pyrolysate Data ^{††}		Mineral/Ash Analyses	
	L+V+ls-F (vol%)	Reactives (vol%)	Porous char (vol%)	Porous char + VM (wt%)	Mineral matter (vol%)	Ash (wt%)
86/002	69.8	65.2	8.8	69.6	9.0	15.0
86/010	72.0	73.6	24.9	84.6	4.8	8.3
86/013	68.2	64.0	31.4	78.4	2.6	9.2
86/016	76.4	92.8	31.5	93.9	19.4	23.1
87/017	76.0	71.1	35.2	84.7	5.0	11.2
87/023	78.1	72.0	27.8	88.4	6.0	15.5

[†] Where: L, V and ls-F represent liptinite, vitrinite and low semi-fusinite respectively, determined by point-counting
^{††} 'Reactives' represents the sum of all macerals up to the l s-f/h s-f 'boundary' determined from reflectograms

^{††} Where: porous char represents cenospheres + cenospheropore + tenui-network, normalised to total material pyrolysed
 VM = material lost presumed as volatiles

The reflectance of mineral constituents varies greatly from 0.2% to 0.8% (%R₀random) for argillaceous material and up to a reflectance value of 18+% for pyrite. An illustration of the problem is given in Figure 7.21.

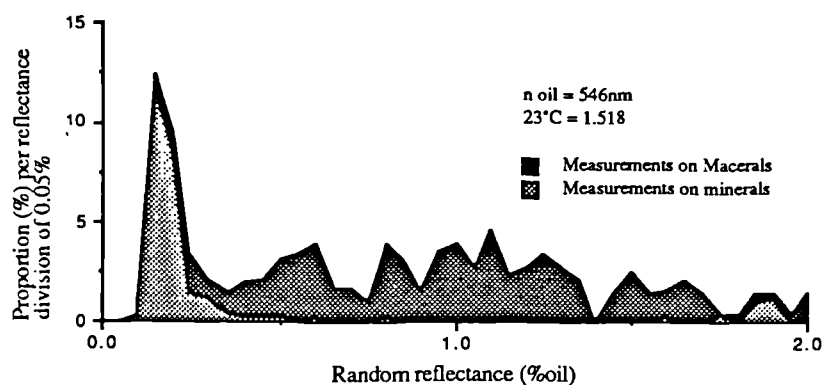


Figure 7.21 A reflectogram for sample 86/003 showing spurious measurements due to mineral matter.

However, it is unlikely that a coal such as 86/003 would be considered for use as a fuel, due to the high mineral content (mineral matter 26 vol%, ash 15 wt% d.b.). But the problem of differentiating between bonafide macerals and minerals must be overcome if the technique is to be automated. At the present moment, the standard point-counting technique offers the most reliable means of differentiating between macerals and minerals, or between the various macerals, or as a technique employed in the assessment of maceral associations (microlithotypes).

7.2.3 Coal and Char Univariate and Multivariate Relationships

7.2.3.1 Univariate Relationships

Vitrinite generates a variety of char types during pyrolysis (1000°C / atmosphere of N₂: Section 7.1). Therefore, the amalgamation of those chars (cenospheres, cenospheropore and tenui-networks) into a general class of '*Porous char*' (macro-porosity 55+%, see Table 6.6) was deemed logical because it simplified the nomenclature and accounted for variations in char type

due to rank. The reference to 'porosity' is a consideration of the large inner chambers within the char and not to the presence of small pores or vents present within char walls, as discussed in the previous section, or to CO₂ surface area determinations.

The relationships between volatile matter content, calorific value and the proportion of porous chars generated during rapid pyrolysis was investigated using a suite of twenty-two coals that vary in rank, petrographic composition and geographic origin (Table 6.4). The maceral and microlithotype analyses for the coals are given in Tables 6.6 and 6.7. Volatile matter content showed no correlation ($R^2 = 0.001$) with the proportion of Porous chars generated during pyrolysis. Coal calorific value yielded a better correlation coefficient ($R^2 = 0.57$) when plotted against the proportion of corresponding porous chars produced during pyrolysis. However, the best correlations were between the proportion of vitrinite macerals (vol%) within each of the petrographically heterogeneous coals and the proportion of porous chars ($R^2 = 0.73$), and between the proportion of vitrinite rich microlithotypes (microlithotype_v) and the occurrence of Porous char ($R^2 = 0.83$, Figure 7.22) for each of the twenty-two coals.

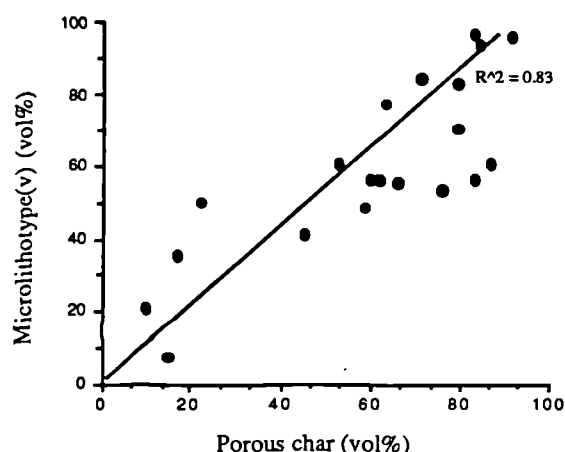


Figure 7.22 The correlation between petrographic composition (microlithotype_v) and the proportion of Porous char generated during pyrolysis for coals of sub-A to mvb rank.

The microlithotype_v class, proposed in this thesis, incorporates the following microlithotype classes: Vitrinite, Clarite, Vitrinite_v and Trimacerite_v. There were no recordings for the sub-class Trimacerite_L. The new term microlithotype_v is an attempt to simplify the nomenclature. However, the relationships within Figure 7.22 could be better defined if the geological age of the coals was considered (Figure 7.23), suggesting the existence of intra-group similarities.

The reason for this correlation is not wholly clear; but, it most probably indicates that the coals, when crushed, produce particles (38 - 75µm) consisting of intimate associations of macerals that may have a collective effect upon the free-radical mechanisms operating during pyrolysis. For example, an association of hydrogen-rich liptinite macerals with hydrogen-poor semi-fusinite may possibly generate the hydrogen-capping moieties required to impart softening or 'fluidity' to the whole particle.

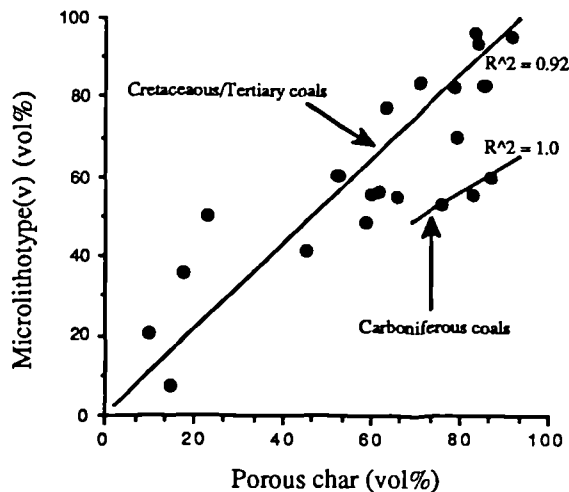


Figure 7.23 Coal microlithotype_v and corresponding Porous chars, indicating the possible influence of 'Provincialism'.

7.2.3.2 Multivariate Relationships and 'Provincialism'

Investigating the relationship between petrographic content (microlithotype_v), calorific value and the rank of the coal samples (Figure 7.24) provided a useful insight into the combined influence of petrographic composition *and* rank upon the calorific value of a given coal.

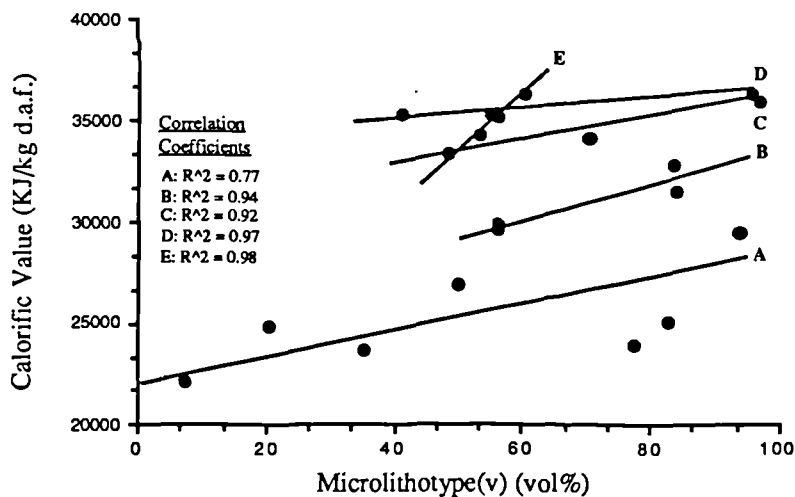


Figure 7.24 The relationship between petrographic composition (microlithotype_v), calorific value, rank (%R_O max) and geological age for coals in the study. The Tertiary /Cretaceous coals are allotted to coal rank as follows: A = 0.5 - 0.59%, B = 0.6 - 0.69%, C = 0.9 - 1.19%, D = 1.2 - 1.39%, the Carboniferous coals E = 0.8 - 0.89%

The relationships within Figure 7.24 indicate the influence of petrographic composition over calorific value for a given rank, especially low rank coals. For example, a coal on the iso-rank line 'A' has a microlithotype_v content of 84% and a comparable calorific value to that of a

slightly higher rank coal (iso-rank line 'B') associated with a microlithotype_v content of 47%. This possibly explains why a low rank vitrinite rich coal with a microlithotype_v content of +80%, imported from South America, competes well with domestic steam raising coals of higher rank but lower microlithotype_v (vitrinite) content.

There are two broad trends apparent within Figure 7.24. The sub-parallel array of regression lines A to D represent a Cretaceous/Tertiary coal data set, whereas the cross-cutting regression line E represents data pertaining to coals of the Carboniferous period. Furthermore, the slight but significant increases in microlithotype_v content for the Carboniferous coals markedly increases the calorific value, whereas comparable increases in petrographic composition for the Cretaceous/Tertiary coals do not affect coal calorific content by the same degree.

The possible role of 'provincialism' upon the behaviour and utilisation characteristics of coals was discussed in Chapter 1 (Page 1). Although differences in coking propensity for Cretaceous and Carboniferous coals have been attributed to aspects of 'provincialism'; there are no studies to date, relating combustion or char-forming behaviour to the same phenomenon. The concept of 'provincialism' used in this thesis is that, despite similarities in petrographic composition, coals from the Carboniferous and Cretaceous/Tertiary coal forming epochs will behave dissimilarly due to a number of possible palaeoenvironmental, palaeogeographical and evolutionary factors (as discussed in Chapter 1) and the different microlithotypes are acknowledged to represent a variety of depositional environments (Chapter 1, Figure 1.6).

Berkowitz,⁴⁶ and van Veen and King⁴⁷ discuss the higher proportion of ether linkages and higher phenolic-OH groups within the Cretaceous coals compared to comparable coals of Carboniferous age, whereas Youtcheff and Given⁴⁸ report significant differences in liquefaction behaviour for coals of Cretaceous and Carboniferous coals. Those studies illustrate that the empirical relationship discussed above possibly reflect fundamental differences in chemical structure and provide additional support to the 'provincialism' postulate invoked in this study between the Cretaceous/Tertiary and Carboniferous coals used.

Concentrating upon the Cretaceous/Tertiary coals, a complex relationship was found to exist between petrographic composition (microlithotype_v), calorific value, coal rank and the proportion of porous chars produced during pyrolysis in the EFR (Figure 7.25).

The lines marked A to D in Figure 7.25 correspond to the regression lines A to D in Figure 7.24, whereas the relationship between all parameters incorporated within Figure 7.25 and the proportion of Porous char generated during pyrolysis is expressed by a *regression plane* ($R^2 = 0.91$) through which it may be possible to relate expected proportions of porous char for other 'unknown' Cretaceous/Tertiary coals. By combining the data from more than one analytical technique, it would appear possible to relate coal characteristics such as rank, petrographic composition and a measure of the heat released during combustion (calorific value) to a given aspect of pulverised coal combustion, in this case the char.

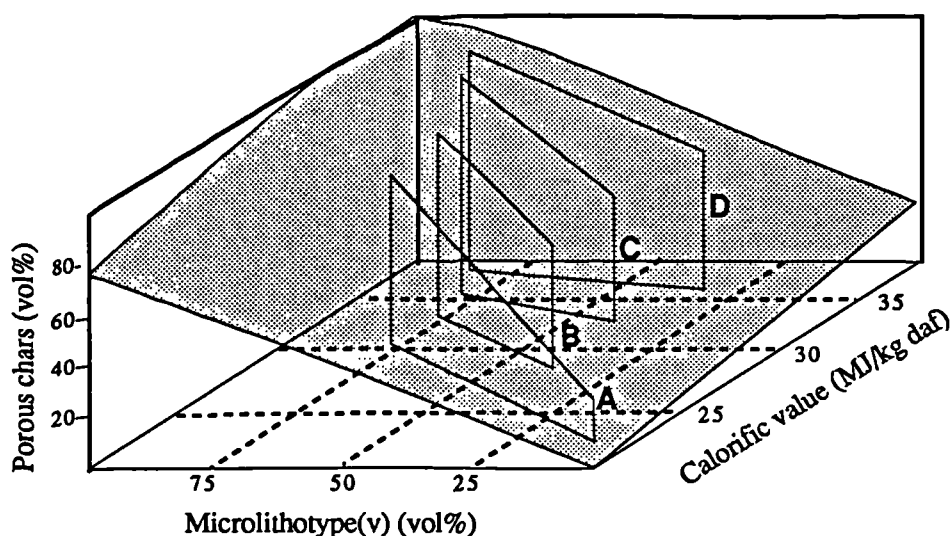


Figure 7.25 A representation of the relationship between calorific value, microlithotype_v content, coal rank (%R_{O,max}) and the proportion of Porous char produced during rapid pyrolysis at 1000°C in N₂ using the EFR. Correlation coefficient $R^2 = 0.91$. The regression lines A → D represent those within Figure 7.24.

However, neither the specific combination of techniques nor the relationships presented in Figures 7.24 and 7.25 are considered definitive, but serve to illustrate the potential of using multivariate techniques when seeking to discriminate between coals of different geological age or origin.

7.2.4 Review

Whole-coal reflectograms offer a means by which petrographic composition may be expressed in terms of 'reactive' or 'non-reactive' constituents, depending upon the utility. However, many technical problems must first be overcome before the technique can be successfully used.

Poor univariate relationships exist between standard analytical techniques (volatile matter content and calorific value) and the char type produced during pyrolysis, in contrast to those that include petrographic composition. However, by incorporating several analytical techniques such as: vitrinite reflectance (rank), calorific value and petrographic composition (microlithotype_v), a relationship was shown to exist that suggests the possible influence of 'provincialism' (depositional environment, flora, coalification history etc.). Using the same coal characterisation parameters, correlated against char type, generated a regression plane through which it would be possible to relate the proportion of porous chars generated during pyrolysis at 1000°C within the EFR to other coals of similar geological age and origin. Such a relationship underlines the usefulness of combining analytical techniques for the purpose of characterising coals of varying utilisation suitability.

7.3 The Effects of Coal Oxidation and Weathering upon Coal Characteristics, Char Morphology and Combustion

7.3.1 Introduction

Nandi *et al.*³ in their investigation into the role of inert coal macerals in pulverised fuel combustion, determined that the combustion efficiencies of coal were inversely related to the (organically) inert content of the coal feedstock during pilot-scale combustion experiments. They included oxidised vitrinite within their category of organically inert material. Axelson *et al.*⁴⁹ in their investigation into the effects of oxidation upon in-situ out-croppings and stockpiled coal, discuss the various problems encountered when attempting to characterise oxidised coal using standard analytical techniques, as noted earlier by other workers.^{50,51} Furthermore, Axelson *et al.*⁴⁹ note the additional complicating factor that petrographic composition has upon standard analytical techniques such as Free Swelling Index, over and above the effects induced by oxidation. The mechanisms of oxidation would appear complex and appear to differ above and below a temperature of 70/80°C.^{27,50-56} Martin *et al.*⁵⁵ using ¹⁸O in their controlled oxidation study, estimated the activation energy for ¹⁸O deposition on the coal surface to be 47.1 kJ mol⁻¹ for a temperature range of 23 to 70°C and 82.0 kJ mol⁻¹ over a temperature range of 70 to 90°C. They also reconciled those differences by inferring the formation of peroxides (Ar-O-O-R/Ar) at low temperatures, compared to higher temperature oxidation that involved the *initial formation of peroxides (Ar-O-O-R/Ar), followed by their decomposition and the subsequent formation of carboxylic acids, thereby largely concurring with earlier work.*^{27,50-54}

However, few studies discuss the effect that the oxidation of pulverised-coal feedstock has upon pyrolysis and combustion using Entrained Flow Reactor (EFR) apparatus. Hamilton⁵ comments on the difference induced in the appearance of char produced on a heated grid after storing the coal for one year. Mahajan *et al.*,⁵⁷ Maloney and Jenkins,⁵⁸ and Tromp *et al.*⁵⁹ investigated the effects of oxidation upon a 'swelling coal' (mvb rank) They comment upon the subsequent enhancement in reactivity, increase in porosity, loss of thermoplasticity and a significant decrease in the production of n-alkane homologues during Curie-point pyrolysis. All three studies involved oxidation temperatures ranging from 50-300°C (typically 120-175°C).

The increase in world coal trade of coal often requires temporary stockpiling at some stage during the shipment of a coal to various points of usage, the possible effects of oxidation upon coal feedstock requires investigation. There are no grounds for assuming that the specifications quoted by the coal vendor or that published characteristics, such as volatile matter content, remain fixed and constant throughout time.

7.3.2 Coal Characterisation: Oxidation and Weathering Effects

Two coals of different coal rank were used in this study (particle size < 1.18mm). The first is a British Coal class 500 (88/024) and the second (88/025) is a class 700 of which the latter is used as a pulverised fuel within a 1,730 MW coal-fired generating station. The proximate analyses of the oxidised coals A24 and A25 show an initial rapid loss in their volatile matter content, as demonstrated in Figure 7.26, with a gradual decrease in the rate of volatile matter content loss as the duration of oxidation increased. The loss in volatile matter content yield for the two coals over time was such that logarithmic curve fitting yields correlation coefficients of $R^2 = 0.97$ and 0.94 for the A24 and A25 coal series respectively. This suggested that no further significant change in volatile matter content yield would occur beyond an oxidation period of 112 days at 100°C and that the greatest changes occurred during the initial oxidation period.

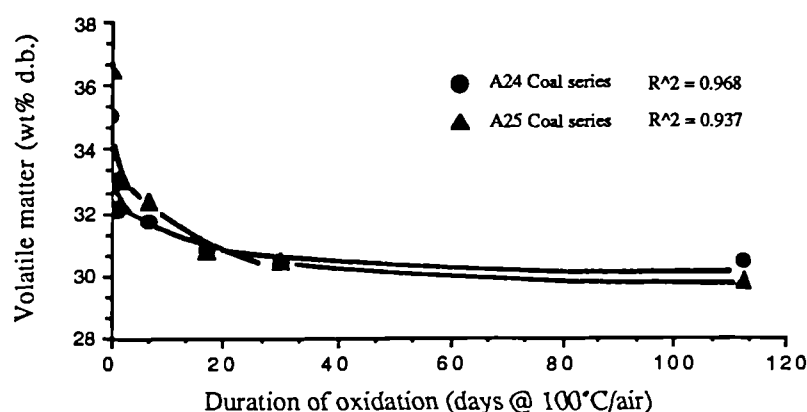


Figure 7.26 The effect of oxidation (air/ 100°C) upon volatile matter content.

The rate of volatile matter loss was greater for the oxidised series of coals than for those weathered over a similar period of time (Figure 7.27). A logarithmic curve was applied to the W25 weathered series which yielded a correlation coefficient of $R^2 = 0.97$, whereas a polynomial applied to the W24 series produced a correlation coefficient of $R^2 = 0.9$, thus suggesting that further decreases in volatile matter content yield would be slight.

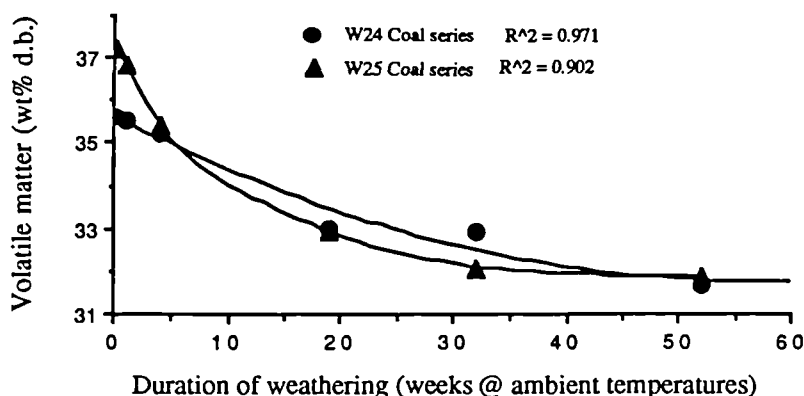


Figure 7.27 The effect of weathering (ambient) upon volatile matter content.

The above trends in volatile matter content yield are augmented by a similar decrease in elemental hydrogen and elemental carbon in preference to oxygen, as noted previously.^{49,50} A cross-plot of the atomic ratios H/C and O/C (Figure 7.28) illustrate the changes in elemental composition through the oxidation of coal in air at 100°C, compared to those changes normally associated with coalification.⁵⁰ Berkowitz⁵¹ considers elemental hydrogen to be sensitive to oxidation, which was also shown to decrease during the weathering (<55 days) of a sample of Illinois N° 6 bituminous coal.⁶⁰

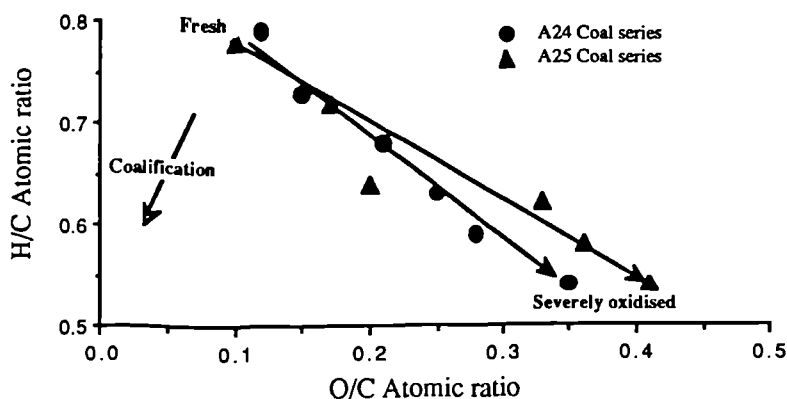


Figure 7.28 Atomic ratio cross-plot for the oxidised coals, showing the decrease in the H/C and an increase in the O/C atomic ratios with increasing duration of oxidation (100°C/air).

The removal of elemental hydrogen was supported in this study by non-quantitative Fourier transform-infra red spectroscopy (FT-IR). The FT-IR spectra (Figures 7.29 and 7.30), stacked for viewing convenience, indicate that the main processes occurring during the oxidation of coals A24 and A25 was the progressive removal of aliphatic hydrocarbons and the inclusion of oxygen bearing functionalities within the molecular structure of the coal. The removal of aliphatic hydrocarbons, such as CH₂ and CH₃ and CH- groups, are indicated by a decrease in the absorption bands occurring at 2920 cm⁻¹, 2850 cm⁻¹ and 1435 cm⁻¹^{19,22,24-26,60} for both coals. The absorption bands occurring between 1580 cm⁻¹ and 1750 cm⁻¹ have been attributed by other workers to specific oxygen bearing functional groups. They include carboxylic acids (1580-1590 cm⁻¹)^{19,20,60} ketones (1620-1700 cm⁻¹),^{23,27} carbonyls in acids (1690-1718) esters (1765 cm⁻¹)^{22,23,24} and anhydrides (1770 cm⁻¹ and 1843 cm⁻¹).^{22,24,28} In both un-oxidised coals (Figures 7.29 & 7.30) the main carbonyl band possibly occurs at 1695 cm⁻¹,^{22,23} but broadens and undergoes a shift to a longer wavelength (1710 cm⁻¹) with prolonged oxidation. This shift could be due to the development of anhydrides, which have been assigned²⁸ to the absorption bands occurring at 1765 cm⁻¹ and at 1845 cm⁻¹.

In contrast, the weathered series of coals (Figures 7.31 and 7.32) show a markedly different trend; the most notable difference being the development of a pronounced, broad, absorption band at ≈3380 cm⁻¹^{22,25} (OH- stretching) after a period of 19 weeks, which is more prominent within the W25 coal series. The OH- stretching band would appear to diminish in coals of both series that have been exposed to the atmosphere for periods of 32 and 52 weeks.

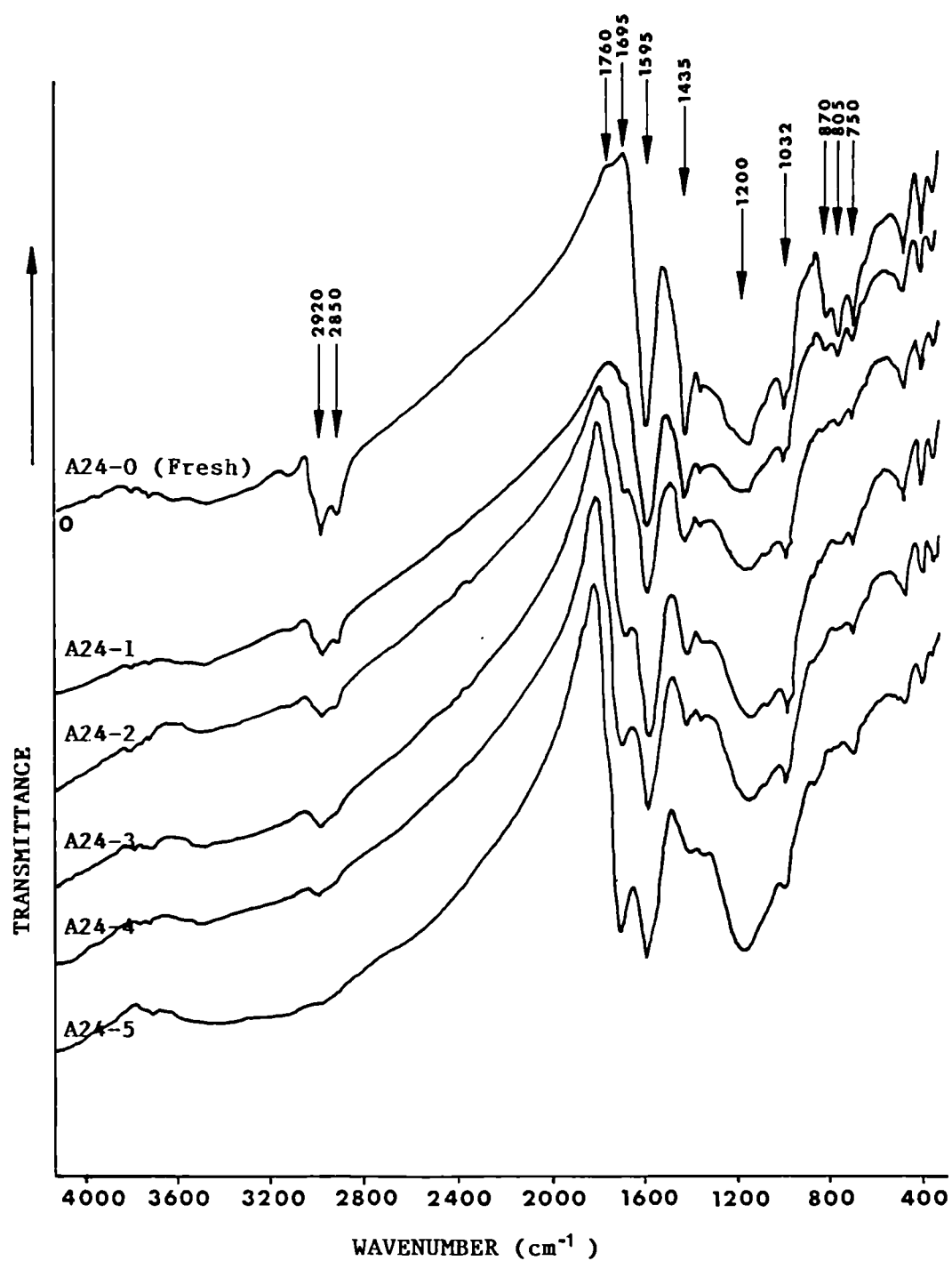


Figure 7.29 FT-IR spectra for the oxidised (100° C/air) A24 coal series, in which the spectra have been stacked for ease of comparison.

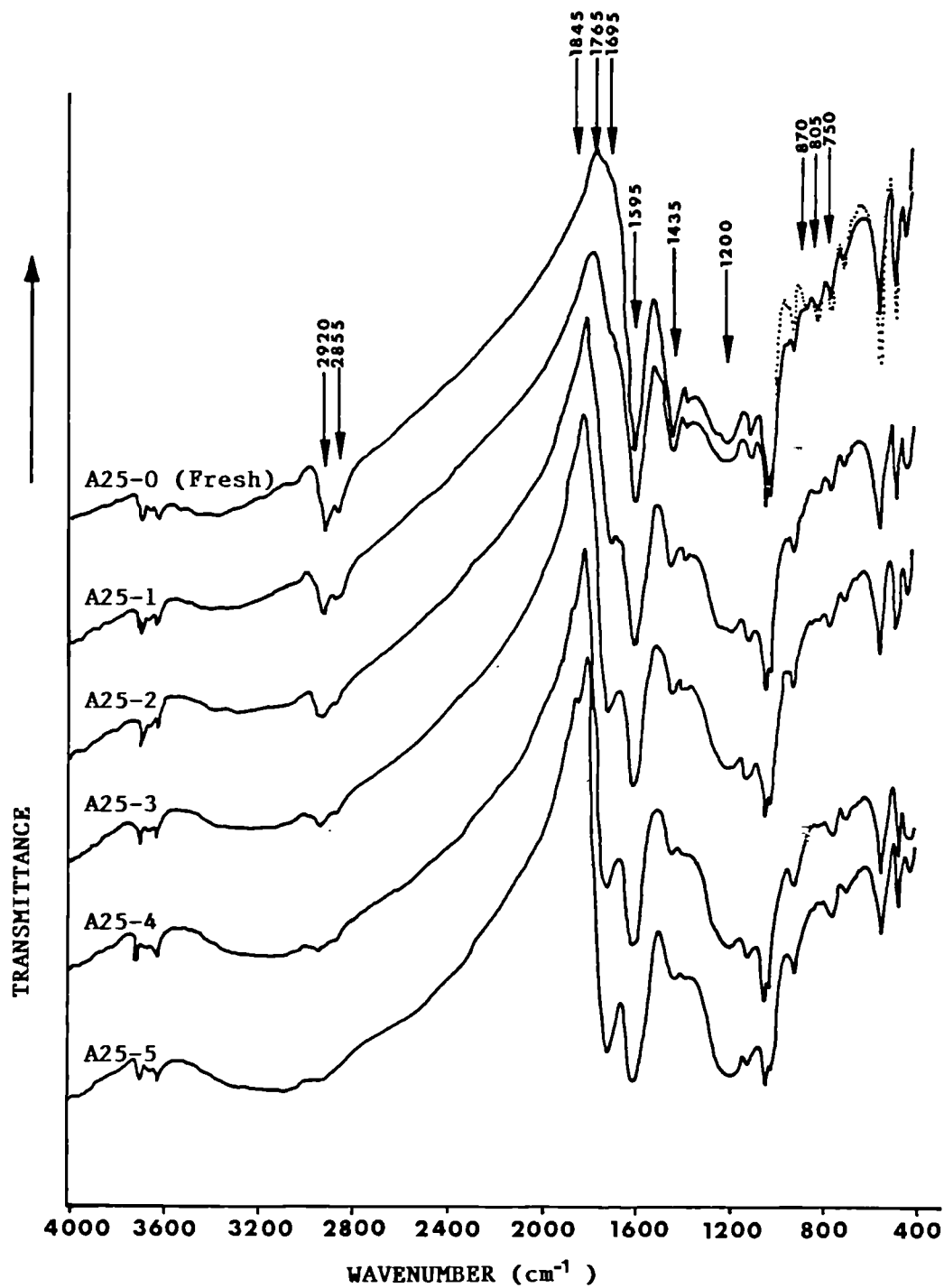


Figure 7.30 FT-IR spectra for the oxidised (100° C/air) A25 coal series, in which the spectra have been stacked for ease of comparison.

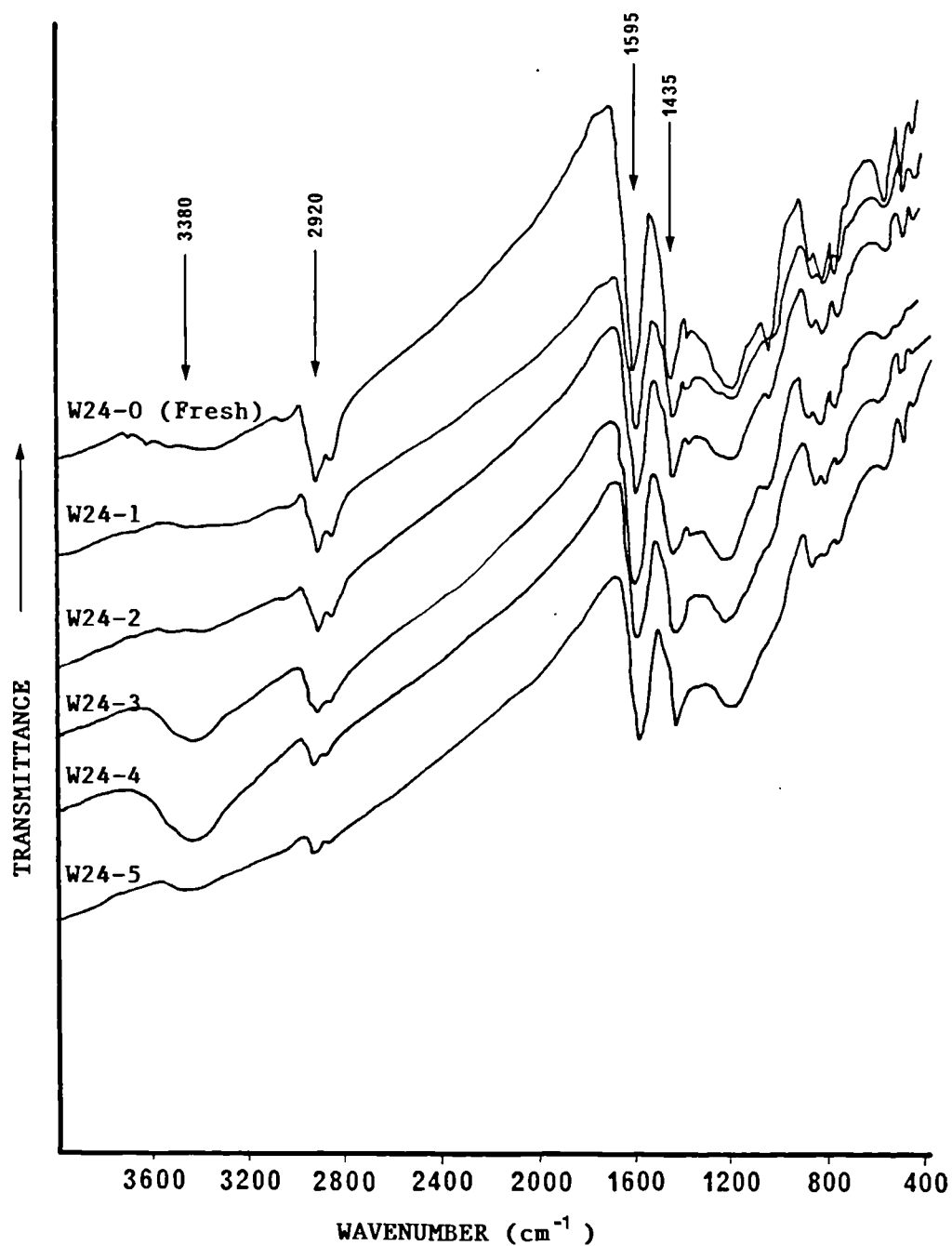


Figure 7.31 FT-IR spectra for the weathered W24 coal series, in which the spectra have been stacked for ease of comparison.

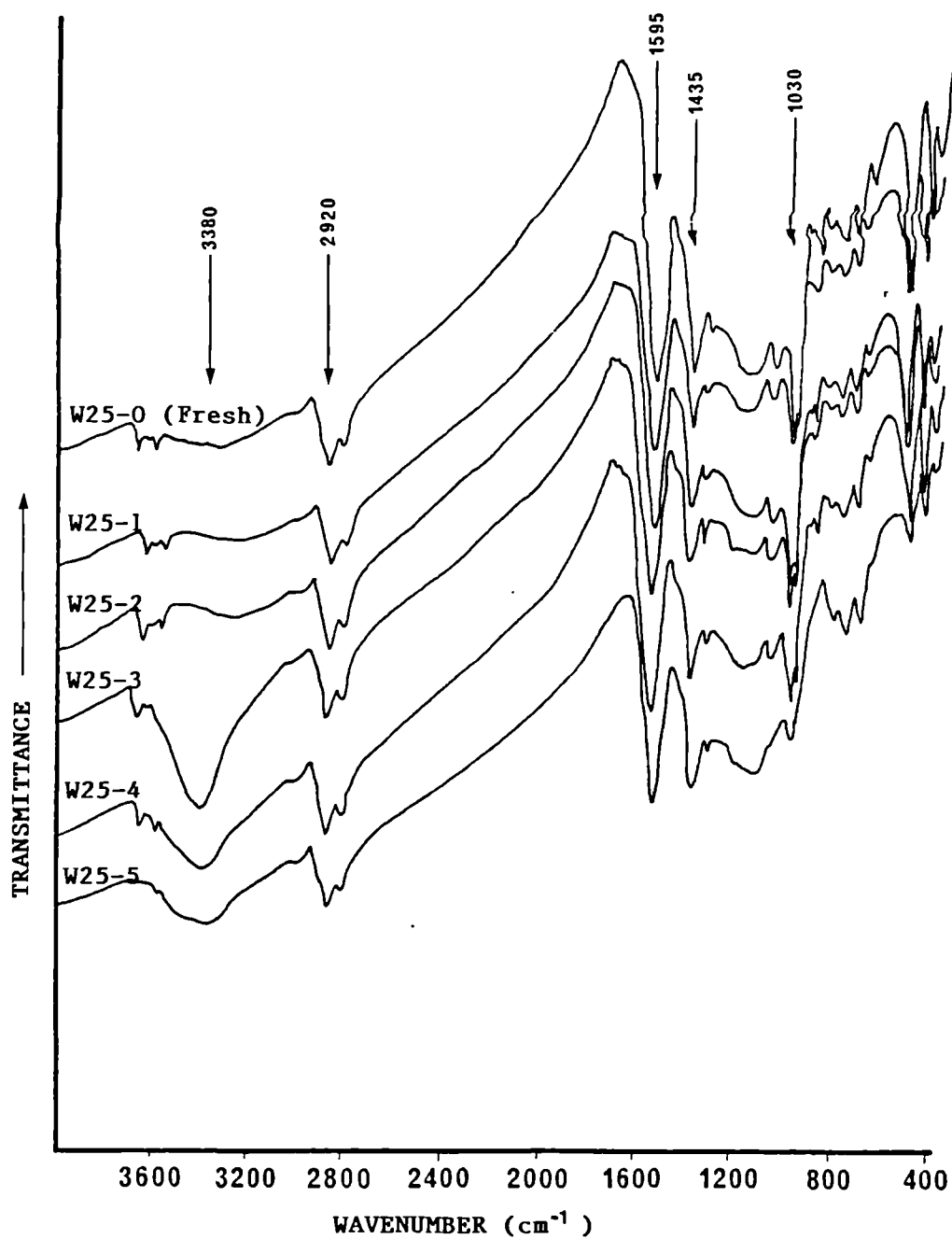


Figure 7.32 FT-IR spectra for the weathered W25 coal series, in which the spectra have been stacked for ease of comparison.

Also, in contrast to the oxidised coal series (100°C/air), the (aliphatic) CH- stretching bands at 2920-2850 cm^{-1} decrease over a longer period of time with respect to the W24 weathered series and appear unchanged within the W25 weathered series. Similarly, there is no carbonyl ($\approx 1595 \text{ cm}^{-1}$) or C-O-C absorption band (1210 - 1230 cm^{-1}) visible within any of the weathered coal spectra.

Clearly, the temperature used within this study governed the structural changes that took place during the oxidative process of coals 88/024 and 88/025. This would support the growing consensus of opinion that different oxidative processes occur above and below 70 to 80°C.

The vitrinite reflectance values (Figure 7.33) increased to approximately 20 to 25% above the values derived from the fresh coals after a period of three months with respect to the oxidised coal series. In contrast, the reflectance values for the weathered coals (Figure 7.34) decreased over the same period of time, thereby concurring with the work of Puttnam *et al.*⁶¹

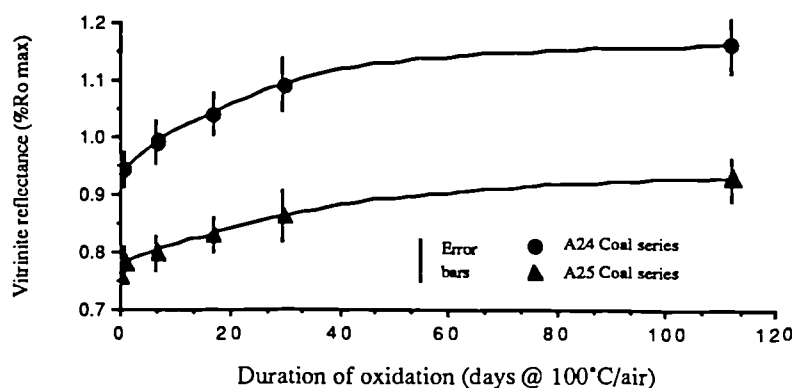


Figure 7.33 The effect of oxidation (100°C/air) upon vitrinite reflectance (%R_o max).

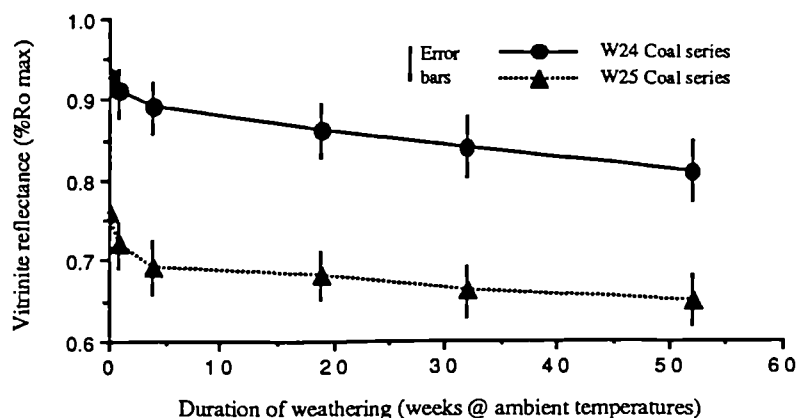


Figure 7.34 The effect of weathering (ambient conditions) upon vitrinite reflectance (%R_o max).

Both Prado⁶² and Cronauer *et al.*⁶³ comment on the absence of visible oxidation rims on low temperature (<150°C) oxidised coals when using plain polarised light. Cronauer *et al.*⁶³ oxidised coals under similar conditions to those used in this study and considered the kinetics of low temperature oxidation to be diffusion controlled. However, they failed to detect the

presence of oxidation rims which would indicate the presence of a reaction front (Chapter 3). Cronauer *et al*⁶³ were, therefore, unable to verify their reaction concept. However, in this study, the presence of rims of low fluorescence (quenched fluorescence) as a direct consequence of oxidation has been demonstrated using fluorescent microphotometry on vitrinite and particles of coal. The rims of quenched fluorescence (Figures 7.35 and 7.36) widen as the period of oxidation increases, until eventually no measurable, or visible, fluorescence remains.

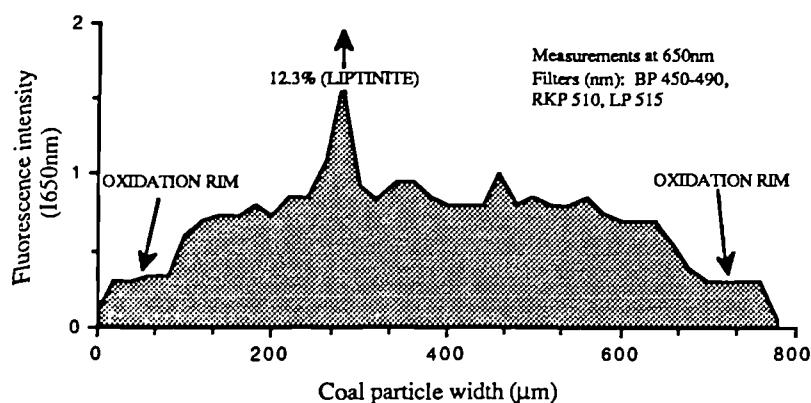


Figure 7.35 The measured fluorescence intensity (% relative to an uranyl glass) across the surface of an oxidised particle of A24-1 coal (100°C/ air, one day).

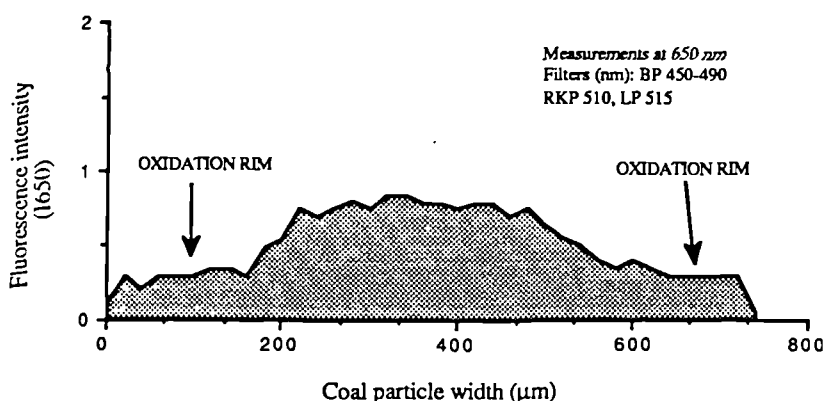


Figure 7.36 The measured fluorescence intensity (% relative to an uranyl glass) across the surface of an oxidised particle of A24-2 coal (100°C/ air, one week).

Therefore, the development of conjugated oxygen bearing groups, during oxidation, is supported by the observed quenching of fluorescence within oxidised coal particles. Ring-bound ketones, for example, have $\pi \rightarrow \pi^*$ and $n \rightarrow \pi^*$ absorbances at 245 nm and 435 nm. The bond between the ketone and the aromatic group is associated with the $\pi \rightarrow \pi^*$ transition, whereas ketones give rise to the $n \rightarrow \pi^*$ transition. The electronic transitions of oxygen bearing groups increase in both wavelength and intensity with an increasing degree of conjugation. Fluorescence intensity measurements conducted at 650 nm across the polished surface of vitrinite particles (Figures 7.35 and 7.36) would appear to verify the diffusional postulate of Cronauer *et al*,⁶³ i.e., that the gas-solid reaction accompanying oxidation appears

to be predominantly diffusional at 100°C a view, however, that is not universally accepted.²⁷ The proportion of oxidised coal may be determined (Figure 7.37) by adapting a model proposed by Bouwman and Freriks¹⁹ and the minimum measured rim-width for a *given particle* size can be determined from the data obtained by particle scanning using the fluorescence microphotometry technique discussed above. However, in the case of the weathered coals, no well defined oxidation rim was discernible within the vitrinite particles.

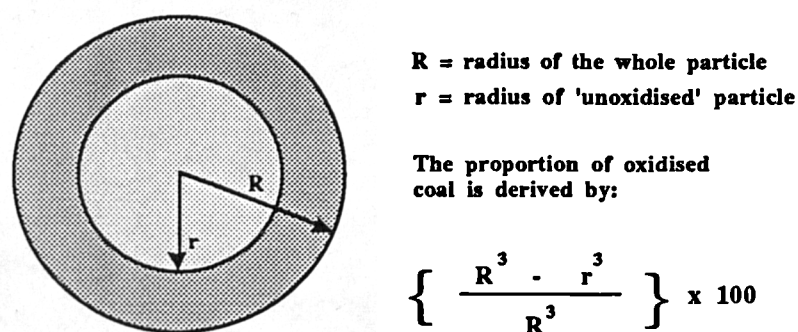


Figure 7.37 A means of calculating the proportion of oxidised coal (100°C/air) using data derived from fluorescence microscopy. (modified and adapted from Bouwman and Freriks¹⁹)

Instead, the fluorescence intensity diminishes gradually across the particle surface (Figure 7.38). This suggests that, under the conditions used in this study, the rate limiting step governing the process of weathering is probably not diffusion, as proposed for the oxidative processes at temperatures of 100°C or more,⁶⁴ since the profiles do not show an abrupt change in fluorescence intensity associated with oxidation at higher temperature (i.e. 100°C).

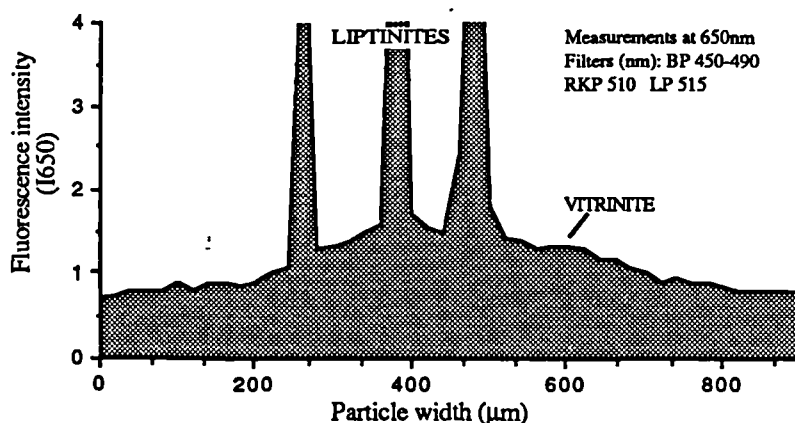


Figure 7.38 The measured fluorescence intensity (%relative to an uranyl glass) across the surface of a particle of W24 coal weathered (ambient) for one month.

Therefore, where oxidation rims are vague, as in the case of weathered coals, the extent of oxidation may be estimated by measuring the intensity of the fluorescence emission at 650 nm. The fluorescence intensity decreases (Figure 7.39) due to oxidation (100°C/air) and also due to progressive weathering, but at differing rates.

Figures 7.39 and 7.40 illustrate the complex nature of weathering and oxidation (100°C/air) phenomena upon vitrinite reflectance and fluorescence emission for the coals studied.

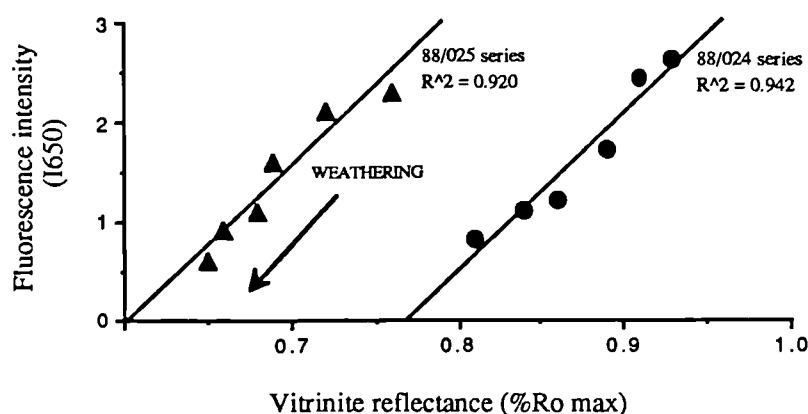


Figure 7.39 A illustration of the effect of progressive weathering (ambient) upon vitritine reflectance and the intensity of vitritine fluorescence.

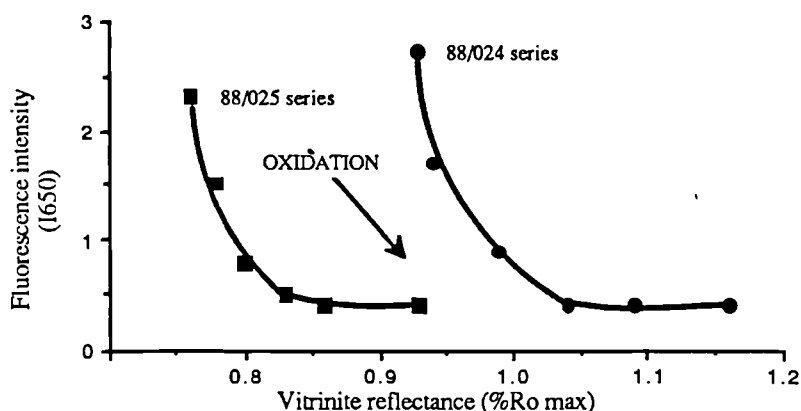


Figure 7.40 Changes in fluorescence intensity and reflectance due to oxidation (100°C/air)

A means of simplifying the phenomena and thereby assisting with the interpretations would be to place both phenomena on a single scale. The proposed Oxidation Quotient (O/Q) is a ratio that combines the fluorescence intensity measurements ($I_{650\text{nm}}$) and vitritine reflectance ($\%R_{0\text{max}}$) values, determined on the same coal under standardised conditions, thereby normalising for rank and the variations induced by the effects of oxidation (i.e. 'pseudo coalification') or weathering at different temperatures. The extent and conditions of oxidation may be effectively assessed through this simple technique:

$$\text{O/Q} = \frac{I_{650\text{nm}}}{\%R_{0\text{max}}} \quad (7.1)$$

where:

- O/Q = the Oxidation Quotient.
- $I_{650\text{nm}}$ = the mean maximum fluorescence intensity of the vitritine measured at 650nm, relative to a known standard (e.g. uranyl glass, LED).
- $\%R_{0\text{max}}$ = the mean maximum reflectance of vitritine.

Values derived for the two coals used within the weathering and oxidation study are presented in Figure 7.41 and in Tables 6.15 to 6.18.

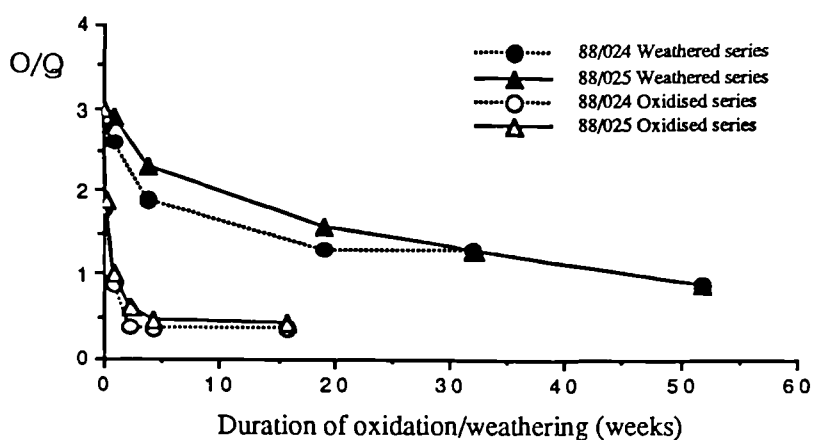


Figure 7.41 Changes in the Oxidation/Quotient (O/Q) with time, given in weeks, for both the oxidised coal series (open symbols) and the weathered coal series (closed symbols).

Measured on the submaceral desmocollinite, the value for the hvA bituminous (88/024) or hvB bituminous (88/025) coal is 2.8 to 3.0, *irrespective of the difference in coal rank for the two coals* (Figure 7.41). This value decreases to 0.35 - 0.4 after oxidation at 100°C for a period of 16 weeks (112 days), whereas the O/Q for coals of the weathered series is 1.3 - 1.6 over the same period of time.

Therefore, the rate at which the quotient changes over a given period of time, reflects the severity (i.e. temperature) of the oxidising/weathering conditions (Figure 7.42). Extreme conditions of oxidation produce a rapid rate of decrease in the O/Q value, whereas the O/Q is unchanged in instances where no oxidation or weathering has occurred. Less severe conditions of oxidation, or weathering, produce a more gradual decrease in the O/Q value over a given period of time.

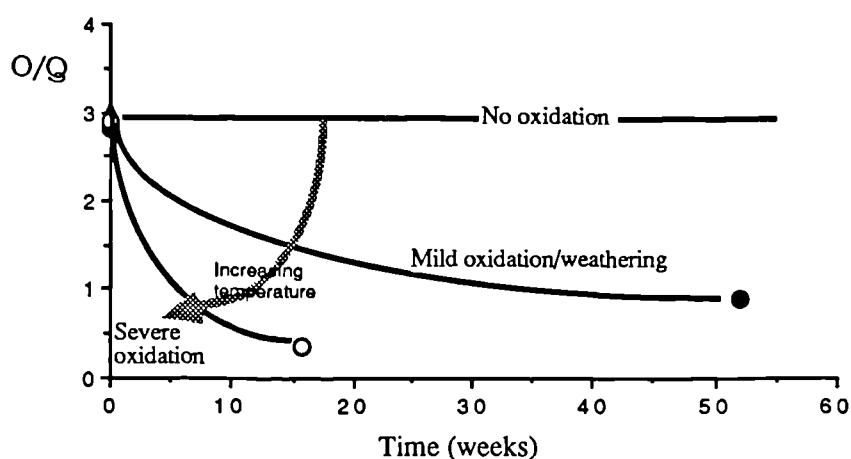


Figure 7.42 A generalised form of Figure 7.41 relating the changes in the slope of the Oxidation Quotient (O/Q) with time to the prevailing conditions of weathering/oxidation.

7.3.3 Char Morphology and Combustion: Oxidation and Weathering Effects

The effects of oxidation upon the morphology of chars produced in the EFR are illustrated in Figures 7.43 and 7.44 for the coal series A24 and A25.

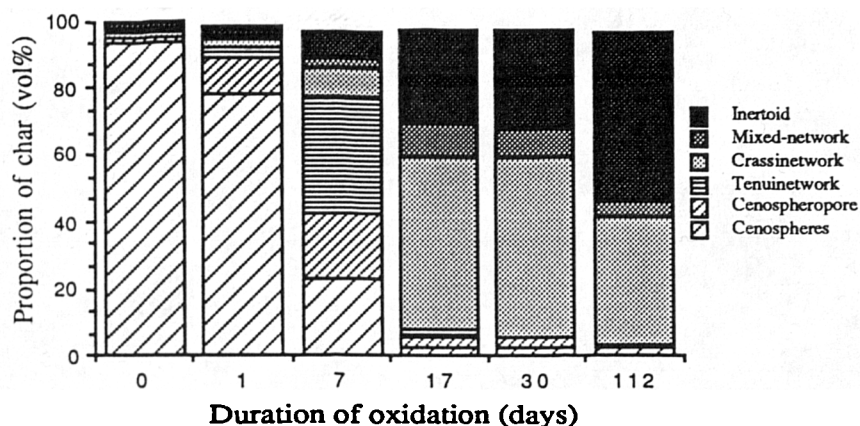


Figure 7.43 Coal series A24 and the change in char type with oxidation (100°C/air).

The initial high proportion of optically anisotropic cenospheres produced during the pyrolysis of the unoxidised coals A24-0 and A25-0 is gradually replaced by chars of lower thermoplasticity, i.e. *cenospheres* → *tenui-network* chars → *inertoids* (dense & solid: see Plate 6).

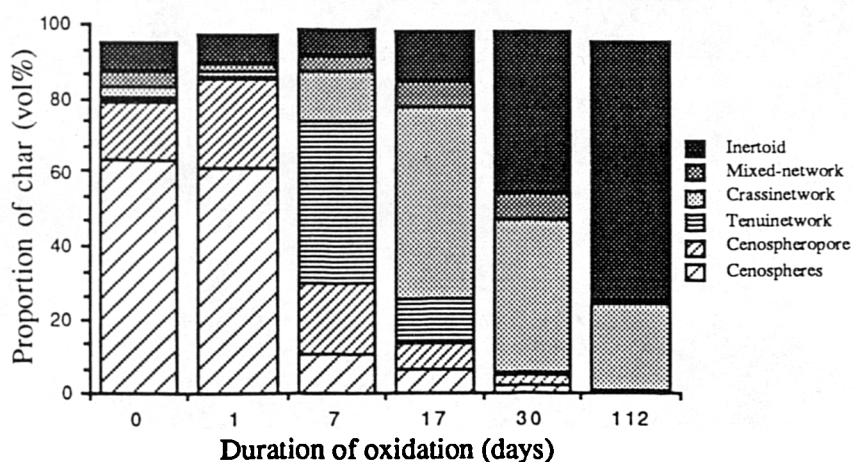
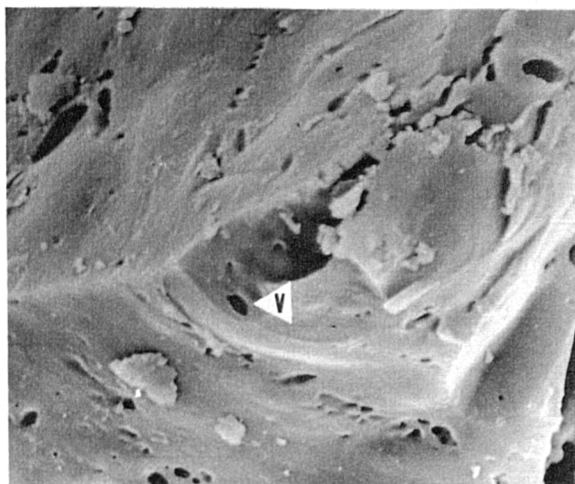


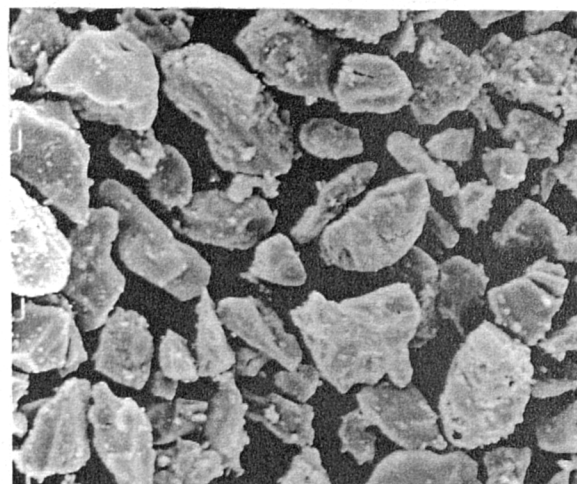
Figure 7.44 Coal series A25 and the change in char type with oxidation (100°C/air).

The effect of oxidation (100°C/air) upon the A24 coal series is very severe. After oxidation at 100°C for one day, the decrease in the proportion of anisotropic char, from an original value of 92.4% down to 34.2%, is subsequently followed by a virtual elimination of all visible optical anisotropy within the char after oxidation at 100°C for one week. The loss of swelling and softening characteristics within the coal series A24 produces a char that is angular, dense and solid in appearance. However, when viewed by SEM (Plates 9a & 9b) the appearance of a high proportion of visible porosity suggested that some in situ devolatilisation occurs during pyrolysis. Such characteristics contrast with those of the chars produced from the fresh coal A24-0 which has a lower proportion of small devolatilisation pores that possess only a few large



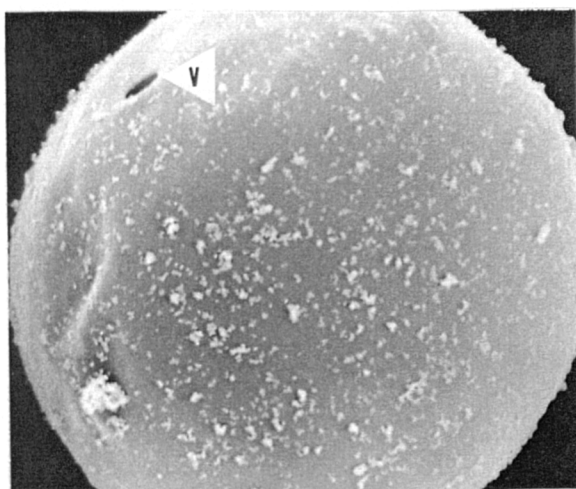
9a 24/5A

7.5µm



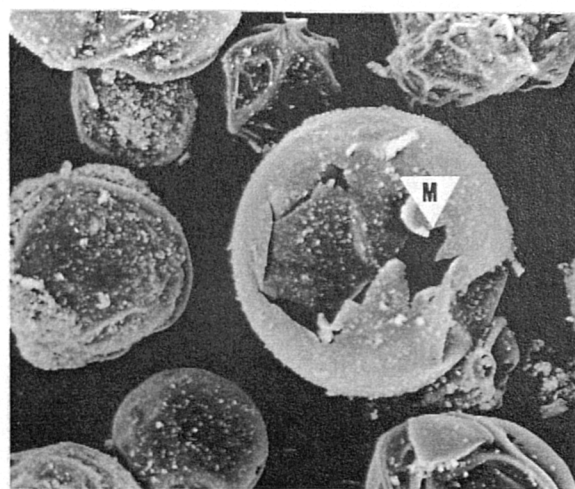
24/5A

100µm



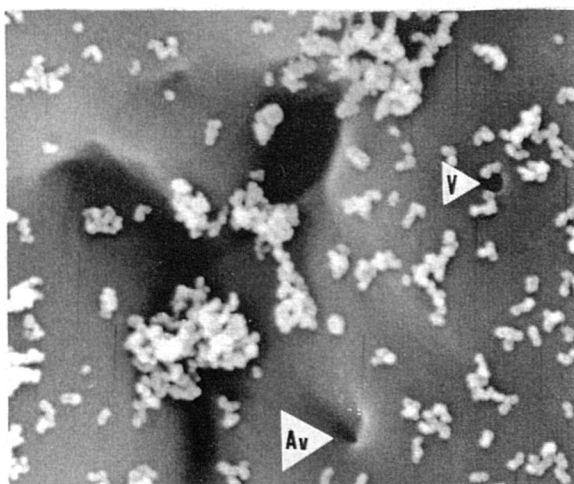
9b 24/0

50µm



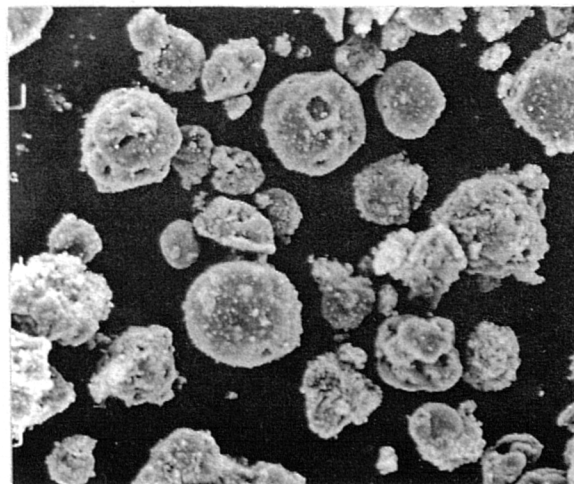
24/0

100µm



9c 24/5W

2µm



24/5W

100µm

Plate 9 Scanning Electron Micrographs of Char from the 88/024 Coal Series

9a, Char derived from oxidised coal (100°C/air, 112 days) showing pronounced char wall vesiculation.

9b, Cenospheres and mechanically damaged cenospheres derived from fresh coal.

9c, Cenospheres derived from a weathered coal (ambient/ 1 year) coal.

(V), devolatilisation vents. (M), mechanical damage. (Av), annealed vent.

(JEOL JSMT20)

vents or signs of mechanical damage. The changes in visible porosity are accompanied by significant changes in micro-porosity, which is indicated by an increase in CO₂ minimum surface area from 60 m² g to 250 m² g. The char burn-out characteristics (Figure 7.45), measured

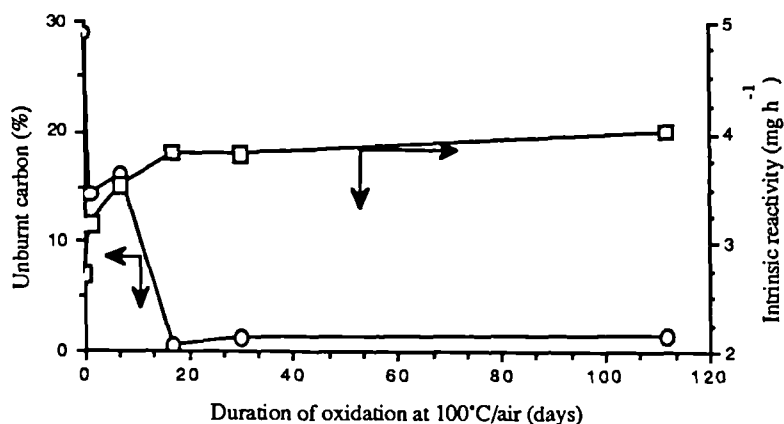


Figure 7.45 The changes in coal char TGA reactivity and in the level of unburnt carbon within the combustion product of char derived from coals of the oxidised series A24.

by the proportion of unburnt carbon remaining within the combustion residue, showed a marked improvement after the oxidation of the parent coal for 17 days at 100°C in air (Table 6.23), coinciding with the loss in optical anisotropy. Despite differences in the initial level of unburnt carbon within the combustion product of chars generated from the fresh coal A25-0 (2.2%) and A24-0 (28.%), the trends and changes that occurred due to progressive oxidation are somewhat similar. Changes in char morphology for the A25 series parallel those of the A24 coal series (Figure 7.44 & Plate 10), although the initial lower degree of swelling and a higher CO₂ surface area during char formation are related to the rank of the coal (section 7.1).

However, differences exist between the A24 and A25 series in the relative combustion efficiencies of the char after prolonged oxidation at 100°C (Figure 7.45 and 7.46). The level of unburnt carbon within the combustion product of the A25 series decreases to almost zero following the oxidation of the parent coal for a period of seven days. Thereafter, the level of unburnt carbon significantly *increases* up to 10.1% after prolonged oxidation (≥ 112 days) of

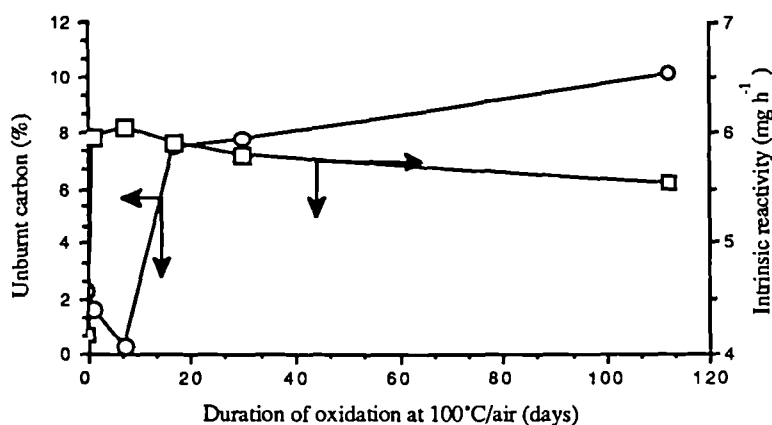
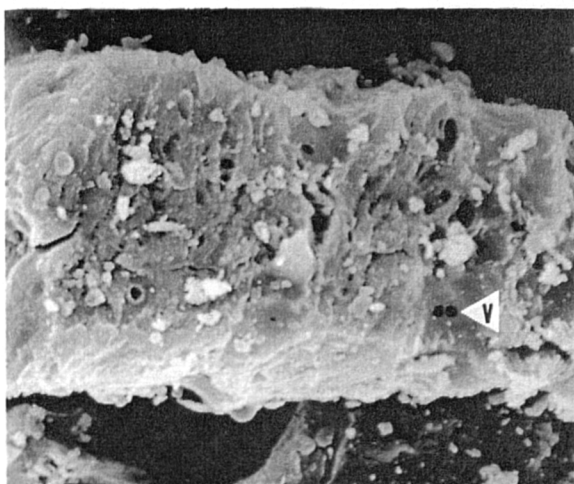


Figure 7.46 The changes in coal char TGA reactivity and in the level of unburnt carbon within the combustion product of char derived from coals of the oxidised series A25.



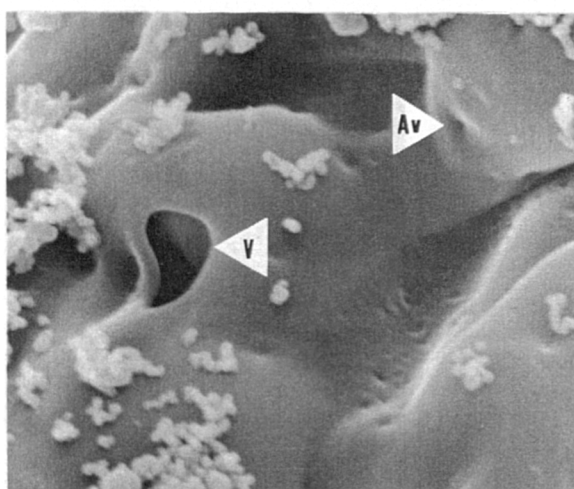
10a 25/5A

10µm



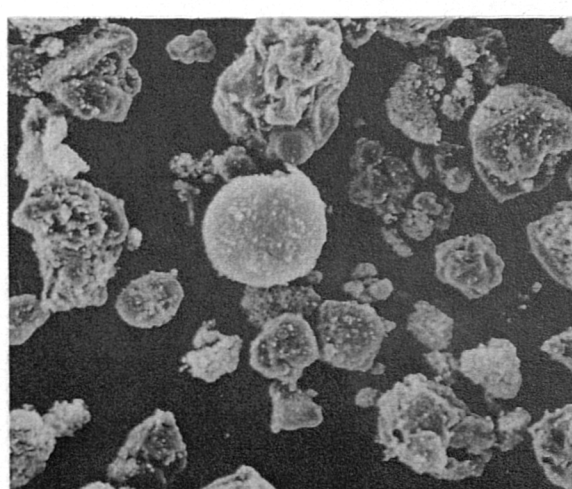
25/5A

100µm



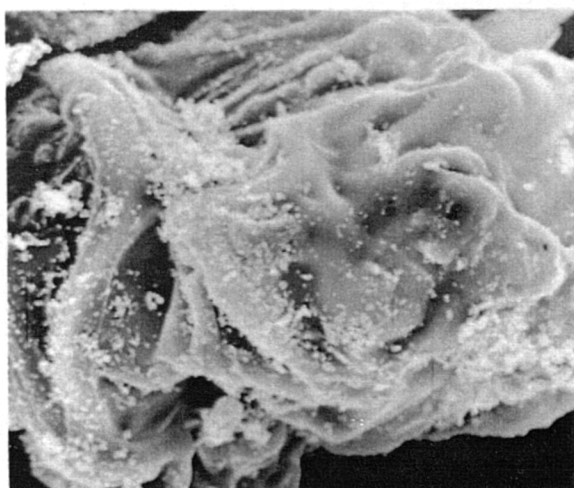
10b 25/0

1µm



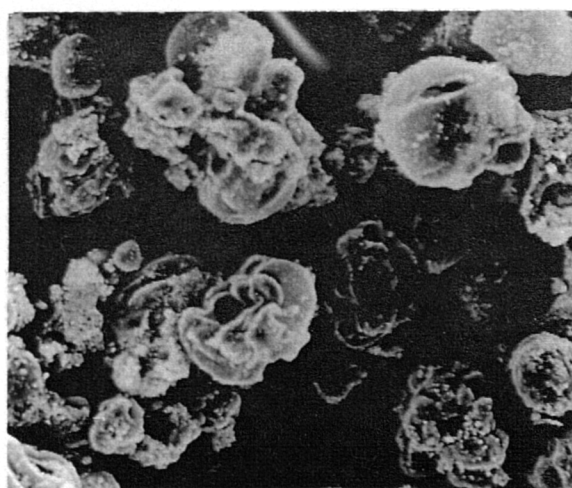
25/0

100µm



10c 25/5W

10µm



25/5W

100µm

Plate 10 Scanning Electron Micrographs of Char from the 88/025 Coal Series

10a, Char derived from oxidised coal (100°C/air, 112 days) showing pronounced char wall vesiculation.

10b, Cenospheres and mechanically damaged cenospheres derived from fresh coal.

10c, Cenospheres derived from a weathered coal (ambient/ 1 year) coal.

(V), devolatilisation vents. (M), mechanical damage. (Av), anealed vent.

(JEOL JSMT20)

the parent coal. This suggests that the oxidation of a swelling coal (i.e. A24 series) significantly improves char gasification, with only a marginal improvement in char burn-out for non-swelling coals (i.e. A25 series). However, there appears to be a point beyond which char burn-out (gasification) is not improved by the oxidation (100°C/air) of parent coals and consequently relative combustion efficiencies decrease, when measured by the level of unburnt carbon within the char combustion residue.

The effect of progressive weathering upon the characteristics of the char, generated during pyrolysis, is to produce numerous changes such as: an overall decrease in the proportion of cenospheres (Figure 7.47), a gradual decrease in optical anisotropy and char swelling, an increase in visible char-wall porosity (Plate 9c), an increase in the intrinsic (TGA) reactivity and a reduction in unburnt carbon within the char combustion residue (Figure 7.48).

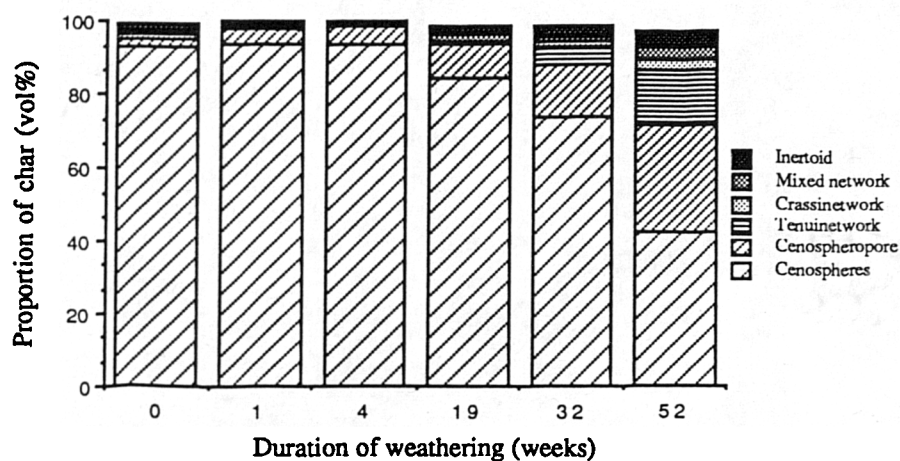


Figure 7.47 Coal series W24 and the change in char type with weathering (ambient).

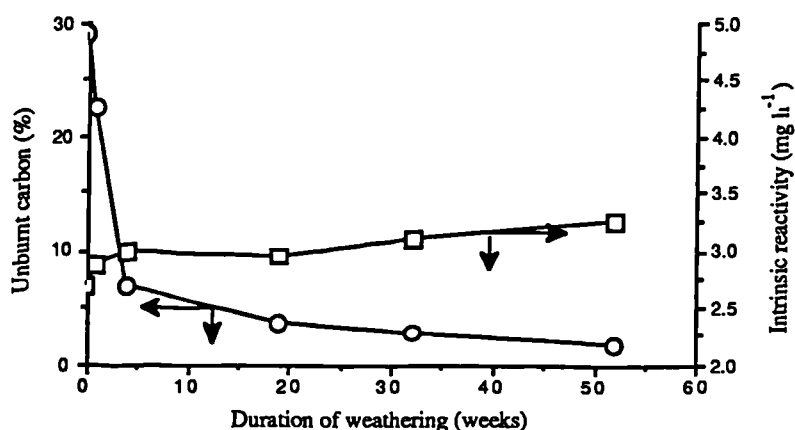


Figure 7.48 The changes in coal char TGA reactivity and in the level of unburnt carbon within the char combustion product derived from the weathered (ambient) coal series W24.

The changes that occurred within the lower rank W25 series (Figure 7.49) also included those changes in char characteristics identified within the W24 series outlined above. The changes included a gradual reduction in char optical anisotropy, a decrease in the proportion of

cenospheres and a concomitant decrease in the proportion of unburnt carbon within the char combustion residue (Figure 7.50).

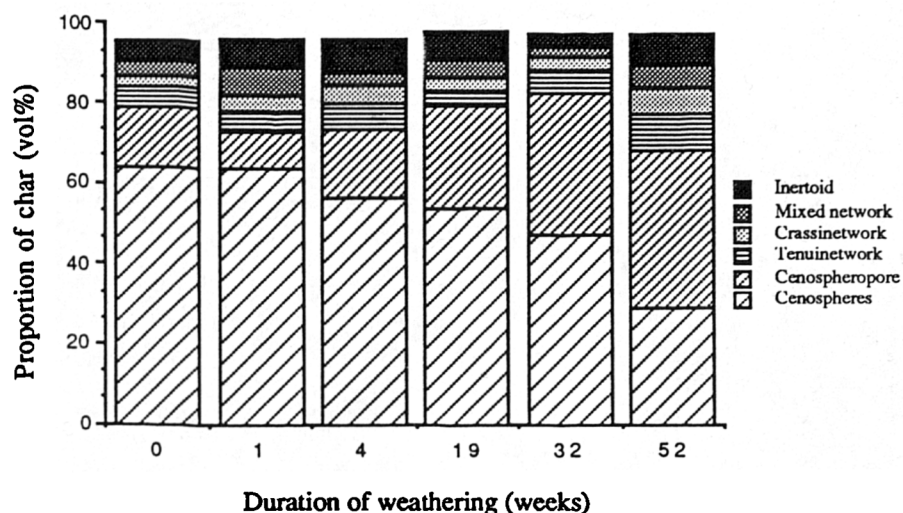


Figure 7.49 Coal series W25 and the change in char type with weathering (ambient).

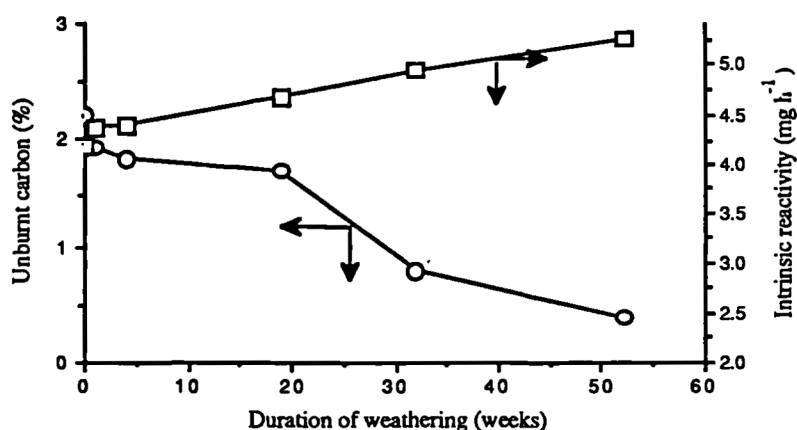


Figure 7.50 The changes in coal char TGA reactivity and in the level of unburnt carbon within the char combustion product derived from coals of the weathered (ambient) series W25.

However, the changes within the char characteristics, wrought by weathering, are less severe than those changes induced by oxidation at 100°C over the same period of time. Similarly, the changes within the char characteristics between the two coal series were subtly different. For example, coal W24-3 showed a significant improvement in char burn-out after weathering for twenty weeks (Figure 7.48) accompanied by a rapid improvement in intrinsic reactivity. After the initial gains in char burn-out efficiency and reactivity, only slight improvements occurred with prolonged exposure to the atmosphere; unlike coals of the W25 series that showed continued gains in reactivity and char burn-out (Figure 7.50).

7.3.4 The Relationship Between Char Formation and Coal Elemental Oxygen Content

The results from this oxidation and weathering study would appear to suggest that limited oxidation at 100°C and the weathering (ambient) of coal feedstock reduces the thermoplastic properties of a coal. These results, therefore, concur with the work of Mahajan *et al.*⁵⁷

The atomic O/C ratios increased within both the oxidised and weathered coals (page 146) but at different rates. There appears to be an inverse relationship between the generation of specific types of char, for example cenospheres, and the atomic O/C ratio of the oxidised or weathered coal from which they are derived (Figure 7.51). Such a relationship is reminiscent of the *cenosphere/atomic O/C ratio* relationship (Figure 7.52) which was discussed previously during the coal rank study (see Figure 7.9, Section 7.1).

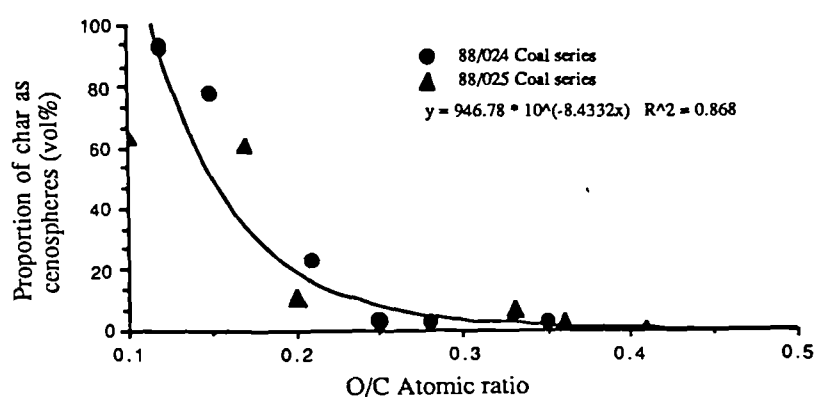


Figure 7.51 The proportion of char occurring as cenospheres and the O/C atomic ratios for the oxidised coals (100°C/air).

The inverse relationship between the proportion cenospheres generated during pyrolysis and the atomic O/C ratio of the parent coals is common to coals and chars of the coal rank (Figure 7.52) and oxidation/weathering study.

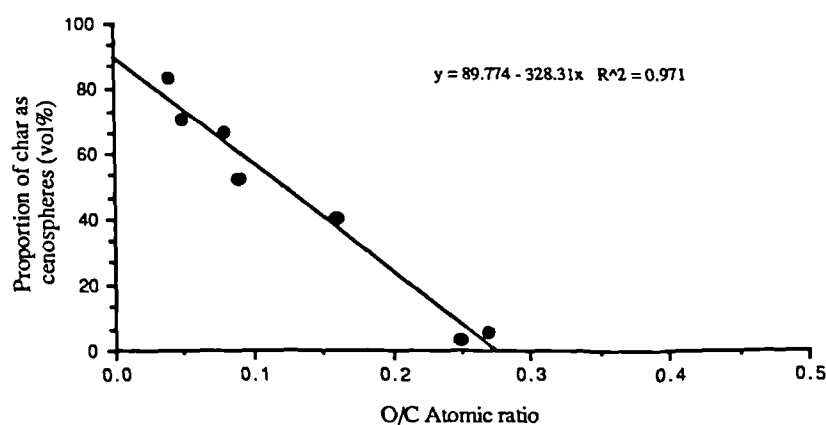


Figure 7.52 The proportion of char occurring as cenospheres and the O/C atomic ratios for the rank series of coals, excluding the semi-anthracite and anthracite.

The relationships discussed above strongly support the current theories on rapid coal pyrolysis mechanisms.^{33,35,36,64} Theories suggesting that the thermal decomposition of oxygen-bearing functional groups, during coal-pyrolysis, play an active mechanistic role in char formation through the generation of hydrogen-scavenging free radicals. Deshpande *et al.*³⁵ discuss the decomposition of carboxyl groups during pyrolysis and they propose that bond formation, within the metaplast, occurs simultaneously with tar evolution at higher heating rates (2.0×10^4 °C s⁻¹). The reduction in thermoplasticity of the metaplast, described by Deshpande *et al.*³⁵ is possibly the result of the formation of hydrogen-scavenging free radicals due to the thermolysis of oxygen-bearing functional groups during coal pyrolysis.

Therefore, the thermoplastic properties of coal during pyrolysis and the formation of hollow single chambered cenospheres, characterised by pronounced swelling, low char wall porosity, low CO₂ surface area and an anisotropic optical texture is inversely related to the proportion of elemental oxygen within the parent coal (Figure 7.53), either as a function of rank or due to oxidation/weathering.

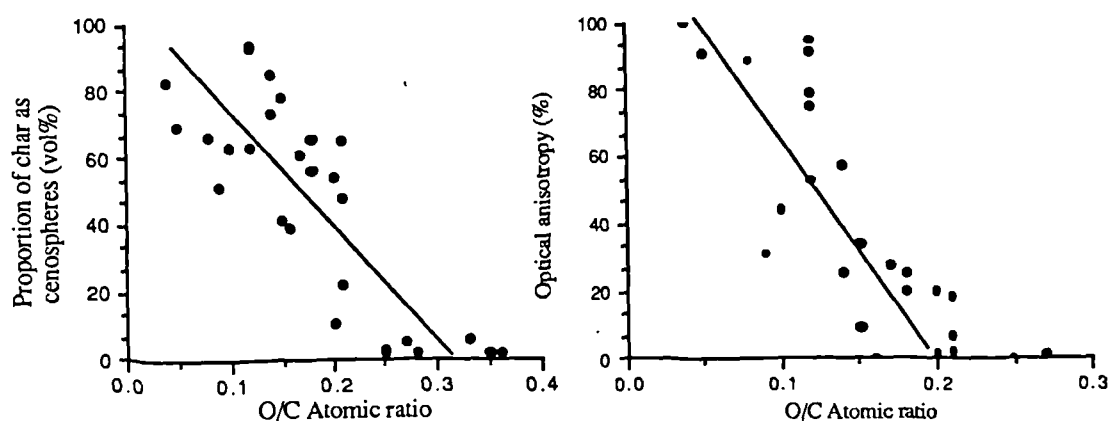


Figure 7.53 The inverse relationship between the Atomic O/C ratio and the proportion of cenospheres (left) and the relationship between the Atomic O/C ratio and optical anisotropy (right).

Therefore, the reduction of donateable hydrogen species, either due to a decrease in coal rank or through the oxidative replacement of alkyl groups by oxygen-bearing functional groups, probably leads to a greater number of hydrogen scavenging free radicals during pyrolysis. In this way, the generation of specific char types can be related to the proportion of elemental oxygen within the coal particle; below an atomic O/C ratio of 0.25 the predominant char is that of the cenosphere variety.

7.3.5 Review

Coal oxidation or weathering affects the values obtained from standard analytical techniques, such as proximate and ultimate analysis and vitrinite reflectance. However, the utilisation of fluorescence microphotometry, in conjunction with vitrinite reflectance through an oxidation

quotient O/Q , can be used as a technique for the detection of oxidation or weathering and appears to be very sensitive to the severity of the oxidation conditions.

The progressive oxidation or weathering of coal effects the physical and structural characteristics of the associated chars produced during coal pyrolysis at 1000°C in an EFR. The formation of chars that are optically isotropic and porous (outer char wall porosity) enhances char gasification during combustion at 1000°C (air) using the EFR apparatus within Northern Carbon Research Laboratories.

The oxidation or weathering of parent coal (or a decrease in coal rank) significantly improves char burn-out, due to the formation of highly vesiculated, fenestrated chars with high CO₂ surface areas and an isotropic optical texture. Char burn-out within the EFR is apparently controlled by the presence or absence of pores within the char wall material, thereby enabling the penetration of gaseous reactants (diffusion) to access the reacting char particle, a characteristic that varies with rank and oxidation or weathering. Such a phenomenon indicates that the combustion of char within the EFR is influenced by the optical texture and the presence or absence of pores within the char wall material (Plates 9 and 10, and also 7 and 8).

However, the question whether the combustion of oxidised or weathered pulverised coal would maintain a self-sustaining flame in a full-size industrial boiler at maximum load cannot be addressed within the present study. The inhibition of volatile matter release due to the promotion of char condensation reactions during the pyrolysis of the pulverised coal suggests that this may not be the case, a point pertaining especially to the more severely oxidised coals (at 100°C / 112 days). Clearly there is need for future work within this area of pulverised coal combustion.

References

1. Street, P.J., Weight, R.P. and Lightman, P. (1969). *Fuel*. **48**, 343-365.
2. Lightman, P. and Street, P.J. (1968). *Fuel*. **47**, 7-28.
3. Nandi, B.N., Brown, T.D. and Lee, G.K. (1977). *Fuel*. **56**, 125-130.
4. Jones, R.B., McCourt, C.B., Morley, C. and King, K. (1985). *Fuel*. **64**, 1460-1467.
5. Hamilton, L.H. (1981). *Fuel*. **60**, 909-913.
6. Oka, N., Msrayama, T., Maksouka, H., Yamada, S., Yamada, V.T., Shinozoki, S., Shibaoka, M. and Thomas, C.G. (1987). *Fuel Proc. Technol.* **15**, 213-224.
7. Tsai, C-Y. and Scaroni, A.W. (1987). *Fuel*. **66**, 200-206.
8. Bengston, M. (1987). *Int. Conf. on Coal Sci.* (Moulijn, J.A., Nater, K.A. and Chermin, H.A.G. Eds.) Elsevier Science Pubs., B.V. Amsterdam. 863-896.
9. Skorupska, N.M., Sanyal, A., Hesselman, G.J., Crelling, J.C., Edwards, I.A.S. and Marsh, H. (1987). *Int. Conf. on Coal Sci.* (Moulijn, J.A., Nater, K.A. and Chermin, H.A.G. Eds.). Elsevier Science Pubs., B.V. Amsterdam. 827-821.
10. Shibaoka, M., Thomas, C.G., Oka, N., Matsuoka, H., Murayama, K. and Tamaru, K. (1986). *Int. Conf. on Coal Science*, Pergamon, Sydney. 665-668.
11. Sanyal, A. (1983). *J. Inst. Energy*. June 92-95.
12. Skorupska, N.M. (1987). Ph.D. Thesis (Unpub) Dept. of Chemistry, University of Newcastle upon Tyne.
13. Jones, R.B., McCourt, C.B., Morley, C. (1985). *Fuel*. **64**, 1460-1467.
14. Bailey, J.G. and Diessel, C.F.K. (1987). Presentation to Committee of the I.C.C.P.,
15. Rymer, T.B. (1970). *Electron Diffraction* Methuen and Co. Ltd London.
16. Laurendau, N.M. (1978). *Prog. in Energy and Combustion Science*. **4**, 221-270.
17. Walker, P.L. Jr., Pusinko, F. Jr., and Austin, L.G. (1959). in: 'Advances in Catalysis, Vol II' (Ely, D.D., Selwood, P.W. and Weisz, P.B. Eds.). Academic Press, New York. 133-221.
18. Suuberg, E.M., Peters, W.A. and Howard, J.B. (1979). 17th Symp. (Int.) Combust. The Combustion Institute, Pittsburg, P.A., 117-130.
19. Bouwman, R. and Frericks, I.L.C. (1980). *Fuel*. **59**, 315-322.
20. Fuller, M.P., Hamadeh, I.M., Griffiths, P.R. and Lowenhaupt, D.E. (1982). *Fuel*. **61**, 529-536.
21. Riesser, B., Starsinic, E., Squires, E., Davis, A. and Painter, P.C. (1984). *Fuel*. **63**, 1253-1261.
22. Rhoads, C.A., Senftle, J.T., Coleman, M.M., Davis, A. and Painter, P.C. (1983). *Fuel*. **62**, 1387-1392.
23. Painter, P.C., Snyder, R.W., Pearson, D.E. and Kwong, J. (1980). *Fuel*. **59**, 282-285.
24. Calemma, V., Rausa, R., Margarit, M. and Girardi, E. (1988). *Fuel*. **67**, 764-765.
25. Zawadzki, J. (1987). *Carbon*. **16**, 491-497.
26. Senftle, J.T., Kuehn, D., Davis, A., Brozoski, B., Rhoads, C. and Painter, P.C. (1984). *Fuel*. **63**, 245-250.
27. Albers, G., Lenart, L. and Olert, H.H. (1974). *Fuel*. **53**, 47-53.
28. Tooke, P.B. and Grint, A. (1983), *Fuel*. **62**, 1003-1008.
29. Lambert, J.B., Shurvell, H.F., Verbit, L., Cooks, R.G. and Stout, G.H. (1976) 'Organic Structural Analysis' Macmillan Publishing Co., In. New York, Collier Macmillan Pubs., London.
30. Speight, J.G. (1978). in: 'Analytical Methods for Coal and Coal Product' (Karr, C. Jr.). Academic Press, Inc. New York. San Fransisco. London. 78-81.
31. Banwell, C.N. (1983) 'Fundamentals of Molecular Spectroscopy', 3rd Edn. McGraw-Hill Ltd. London.
32. Niksa, S. and Kerstein, A. R. (1987). *Fuel*. **66**, 1389-1399.
33. Bruinsma, O.S.L. (1988) Ph.D Thesis. University of Amsterdam. Krips Repro Meppel, Amsterdam.
34. Solomon, P.R. and Hamblen, D.G. (1985) in: 'Chemistry of Coal Conversion' (Schlosberg R.H. Ed.). Plenum Press. New York. 121.
35. Deshpande, C.V., Solomon, P.R. and Serio, M.A. (1988). *ACS Div. of Fuel Chem.* **33**, No 2. 310-321.
36. Moulijn, J.A. and Tromp, P.J.J. (1986). in: 'New Trends in Coal Science' (Yürüm, Y. Ed.) Kluwer Academic Press Dodecht, Boston, London. 433-480.
37. Jüngten, H. (1987). *Erdöl und Kohle, Erdgas*. **40**, 153-165.

38. Suuberg, E.M., Unger, P.F. and Lilly, W.D. (1985). *Fuel*. **64**, 956-962.
40. McCartney, J.T. and Hofer, L.J.E. (1955). *Analytical Chem.* **27**, 1320-1325.
41. McCartney, J.T., O'Donnell, H.J. and Ergun, S. (1971). *Fuel*. **50**, 226-235.
42. Davis, A. and Vastola, F.J. (1977). *J. of Microscopy* **109**, 3-12.
43. Pitt, G.J. and Dawson, K.M. (1979). *J. of Microscopy* **116**, 321-328.
44. Lee, J.B. (1985) *J. of Microscopy*. **137**, 145-154.
45. Jones, R.B., Morley, C. and McCourt, C.B. (1985), *Proc. Int. Conf. on Coal Science*, Sydney Australia Pergamon Press. Sydney 669-672.
46. Berkowitz, N., Fryer, J.F., Ignasiak, B.I. and Szladow, A.J. (1974). *Fuel*. **53**, 141.
47. van Veen, J.A.R., King, K. (1987). *Fuel Proc. Technol.* **16**, 3-17.
48. Youtcheff, J.S. and Given, P.H. (1982). *Fuel*, **61**, 980-987.
49. Axelson, D.E., Mikula, R.J. and Munoz, V.A. (1987). *Int. Conf. on Coal Science* (Moulijn J.A., Nater, K.A., Chermin, H.A.G. Eds.), Elsevier Science Pubs., B.V. Amsterdam, 419-422.
50. van Krevelen, D.W. and Schuyer, J. (1957) 'Coal Science' Elsevier Amsterdam, London, New York, Princeton.
51. Berkowitz, N.L. (1979) 'An Introduction to Coal Technology'. Academic Press, New York.
52. Chamberlain, E.A.C., Barrass, G. and Thirlaway, J.T. (1976). *Fuel*. **55**, 217-223.
53. Larsen, J.W., Lee, D., Schmidt, T., and Grint, A., (1986). *Fuel*. **65**, 595-596.
54. Jakab. E., Hoesterey, B., Windig, W., Hill. G.R. and Meuzelaar. H.L.C. (1988). *Fuel*. **67**, 73-79.
55. Martin. R.R., MacPhee, J.A., Workinton, M. and Lindsay, E. (1989). *Fuel*. **68**, 1077-1079.
56. Rausa, R., Calemme, V., Ghelli, S. and Girardi, E. (1989). *Fuel*. **68**, 1168-1173.
57. Mahajan, Om.P., Komatsu, M. and Walker, Jr., P.L. (1980). *Fuel*. **59**, 3-10.
58. Jenkins, R.G., Nandi, S.P. and Walker, Jr. P.L. (1973). *Fuel*. **52**, 288-293.
59. Tromp, P.J.J., Kapteijn, F., Boon, J.J. and Moulijn, J.A. (1987). *Int. Conf. on Coal Science* (Moulijn J.A., Nater, K.A., Chermin, H.A.G. Eds.), Elsevier Science Pubs., B.V. Amsterdam, 537-541.
60. Liotta, R., Brons, G. and Isaacs, J. (1983). *Fuel*. **62**, 481-791.
61. Puttmann, W., Steffens, K. and Kalkreuth, W. (1987). *Int. Conf. on Coal Science* (Moulijn J.A., Nater, K.A., Chermin, H.A.G. Eds.), Elsevier Science Pubs., B.V. Amsterdam, 411-414.
62. Prado, J.G. (1977) *J. of Microscopy* **109**, 85-92.
63. Cronauer, D.C., Ruberto, R.G., Jenkins, R.G., Davis, A., Painter, P.C., Hoover, D.S., Starsinic, M.E. and Schlyer, D. (1983). *Fuel*. **62**, 1124-1132.
64. Solomon, P.R., Hamblen, D.G., Carengelo, R.M., Serio, M.A. and Deshpande, G.V. (1988) *Combust. Flame*. **71**, 137-146.

CHAPTER EIGHT

Conclusions

8.1 Overall Conclusions

Several relationships were investigated between the morphology of the chars produced during the rapid pyrolysis of pulverised coal and various analytical and coal characterisation techniques. Many complex relationships, hitherto not investigated, were studied using laboratory based techniques culminating in the development of relationships and techniques for the assessment of coal feedstock of varying rank, petrographic composition, geological age and degree of oxidation/weathering.

8.2 Specific Conclusions

8.2.1 The Influence of Coal Rank upon Char Morphology and Combustion

- 8.2.1.1 The rank of a vitrinite rich coal strongly influences the morphology of the char generated by pyrolysis at 1000°C in an entrained flow reactor (EFR), and the results within this study concur with those of Street *et al.*,¹ Shibaoka *et al.*,² Oka *et al.*,³ and Hamilton.^{4,5} In addition to the influence coal rank exerts over the *morphology* of the char, the characteristics of the respective char types vary in response to the rank of the parent coal. Low rank vitrinite rich coals (sub-bituminous to high volatile C bituminous) generate hollow, multi-chambered, highly vesiculated, fenestrated, optically isotropic chars (*network* variety). Network chars have high CO₂ surface areas (200 m² g⁻¹) and pores (<5µm diameter) which are visible within the walls of the char when using SEM or TEM.

With an increase in coal rank to medium volatile bituminous, the network chars are systematically replaced by hollow, single-chambered, optically anisotropic chars (*cenospheres*) that are typified by low CO₂ surface areas (20 m² g⁻¹) and an apparent lack of porosity within the char wall. In contrast, the hollow, single to multi-chambered, optically anisotropic chars derived from a semi-anthracite have an associated inter-connected porosity within the walls of the char and an associated CO₂ surface area of 160 m² g⁻¹; whereas, anthracites do not form a char under the experimental conditions used, but generate solid dense particles that do not vesiculate.

- 8.2.1.2 There is an inverse relationship between the proportion of cenospheres generated during pyrolysis at 1000°C in an EFR and the elemental oxygen content of the coal. Correlation coefficients of $R^2 = 0.97$ and 0.95 indicate that the inverse and normal relationships between the elemental oxygen content of the parent coal and the proportion of cenosphere or network chars respectively are excellent. Better correlation coefficients are obtained when considering the atomic O/C ratio and the generation of cenospheres or network chars ($R^2 = 0.97$ & 0.98 respectively). Below an atomic O/C ratio of 0.25 to 0.2 the predominant char is network; whereas, a vitrinite rich coal (excluding anthracites) with an atomic O/C ratio between 0.25 to 0.2 and 0.01 generates cenospheres predominantly.
- 8.2.1.3 The efficiency of char combustion also varies with the rank of the parent coal, when using a laboratory based EFR at 1000°C under standardized conditions. A summary of the char and associated combustion characteristics (burn-out), and coal atomic O/C ratio is given in Figure 8.1.

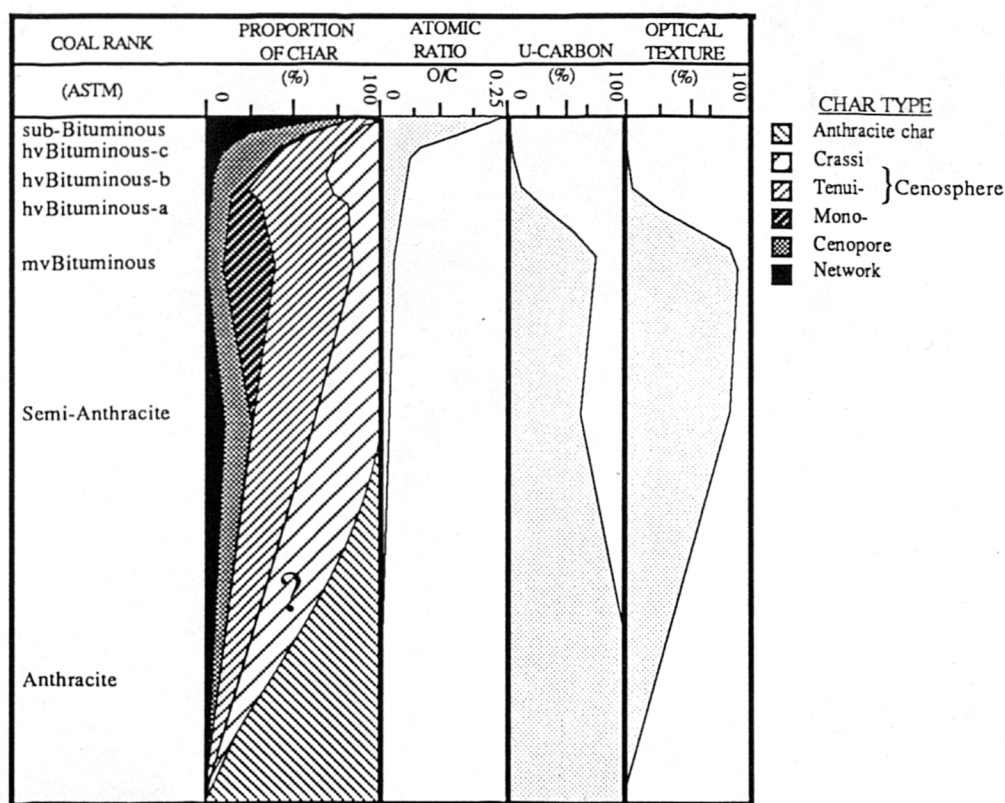


Figure 8.1 A summary of the characteristics of the vitrinite coals used for the Coal Rank, Char morphology and Combustion Study (rank, atomic O/C ratio), char type, optical texture and char combustion efficiency (burn-out).

The chars associated with lower levels of unburnt carbon within the combustion residue are those chars (predominantly network) that are derived from the sub-

bituminous and high volatile B bituminous coals. Relatively higher amounts of unburnt carbon (up to 16%) within the combustion residue are associated with the optically anisotropic cenospheric chars derived from the medium volatile bituminous coal with low CO₂ surface areas and low char wall porosity. The optically anisotropic semi-anthracite chars have lower levels of unburnt carbon within the combustion residue than the optically anisotropic medium volatile bituminous chars. This is attributed to the higher char-wall porosity and higher CO₂ surface area within the semi-anthracite char. In contrast, the anthracite, which does not produce a vesiculated char, is associated with the highest level of un-burnt carbon (60%) within the combustion residue.

The physical and structural characteristics of the char strongly influence carbon burn-out efficiencies. Because the highest combustion efficiencies are associated with chars possessing an accessible inter-connected char wall porosity, the diffusion of the gaseous reactant into the char would appear to be an important mechanism operating within the EFR during the combustion of the char at 1000°C.

8.2.2 Coal and Char Characterisation and Correlations

- 8.2.2.1 The possible use of coal reflectograms, as a means of characterising coal, has an element of objectivity compared to maceral analysis. However, the application of the technique as a means of discriminating between coals of differing combustion characteristics still requires further investigation to overcome the inherent technical difficulties associated with the technique. These differences include the ability to discriminate between macerals and epoxy binder, maceral and minerals, and maceral boundary situations. Furthermore, the data must be related to a particular utility or need (e.g. coal classification) in a simple, intelligible format. A simple sub-division into 'reactives' and un-reactives' is suggested.
- 8.2.2.2 For the coals used, poor univariate relationships exist between the morphology of the chars produced during pyrolysis and the calorific value, or proximate analyses of the parent coals.
- 8.2.2.3 The most successful univariate relationship found was between the proportion of 'porous char' and the petrographic composition of the parent coal, expressed as a microlithotype_v content (vol %). The relationship holds, irrespective of coal rank, but appears dependent upon the geological age of a coal. The new term *microlithotype_v* was created in an attempt to simplify existing petrographic nomenclature and represents a general class of vitrinite-rich microlithotypes (Vitrinite, Clarite_E, Clarite_V, Vitrinertite_V, Duroclarite and Vitinertoliptite).

8.2.2.4 A relationship exists between calorific value (d.a.f.), petrographic composition (microlithotype_v) and coal rank, for those coals studied. A combination of those parameters also differentiates between coals of different geological age and rank. Furthermore, the combination of microlithotype_v and calorific value can be related to the proportion of 'porous chars' produced during rapid pyrolysis and serves to illustrate the use of characterising coals for a specific purpose by combining various properties. The inter-relationship between 'porous char', microlithotype_v and calorific value forms the basis of a relationship through which the proportion of highly porous char may be estimated for Cretaceous-Tertiary coals.

8.2.3 The Effects of Coal Oxidation and Weathering upon Coal Properties, Char Morphology and Combustion

8.2.3.1 The values for proximate and ultimate analysis and vitrinite reflectance differ to those values obtained on fresh samples of the same coal, due to changes that occur within the chemical and physical structure of the coal in response to oxidation (100°C/air) or weathering (ambient). In response to oxidation (100°C/air) or weathering (ambient), the volatile matter content, elemental hydrogen and carbon decrease, the elemental oxygen increases, whereas the vitrinite reflectance either increases (oxidation, 100°C/air) or decreases (weathering).

8.2.3.2 Vitrinite fluorescence measured at 650 nm decreases due to the oxidation (100°C/air) and weathering of coal. The rate at which the intensity of the fluorescence decreases over a given period of time depends primarily upon the severity of the oxidising conditions used (temperature) and the particle size. Furthermore, when oxidising coals at 100°C, rims of quenched fluorescence are apparent. The presence of rims of quenched fluorescence lends support to a previous postulate⁶ that the kinetics of oxidation are diffusion controlled.

8.2.3.3 A technique capable of detecting the presence of oxidation and/or weathering based upon quantitative vitrinite fluorescence microphotometry (I_{650}) and vitrinite reflectance (% R_o max) was developed. This is presented as an Oxidation Quotient (O/Q), in which:

$$O/Q = \frac{I_{650}}{\%R_o\max} \quad (8.1)$$

The rate at which the quotient decreases was shown to be largely dependent upon the temperature at which the oxidation/weathering occurred for a given particle size range. The ratio normalises for the variable changes in vitrinite reflectance (increase or decrease) that occur due to (*pseudo coalification*) progressive oxidation (100°C/air) or weathering (ambient).

- 8.2.3.4 The progressive oxidation or weathering of coal effects the physical and structural characteristics of the associated chars. Due to progressive oxidation or weathering, cenospheres are superceded by network chars which in turn are superceded by chars of a less vesiculated character. The loss of swelling and softening characteristics, the decrease in the proportion of anisotropic char and an increase in CO₂ surface area within the char are attributable to the effects of oxidation or weathering upon the parent coal. However, the rate at which such changes occur is dependent upon the severity of the oxidative conditions; the process being more gradual with respect to the weathered coals compared to those coals oxidised at 100°C in air.

The transformation of char from cenosphere to other morphological types correlates with the atomic O/C ratio of the oxidised or weathered coal. Coals in which the atomic O/C ratio is greater than 0.25 produce minor amounts of cenospheres during pyrolysis. A similar relationship between coal rank and the proportion of cenospheres generated during pyrolysis exists for vitrinite rich coals (See 8.2.2.3). Because a common relationship exists between the atomic O/C ratio of the parent coal and the proportion of cenospheres generated during pyrolysis, either due to coal rank *or* due to oxidation or weathering phenomena, strongly supports current theories on rapid coal pyrolysis mechanisms that implicates the role of free radicals in the generation of char.

- 8.2.3.5 The formation of chars which are optically isotropic, porous and associated with a higher CO₂ surface area, due to the oxidation or weathering of the parent coal, are associated with an enhanced char combustion characteristic at 1000°C using the EFR, which is similar to a lowering of coal rank.

References

1. Street, P.J., Weight, R.P. and Lightman, P. (1969). *Fuel*, **48**, 343-365.
2. Shibaoka, M., Thomas, C.G., Oka, N., Matsuoka, H., Murayama K. and Tamaru K. (1968). *Inst. Conf. on Coal Science*, Pergamon, Sydney, 665-668.
3. Oka, N., Murayama, T., Matsuoka, H., Yamada, S., Yamada, T., Shinozaki, S., Shibaoka M. and Thomas, C.G. (1987). *Fuel Proc. Technol.* **15**, 213-224.
4. Hamilton, L.H. (1980). *Fuel*, **59**, 112-116.
5. Hamilton, L.H. (1981). *Fuel*, **60**, 909-913.
6. Cronauer, D.C., Ruberto, R.G., Jenkins, R.G., Davis, A., Painter, P.C., Hoover, D.S., Starsinic, M.E. and Schlyer, D. (1983). *Fuel*, **62**, 1125-1132.

Appendix A

Glossary of Terms Used

Glossary of Terms Used

abiotic	(grk: αβιος without life).
ablation	the action, or process, of removing or wearing away material by ice or water.
abscission	(lat: <i>abscissio</i> cut off) the state of being cut off, separated.
actinomyces	filamentaceous bacteria.
aerobic	pertaining too conditions in which oxygen is supplied by air.
allochthonous	not indigenous, transported from the place of origin to the place of deposition.
anaerobic	processes that occur in the absence of air.
angiosperms	(grk: σπερμος – ος) a plant which has its' seed enclosed in a seed-vessel (eg beech).
anisotropy	(grk: ανισος unequal) a substance possessing different physical properties in different directions.
anthracite	coal of high rank, characterized by low volatile matter content (>8%) high carbon content (>91%) and high vitrinite reflectivity (greater than Roil 2.5%).
arborescent	(lat: <i>arbor</i> tree) tree-like in general appearance, having a woody stem and branching.
aromaticity	the degree to which a cyclic organic compound containing double bonds within the molecular structure, exhibits the high stability, and specific reactivity characteristic of benzene and its derivatives.
ash	the non-volatile inorganic residue remaining after the combustion of organic material (i.e. coal).
A.S.T.M.	American Society for Testing, Materials).
attemperation	a means of regulating steam temperature by diluting high temperature, saturated, steam with low-temperature water, thereby introducing wet steam of lower enthalpy to the superheaters.
autochthonous	indigenous, derived from within the same area.
bedding-plane	a term relating to the plane orientated in space that contains the original attitude of the sediments during deposition.
bireflectance	an expression of the increasing degree of order achieved by the aromatic lamellae within a given particle of vitrinite, determined by: %R _o max - %R _o min.
bituminous coal	a coal of medium rank, where the vitrinite reflectance lies between R _o max 0.5 % and 1.9% and is subdivided into high, medium and Low volatile bituminous.
bitumen	(lat: <i>pix</i> pitch) various volatile hydrocarbons that soluble in common organic solvents, or distilled from the solid matrix by the application of heat <i>pyrobitumen</i> .
bright coal	a macroscopic description, synonymous with the term <i>vitrain</i> .
carboniferous	a geological period extending from 345 - 280 Ma (duration 65 Ma).
caking coal	a coal which has a softening propensity (partial or complete), upon heating or agglomeration and goes through a thermoplastic phase.
cathorimetry	a means of detecting and analysing gaseous material using a Thermal Conductivity Detector (T.C.D.), which is based upon the principle of the Wheatstone bridge. The detector consists of two parallel resistance branches, the passage of gas over one resistance branch produces a change in resistance that is proportional to the amount of gas flowing over it.
char	an isotropic or anisotropic carbonisation product due to the rapid pyrolysis of a natural or synthetic organic material which may show evidence of <i>plasticity</i> or devolatilisation due to pyrolysis.
channel sample	a method of sampling a coal seam, in which a vertical channel cut into a seam provides a representative sample of that seam at the point of sampling.
clarain	a macroscopic description of coal possessing a lustre between that of vitrain (very bright) and durain (very dull). Microscopically a clarain may contain vitrite, clarite and some durite.

clarite	a microscopical term. A bimaceral microlithotype composed of exinite and vitrinite.
cretaceous	a geological period extending from 136 - 64 Ma (duration 72 Ma).
coalification	the process(es) responsible for the transformation of plant remains into coal.
coal rank	a measure of the degree of coalification.
combustion	a chemical reaction, or complex of chemical reactions, in which a substance combines with oxygen producing heat, light and flame.
cyclothem	a rhythmic sequence of sedimentation represented as <i>a-b-c-b-a</i> .
devolatilisation	the process of volatile loss, usually a thermal decomposition phenomenon.
dull coal	A macroscopic description, synonymous with durain, possessing a greasy lustre. Microscopically, these coals are composed of the microlithotypes durite and clarite.
durain	See Dull coal.
durite	a microscopical term. A bimaceral microlithotype composed of inertinite and exinite.
epiric	a small enclosed sea, surrounded by land.
excess air	air that is used over and above that which is theoretically required for combustion, eg 125% total air means 100% theoretical air plus 25% excess air.
exinite	a microscopical term. A maceral group consisting of sporinite, cutinite, alginite, resinite and liptodetrinite, now superceded by the term <i>liptinite</i> .
facies	the general aspect or appearance.
fly ash	very fine (< 10 µm) particles of ash due to the combustion of mineral matter that is incorporated within the coal.
fixed carbon	the residual carbon remaining after the removal of hydrocarbons by thermal distillation (pyrolysis) in an inert atmosphere.
fractional burn-off	this is the weight loss observed during the combustion of char and is attributed to the conversion of char carbon to gaseous products.
fractional conversion	this is the weight loss observed during the combustion of coal. The weight loss is made up of volatile matter loss and combustion of the char.
fusain	a macroscopic description. An extremely dull coal, possessing a silky lustre and resembles wood charcoal.
fusinite	a microscopical term. A monomaceral microlithotype composed of inertinite.
gasification	the conversion of a solid or liquid to a lower molecular weight gaseous material (e.g. $C + O_2 \rightarrow CO_2$).
graphitic	a term used to describe carbonaceous material possessing areas of three-dimensional crystalline long range order, thereby generating an <i>optical texture</i> .
graticule	a scale, or a network of fine lines, in the ocular of the microscope.
gyttja	(Swd: <i>gyttja</i> mud) Swedish name for black or brown sapropelic ooze.
gametophyte	haploid phase of the life-cycle of a plant on or within gametes are borne.
heterosporous	a condition in which two types of spores are produced: megaspores (large: female) and microspores (small: male), all seed plants are heterosporous.
homosporous	a condition in which one type of spore is produced.
humic coals	coals, often banded, that have been formed from the accumulation of vegetable debris that have maintained some morphological organisation.
humic micelles	a cluster or group of molecules that by the process of coalification lose their acid nature, by the removal of functional groups, transforming humic acids to humins.
I.C.C.P.	International Committee for Coal Petrology.
inertite	a microscopical term. A monomaceral lithotype composed predominantly of inertinite.
inertinite	a microscopical term. A maceral group, consisting of fusinite, semifusinite, sclerotinite, micrinite, macrinite and inertodetrinite.
isorank	an expression that indicates points on a diagram that are of the same or similar rank.
isotropic	a term used to describe an optical texture in which there is no three-dimensional crystalline order discernable at the operating magnification
'K factor'	a calibration factor used in the calculation of the percentage elemental composition of an unknown.

ITZC	Inter-tropical-convergence-zone a belt of converging trade winds and rising air that encircles the earth at the equator, the rising air produces frequent storms.
leaf abscission	see <i>abscission</i> .
liptite	a microscopical term. A monomaceral lithotype composed predominantly of exinite (liptinite) macerals.
liptinite	a microscopical term, which is synonymous but replaces the older term exinite.
lithotype	a macroscopic description, which is used to describe the macroscopically recognisable bands in coal seams, for example vitrain.
limnic	(grk: λιμνε marshy land) coal deposits formed inland in fresh-water basins or bogs.
maceral	(lat: <i>macerare</i> macerate) organic units in coal analogous to rock minerals, names terminate with the suffix <i>-inite</i> . (Stopes, M. 1935).
meristem	a region in a plant composed of cells in which cell division occurs (i.e. terminations of roots, stems and leaves)
meta-	from the Greek μετα <i>meta</i> after, following.
metaplast	an unstable intermediate <i>plastic</i> phase through which the final char is formed during the pyrolysis or carbonisation of coal.
microlithotype	a microscopical term. An association of macerals occurring in bands more than 50 μm thick, used when characterizing a polished particulate mount block of coal.
mineral matter	the inorganic matter contained within a coal, which was incorporated prior to, or during deposition, being intimately associated with the macerals (syngenetic), or incorporated after deposition and found in crevices or cleats (epigenetic).
moisture content	the analysis of chemisorbed and natural moisture (not including visible surface water) that is released by thermal distillation at low temperatures (105 °C to 130 °C).
morphology	the study of the physical form and structure of a material.
mycelium	the vegetative thallus of many fungi, composed of many hyphae growing closely together.
NO_x	nitrogen oxides
ombrogenous	(grk: ομβρος shower of rain) sustained directly by rainwater.
optical texture	a description of the surface appearance of carbonaceous material in polarised light, isotropic material appears uniform, whereas anisotropic material will have a particular texture (e.g. mosaic, etc) due to the orientation of graphitic regions within the carbonaceous structure.
ortho-	from the Greek ορθος <i>ortho</i> straight.
overburden	a term referring to the rocks or soil that overlies the specific mineral or rock of interest.
oxidation	a substance undergoes oxidation if it gains oxygen ($2\text{Mg} + \text{O}_2 \rightarrow 2\text{MgO}$), or loses hydrogen ($\text{CH}_4 + \text{Cl}_2 \rightarrow \text{CH}_3\text{Cl} + \text{HCl}$) or loses electrons ($\text{Cu} \rightarrow \text{Cu}^{2+} + 2\text{e}^-$).
palaeo-	from the greek palios: ancient, of ancient times.
parenchyma	the fundamental cell type of all plants, these cells are large and isodiametric and considered to be the primitive cells.
particulate block	a solid block consisting of particles of crushed coal, that is representative of the whole sample, bound in epoxy resin, cast in a mould with one face ground and polished. Often referred to as grain mount.
peat	(Anglo-lat: <i>peta</i>) a product of the incomplete and partial decay of plant matter.
periderm	the outermost, secondary, corking or woody tissue produced by most perennial gymnosperms and angiosperms.
petrography	(grk: πετρα rock) the scientific description of the composition and formation of rocks: descriptive petrology.
petrology	see petrography, the branch of geology that deals with the origin, structure and composition of rocks etc.
pleom illuminator	an attachment to the microscope that facilitates the filtering of excitation and emitted light during incident fluorescent light microscopy.
point counter	a device that when attached to the microscope stage, is capable of registering the

	number of counts in each selected maceral category during several traverse across the surface of a particulate block. For each traverse, the particulate block is automatically advanced by a preselected interval (in microns). The lateral movement being activated by the counter mechanism.
phytogeographic provincialism	(grk: <i>θντον</i> plant) the geographic distribution of plants. an area (of rocks etc) that appear to have similar characteristics, suggesting a similarity of origin, but differing in some aspect from adjacent regions.
proximate analysis	an analytical technique based upon weight loss of a sample (i.e. coal) at elevated temperatures, a means of determining moisture content, volatile matter, fixed carbon and ash.
pseudo-vitrinite	pseudo-vitrinite differs from vitrinite by: 1. a slightly higher reflectance; 2. the presence of slightly curved slit-like openings; 3. the presence of cell structure; 4. stepped boundaries of the grains; 5. presence of fissures; 6. higher relief; 7. the absence of pyrite.
pyrobitumen	see bitumen.
pyrolysis	(grk: <i>Πυροσ</i> fire, and <i>λυσισ</i> loose) the thermal decomposition of a substance that does not involve combustion of the pyrolysates.
pyrolysate	material that is thermally distilled during pyrolysis, that encompasses gaseous and liquid (at RTP) material.
radical	molecules with unpaired electron(s) and therefore generally very reactive (e.g. $\cdot\text{CH}_3$ or $\cdot\text{OH}$).
random sample	Utilizing a sampling technique in which coal is selected from the same seam but from various locations within the workings of the coal mine.
rank	the rank of a coal is characteristic of the stage reached during the course coalification which begins with decayed vegetable matter and ends with meta-anthracite.
rhizome	a stem which grows beneath the surface of, or along, the ground.
reflectance	this is the percentage of normal incident light reflected from a polished surface measured in a medium of known refractive index (e.g. oil with an R.I. of 1.518 at 23 °C) and at a specific wavelength of light (546 nm).
sporangium	any spore producing cell or structure.
sapropel	(grk: <i>σαπρος</i> putrid, <i>πηλος</i> mud) formed completely from decomposed aquatic organisms (e.g. algae) found in anaerobic environments on the bottom of lakes and seas (Potonie, H., 1904).
sapromixtite	(grk: <i>σαπρος</i> putrid, <i>μυξα</i> slime) originally Tomite (Tom River: Siberia) thought to be a variety of 'algal coal' (Zalessky, M.D., 1915).
stoichiometry	weight relations between elements and compounds in chemical reactions.
ternary plot	a three sided graph onto which normalized data is plotted.
tertiary	the period of geological time which followed the cretaceous up to the present time, having a duration of 65 million years.
thermo-gravimetry	the simultaneous monitoring of weight (loss/gain) during heating under controlled conditions.
thermo-plastic	a material that <i>softens</i> at elevated temperature and is able to re-soften when re-exposed to similar temperatures
thermo-setting	a material that <i>sets</i> at elevated temperature after softening and is unable to re-soften when re-exposed to similar temperatures.
ultimate analyses	an analytical technique that is intended to provide information on the moisture content, mineral matter content (as ash) and the elemental composition (C, H, N, O, S) of coal.
vascular tissue	(lat: <i>vasculum</i> vessel) tissue which contains vessels or ducts for conveying fluids.
vacuols	(lat: <i>vacuus</i> empty) cavities that may have contained gas or fluids.
vertical illuminator	an attachment to the microscope that facilitates the illumination of a sample from above, rather than below the microscope stage (as in the case of transmitted light microscopy). It consists of a prism or "coated coverslip" (glass plate reflector) providing near incident light.
vitrain	a macroscopic description. An extremely bright coal possessing a vitreous lustre, composed predominantly of vitrinite.

vitrinite	a microscopical term. A maceral group consisting of the macerals: Telinite, collinite and vitrodetrinite .
vitrite	a microscopical term. A monomaceral microlithotype composed predominantly of the macerals vitrinite.
volatiles volatile matter	a substance that readily passes into a <i>vapour</i> : having a high vapour pressure, (proximate analysis term) the volatile matter <i>content</i> consists of material lost when heated up to 900 °C, corrected for moisture. The products mainly consist of hydrogen, carbon monoxide, carbon dioxide, methane, other hydrocarbons, tar vapours, and water vapours.
v-steps	reflectance intervals of 0.05 % (1/2 V-steps) or intervals of 0.1% (V-step) into which individual measurements are placed when plotting reflectance data on a histogram.
xylem	the vascular tissue responsible for transporting water and mineral nutrients throughout the plant.

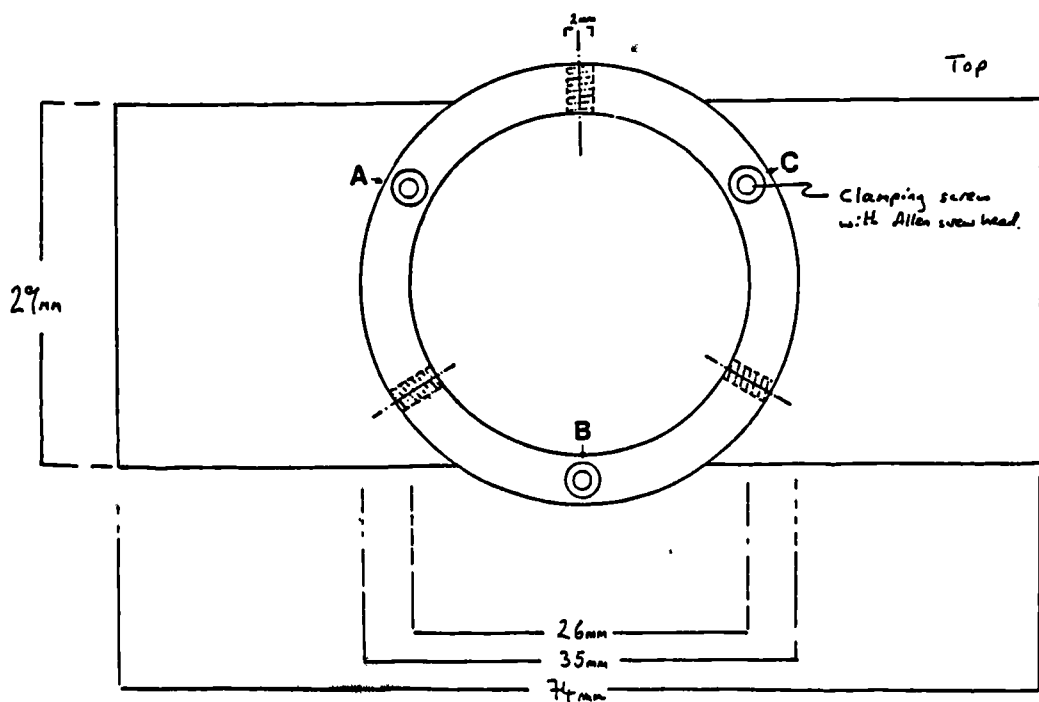
Abbreviations

a ⁻¹	year
C	Celcius
g	gram
h	hour
kg	kilogram
K	Kelvin
l	litre
m	metre
Ma ⁻¹	millions of years
mm	millimetre
µm	micron
mol	mole
m mol	millimoles
ms	milliseconds
MW	megawatt
n	refractive index (if undefined)
nm	nanometre
s	second
t	tonn
v	volt
w	watt

Appendix B

Line Drawings

Steve Bend (w.c.u.)



Plans for a vibrating unit to assist in the fuel feeder system of the Entrained Flow Reactor.

